# Studies on Ceramic Membrane, Sonication and Hybrid Processes for the Clarification of Vegetable Juices and Extracts

*Thesis submitted in partial fulfillment of the*

*requirements for the degree of*

**DOCTOR OF PHILOSOPHY**

*by*

*Sushma Chakraborty*
*Roll No.: 156107040*


**Department of Chemical Engineering**

**Indian Institute of Technology Guwahati**

**Guwahati–781039, India**

**March, 2021**

TH-2589_156107040

# Studies on Ceramic Membrane, Sonication and Hybrid Processes for the Clarification of Vegetable Juices and Extracts

Sushma Chakraborty

TH-2589_156107040

TH-2589_156107040

# Studies on Ceramic Membrane, Sonication and Hybrid Processes for the Clarification of Vegetable Juices and Extracts

*Thesis submitted in partial fulfillment of the*

*requirements for the degree of*

**DOCTOR OF PHILOSOPHY**

*by*

*Sushma Chakraborty*
*Roll No.: 156107040*


**Department of Chemical Engineering**
**Indian Institute of Technology Guwahati**
**Guwahati – 781039, India**

**March, 2021**

TH-2589_156107040

TH-2589_156107040

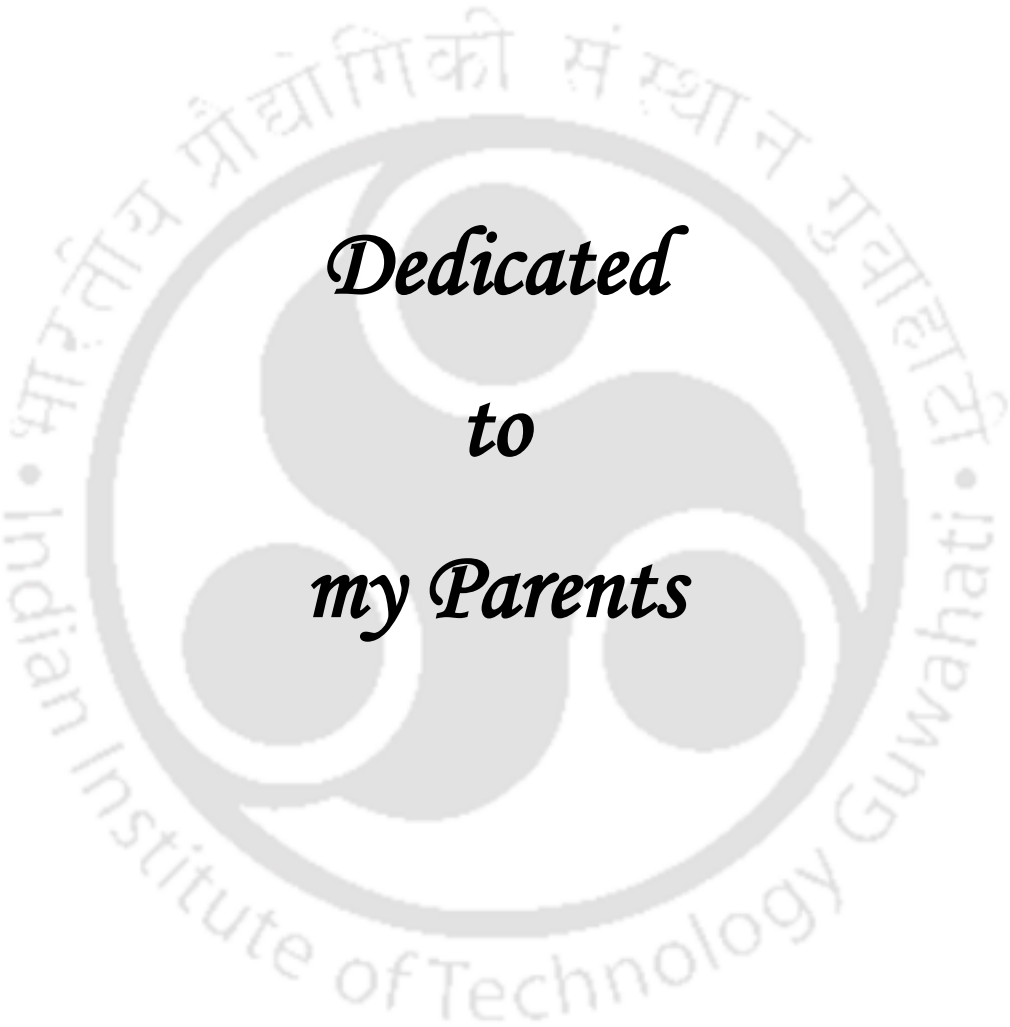

*Dedicated*

*to*

*my Parents*

TH-2589_156107040

TH-2589_156107040

**Department of Chemical Engineering**
**Indian Institute of Technology Guwahati**
**Guwahati – 781039, Assam, India**

# CERTIFICATE

It is certified that the work contained in this thesis entitled **"Studies on Ceramic Membrane, Sonication and Hybrid Processes for the Clarification of Vegetable Juices and Extracts"** submitted by **Ms. Sushma Chakraborty** for the award of the degree of Doctor of Philosophy has been carried out in the Department of Chemical Engineering, Indian Institute of Technology Guwahati under our supervision. To the best of our knowledge, this work is not submitted elsewhere for the award of any other degree or diploma.

**(Prof. Ramagopal V. S. Uppaluri)**
**Department of Chemical Engineering**
**IIT Guwahati, Guwahati - 781039**

**(Prof. Chandan Das)**
**Department of Chemical Engineering**
**IIT Guwahati, Guwahati - 781039**

TH-2589_156107040

TH-2589_156107040

# *Acknowledgements*

This Ph.D. thesis would not have been possible to complete without the help and support of many individuals associated directly or indirectly with the research work. It is my utmost pleasure to pen down these names and acknowledge them for their unconditional care and efforts.

At the very onset, I would like extend my sincere sense of gratitude to my supervisors, Prof. Ramagopal V.S. Uppaluri and Prof. Chandan Das, Department of Chemical Engineering, IIT Guwahati, for their continuous guidance, support and motivation during my Ph.D. tenure at IIT Guwahati. Their immense help throughout, has encouraged me to materialize the research ideas which eventually led to successful completion of this work. I would also like to thank them for providing a very healthy and friendly working environment and flexible work timings. They were always available for having a discussion at any point of time which is very much required for carrying out a productive work. I am glad to have worked under their supervision and will be forever grateful to them.

I am also thankful to my honourable doctoral committee members, Prof. G. Pugazhenthi and Prof. K. Mohanty from Department of Chemical Engineering, IIT Guwahati and Prof. R. Tamuli from Department of Bioscience and Bioengineering, IIT Guwahati for providing highly valuable suggestions, relevant insights and thought provoking ideas during the seminars that helped me to significantly improve my research work.

I am grateful to Prof. Anugrah Singh, Head of the Department of Chemical Engineering, IIT Guwahati and Prof. Bishnupada Mandal, former Head of the Department of Chemical Engineering, IIT Guwahati, for giving me an opportunity to pursue my Ph.D. in this prestigious department. My sincere thanks to Prof. P. Saha, Prof. M. K. Purkait, Prof. S.

TH-2589_156107040

Senthilmurugan, Prof. P. Tiwari, Prof. P. Ghosh, Prof. A. K. Golder, Prof. S. K. Majumdar, Prof. P. Kotecha, and, Prof. V. Katiyar from Department of Chemical Engineering, IIT Guwahati, for their direct and indirect involvements in my academia during my Ph.D. tenure.

The acknowledgement would not be complete without appreciating the support received from the scientific officers and other staffs of Department of Chemical Engineering and Department of Mechanical Engineering, IIT Guwahati. I would also like to thank the scientific officers of University Science Instrumentation Centre (USIC), Gauhati University, for permitting me to use their research facilities. I also thank the Central Instruments Facility (CIF), IIT Guwahati for providing me the facility of high-end and sophisticated instruments which were necessary for this research work.

The working environment in the laboratory has been enjoyable and pleasing because of my labmates and I am extremely thankful to my labmates and colleagues, Dr. Srinu, Ms. Aritra, Mr. Imdad, Ms. Preetisagar, Ms. Srimonti, Ms. Poushali, Ms. Udaratta, Mr. Prabhat, Mr. Kamal, Mr. Nuruzzaman, Ms. Kumudhini, Ms. Tinka, Mr. Simons, Mr. Jay, Mr. Pankaj, Ms. Deepshikha, Mr. Abhradip, Ms. Mounika, Dr. Supriyo, Dr. Suman, Mr. Atanu, Mr. Abhik, Mr. Chinna, and Mr. Barun, for their help and support in some form or the other.

I could not be more thankful to my friends for their constant and endless support they have always shown towards me. Having said that, I would like to thank Ms. Kajal, Ms. Sutapa, Mr. Piyal, Mr. Siddharth, Mr. Jinesh, Ms. Surabhi, Ms. Nilanjana, Mr. Sunil, Ms. Ananya, and Ms. Satarupa. They were always there for me at my highs and lows, which have made my stay at IIT Guwahati easier, fun and homely. I convey my special thanks to Ms. Kajal for always being there by my side and supporting me throughout.

I am forever grateful and indebted to my extremely loving and caring parents, Mr. Jhulan Chakraborty and Mrs. Dolly Chakraborty; my brother, Mr. Krishna Chakraborty; and my



TH-2589_156107040

sister-in-law, Mrs. Priya Sharma Chakraborty for putting their belief in me. It is because of their prayers, uncountable sacrifices and patience that I have reached this far. They have always encouraged me to put extra and sincere efforts in everything I do.

I thank the Almighty for His blessings He has bestowed upon me and for giving me the strength and wisdom to achieve this academic goal.

Last, but not the least, I am grateful to all who have been directly or directly associated in my work during all these years.

Sushma Chakraborty

(chakraborty.sushma@gmail.com)

Indian Institute of Technology Guwahati

TH-2589_156107040

# *Abstract*

Functional fruits and vegetables are important sources to provide bioactive compounds and natural phytochemicals and thereby nurture human metabolism and enhance immunity. Thus, significant emphasis is required towards the production of fruit and vegetable juices and extracts to serve as health and nutritional supplements.

Among alternate methods of fruit and vegetable juice/extract processing, enzymatic pretreatment, centrifugation, membrane separation, mechanical and ultrasound assisted agitation could be regarded to be the most inexpensive methods in comparison with the expensive technologies such as freeze processing, thermal processing, supercritical extraction etc.. Therefore, among the non-thermal processing methods that are gradually gaining popularity, microfiltration (MF), ultrafiltration and ultrasound-assisted extraction (UAE) could be considered as highly competitive due to their inherent advantages such as high efficiency, low cost, easy operation, low temperature requirement, low solvent requirement (for extraction), low pressure (for membrane separation) and ease of cleaning (for membrane separation). Further, few studies elaborate towards hybrid processes (such as centrifugation-MF and UAE-MF) to achieve the desired targets of better clarification, enhanced yield etc..

Considering these issues, the Ph.D. thesis devotes towards the development of microfiltration and ultrasound assisted extraction methods for the clarification and production of vegetable juices and extracts. The optimality of microfiltration system has been addressed in terms of alternate membrane morphologies, variable trans-membrane pressure and feed constitution. Similarly, a design of experiments approach has been followed to address optimality of ultrasound assisted extraction systems. Among many varieties of vegetables available for such investigations, the thesis devotes towards bottle gourd juice and bitter gourd extracts due to their excellent nutritional supplement and medicinal applications. Further, the thesis gains its prominence due to the potential to achieve clarified bottle gourd juices and bitter gourd extracts as viable products in the commercial arena.

Adopting uniaxial dry compaction method to fabricate kaolin based low cost ceramic membranes, the membrane characterization methodology emphasized upon the determination of average pore size, porosity and flexural strength. Field emission scanning electron microscopy (FESEM) was adopted to supplement the data obtained from these characterizations. Microfiltration studies targeted flux decline studies, membrane cleaning

TH-2589_156107040

steps, determination of flux decline coefficient (FDC) and flux recovery ratio (FRR), fouling characteristics (adopting Hermia and Bolton's models to evaluate most competent fouling mechanism to represent pertinent flux decline) and resistances (reversible, irreversible and support resistances)), and morphological changes associated with fouling. Response surface methodology based design of experiments was followed during ceramic membrane fabrication and optimization of ultrasound assisted extraction process.

The hierarchy of the overall PhD thesis methodology is as follows. Firstly, the saw dust based low cost ceramic membranes were fabricated using uniaxial dry compaction method. For this purpose, the experimental designs were generated using mixture model design (MMD) based response surface methodology (RSM). Following this, a variation in membrane properties (pore size, porosity and permeability) was targeted through variations in saw dust particle size (39 – 254 µm) and composition (1 – 8 wt.%) and compositions of other precursors (0.5 to 2.0 variation in kaolin to feldspar ratio and 7.5 – 15 wt.% variation in binder compositions). Thereby, defect free low cost ceramic membranes CM1 – CM7 and VCM1 – VCM6 have been fabricated with wider membrane morphological characteristics. The membranes have been characterized to possess wider average pore size (0.09 – 1.39 µm) and porosity (14.08 – 30.43 %). Empirical models have also been evaluated to visualize upon the associated nonlinearities between responses and process variables. Thereafter, the thesis devotes towards the selection of few membranes (pore size: 1 (CM1), 0.75 (CM3) and 0.45 (CM7) µm) for the microfiltration of bottle gourd juice. Various combinations of pressure differentials (103.4, 137.9 and 172.4 kPa) and feedstocks (fresh, filtered and centrifuged juice) were considered to determine optimal conditions that yield best combinations of trans-membrane flux and permeate quality. Finally, for the production of bitter gourd juice extract, aqueous extracts were prepared using UAE process by considering temperature (25 – 80 °C), time (1 – 15 min) and concentration (0.1 – 0.5 g/mL) as independent variables. In due course of such process, the maximization of antioxidants and polyphenol content was targeted along with the minimization of protein content in the aqueous extract. Both continuous and pulse mode of sonication were adopted to identify best mode of operation along with optimal process parameters. Following this, hybrid UAE-MF process was targeted with various combinations of membrane morphologies (CM1, CM3 and CM7) and pressure differentials (103.4 – 172.4 kPa) to thereby determine the optimal membrane process parameters for the achievement of permeate product with better shelf life and nutritional characteristics.



TH-2589_156107040

Based on MMD, the optimal membrane composition (without considering flexural strength) obtained was 48.19 wt.% kaolin, 28.62 wt.% feldspar, 8.19 wt.% saw dust, 7.5 wt.% sodium metasilicate and 7.5 wt.% boric acid for which optimal pore size and porosity obtained were 1.00 µm and 28.47 %, respectively. The RSM based MMD can be regarded as a very important tool for compositional optimization. The pore size and porosity of the membranes could be significantly reduced to reach the lower values of 0.45 µm with 16.29 % porosity through a reduction in the average particle size of the saw dust (39 µm) and composition (1 wt.%). Further reduction in pore size and porosity of 0.09 µm and 14.09 % respectively were achieved for kaolin to feldspar ratio of 1.68 and binder constitution of 15 wt.%. In other words, nanofiltration membranes have been successfully fabricated through variations in the membrane precursor compositions. The fresh bottle gourd juice processed with 1 µm average pore size membrane (CM1) provided best performance in terms of good combinations of clarity (92.46 %), microbial and protein rejection (99.37 % and 71.60 %). The membrane exhibited transmembrane flux of $0.18 \times 10^{-5} – 3.12 \times 10^{-5}$ $m^3.m^{-2}.s^{-1}$ for a variation in time from 0 – 80 min during dead end MF. The conceptual cost of CM1 membrane was evaluated to be 440 $\$/m^2$. Thereby, conceptual cost analysis based approach indicated that the bottle gourd juice processing cost is about 0.37 – 1.19 $/L. Also, microfiltration of alternate feed systems (fresh, paper filter and centrifuged bottle gourd juice) using alternate membranes (CM1, CM3 and CM7) and variant pressure differentials (103.4, 137.9 and 172.4 kPa) affirmed that fresh bottle gourd juice with CM3 membrane at 137.9 kPa provided best performance and the transmembrane flux varied from $0.08 \times 10^{-5} – 1.35 \times 10^{-5}$ $m^3.m^{-2}.s^{-1}$ for a variation in time from 0 – 80 min. For bitter gourd extraction, compared to normal and pulsed mode UAE, the RSM based optimization approach affirmed that the pulse mode of UAE performed optimally at 68.4 °C temperature, 12 min extraction time and 0.25 g/mL bitter gourd to water ratio. Thereby, the produced bitter gourd water extracts possessed antioxidant activity of 77.9 %, total polyphenols content of 104.5 mg GAE/g and total soluble proteins content of 42.1 mg/1000 mL. For the hybrid UAE-microfiltration process, the CM3 membranes performed optimally at 137.9 kPa applied pressure at which the permeate flux varied from $8.09 \times 10^{-6} – 3.34 \times 10^{-5}$ $m^3.m^{-2}.s^{-1}$ for a time period of 0 – 60 min. The clarified bitter gourd juice extract possessed 25.23 mg/1000 mL protein (46.74 % rejection), 56.68 % antioxidant activity, 75.87 mg (GAE)/g polyphenols content, 1259.27 mg/1000 mL carbohydrate, 0.049 A color and 98.17 % clarity.



TH-2589_156107040

In summary, the PhD thesis provided useful insights towards the promising performance of low cost ceramic membrane based microfiltration technologies and ultrasound-assisted extraction process for the production of organic bottle gourd and bitter gourd juices and extracts. Both processes are simple to envisage upon and are susceptible for cost effective scale up. Specific novelty of the thesis is towards the application of low cost ceramic membranes for the clarification of said vegetable juices and extracts, which also advocates upon the affirming of ultrasound assisted vegetable extraction and hybrid membrane - sonication process for juice and extract clarification. Throughout the PhD thesis, response surface methodology has been used as an efficient tool to supplement the research findings. These findings are expected to further enhance the application of said technologies for vegetable juice and extract production.



TH-2589_156107040

# *Contents*



TH-2589_156107040

TH-2589_156107040

TH-2589_156107040

# *List of Tables*



TH-2589_156107040

TH-2589_156107040

# *List of Figures*



TH-2589_156107040

# *Nomenclature*

## Abbreviation

| | |
|---|---|
| AA | Antioxidant Activity |
| ANOVA | Analysis of Variance |
| BSA | Bovine Serum Albumin |
| CFU | Colony Forming Units |
| DCPIP | 2, 6-dichlorophenol indophenol sodium salt |
| DPPH | 2,2-diphenuyl-1-picrylhydrazyl |
| DOE | Design of Experiments |
| FDC | Flux Decay Coefficient |
| FESEM | Field Emission Scanning Electron Microscopy |
| FRR | Flux Recovery Ratio |
| GAE | Gallic Acid Equivalent |
| GRG | Generalized Reduced Gradient |
| LCCM | Low Cost Ceramic Membranes |
| MF | Microfiltration |
| MMD | Mixture Model Design |
| NBM | Nano Ball Milled |
| RSM | Response Surface Methodology |
| TDS | Total Dissolved Solids |
| TGA | Thermogravimetric Analyzer |
| UAE | Ultrasound-assisted Extraction |
| UF | Ultrafiltration |

TH-2589_156107040

## Nomenclatures

| | |
|---|---|
| CM1 | Optimized LCCM based on RSM study |
| CM2 – CM4 | LCCM samples prepared with variation in saw dust composition |
| CM5 – CM7 | LCCM samples prepared with variation in saw dust particle size |
| VCM1 – VCM6 | LCCM samples prepared with variation in feldspar to kaolin ratio and binder content |

## Notations

| | |
|---|---|
| $\varepsilon_m$ | Volumetric porosity of the membrane, % |
| $\varepsilon_{m,t}$ | Volumetric porosity of the membrane at time t, % |
| $w_1$ | Weight of dry membrane, kg |
| $w_2$ | Weight of wet membrane, kg |
| $\rho_w$ | Density of water, $kg.m^{-3}$ |
| $d_m$ | Diameter of the membrane, $m^2$ |
| $T$ | Thickness of the membrane, m |
| $L_m$ | Average hydraulic permeability, $m^3.m^{-2}.s^{-1}.Pa^{-1}$ |
| $F$ | Flexural Strength of the membrane, MPa |
| $J_w$ | Pure water flux of the membrane, $m^3.m^{-2}.s^{-1}$ |
| $J_0$ | Initial water flux of the membrane, $m^3.m^{-2}.s^{-1}$ |
| $J_p$ | Water flux of the fouled membrane, $m^3.m^{-2}.s^{-1}$ |
| $J_c$ | Pure water flux of the cleaned membrane, $m^3.m^{-2}.s^{-1}$ |
| $V_s$ | Volume of the setup, $m^3$ |



TH-2589_156107040

| | |
|---|---|
| $A_m$ | Effective permeable area of the membrane, $m^2$ |
| $t$ | Time required for the entire volume of water to flow out of the setup, s |
| $J_{p,t}$ | Permeate flux at time t, $m^3.m^{-2}.s^{-1}$ |
| $V_t$ | Volume of the permeate collected at time t, $m^3$ |
| $t_t$ | Instantaneous time, s |
| $\Delta P$ | Applied pressure, kPa |
| $\eta_w$ | Viscosity of water, Pa.s |
| $\eta_p$ | Viscosity of the permeate, Pa.s |
| $d_p$ | Average membrane pore diameter, m |
| $d_t$ | Average membrane pore diameter at time t, m |
| $l$ | Length of the membrane, m |
| $l_t$ | Length of the membrane at time t, m |
| $C_p$ | Microbial concentration of permeate sample, $CFU.mL^{-1}$ |
| $C_f$ | Microbial concentration of feed sample, $CFU.mL^{-1}$ |
| $R_t$ | Total fouling resistance, $m^2.m^{-3}$ |
| $R_m$ | Hydraulic resistance or membrane resistance, $m^2.m^{-3}$ |
| $R_r$ | Reversible resistance, $m^2.m^{-3}$ |
| $R_i$ | Irreversible resistance, $m^2.m^{-3}$ |
| $k_c$, $K_b$ | Complete pore blocking coefficient |
| $k_s$, $K_s$ | Standard pore blocking coefficient |
| $k_i$, $K_i$ | Intermediate pore blocking coefficient |
| $k_{cf}$, $K_c$ | Cake filtration coefficient |
| $A$ | Absorbance at 660 nm |



TH-2589_156107040

| | |
|---|---|
| $V_1$ | DCPIP dye solution consumed to turn blank sample pink, mL |
| $V_2$ | DCPIP dye solution consumed to turn the juice samples pink, mL |



TH-2589_156107040

# Chapter 1:

## Introduction and Literature Review

TH-2589_156107040

TH-2589_156107040

# *Chapter 1*

# Introduction and Literature Review

*This chapter briefs about the fundamentals associated with vegetable and fruits juice processing technology. Section 1.1 provides a background of the work presented in the thesis. Section 1.2 gives an overview available techniques associated with food processing industries. The plants derivatives targeted in this Ph.D. thesis have been discussed in section 1.3. Section 1.4 addresses available prior art for ceramic membrane fabrication and its utilization in juice processing along with sonication extraction process used in extraction of bioactive compounds from plant derivatives. Following the prior art, section 1.5 gives a description about the lacunae identified from the literature review. Thereafter, section 1.6 conveys the broad objectives of the thesis followed with thesis organization related details in section 1.7.*

## 1.1 Background

### 1.1.1 Vegetable Juice and Extract Products

Wide varieties of nutritional compounds exist in fruits and vegetables. Human consumption of appropriate quantities of fruits and vegetables has been well documented to reduce and prevent the risks of degenerative diseases. This is due to the greater content of phytochemicals in such horticultural produce (Cassano et al., 2009; Rawson et al., 2011). Thus, significant emphasis and growing demand is evident for the transformation of organic plant resources as functional food supplements, additives and products.

TH-2589_156107040

While horticultural produces may be conventionally consumed without applying food preservation techniques to enhance their shelf life and value, globalization past world economy enabled significant variations in the habitat of a modern man. Extremely busy lifestyle, round the clock engagement in professional and social circles, awareness towards bettering nutrition through food supplements have altogether propelled the need for food preservation based development of nutritional supplements such as horticultural extracts, fruit juices etc.

In the wide varieties of vegetable produces, few food and nutritional supplements in the contemporary lifestyle of humanity can be briefly mentioned as follows:

a) Bottle gourd Juice: Among wide varieties of horticultural produces, bottle gourd is well known for its several health benefits and hence clarification of bottle gourd juice is often targeted (Rahman, 2003; Sharma et al., 2012).

b) Bitter gourd extract: Bitter gourd is another organic functional vegetable which is becoming popular given its functionally rich constituents has been reported to have applications in food, health care and medicinal industries (Lucas et al., 2010; Tan et al., 2016).

c) White-pumpkin juice: White pumpkins are highly nutritious and are specially used as weight loss supplements (Ravi et al., 2010; Yadav et al., 2010).

d) Night-jasmine extract: The medicinal benefits of plants are not limited to its fruits and vegetables. The leaves of some plants contains several bioactive components which are beneficial to human health and helps to cure various diseases such as leaves of night jasmine plants (Shrivastava and AK, 2018; Singh and Vyas, 2018).

e) Guava-leaf extract: Similar to night jasmine leaves, guava leaf extracts are also becoming popular due to its medicinal value in terms of higher dosage of anti-oxidants (Barbalho et al., 2012; Laily et al., 2015).



TH-2589_156107040

### 1.1.2 Overview of Vegetable and Fruit Juice Production Processes

Food processing is inevitable to enhance shelf life of perishable fruits and vegetables (Kubde et al., 2010; Mondal et al., 2016; Shah et al., 2010). Till date, various conventional and frontier methods of vegetable and fruit juice processing have been reported. Food, beverage and vegetable processing involves the integration of alternate techniques to achieve the desired objectives. Often, a combination of several operations is required to meet the stringent needs of processed horticultural produces. A typical vegetable and fruit juice processing scheme involves the sequential operations of sorting and washing, pressing and extraction, heating/blanching, clarification/centrifugation/enzymatic treatment, filtration, pasteurization and finally concentration (Jiménez-Sánchez et al., 2017). Among these, mechanical pressing and extraction, heating/blanching, clarification and filtration are very important steps to achieve various objectives that cannot be achieved by any of these processes on their own. While mechanical pressing and extraction facilitates the removal of pulpy content from the juice, the heating and blanching operation is effective to reduce pathogens and germs that enormously detriment shelf life of the processed juice systems. Clarification/centrifugation/enzymatic treatment removes colloids, macromolecules, pectin and other harmful matter that serve as useful sites to enhance deterioration of processed juices (Emani et al., 2013; Nandi et al., 2009). Filtration aids in the removal of unwanted substances and achieve better clarity of the product. Thereby, the sequence of operations enable better shelf life and improved characteristics of the product.

Certain disadvantages in the above cited sequential unit operations are as follows. Firstly, heating and blanching are ineffective to retain heat sensitive compounds such as antioxidants, which are well known for their nutritional benefits (Heldman and Hartel, 1999; Mújica-Paz et al., 2011). Secondly, enzymatic treatment involves the usage of expensive enzymes that further complicate the processing due to additional enzyme deactivation procedures that are



TH-2589_156107040

essential to retain better shelf life of the processed horticultural produce (Sharma and Van Sumere, 1992). Thirdly, mechanical extraction and pressing are inevitable to separate pulpy materials but offer poor extraction efficiency (Wang et al., 2020). Fourthly, centrifugation despite being highly effective is not cost effective for large scale processing (Wang et al., 2007).

### 1.1.3 Frontier Process Technologies for Vegetable Juice and Extract Production

To overcome the limitations of various conventional technologies mentioned in the previous section, wherever possible, process improvement can be targeted with the replacement of one, two, or fewer combinations of processes/operations with advanced process technologies. Notable issues with respect to such avenues have been outlined as follows:

a) Conventional process operations such as centrifugation, enzymatic treatment, filtration can be replaced with membrane processes such as microfiltration and ultrafiltration. By doing so, the desired objectives of colloidal particulate removal, retention of phytochemicals and other functional nutrients and significant reduction in microbial content can be altogether achieved through either microfiltration or a combination of microfiltration and ultrafiltration technologies. Such technologies are well known to have promising features such as lower processing cost, room temperature operation, lower energy consumption, scalability, elimination of external chemical usage and higher productivity (Grampp et al., 1978; Urošević et al., 2017).

b) Further, pasteurization and concentration using low pressure evaporation can be replaced using reverse osmosis membrane technology. Thereby, non-thermal processing can be effectively introduced to replace conventional operations involving thermal processing. Further, expensive centrifugation can be replaced with low cost



TH-2589_156107040

membrane technologies. Thereby, drawbacks of the mentioned technologies can be overcome (Mújica-Paz et al., 2011).

c) Many vegetable and fruit juice clarification techniques do not wish to omit centrifugation due to being a non-thermal process. Therefore, centrifugation and enzymatic treatment are often suggested in few literatures to supplement membrane technologies. In this regard, it can be noted that utilization of low cost membrane materials with appropriate morphological characteristics can enable replacing centrifugation with several membrane processes (Emani et al., 2013; Nandi et al., 2009; Nandi et al., 2011).

d) Ultrasound assisted extraction enables replacement of several unit operations such as pressing and extraction, heating/blanching, clarification/centrifugation/enzymatic treatment. Thereby, disadvantages of mechanical extraction or chemical extraction can be overcome through the sonication assisted extraction process. Further, higher quantities of phytochemicals can be obtained through sonication. This is due to the role of cavitation phenomena that significantly facilitate penetration of solvents into the bubbles formed in the liquid media and thereby enhances transport from the solid to the liquid phases (Caldas et al., 2018).

### 1.1.4 Summary

In summary, prominent operations for vegetable juice clarification include conventional (enzymatic treatment, centrifugation, straining and screening, freezing, thermal processing) and frontier technologies (membrane separation and ultrasound assisted extraction). Further, to produce organic juices which are gold standard in naturopathy and Ayurveda systems of medicine, very few technologies are promising as competent technologies to achieve desired objectives.



TH-2589_156107040

Conventional juice clarification requires a combination of three processes namely physical, mechanical and chemical processes. Microfiltration/Ultrafiltration, Centrifugation and Ultrasound assisted extraction can be visualized to be competent technologies to enhance process simplification and effective integrated processing. The following sections provide an overview of these important process technologies namely membrane technology, centrifugation and sonication.

## 1.2 Sustainable Vegetable Juice and Extract Processing Technologies

### 1.2.1 Centrifugation

Centrifugation process involves utilization of a centrifugal force to drive the separation of solids suspended in fluid due to varied density with respect to the fluid. The applied centrifugal force is higher than the gravitational force (Stephenson, 2016). In fruit/vegetable juice processing units, enhanced shelf life is targeted through the removal of undesirable macromolecules that exist in the raw juice. Thus, centrifugation enables removal of suspended constituents from juices and extracts. The efficiency of centrifugation process is dependent upon particle size of the suspended solids, difference in the densities of particles with respect to the fluid, fluid viscosity, and rotation speed (Poole, 2009). Primarily, centrifugation is deployed as a pretreatment process to eliminate heavier and larger particulates prevalent in the raw samples and thereby achieve juice with better clarity for subsequent processing units. Upon combining with membrane technology, the centrifugation is very effective. This is due to the removal of macromolecules that clog the membrane pores with the centrifugation step prior to membrane based clarification of fruit/vegetable juices. Thereby, such hybrid process facilitates better functionality of the membrane process and its efficiency (Tarazona-Díaz and Aguayo, 2013).



TH-2589_156107040

### 1.2.2 Ultrasound-assisted Extraction

Since plant species are rich in phytochemicals, extraction may serve as one of the best techniques to extract better the said compounds in comparison with conventional technologies. Contrary to other unit operations, extraction requires a medium (solvent) to facilitate transportation of essential nutrients from the source to solvent media. The solvent plays a vital role in determining the efficiency of an extraction process and therefore its choice is very crucial.

Various extraction methods that could be used to target extraction of plant based bioactive compounds. Conventional vegetable processing methods adopted for the extraction of plant resources refer to mechanical agitation, boiling and soxhlet extraction (Azmir et al., 2013). Advanced methods include supercritical fluid extraction, ohmic heating extraction, microwave heating extraction, extraction assisted with accelerated solvents, pressurized liquid extraction, sub-critical water extraction, extrusion, and enzymatic digestion, extraction with pulsed electric field and ultrasound-assisted extraction (UAE).

Among all these process, UAE method serves as the most suitable, economic and an efficient technique. Ultrasonic waves during UAE process create cavitation that enables greater penetration of solvents into the cellular matrix and rapid movement of molecules due to mechanical rupture and breakage of the cell walls. Two main phenomena drive UAE namely diffusion across the cell wall and their transport into the solvent after breakage of the cell walls (Azmir et al., 2013; Mason, 1996). Due to combinatorial effect of cavitation, mechanical agitation and thermology, sonication facilitates higher mass transport of bioactive constituents from plant resources to the solvent media (Bonfigli et al., 2017; Fang et al., 2014; He et al., 2016).



TH-2589_156107040

UAE can be concluded to be a simple, easy and inexpensive technique that facilitates lower solvent consumption, lower process temperature, extraction time and greater extraction efficiency and hence has a wider scope for application in chemical and food industries (Chemat et al., 2017; Sutanto et al., 2015). The UAE process can also be integrated with other processes such as membrane separation processes to enable a hybrid system for the enhanced and efficient selective transfer of nutrients from fruit and vegetable beverages to the solvent media.

### 1.2.3 Membrane Technology

Membrane technology constitutes a physical semi-permeable barrier or membrane to selectively allow one or more components to pass through it and thereby restrict other components in the feed system. Typically, membrane filtration is driven with the variations in physical and chemical properties of the components prevalent in the feed system. These refer to size (membrane filtration), charge (electro dialysis, ion exchange, electrophoresis), affinity (pervaporation, reverse osmosis), vapor pressure (membrane distillation) and chemical nature of molecules (carrier mediated membrane processes). Thus, driving forces in membrane process can be either pressure gradient or concentration gradient or electric potential gradient or temperature gradient (Dutta, 2009; Mulder, 1996).

Membrane technology has emerged to be a very important separation process in various industries such as, food and beverage industries, industrial wastewater treatment, pharmaceutical industries, air purification and other allied industries (Issaoui and Limousy, 2019). While polymeric membrane systems are widely deployed, the commissioning of ceramic membranes is on the rise in many industrial installations. Compared to polymeric membranes, ceramic membranes are promising from the perspectives of their higher chemical and thermal stability, higher strength, lower maintenance issues, ease of operation and



TH-2589_156107040

scalability (Obada et al., 2017; Yang and Tsai, 2008). However, the primary drawback of ceramic membranes is with respect to their higher cost in comparison with polymeric membranes. Due to this reason, the application of ceramic membranes in industrial scale applications is restricted. To overcome this problem, low cost ceramic precursors can be used that enable a moderate reduction in sintering temperature and processing costs.

#### 1.2.3.1 Ceramic Membranes

With greater chemical resistance in comparison with the polymer membrane, ceramic membranes are becoming gradually popular for application in commercial separation operations. Thus, with better mechanical strength, higher flux and improved shelf life, ceramic membranes omit requirements associated to enhanced cleaning, module replacement and disposal of the used unit. Colloids, suspended solids, bacteria, algae, viruses, fungi and dissolved organics can be easily removed using ceramic membranes. A primary limitation of the ceramic membrane is with respect to its cost. Materials such as alumina and zirconia demand higher material cost as well as sintering temperature, which can be overcome by using cheaper materials such as clay, diatomaceous earth, etc. Due to ceramic membranes possessing higher pore size than the polymeric membranes, they can be deployed widely for size based separation. Therefore, to enhance better utility of ceramic membranes, cheaper materials with lower pore sizes are to be targeted using expensive materials such as clay.

#### 1.2.3.2 Applications of Ceramic Membranes

There are several applications of ceramic membranes in various process industries. Some of them are as listed below:

1. Waste water treatment such as treatment of oily waste waters, paper and pulp effluents and tannery waste waters.



TH-2589_156107040

2. Potable water production involving the separation of bacteria and other micro-organisms from contaminated water resources.
3. Juice Clarification and especially for mosambi, orange, pineapple and sugarcane juices.
4. Bio separation technologies targeting protein recovery, production of antibiotics and fat separation from milk.

### 1.2.4 Hybrid Process Technologies

The above mentioned technologies do have numerous applications in various food industries. Despite this, contemporary emphasis has also been given towards development of hybrid processes for vegetable juice and extract processing applications. In the field of membrane technology, hybrid MF-UF process and hybrid MF-centrifugation processes have received considerable attention by various research groups. Such hybrid processes offer promising performance due to better processing efficiency, high product quality, ease of separation/concentration and reduction or mitigation of membrane fouling characteristics. Among all these, the mitigation of fouling characteristics is by far the most important feature of a hybrid system that enables better shelf life of the membrane systems. The PhD thesis targets efficacy of hybrid UAE-MF process system with respect to improvising product quality and reducing membrane fouling characteristics. The hybrid processes are also relevant for systems in which non-juicy fruits/vegetables are to be processed. This is due to the reason that direct processing of juices from such sources is not possible. Thus, hybrid processes can be regarded to be much more beneficial to achieve juices and extracts from vegetables with better retention of phytochemicals.



TH-2589_156107040

## 1.3 Targeted Vegetable Juices and Extracts

Among the various available plant derivatives containing medicinal and nutritional properties, the thesis aim to target some highly valuable yet least explored species. This includes vegetables such as bottle gourd and bitter gourd.

Bottle gourd, *Lagenaria siceraria*, popular Asian vegetable in the *cucurbitaceae* family (Mashilo et al., 2017), is well known for its several health benefits. Bottle gourd juice have excellent medicinal applications to serve as an active ingredient to treat diseases such as diabetes mellitus, flatulence, diarrhea and liver diseases, cardiovascular diseases and hypertension in naturopathy and Ayurveda systems of medicine (Ghule et al., 2006). Due to these potential benefits, clarification of *Lagenaria siceraria* juice is often targeted.

Bitter gourd (*momordica charantia*), another organic and natural functional food is becoming popular due to its several health benefits (Habicht et al., 2011). Belonging to the Cucurbitaceae family and being cultivated in Asian, African and South American countries, bitter gourd possesses large quantities of bioactive compounds and hence indicates wider medicinal benefits (Krawinkel and Keding, 2006; Zhang et al., 2016). Typical bitter gourd constituents include proteins, terpenoids, alkaloids, saponins, flavonoids, amino acids, fatty acids and polysachharides, such as, antioxidants, neuroprotective compounds, antidiabetics, and antitumor compounds (Krawinkel and Keding, 2006; Sathishsekar and Subramanian, 2005; Yan et al., 2019). Given such functionally rich constitution, bitter gourd apart from culinary usage has been reported to have applications in food, health care and medicinal industries.



TH-2589_156107040

## 1.4 Prior Art

The Ph.D. thesis aims to target ceramic membrane applications for beverage processing scenarios. To enhance economic effectiveness of the ceramic membranes, low cost ceramic membranes are targeted in this work using organic pore former such as sawdust. Beverage processing applications targeted in this work refer to extraction and clarification of vegetable juices such as bottle gourd juice and bitter gourd extracts. These vegetable juices are becoming popular as nutritional supplements and ceramic membrane technology has not been investigated for these applications till date. Thus, the targeted prior art has been classified into the following sections namely:

a) Compositional optimization using of low cost ceramic membranes.
b) Fabrication of sawdust based low cost ceramic membranes (LCCM).
c) Microfiltration of vegetable juices using LCCM.
d) Ultrasound-assisted extraction of bioactive compounds.
e) Feasibility of membrane technology in hybrid juice processing systems.

A brief account of available state-of-the-art has been presented in the following sub-sections.

### 1.4.1 Compositional Optimization of Low Cost Ceramic Membranes

Conventionally, the identification of optimal precursor formulations during low cost ceramic membrane fabrication was based on a trial and error approach. Nandi et al. (2008) fabricated ceramic membranes using low cost precursors such as quartz (15 wt.%), kaolin (40 wt.%), calcium carbonate (25 wt.%), sodium carbonate (10 wt.%), sodium metasilicate (5 wt.%) and boric acid (5 wt.%) and variable sintering temperatures (850, 900, 950 and 1000 °C). Subsequently, using a trial and error approach, the authors identified optimal sintering temperature to be about 850 °C (Nandi et al., 2008). Similarly, along with additional feldspar (16 wt%), Nandi et al. (2009, 2010) considered an insignificant modification to other



TH-2589_156107040

precursor materials and thereby fabricated defect free ceramic membranes using the sintering process (Nandi et al., 2009; Nandi et al., 2010). Varying sintering temperatures from 900 – 1000 $^{o}$C, Vasanth et al. (2011) inferred that an appropriate combination of kaolin (50 wt.%), quartz (25 wt.%) and calcium carbonate (25 wt.%) precursors were appropriate to achieve microfiltration range low cost ceramic membranes. Later, the authors conducted microfiltration studies using the said ceramic membranes for the separation of oil-water emulsions and microbes from synthetic solution systems. The authors affirmed that the optimal sintering temperature is about 900 °C at which the pure water flux varied from $2 \times 10^{-4}$ – $10 \times 10^{-4}$ $m^3.m^{-2}.s^{-1}$ for a variation in pressure from 70 – 340 kPa (Vasanth et al., 2011). The trial and error based investigations of Emani et al. (2013) indicated a new inorganic precursor formulation (kaolin (40 wt.%), quartz (15 wt.%), sodium carbonate (10 wt.%), calcium carbonate (25 wt.%), sodium metasilicate (5 wt.%), boric acid (5 wt.%)) that can be mixed with 2 % polyvinyl alcohol (PVA) solution to thereby fabricate defect free low cost ceramic membranes. The authors adopted dry compaction method and regarded fabricated pressure as a variable (29 – 49 kPa). Thereafter, the membrnes were applied for fruit juice clarification studies (Emani et al., 2013). Kaniganti et al. (2015) fabricated ceramic membranes with low cost precursor materials such as kaolin, quartz, calcium carbonate, sodium carbonate, boric acid, sodium metasilicate and PVA and utilized the membranes for the microfiltration of bacteria solution (Kaniganti et al., 2015). On the other hand, Wei et al. (2016) targeted the utilization of both fly ash (70 – 100 wt.%) and calcium carbonate (0 – 30 wt.%) as membrane precursors to thereafter achieve disc shaped membranes by using 5 wt% PVA solution as an organic binder to the system. The authors varied sintering temperatures in the range of 1200 – 1350 °C during low cost ceramic membrane fabrication.

It can be observed that in most cases, due to easy availability and efficient pore formation, calcium carbonate was used as the pore forming agent. However, in preliminary



TH-2589_156107040

investigations conducted by our research group, it has been evaluated that these membranes had an inherent disadvantage in terms of carbonate leaching during microfiltration test runs which resulted in undesirable enhanced pH in the permeate sample. To circumvent this problem, the approach taken by Bose et al. (2013) could be relevant, as the authors used sawdust (10 – 30 wt.%) but not carbonates as pore former in due course of membrane fabrication. Other precursors used by the authors include kaolin (30 – 50 wt.%), quartz (0 – 30 wt.%) and feldspar (0 – 40 wt.%) (Bose and Das, 2013). The membrane sintering was carried out in the temperature range of 550 – 700 °C. The sawdust based membranes exhibited promising characteristics of mechanical strength (2 MPa), pore size (0.19 – 0.35 µm) and porosity (21 – 30 %). Hence, to avoid the problem associated to carbonate leaching in due course of microfiltration, sawdust is a very useful alternative low cost pore former. Table 1.1 summarizes some of the most competent literatures available for the fabrication of ceramic membranes.

Response Surface Methodology (RSM) is an optimization tool used to conduct detailed optimization of a process involving parametric as well as compositional optimization. The overall technique is easier, reasonably accurate and involves integrated simulation and experimental approach. The most commonly used RSM tool is the central composite design (CCD) that targets optimization of various process parameters or composition of few components.

Till date, very few research groups targeted RSM design methodology for ceramic membrane fabrication. Hubadillah et al. (2016) deployed historical data design (HDD) based response surface methodology to optimize process parameters in due course optimization. The authors varied sintering temperature (800 – 1200 °C), bore fluid flowrate (3 – 5 $mL.min^{-1}$) and metakaolin content (37.5 – 45 wt.%) to thereby determine their influence upon the mechanical strength of kaolin and tripolyphosphate based ceramic hollow fiber membranes



TH-2589_156107040

(Hubadillah et al., 2018). Suresh et al. (2016) employed central composite design (CCD) for the optimization of process variables (feed concentration and applied pressure) associated to optimality of flux and rejection. The authors deployed three distinct ceramic morphologies (1.36, 1.41 and 1.53 µm) (Suresh et al., 2016). With optimal process parameters of 97% rejection, $2.6 \times 10^{-4}$ $m^3.m^{-2}.s^{-1}$ flux at 345 kPa pressure and 176.07 mg/L feed concentration, the optimal membrane performance was inferred to correspond to that of the 1.36 µm membrane.

Supplemented with experimental investigation based membrane characterization parameters, Bose et al. (2014) conducted detailed investigations using CCD based RSM design with respect to optimality of binder (boric acid (4.21 – 10.79 wt.%) and sodium metasilicate (4.21 – 10.79 wt.%)) composition and fabrication pressure (7.23 – 12.39 MPa) in due course of ceramic membranes fabrication using kaolin, feldspar and sawdust (Bose and Das, 2014). Thereby, the authors inferred that for an optimal fabrication pressure of 9.81 MPa, the optimal precursor concentration corresponds to 7.5 wt.% for both sodium metasilicate and boric acid.

Using a CCD based RSM approach, Arzani et al. (2016) studied the alkali leaching of free silica on the porosity of ceramic membranes fabricated using raw kaolin at a sintering temperature of 1150 $^oC$ (Arzani et al., 2016). For a variation in leachant (NaOH) concentration of 15 – 30 wt%, 4 – 8 h of leaching time, 45 – 75 $^oC$ leaching temperature, the optimal membrane porosity was evaluated to be 49.4 % for an average membrane pore size of 1.79 µm.

A careful insight into CCD indicates that CCD fails in circumstances that require optimization of all components in a mixture due to interaction between raw materials effecting overall system performance. For such cases, mixture model designs are used. The



TH-2589_156107040

most common research field for the deployment of mixture model based RSM methodology is the pharmaceutical sector in which the optimization of each component of a drug formulation is desired. Few literatures indicated its relevance and competence. Furlanetto et al. (2011) utilized the mixture design approach to optimize formulations of microemulsions associated to lipophilic drug delivery (Furlanetto et al., 2011). El-Malah et al. (2006) investigated the effect of Carbopol, lactose and Polyox concentrations on the rate of release of thyophylline drug through the ternary matrix using D-optimal mixture model (El-Malah et al., 2006). Mura et al. (2005) also optimized the composition of glibenclamide tablet using the D-optimal mixture design (Mura et al., 2005). However, RSM based mixture design for ceramic membrane fabrication has not been targeted to achieve optimized membrane precursor compositions. Table 1.2 summarizes relevant literature data for the utility of RSM to achieve compositional optimization.

### 1.4.2 Fabrication of Sawdust based Low Cost Ceramic Membranes

Notable low cost precursors for ceramic membranes have been suggested to be natural clay, dolomite, kaolin, fly ash and apatite powder (Obada et al., 2017). Hence, compared to ceramic membranes prepared with expensive precursors such as alumina, sodium carbide and titania (Jeong et al., 2017; Lorente-Ayza et al., 2015), low cost ceramic membranes fabricated from materials such as clay shall have similar performance efficiency, mechanical, chemical and thermal stability but lower cost. The lower cost of clay based ceramic membranes is due to utilization of inexpensive precursors and lower sintering temperatures.



TH-2589_156107040

TH-2589_156107040



**Table 1.1: Compositional and morphological parametric data of low cost ceramic membranes.**

| S. No. | Membrane Precursor Materials | Membrane Properties | Applications | Authors |
|---|---|---|---|---|
| 1 | • Fly Ash (0 – 30 wt.%)<br>• Calcium Carbonate (0 – 30 wt.%)<br>• PVA (5 wt.%)<br>• Ethanol (rest) | • Porosity: 31 – 49.6 %<br>• Average Pore Size: 0.5 – 4.3 μm<br>• Flexural Strength: 90 MPa | NA | Wei et al. (2016) |
| 2 | • Kaolin (NA)<br>• Feldspar (NA)<br>• Sawdust (NA)<br>• Sodium Metasilicate (4.21 – 10.79 wt.%)<br>• Boric Acid (4.21 – 10.79 wt.%) | • Porosity: 21 %<br>• Flexural Strength: 2 MPa | NA | Bose et al. (2014) |
| 3 | • Kaolin (30 – 50 wt.%)<br>• Quartz (0 – 30 wt.%)<br>• Feldspar (0 – 40 wt.%)<br>• Sawdust (10 – 30 wt.%) | • Porosity: 34 %<br>• Average Pore Size: 0.13 μm<br>• Nitrogen Gas Permeability: $3.71\times10^{-3}$ $m^3.m^{-2}.s^{-1}.kPa^{-1}$ | NA | Bose et al. (2013) |
| 4 | • Kaolin (40 wt.%)<br>• Quartz (15 wt.%)<br>• Sodium Carbonate (10 wt.%)<br>• Calcium Carbonate (25 wt.%)<br>• Sodium Metasilicate (5 wt.%)<br>• Boric Acid (5 wt.%)<br>• Polyvinyl Alcohol (2 %) | • Porosity: 35.4 – 39.4 %<br>• Average Pore Size: 0.89 – 1.85 μm<br>• Flexural strength: 7.81 – 11 MPa | • Juice Clarification | Emani et al. (2013) |
| 5 | • Quartz (3 g)<br>• Kaolin (10 g)<br>• Sodium Carbonate (2 g)<br>• Feldspar (3 g)<br>• Sodium Metasilicate (1 g)<br>• Boric Acid (1 g)<br>• Distilled Water (7 g) | • Porosity: 23.6%<br>• Average Pore Size: 0.285 μm | • Juice Clarification<br>• Oily Wastewater Treatment | Nandi et al. (2009, 2010) |

TH-2589_156107040



**Table 1.2: Literature reported data summary of optimization software based best choice of composition and process parameters.**

| S. No. | Optimization Software | Parameters Optimized | Predicted optimal values from design | Optimal values obtained from experiments | Authors |
|---|---|---|---|---|---|
| 1 | Design Expert (RSM- Central Composite Design) | • Composition of NaOH solution (35 %)<br>• Leaching Time (8 h)<br>• Leaching Temperature (75 °C) | • Membrane Porosity: 49.4 % | • Membrane Porosity: 48.3 % | Arzani et al. (2016) |
| 2 | Design Expert (RSM-Central Composite Design) | • Composition of<br>  • Boric Acid (7.5 %)<br>  • Sodium Metasilicate (7.5 %)<br>• Fabrication pressure (9.81 MPa) | • Membrane Porosity: 20.59 %<br>• Flexural Strength: 11.55 MPa | • Membrane Porosity: 21 %<br>• Flexural Strength: 11.68 MPa | Bose et al. (2014) |
| 4 | NEMROD-W (D-optimal mixture design) | Composition of<br>• Tween 20 and Transcutol mixture (1:1, v/v) (78 %)<br>• Labrafac-hydro (5 %)<br>• Water (17 %) | • Dissolved Efficiency at<br>  • 30 °C: 10.30 %<br>  • 60 °C: 19.82 %<br>• Dissolved Percentage at<br>  • 30 °C: 22.41 %<br>  • 60 °C: 37.46 % | • Dissolved Efficiency at<br>  • 30 °C: 20.0 %<br>  • 60 °C: 30.1 %<br>• Dissolved Percentage at<br>  • 30 °C: 29.4 %<br>  • 60 °C: 53.2 % | Furlanetto et al. (2011) |
| 5 | Design Expert (D-optimal mixture design) | Composition of<br>• Carbopol (10.53 mg)<br>• Lactose (76.47 mg)<br>• Polyox (162.99 mg)<br>• Thyophylline (100 mg) | • Drug Release in<br>  • 2 h: 20.4 %<br>  • 4 h: 36 %<br>  • 6 h: 52.4 %<br>  • 8 h: 72.2 %<br>  • 12 h: 95.1 % | • Drug Release in<br>  • 2 h: 13.9 %<br>  • 4 h: 31.9 %<br>  • 6 h: 53.4 %<br>  • 8 h: 71.6 %<br>  • 12 h: 100 % | Malah et al. (2006) |
| 6 | NEMROD-W (D-optimal mixture design method) | Composition of<br>• Glibenclamide (6.25 %)<br>• Natrosol (2.5 %)<br>• Sorbitol (46.5 %)<br>• Stearic Acid (1.00 %)<br>• PVP (3.75 %) | • Relative enthalpy per unit mass: 40.99 J g−1 | Not reported | Mura et al. (2005) |

Using suitable pore forming agents, various alternate methods for fabricating ceramic membranes include combustion synthesis, freeze drying, gel casting, sintering, dry pressing, slip casting, isopressing and electrophoretic decomposition (Feng et al., 2013; Sarikaya and Dogan, 2013). Among these, sintering with an appropriate pore former is the simplest, easiest and most inexpensive fabrication process and hence is the most commonly deployed fabrication method (Nie et al., 2011).

A primary challenge during partial sintering is to achieve controllable or tailored pore size and porosity of the ceramic membranes using pore formers. The pore formers enable the formation of stable pores and also offer alternate options to enhance chemical stability. For example, $CaCO_3$ pore former may provide inexpensive membranes but may leach calcium as $Ca(OH)_2$ during microfiltration to potentially alter the permeate pH. Thereby, such membranes can be ineffective for the real application of low cost ceramic membranes to process moderately acidic feed systems such as fruit and vegetable juices. Therefore, appropriate pore former needs to be chosen from integrated perspectives of pore size, porosity and chemical stability of membranes as well as products such as clarified juices using low cost ceramic membranes.

During a sintering process, the pore formers being combustible materials, undergo decomposition or burning to create well defined pores (Haugen et al., 2018; Horri et al., 2012). Organic pore formers are usually selected based on the formation of minimum quantity of residual carbon due to oxidation and decomposition during sintering (Sarikaya and Dogan, 2013). In order to incorporate pores in the ceramic membrane structure, researchers till date adopted carbon based natural pore forming agents such as sawdust, starch, cotton, rice husk, poppy seeds, carbon fibers, wheat particles and natural polymers (Li and Li, 2007; Liu et al., 2016; Obada et al., 2017; Xavier et al., 2019). Gel casting, injection



TH-2589_156107040

moulding techniques are usually adopted to achieve porous structures through the addition of such pore formers in the ceramic membrane precursor mix. The quantity, shape and size of the pore forming agents strongly influence the desired combinations of pore size and porosity of the membranes (Horri et al., 2012). Therefore, customizing such pore forming agent parameters would enable a deeper understanding towards the desired characteristics of the ceramic membranes, including the membrane mechanical strength. In other words, research needs to target the optimality of pore forming agents in conjunction with low cost precursors to achieve low cost ceramic membranes by adopting inexpensive fabrication methods.

The available prior art in the field of organic and inorganic pyrolyzable pore formers for ceramic membrane fabrication indicates distinct and variegated characteristics in terms of average membrane pore size and porosity. Yang and Tsai (2008) used corn starch of particle size 53 µm (quantity 0 – 15 wt.%) as the pore forming agent along with other components such as alumina and bentonite to achieve ceramic membranes of pore size and porosity ranging from 1 – 2.1 µm and 23.44 – 43.96 %, respectively (Yang and Tsai, 2008). The use of potato starch as a pore former and its quantity varied form 0 – 30 wt.% was investigated by Ayza et al. (2015) and ceramic membranes with pore sizes ranging from 0.23 – 2.35 µm and porosities ranging from 44.9 – 67.3 % were achieved with kaolin and alumina being other components of the mixture (Lorente-Ayza et al., 2015). In another study, rice husk with particle size ranging from 75 – 600 µm was used as a pore forming agent along with sucrose and alumina to achieve membranes ceramic membranes possessing wider pore sizes (50 – 516 µm (horizontal length) and porosity (20 – 66 %) (Mohanta et al., 2014). In summary, depending verily upon the particle size and concentration of pore formers deployed to achieve desired combinations of average pore size and porosity, the wider combinations of membrane porosities (20 – 70 %) and average pore sizes (0.26 – 10.21 µm) can be achieved using organic pore formers (Lorente-Ayza et al., 2015; Lv et al., 2013; Mingyi et al., 2010;



TH-2589_156107040

**Table 1.3: Literature data summary of low cost pore former based ceramic membranes**

| S. No. | Pore Former | Other Components (wt.%) | Pore Size (µm) | Porosity (%) | Authors |
|---|---|---|---|---|---|
| 1 | Corn Starch<br>Quantity: 0-15 wt.%<br>Particle Size: 53 µm | Alumina: 75 – 90<br>Bentonite: 10 | 1 – 2.1 | 23.44 – 43.96 | Yang and Tsai, 2008 |
| 2 | Cationic manioc starch (CMS) grade Superion 300<br>Quantity: 0 – 15 wt.%<br>Particle Size: 23.26 µm | Egg Shell: 0 – 15<br>Water: 10<br>Natural Clay: 75 – 85 | – | 35.50 – 56.30 | Xavier et al., 2019 |
| 3 | Potato Starch<br>Quantity: 0 – 30 wt.% | Kaolin: 35 – 50<br>Alumina: 35 – 50 | 0.23 – 2.35 | 44.9 – 67.3 | Ayza et al., 2015 |
| 4 | Rice Husk<br>Quantity: 5 – 40 wt.%<br>Particle Size: 75 – 600 µm | Sucrose: 20<br>Alumina: 40 – 75 | Fine pores: 4<br>Interconnected Pores: 50 – 516 (length) | 20 – 66 | Mohanta et al., 2014 |

Mohanta et al., 2014; Obada et al., 2017; Sarikaya and Dogan, 2013; Xavier et al., 2019; Yang and Tsai, 2008). The inorganic pore former particle size could not be mostly controlled and only pore former concentration has a strong role to influence membrane porosity and pore size for such pore forming agents (Li et al., 2014; Li and Li, 2007; Mingyi et al., 2010). Table 1.3 summarizes the most appropriate literatures available for the fabrication low cost ceramic membrane.

It is apparent from the available prior art that the variation in pore sizes and porosities for alternate choices of pore formers, particle sizes and concentrations have been studied in few literature for ceramic membrane fabrication. It is apparent that for the case of natural low cost pore formers such as corn starch, potato starch, rice husk, etc., microfiltration membranes with larger pore sizes (0.23 – 4 µm) and wider porosities (20 – 67.3 %) were obtained.

### 1.4.3 Juice and Extract Microfiltration using Low Cost Ceramic Membranes

In the past decade, there has been a renewed and enhanced interest for further applications of membrane technology in food industries through the microfiltration and ultrafiltration of fruit



TH-2589_156107040

and vegetable juices (Cui and Muralidhara, 2010). In a membrane separation process, the product quality and process efficiency depends to a significant extent on the membrane pore size distributions, configurations and transmembrane pressures (TMP) used to carry out the separation. Therefore, many researchers attempt to identify optimal combination of pore sizes and TMPs to maximize membrane flux, minimize irreversible fouling and optimize product nutritional characteristics. Polysulfone (PS), polyethersulphone (PES) and polyvinylidene fluoride (PVDF) membranes with average pore sizes of 0.1 µm and 0.45 µm (for PS) and 0.3 µm (PES and PVDF) were considered to achieve very good retention of sugars from pineapple juice. The authors deployed two alternate geometries namely plate/frame and tubular modules in their investigations. Based on optimal combinations of flux and permeate characteristics, the authors opined that the optimal process system corresponds to 0.3 µm PES membrane being operated in a tubular geometry at 2 bar transmembrane pressure. Under these conditions, optimal permeate and sugar recovery have been obtained as 46.8 $L.m^{2}.h^{-1}$ and 81.32 % respectively (De Carvalho et al., 2008).

Using similar membranes (PVDF membranes with an average pore size of 0.22 and 0.45 µm), Mirsaeedghazi et al. 2010 conducted pomegranate juice clarification (Mirsaeedghazi et al., 2010). Compared to the higher average pore size membrane, significant flux decline (17 – 3 $L.m^{-2}.h^{-1}$) and flow resistances ($5 \times 10^{9}$ – $4.43 \times 10^{10}$ $m^{2}.kg^{-1}$) have been analyzed by the authors for the 0.22 µm membrane. Further, the lower pore size membrane enabled a product quality in terms of higher higher reduction in turbidity (484 – 3.21 NTU) and color (1.473 – 0.562) and TSS content (16.27 – 15.13 °Brix). In other words, membrane morphology and applied pressure can be analyzed to have profound influence on pertinent flux decline, irreversible fouling and product quality. Using 0.1 and 0.2 µm average pore size polymeric membranes, another research group carried out pineapple juice MF at an applied pressure of



TH-2589_156107040

1 bar. The authors inferred that the membrane with wider average pore size performed best in terms of flux, product quality and irreversible fouling (Laorko et al., 2010).

Compared to polymeric membranes investigated till date, the optimality of membrane morphology and applied pressure were not widely studied using ceramic membranes. Deploying ceramic membranes with larger average pore sizes (0.77 µm to 1.54 µm), Nandi et al. (2011) carried out mosambi juice clarification in the wider applied pressure range of 41.4 – 165.5 kPa (Nandi et al., 2011). Further, the authors also considered enzymatic pre-treatment for the said membranes to thereby infer that the ceramic membrane with an average pore size of 0.77 µm performed best in terms of very good characteristics associated to color (0.076) and clarity (94.39 %) of the microfiltration based clarified juice. Corresponding trans-membrane flux and applied pressure for the membrane have been evaluated to be $14.07 \times 10^{-6}$ – $60.64 \times 10^{-6}$ $m^3.m^{-2}.s^{-1}$ and 82.7 kPa.

Vladisavljevic et al. (2013) carried out raspberry juice clarification studies using various combinations of membrane materials, configurations and morphology (Vladisavljević et al., 2013). The authors deployed membranes with variant pore size characteristics. These include an ultrafiltration range inorganic tubular membrane possessing an average molecular weight cut off (MWCO) of 30 – 300 kDa, polysulfone hollow fiber ultrafiltration membrane with a MWCO of 30 kDa and a multichannel ceramic microfiltration membrane possessing an average pore size of 0.2 µm. Among the three deployed membranes, the ceramic membrane provided higher permeate flux of 170 $L.m^{-2}.h^{-1}$, higher pectin removal and complete recovery of TSS and citric acid.

Targeting clarification of lime juice, Jegatheesan at al. (2009) considered alternate membranes with variegated average pore sizes (Jegatheesan et al., 2009). Tubular ceramic membranes (0.02 – 0.1 µm variegated average pore size) were considered for wider applied



TH-2589_156107040

pressure range (1 – 3 bar). Among all investigated membranes, the authors inferred that the membrane with 0.1 µm average pore size performed optimally with higher trans-membrane flux of 64.2 $L.m^{-2}.h^{-1}$ at 3 bar applied pressure. However, based on severity of fouling, the authors indicated that the membrane with an average pore size of 0.05 µm is to be considered optimal. For all cases, the clarified lime juice quality was found to be similar.

Among several perishable vegetables, bottle gourd (*Lagenaria siceraria)* is well - known from the perspective of abundance, wider consumption and medicinal benefits. The vegetable has been classified to possess multiple vitamins, assists to prevent constipation, reduce weight, treats insomnia, maintains body pH and also acts as an antidote to certain poisons (Bhat and Sharma, 2016; Minocha, 2015; Mondal et al., 2016) The phytochemicals and bioactive constituents prevalent in bottle gourd enables the vegetable as an important source of nutrients. Mondal et al. (2016) deployed hollow fibre polymeric membranes (with an MWCO in the range of 42 – 127 kDa) for the comparative assessment of ultrafiltration and microfiltration technologies towards bottle gourd juice clarification. The authors reported that the microfiltration membrane process being operated at 104 kPa performed optimally in terms of very good product quality and minimum fouling. Under these conditions, a flux of 45 $L.m^{-2}.h^{-1}$ was achieved for a cross flow rate of 20 $L.h^{-1}$ (Mondal et al., 2016). Table 1.4 summarizes the work carried out by Mondal et al. (2016) for bottle gourd juice clarification using hollow fiber membranes. From a modeling perspective, it can be analyzed that during membrane filtration, the deposition of macromolecules on the surface or the membrane matrix may lead to the most critical issue of membrane fouling. In order to develop a better understanding of the fouling mechanism, researchers have proposed various mathematical expressions to describe the pore blocking behavior. Typically, there are four common mechanistic models available which includes standard pore blocking, intermediate pore blocking, complete pore blocking and cake filtration (Hermans and Bredée, 1935). Hermia



TH-2589_156107040

later modified the models for constant pressure dead end operation using power law models (Hermia, 1982). These models have been investigated significantly to understand the pertinent fouling characteristics (Almandoz et al., 2010; Bowen et al., 1995; Cassano et al., 2008; Li et al., 2018; Nandi et al., 2011; Suki et al., 1984). Alternatively, based on Darcy's Law, Bolton et al. (2006) developed more appropriate models to describe the fouling behavior and evaluate fouling coefficients associated to each model (Bolton et al., 2006). Till date, very few articles adopted models proposed by Bolton et al. (2006) in their investigations (Kim and DiGiano, 2009; Shi et al., 2019).

### 1.4.4 Ultrasound-assisted Extraction of Bioactive Compounds

The conventional methods associated with extraction suffer with the limitations of lower efficiency or extraction of desired bioactive constituents, longer extraction time and larger solvent consumption (Caldas et al., 2018; Li et al., 2013). A suitable modification to these approaches is to utilize hot solvents.

The utilization of hot solvents in such processes facilitates better extraction efficiency and reduces extraction time but suffers with the limitation of the product quality as bioactive constituents are heat sensitive and susceptible to chemical changes. To circumvent these issues, non-conventional extraction methods have been suggested. Except a few, several of these processing methods are expensive and non-scalable and among these, ultrasound–assisted extraction appears to be promising with moderate enhancement in processing cost and good scalability (Azmir et al., 2013).



TH-2589_156107040

TH-2589_156107040



**Table 1.4: Data summary of membrane based bottle gourd juice clarification studies.**

| Process | Parameters | | | | | | | | | | | | Literature |
|---|---|---|---|---|---|---|---|---|---|---|---|---|---|
| | Membrane Process | | | | | Permeate quality | | | | | | | |
| | Pore Size (µm) | Applied Pressure (kPa) | FRR | FDC | Protein Removal (%) | Constituents | Total Phenolics (mg GAE/100g) | Total Flavonoids (mg/100g) | Color (A) | Clarity (%T) | pH | Microbial Content (CFU/mL) | |
| Micro-filtration | 0.20 | 123 | — | — | 63.46 | Feed | 17.7 | — | 3.57 | 4.1 | 4.6 | NA | Mondal et al. (2016) |
| | | | | | | Permeate | 7.9 | — | 0.4 | 76.5 | 5.8 | NA | |
| Hybrid micro-filtration and ultra-filtration | 0.017 | 104 | 85 | 40 | 82.41 | Feed | 17.7 | — | 3.57 | 4.1 | 4.6 | NA | |
| | | | | | | Permeate | 3.9 | — | 0.14 | 94.8 | 4.7 | NA | |

Advances in food biochemistry and nutrition provided valuable insights with respect to antioxidants, phenolic compounds and proteins, all of which exist in abundance in plant extracts (Sasidharan et al., 2011). While antioxidants are instrumental to protect human body cells from free radicals generated oxidative stress and inhibit cellular and metabolic injury, accelerated ageing, cardiovascular diseases, cancer, and neurodegenerative diseases; phenolic compounds being secondary metabolites and a class of antioxidants as well reduce oxidative stress based free radical generation (Alberti et al., 2014; Kubola and Siriamornpun, 2008). On the other hand, proteins being the building blocks of human body contribute towards repair mechanisms associated to bones, muscles, skin and blood (Trumbo et al., 2002). Functional food products in aqueous media do not advocate on higher protein content, due to their detrimental role in enhanced food degradation and poisoning.

Till date, UAE has been successfully deployed for the extraction of bioactive compounds from various plants containing medically bioactive constituents such as tea (Bakht et al., 2018), purple sweet potatoes (Cai et al., 2016), blueberry (*Vaccinium ashei*) wine pomace (He et al., 2016), *Limonium sinuatum* (Xu et al., 2017), *Eclipta prostrate L* (Fang et al., 2014), grape pomace (Bonfigli et al., 2017), *Momordica charantia* (Sutanto et al., 2015), mulberry (*Morus nigra*) pulp (Espada-Bellido et al., 2017), *Lycium ruthenicum* Murr. Fruit (Chen et al., 2018), *Cassia auriculata* leaves (Sharmila et al., 2016), *Rheum moorcroftianum* (Pandey et al., 2018) and *Melissa officinalis L.* (Caleja et al., 2017).

In order to carry out efficient optimization of extraction parameters associated to a plant extraction process, statistical tools such as response surface methodology (RSM) may be utilized. Such an approach reduces the number of experiments, provides better data interpretation and assists to identify critical interaction amongst various parameters. In the vast field of food science and technology, RSM has been successfully used by researchers as an optimization tool to carefully and precisely optimize extraction processes (Gan and Latiff,



TH-2589_156107040

2011; Gong et al., 2012; Ilaiyaraja et al., 2015; Jiang et al., 2017). In the specific field of bioactive compounds extraction from plant resources, RSM has been applied in few investigations involving UAE (Chen et al., 2018; Deshaware et al., 2017; Fang et al., 2014; Pandey et al., 2018; Xu et al., 2015). For many such cases, typical solvent media deployed for extraction refer to water, methanol, ethanol, hexane, propane, $CO_2$, acetone, ethyl acetate and ionic liquids (Do et al., 2014; Kou et al., 2018; Pintać et al., 2018; Wang and Weller, 2006; Xu et al., 2015). While some of these solvents enable better extraction efficacies, they are toxic and harmful to human health. Hence, from cost, health and toxicity perspectives, among all solvents, water can be regarded as the ideal extractant.

Very few research groups targeted the extraction of bioactive constituents from bitter gourd vegetable. Kubola and Siriamornpun (2008) conducted hot water extraction by boiling the bitter gourd in water for 5 mins and indicated good antioxidant activity (53.24 ± 1.63) for an optimal vegetable to water concentration of 0.2 g/mL (Kubola and Siriamornpun, 2008).

**Table 1.5: Prior art data of bioactive compound extraction schemes from bitter gourd vegetable.**

| Extraction Process | Temperature (°C) | Time (min) | Concentration (g/mL) | Antioxidant Activity (%) | Total Phenolics (mg (GAE)/g) | Total Soluble Protein (mg/100 mL) | Literature |
|---|---|---|---|---|---|---|---|
| Boiling | NA | 5 | 0.2 | 53.9 ± 0.73 | 3.24 ± 1.63 | - | Kubola and Siriamornpun (2008) |
| UAE | 25 | 5 | 0.025 | 22 | 4.5 | - | Sutanto et. al. (2015) |
| Normal SLE | 65 | 5 | 0.025 | 19 | 3.7 | - | |



TH-2589_156107040

Sutanto et al. (2015) carried out a comparative study between UAE and solid - liquid extraction (SLE) for the recovery of antioxidants and total phenolics form bitter gourd. However, as compared to SLE, the performance of UAE was found to be better in terms of lower extraction temperature (25 °C) and better antioxidants (22 %) and total phenolics (4.5 mg (GAE)/g)) content in the extract (Sutanto et al., 2015). Table 1.5 summarizes the literatures available for extraction of bioactive compounds from bitter gourd.

### 1.4.5 Feasibility of Membrane Technology in Hybrid Horticultural Extract Production Process

A hybrid food processing system constitutes two or more conventional/non-conventional food processing technologies. The primary objective of such system is to enhance the quality of horticultural juices and extract production. Since the raw or fresh juice from such sources possess higher content of colloidal and suspended solid constituents, the clarification of such juice systems using microfiltration process technology is not promising due to higher degree of insitu fouling. Typically, such operations will involve clarification of juices/extracts from particles such that the size of such particles are larger than the membrane pores. To circumvent the issue of higher degree of fouling, certain pretreatment methods are followed prior to membrane separation. These pretreatment processes are very likely to involve either one or a combination of other thermal and non-thermal pretreatment processes such as enzymatic treatment, centrifugation, liming, extraction, adsorption, pasteurization or vacuum filtration (Tiwari et al., 2009). Following such pre - treatment step, the membrane process system can comprise of either one or combination of alternate membrane separation processes such as microfiltration, ultrafiltration, nanofiltration or reverse osmosis (Jegatheesan et al., 2009; Mondal et al., 2016; Pauer et al., 2013). On a large scale basis,



TH-2589_156107040

enzymatic treatment and centrifugation are familiar pre-treatment methods to supplement membrane process systems in due course of obtaining horticultural juice and extract products.

The available prior art in the field of membrane based hybrid process systems for horticultural juice and extract products is affirming that very few research groups have focused on the said area of research. Machado et al. (2012) and Laorko et al. (2013) adopted enzymatic treatment using Ultrazym® AFPL and pectinase enzymes followed with microfiltration based clarification to produce better quality açaí pulp and pineapple juice, respectively. Similar investigations have been carried out by Cassano et al. (2008, 2009). The authors adopted pectinase based enzymatic treatment and subsequent ultrafiltration based clarification to produce better quality kiwifruit and clementine mandarin juices (Cassano et al., 2008; Cassano et al., 2009; Laorko et al., 2013; Machado et al., 2012). On the other hand, enzymatic treatment followed with a combination of microfiltration and ultrafiltration was reported by De Carvalho et al. (2008) and Laorko et al. (2010). The authors respectively utilized Ultrazym 100G and pectinase enzymes for the treatment of pineapple juice and targeted a comparative assessment of enzymatic treatment with the microfiltration process (De Carvalho et al., 2008; Laorko et al., 2010). The authors identified best combinations of process parameters based on the retention and rejection of juice constituents, membrane fouling and flux decline characteristics.

The efficacy of centrifugation as an effective pre-treatment process was reported by the literature to remove colloidal particles prior to membrane filtration for the production of better quality kiwi juice, crude pineapple waste extracts and soy extracts (Nor et al., 2015; Pauer et al., 2013; Qin et al., 2015). A combination of enzymatic treatment, centrifugation and microfiltration process have been targeted by Nandi et al. (2009, 2011) and Emani et al. (2013) for the clarification of mosambi juice (Emani et al., 2013; Nandi et al., 2009; Nandi et al., 2011). Based on their investigations, the authors recommended enzymatic treatment



TH-2589_156107040

followed with centrifugation as the most effective step to enhance the product quality and mitigate membrane fouling characteristics. The product quality was also evaluated to enhance significantly in terms of color and clarity of the juice. Few research groups targeted liming followed with membrane filtration for the clarification of sugarcane juices (Jegatheesan et al., 2009; Li et al., 2018; Shi et al., 2019). These articles affirmed that liming followed with subsequent heating of the juice system enabled removal of impurities prevalent in the raw juice system through the principles of coagulation and precipitation. For the membrane filtration process, pre-treatment using rotary vacuum filtration was investigated by Almandoz et al. (2010) for the clarification of corn syrup. The authors used diatomaceous earth and activated carbon to considerably reduce the turbidity of the raw syrup (Almandoz et al., 2010). In another investigation, adsorption using zirconia pellets was used as a pretreatment process to reduce unstable proteins prevalent in the raw wine system. Thereafter, microfiltration based clarification enabled achievement of both enhanced quality of the final wine product and enhanced permeate flux of the membrane system (Salazar et al., 2007).

Apart from the above mentioned pretreatment processes, a combination of various membrane filtration processes (microfiltration/ultrafiltration and ultrafiltration/nanofiltration) have also been deployed successfully to improve juice clarity and enhance concentration of desired essential nutrients in sugarcane juice, soy extracts and bottle gourd vegetable juice systems (Jegatheesan et al., 2009; Mondal et al., 2016; Pauer et al., 2013).

On the other hand, for the case of fruits, leafy and few other vegetables and seeds, juice could not be produced directly using juicers and blenders. For such cases, extraction is deployed as a viable process technology to recover important and essential phytochemicals from such horticultural produces. Few investigations report upon the efficacy of extraction processes for various horticultural produces. Balyan et al. (2016) used a simple distillation process for the aqueous extraction of bioactive compounds from jamun seed powder. Thereafter, the authors



TH-2589_156107040

clarified and concentrated the extracts using a combination of ultrafiltration and nanofiltration processes respectively (Balyan and Sarkar, 2016). Similarly, Jain et al. (2018) deployed solid – liquid extraction (SLE) process as a pre-treatment process to enable the microfiltration membrane technology based extraction of essential nutrients from bitter gourd vegetable. Using the hybrid process, the authors attempted to improve and refine the quality of the aqueous vegetable extract (Jain et al., 2018). The optimal hybrid SLE-MF configuration enabled the production of high quality clarified bitter gourd extract in terms of higher polyphenol content, appropriate protein content, enhanced combinations of color (0.07 – 0.19 A) and clarity (77.97 – 86.01 %), maximum flux decline ratio of 64% at a trans-membrane pressure of 173 kPa. However, the authors utilized hollow fiber polymeric membranes but not low cost ceramic membranes. Thereby, the overall cost of juice processing is expected to be high.

A summary of the relevant data for the vegetable juice/extraction system targeted in this work has been presented in Table 1.6 (a) and (b). This refers to the data reported by Jain et al. (2018). In summary, the available prior art with respect to existing process hybrid process technologies for horticultural juice/extract production affirm that hybrid processes are beneficial to enhance the quality of juice or extracts. Thereby, they are bound to gain considerable interest for commercial application in the juice and beverage industries in the near future.

For the chosen bitter gourd vegetable in the PhD thesis, the primary emphasis is upon the maximization of the extraction of bioactive compounds from the said vegetable using ultrasound assisted extraction (UAE) process. Compared to the solid-liquid extraction process, the UAE has better performance in terms of enhanced extraction of bioactive compounds.



TH-2589_156107040

**Table 1.6: Literature reported data of bitter gourd juice extract produced with conventional extraction-membrane hybrid process (a) feed and permeate characteristics, and (b) process parameters**

| S. No. | Parameters | Feed | Permeate |
|---|---|---|---|
| 1 | Proteins (mg/L) | 171.2 ± 6.8 | 104.6 – 137.0 |
| 2 | Polyphenols (mg GAE/100 mL) | 22.1 ± 2.4 | 10.6 – 14.5 |
| 3 | Color (A) | 0.85 ± 0.07 | 0.07 – 0.19 |
| 4 | Clarity (% T) | 35.71 ± 3.4 | 77.97 – 86.01 |

**(a)**

| S. No. | Process Parameters | | | |
|---|---|---|---|---|
| | Extraction | | Membrane Filtration | |
| 1 | Time (min) | 95 | Membrane Material | Hollow fiber polyacrylonitrile polymeric membranes |
| 2 | Temperature (°C) | 68 | Trans-membrane Pressure (kPa) | 35 – 173 |
| 3 | Concentration (g/mL) | 0.48 | Cross Flow Rate (L/h) | 10 - 30 |

**(b)**

Thus, the hybrid UAE-MF system is anticipated to serve better than the solid liquid extraction - MF hybrid system. Further details of the UAE process efficacy have been presented in the earlier sections of the thesis. Thereby, the UAE-MF hybrid process is anticipated to enhance the extract quality and improve efficiency of the overall process.

## 1.5 Research Gaps

Based on the literature review discussed in the previous section, the following lacunae have been identified.



TH-2589_156107040

### 1.5.1 MMD Based Compositional Optimization of Saw Dust based Low Cost Ceramic Membranes

From literature survey, it has been observed that organic pore former enable variation in pore sizes and porosities of the membranes (Lorente-Ayza et al., 2015; Lv et al., 2013; Mingyi et al., 2010; Mohanta et al., 2014; Obada et al., 2017; Sarikaya and Dogan, 2013; Xavier et al., 2019; Yang and Tsai, 2008). Literature affirms that membranes with wider pore size distributions (0.26 – 10.21 μm) can be achieved through the deployment of pore formers of higher particle size (7.43 – 600 μm) and concentration (5 – 40 wt.%).

Bose et al. (2013) optimized the composition of sawdust based membrane using trial and error method. The authors generated few experimental data sets and considered binder optimality in the precursor materials (Bose and Das, 2013). While studying the effect of binder constituents, Bose et al. (2014) optimized the composition of binders viz. boric acid and sodium metasilicate and fabrication pressure using RSM. In other words, the authors did not consider the optimization of other components (Bose and Das, 2014). Precisely, the investigation did not emphasize upon detailed optimization of other membrane precursors (such as kaolin, feldspar and sawdust) to achieve optimal combinations of pore size, porosity and flexural strength.

Also, in the chosen field of RSM design methodology based optimal fabrication of low cost ceramic membranes, only few research groups contributed (Arzani et al., 2016; Bose and Das, 2014; Hubadillah et al., 2018). Among these, it can be observed that the design methodology adopted by the authors referred to either CCD or HDD. While these design methodologies are effective to identify optimal parameters in relevant case studies, they do have limitations in comparison with the mixture model design (MMD) methodology. It is well known that HDD design methodology involves manual setting of design runs and data



TH-2589_156107040

sets and hence limitations of human intellect via trial and error methodology may restrict further insights into the identification of optimal parameter set. Further, a comparison between MMD and CCD approaches for membrane precursor composition optimization indicates that MMD has greater flexibility to vary compositions within a maximum total precursor composition which is not the case for CCD. In other words, MMD offers greater flexibility to systematically identify optimal precursor formulations in comparison with CCD.

Considering these important lacunae namely due consideration of sawdust based ceramic membrane complete compositional optimization and deployment of mixture model based RSM approach, the first major gap in the literature can be addressed to obtain useful insights into the role of compositional optimality in influencing sawdust based LCCM fabrication. The competence of D-optimal mixture design can be as well understood to achieve desired combinations of optimal responses for optimized precursor composition.

### 1.5.2 Fabrication of sub-micron range LCCM

It is also well known that many microfiltration applications require lower pore sizes and hence the application of such membranes reported in the literature are confined to specific feedstocks and concentrations. To enhance the applicability of low cost ceramic membranes in beverage processing applications such as vegetable juice clarification, it is necessary to significantly reduce pore size and achieve membranes within the sub-micron range average pore size value. Natural organic pore formers such as sawdust are to be utilized.

The available prior art affirms that sawdust based LCCM fabrication has not been targeted from the perspective of sub-micron range average pore size achievement through the alternation of sawdust average particle size and concentration. The existing literature confines towards the utilization of few pore formers such as potato starch to achieve sub-micron range



TH-2589_156107040

ceramic membranes. However, it is well known that potato starch is considerably expensive when compared to sawdust. Also, it shall be noted that the literature refers to utilization of rice husk as organic pore former, but ceramic membranes with significantly higher average pore size (50 µm) have been achieved. Hence, sub-micron range ceramic membrane fabrication was not effectively addressed in the available prior art using waste materials such as sawdust. In summary, the influence of sawdust average particle size and porosity are to be studied so as to achieve sub-micron range LCCM.

### 1.5.3 Vegetable Juice Clarification using Low Cost Ceramic Membranes

Available literature focused extensively towards optimality of membrane morphology and TMP for polymeric membranes for fruit juice clarification. Few literatures also provided similar methodologies for ceramic membrane based fruit juice clarification. Only one literature focused towards bottle gourd vegetable juice clarification and with polymeric membranes. Ceramic membranes have not been investigated till date for clarification of vegetable juices such as bottle gourd juice. Also, model based irreversible and reversible fouling analysis was targeted by many research groups to identify optimality of feedstock using Hermia fouling models. For few cases, the alternate Bolton models were deployed. However, detailed fouling assessment was missing along with the role of ceramic membrane morphology influencing the permeate quality and fouling characteristics. In summary, despite greater utility of polymeric membranes for juice processing application, due to several limitations associated with the polymeric membranes in terms of higher fouling and narrow pore sizes, ceramic membranes can suite better the needs of commercial and industrial juice processing. In other words, given the significant surge in development of nutritional beverages using vegetable juices such as bottle gourd juice, ceramic membrane clarification



TH-2589_156107040

research needs to be extended to gain useful insights into optimality of membrane morphologies, feed stock alternatives and TMPs.

### 1.5.4 Ultrasound-assisted Vegetable Extraction of Bioactive Compounds

The RSM based UAE of bitter gourd has not been investigated till date and the available niche data indicates poor quality of extraction from the perspective of the UAE. Kubola et al. optimized the UAE process for bitter gourd extraction, however, they did not optimize the temperature and time of extraction. The concentration was also optimized with trial and error method instead of using any superior optimization tool. Sutanto et al. (2015) conducted UAE using water as extractant using trial and error method (Sutanto et al., 2015). However, the advantage of using RSM over trial and error method is significant, since, RSM is a statistical tool which provides a better understanding of the interactions between various independent variables in terms of desired results (maximization or minimization) of the output variables. Hence, the optimized results produced by RSM may be devoid of experimental design immaturity and could be more appropriate in terms of parametric optimality and associated reduction in process costs. Considering RSM based UAE of bitter gourd using aqueous extractant as the central objective, this work targets the evaluation of the effect of control variables (such as time of extraction, extraction temperature and bitter gourd to water ratio) on the optimality of desired combinations of bioactive constituent concentrations (maximum concentrations of antioxidant activity and polyphenols and minimum concentration of proteins) in the extract phase during UAE plant extraction process. Central composite design (CCD) based RSM can be deployed to design the experiments for model development and optimization of process variables.



TH-2589_156107040

### 1.5.5 Efficacy of Ceramic Membrane - Sonication Hybrid Extraction process

The extensive literature survey reported in the PhD thesis in the field of hybrid process systems for horticultural extract production have clearly demonstrated upon its prominence. However, it is to be noted that most literature dealt with common pretreatment processes such as centrifugation and enzymatic treatment. Research investigations that focused towards the combination of extraction and membrane filtration are scarce. Also, conventional solid - liquid extraction and heating have been reported as prior pre-treatment steps in the literature. Contemporary importance on advanced extraction methods emphasizes upon the utilization of ultrasound assisted extraction process. This has not been explored till date in the context of hybrid juice processing system. Also, hybrid processing of bitter gourd, a prominent vegetable to serve as a nutritional and medicinal supplement has not been given much attention in the food/agro processing sector. Till date, only one literature (Jain et al. (2018)) has addressed the vegetable processing using a hybrid system. However, the process requires a matured outlook in terms of juice quality (enhanced content of nutritional constituents in the extract) and better storage indicators (with minimal protein content) (Jain et al., 2018). In summary, despite considering a hybrid system to achieve clarified bitter gourd juice extract, the authors (Jain et al (2018)) deployed a simple solid-liquid extraction system but not the ultrasound assisted extraction process. The UAE system is well known to provide enhanced extraction efficacy in comparison with the solid-liquid extraction process. Thus, addressing such lacunae in the only available literature in the field of study, hybrid system efficacy needs to target the combination of UAE-MF process using a low cost ceramic membrane system. Thereby, better extract product characteristics can be achieved.



TH-2589_156107040

## 1.6 Objectives of the Ph.D. Thesis

The overall objective of the thesis is to develop a suitable technology for vegetable juice processing. To attain the overall objective, membrane filtration and ultra-sonication techniques have been investigated and optimality of process characteristics were targeted. Firstly, low cost ceramic membranes with green pore former were prepared. Microfiltration of bottle gourd was than carried out varying the process parameters and membrane pore sizes. Further, ultrasound-assisted bitter gourd juice extraction was carried out so as to optimize the extraction of bioactive compounds prevalent in the vegetable using water as extracting phase. To further optimize the extract quality, hybrid membrane process involving a combination of microfiltration and sonication have been targeted. Considering these broad directives, the objectives of the thesis have been set as follows:

a. RSM based optimization of sawdust based precursor composition to achieve optimal low cost ceramic membranes.
b. Investigation on structural changes in ceramic membranes based on variation in sawdust pore former particle size and concentration.
c. Optimization of microfiltration process for the production of market compatible bottle gourd juice using low cost ceramic membranes with due consideration of fouling characteristics.
d. RSM based ultrasound assisted extraction of bioactive compounds from bitter gourd.
e. Hybrid UAE-Microfiltration process for refining of bitter gourd extract

## 1.7 Organization of the Thesis

In this section, a short description of the chapters in the PhD thesis is being presented in the following paragraphs.



TH-2589_156107040

Chapter 2 summarizes materials and methods that were adopted to carry out the PhD thesis. These are (a) materials required to carry out the thesis work, (b) procedure adopted for the fabrication of sawdust based low cost ceramic membranes, (c) theoretical analysis of techniques deployed for compositional optimization using RSM, (d) procedures and theoretical methodologies associated to microfiltration of bottle gourd juices and ultrasound assisted bitter gourd juice extracts, (e) analytical methods followed to determine the physico-chemical properties as well as nutrient analysis of juice samples, and (f) ultrasound assisted extraction process deployed for bioactive constituents extraction from bitter gourd juice.

Chapter 3 addresses the relevance of D-optimal mixture model based RSM design methodology for the optimal fabrication of sawdust based low cost ceramic membranes. The RSM design methodology has been validated by targeting alterations in the composition of kaolin, feldspar and sawdust precursors in due course of low cost ceramic membrane fabrication. Experimental findings of key dependent membrane product variables namely average pore size, average porosity and flexural strength have been regarded as biases to identify optimal kaolin, feldspar and sawdust precursor compositions. Further, a comparative study has also been conducted to evaluate upon the sensitivity of optimal compositions with respect to consideration of flexural strength as a response variable.

Chapter 4 addresses the effect of pore former (sawdust) characteristics on the properties (pore size and porosity) of low cost ceramic membranes. Two approaches were followed to effectively reduce the pore size. Firstly, the pore size reduction was targeted through the variation of sawdust concentration in the overall membrane precursor formulation and lowest achievable pore size was determined. Thereafter, further reduction in the pore size has been targeted through the reduction of average particle size of the sawdust precursor. While porosity was determined using the Archimedes' principle, pure water experiments conducted under dead-end filtration mode enabled the determination of average membrane pore size. An



TH-2589_156107040

empirical model has been as well developed to quantify the variation of average pore size and porosity on the average particle size and concentration of the sawdust precursor.

Chapter 5 targets the application of kaolin based low cost ceramic micro-filtration membrane (average porosity and pore size of 1 μm and 28.47 % respectively) for bottle gourd juice clarification. The treatment has been carried out at different trans-membrane pressures (103.4 - 172.4 kPa) and with two types of juice samples (fresh juice and centrifuged juice). In addition to pertinent flux decline, feed and permeate quality has also been evaluated in terms of nutritional content (carbohydrate content, protein content, vitamin C content, total flavonoids and total phenol content) and physico-chemical parameters (pH, salt content, TDS, color and clarity).

Chapter 6 addresses the combinatorial optimality of membrane morphology and process parameters during dead-end microfiltration of bottle gourd juice. Sawdust and kaolin based low cost ceramic membranes with varied morphology were considered to evaluate their microfiltration performance. Fresh, paper filtered and centrifuged juice samples were considered along with trans-membrane pressure differential variation for the chosen membranes. Combinatorial optimality was based on flux decline trends, fitness of fouling models, irreversible and reversible fouling data, irreversible permeation resistance and nutritional analysis of the permeate samples. An interesting feature of this work is with respect to feed constitution playing a critical role in influencing the optimal choice of membrane morphology and transmembrane pressure differentials.

Chapter 7 presents the ultrasound-assisted extraction of antioxidants, total phenolics and soluble proteins from bitter gourd (*momordica charantia*). For comparative purposes, two modes of sonications, namely, normal and pulsed mode have been considered and the



TH-2589_156107040

response variables have been evaluated as a function of temperature, extraction time and vegetable to water ratio using response surface methodology based design of experiments.

Chapter 8 elaborates upon the findings of the hybrid UAE-MF system for the production of better quality bitter gourd extract product. The extract obtained with best choice of UAE system process parameters has been considered as feed to the MF system. The carried out investigations targeted identification of optimal membrane morphology and trans-membrane pressure differential parameters for the maximization of desired nutritional characteristics and minimized protein content in the juice samples. Also, fouling characteristics of the flux decline data of the MF system has also been addressed and the obtained results have been detailed in this regard.

Chapter 9 summarizes notable conclusions of the work reported in the PhD Thesis. Following this, a brief overview of future research perspectives has been presented.

## References

1. Alberti, A., Zielinski, A.A.F., Zardo, D.M., Demiate, I.M., Nogueira, A., Mafra, L.I., 2014. Optimisation of the extraction of phenolic compounds from apples using response surface methodology. Food Chemistry 149, 151-158.
2. Almandoz, C., Pagliero, C., Ochoa, A., Marchese, J., 2010. Corn syrup clarification by microfiltration with ceramic membranes. Journal of Membrane Science 363, 87-95.
3. Arzani, M., Mahdavi, H.R., Bakhtiari, O., Mohammadi, T., 2016. Preparation of mullite ceramic microfilter membranes using Response surface methodology based on central composite design. Ceramics International 42, 8155-8164.



TH-2589_156107040

4. Azmir, J., Zaidul, I., Rahman, M., Sharif, K., Mohamed, A., Sahena, F., Jahurul, M., Ghafoor, K., Norulaini, N., Omar, A., 2013. Techniques for extraction of bioactive compounds from plant materials: A review. Journal of Food Engineering 117, 426-436.
5. Bakht, M.A., Geesi, M.H., Riadi, Y., Imran, M., Ali, M.I., Ahsan, M.J., Ajmal, N., 2018. Ultrasound-assisted extraction of some branded tea: Optimization based on polyphenol content, antioxidant potential and thermodynamic study. Saudi Journal of Biological Sciences.
6. Balyan, U., Sarkar, B., 2016. Integrated membrane process for purification and concentration of aqueous *Syzygium cumini* (L.) seed extract. Food and Bioproducts Processing 98, 29-43.
7. Barbalho, S.M., Farinazzi-Machado, F., de Alvares Goulart, R., Brunnati, A.C.S., Otoboni, A., Ottoboni, B., 2012. *Psidium guajava* (Guava): A plant of multipurpose medicinal applications. Medicinal and Aromatic Plants 1, 2167-0412.1000104.
8. Bhat, S., Sharma, H.K., 2016. Combined effect of blanching and sonication on quality parameters of bottle gourd (*Lagenaria siceraria*) juice. Ultrasonics Sonochemistry 33, 182-189.
9. Bolton, G., LaCasse, D., Kuriyel, R., 2006. Combined models of membrane fouling: development and application to microfiltration and ultrafiltration of biological fluids. Journal of Membrane Science 277, 75-84.
10. Bonfigli, M., Godoy, E., Reinheimer, M.A., Scenna, N.J., 2017. Comparison between conventional and ultrasound-assisted techniques for extraction of anthocyanins from grape pomace. Experimental results and mathematical modeling. Journal of Food Engineering 207, 56-72.
11. Bose, S., Das, C., 2013. Preparation and characterization of low cost tubular ceramic support membranes using sawdust as a pore-former. Materials Letters 110, 152-155.



TH-2589_156107040

12. Bose, S., Das, C., 2014. Role of binder and preparation pressure in tubular ceramic membrane processing: design and optimization study using response surface methodology (RSM). Industrial & Engineering Chemistry Research 53, 12319-12329.
13. Bowen, W., Calvo, J., Hernandez, A., 1995. Steps of membrane blocking in flux decline during protein microfiltration. Journal of Membrane Science 101, 153-165.
14. Cai, Z., Qu, Z., Lan, Y., Zhao, S., Ma, X., Wan, Q., Jing, P., Li, P., 2016. Conventional, ultrasound-assisted, and accelerated-solvent extractions of anthocyanins from purple sweet potatoes. Food Chemistry 197, 266-272.
15. Caldas, T.W., Mazza, K.E., Teles, A.S., Mattos, G.N., Brígida, A.I.S., Conte-Junior, C.A., Borguini, R.G., Godoy, R.L., Cabral, L.M., Tonon, R.V., 2018. Phenolic compounds recovery from grape skin using conventional and non-conventional extraction methods. Industrial Crops and Products 111, 86-91.
16. Caleja, C., Barros, L., Prieto, M., Barreiro, M.F., Oliveira, M.B.P., Ferreira, I.C., 2017. Extraction of rosmarinic acid from *Melissa officinalis* L. by heat-, microwave-and ultrasound-assisted extraction techniques: A comparative study through response surface analysis. Separation and Purification Technology 186, 297-308.
17. Cassano, A., Donato, L., Conidi, C., Drioli, E., 2008. Recovery of bioactive compounds in kiwifruit juice by ultrafiltration. Innovative Food Science & Emerging Technologies 9, 556-562.
18. Cassano, A., Tasselli, F., Conidi, C., Drioli, E., 2009. Ultrafiltration of Clementine mandarin juice by hollow fibre membranes. Desalination 241, 302-308.
19. Chemat, F., Rombaut, N., Sicaire, A.-G., Meullemiestre, A., Fabiano-Tixier, A.-S., Abert-Vian, M., 2017. Ultrasound assisted extraction of food and natural products. Mechanisms, techniques, combinations, protocols and applications. A review. Ultrasonics sonochemistry 34, 540-560.



TH-2589_156107040

20. Chen, S., Zeng, Z., Hu, N., Bai, B., Wang, H., Suo, Y., 2018. Simultaneous optimization of the ultrasound-assisted extraction for phenolic compounds content and antioxidant activity of *Lycium ruthenicum* Murr. fruit using response surface methodology. Food Chemistry 242, 1-8.
21. Cui, Z., Muralidhara, H., 2010. Membrane technology: a practical guide to membrane technology and applications in food and bioprocessing. Elsevier.
22. De Carvalho, L.M.J., De Castro, I.M., Da Silva, C.A.B., 2008. A study of retention of sugars in the process of clarification of pineapple juice (*Ananas comosus*, L. Merril) by micro-and ultra-filtration. Journal of food engineering 87, 447-454.
23. Deshaware, S., Gupta, S., Singhal, R.S., Variyar, P.S., 2017. Enhancing anti-diabetic potential of bitter gourd juice using pectinase: a response surface methodology approach. LWT 86, 514-522.
24. Do, Q.D., Angkawijaya, A.E., Tran-Nguyen, P.L., Huynh, L.H., Soetaredjo, F.E., Ismadji, S., Ju, Y.-H., 2014. Effect of extraction solvent on total phenol content, total flavonoid content, and antioxidant activity of *Limnophila aromatica*. Journal of Food and Drug Analysis 22, 296-302.
25. Dutta, B.K., 2009. Principles of mass transfer and separation processes. The Canadian Journal of Chemical Engineering 87, 818-819.
26. El-Malah, Y., Nazzal, S., Khanfar, N.M., 2006. D-optimal mixture design: optimization of ternary matrix blends for controlled zero-order drug release from oral dosage forms. Drug Development and Industrial Pharmacy 32, 1207-1218.
27. Emani, S., Uppaluri, R., Purkait, M.K., 2013. Preparation and characterization of low cost ceramic membranes for mosambi juice clarification. Desalination 317, 32-40.
28. Espada-Bellido, E., Ferreiro-González, M., Carrera, C., Palma, M., Barroso, C.G., Barbero, G.F., 2017. Optimization of the ultrasound-assisted extraction of anthocyanins



TH-2589_156107040

and total phenolic compounds in mulberry (*Morus nigra*) pulp. Food Chemistry 219, 23-32.

29. Fang, X., Wang, J., Wang, Y., Li, X., Zhou, H., Zhu, L., 2014. Optimization of ultrasonic-assisted extraction of wedelolactone and antioxidant polyphenols from *Eclipta prostrate* L using response surface methodology. Separation and Purification Technology 138, 55-64.
30. Feng, Y., Wang, K., Yao, J., Webley, P.A., Smart, S., Wang, H., 2013. Effect of the addition of polyvinylpyrrolidone as a pore-former on microstructure and mechanical strength of porous alumina ceramics. Ceramics International 39, 7551-7556.
31. Furlanetto, S., Cirri, M., Piepel, G., Mennini, N., Mura, P., 2011. Mixture experiment methods in the development and optimization of microemulsion formulations. Journal of Pharmaceutical and Biomedical Analysis 55, 610-617.
32. Gan, C.-Y., Latiff, A.A., 2011. Optimisation of the solvent extraction of bioactive compounds from *Parkia speciosa* pod using response surface methodology. Food Chemistry 124, 1277-1283.
33. Ghule, B., Ghante, M., Saoji, A., Yeole, P., 2006. Hypolipidemic and antihyperlipidemic effects of *Lagenaria siceraria* (Mol.) fruit extracts.
34. Gong, Y., Hou, Z., Gao, Y., Xue, Y., Liu, X., Liu, G., 2012. Optimization of extraction parameters of bioactive components from defatted marigold (*Tagetes erecta* L.) residue using response surface methodology. Food and Bioproducts Processing 90, 9-16.
35. Grampp, E., Schmitt, R., Urlaub, R., 1978. Method for clarification of fruit juice. Google Patents.
36. Habicht, S.D., Kind, V., Rudloff, S., Borsch, C., Mueller, A.S., Pallauf, J., Yang, R.-y., Krawinkel, M.B., 2011. Quantification of antidiabetic extracts and compounds in bitter gourd varieties. Food Chemistry 126, 172-176.



TH-2589_156107040

37. Haugen, A., Geffroy, A., Kaiser, A., Gil, V., 2018. MgO as a non-pyrolyzable pore former in porous membrane supports. Journal of the European Ceramic Society 38, 3279-3285.
38. He, B., Zhang, L.-L., Yue, X.-Y., Liang, J., Jiang, J., Gao, X.-L., Yue, P.-X., 2016. Optimization of ultrasound-assisted extraction of phenolic compounds and anthocyanins from blueberry (*Vaccinium ashei*) wine pomace. Food Chemistry 204, 70-76.
39. Heldman, D.R., Hartel, R.W., 1999. Pasteurization and blanching, Principles of food processing. Springer, pp. 34-54.
40. Hermans, P., Bredée, H., 1935. Zur kenntnis der filtrationsgesetze. Recueil des Travaux Chimiques des Pays-Bas 54, 680-700.
41. Hermia, J., 1982. Constant pressure blocking filtration laws-application to power-law non-Newtonian fluids. Chemical Engineering Research and Design 60, 183-187.
42. Horri, B.A., Selomulya, C., Wang, H., 2012. Characteristics of Ni/YSZ ceramic anode prepared using carbon microspheres as a pore former. International Journal of Hydrogen Energy 37, 15311-15319.
43. Hubadillah, S.K., Othman, M.H.D., Matsuura, T., Ismail, A., Rahman, M.A., Harun, Z., Jaafar, J., Nomura, M., 2018. Fabrications and applications of low cost ceramic membrane from kaolin: A comprehensive review. Ceramics International 44, 4538-4560.
44. Ilaiyaraja, N., Likhith, K., Babu, G.S., Khanum, F., 2015. Optimisation of extraction of bioactive compounds from *Feronia limonia* (wood apple) fruit using response surface methodology (RSM). Food Chemistry 173, 348-354.
45. Issaoui, M., Limousy, L., 2019. Low-cost ceramic membranes: Synthesis, classifications, and applications. Comptes Rendus Chimie 22, 175-187.



TH-2589_156107040

46. Jain, A., Sengupta, S., De, S., 2018. Fundamental understanding of fouling mechanisms during microfiltration of bitter gourd (*Momordica charantia*) extract and their dependence on operating conditions. Food and Bioprocess Technology 11, 1012-1026.
47. Jegatheesan, V., Phong, D., Shu, L., Aim, R.B., 2009. Performance of ceramic micro-and ultrafiltration membranes treating limed and partially clarified sugar cane juice. Journal of Membrane Science 327, 69-77.
48. Jeong, Y., Lee, S., Hong, S., Park, C., 2017. Preparation, characterization and application of low-cost pyrophyllite-alumina composite ceramic membranes for treating low-strength domestic wastewater. Journal of Membrane Science 536, 108-115.
49. Jiang, H.-L., Yang, J.-L., Shi, Y.-P., 2017. Optimization of ultrasonic cell grinder extraction of anthocyanins from blueberry using response surface methodology. Ultrasonics Sonochemistry 34, 325-331.
50. Jiménez-Sánchez, C., Lozano-Sánchez, J., Segura-Carretero, A., Fernández-Gutiérrez, A., 2017. Alternatives to conventional thermal treatments in fruit-juice processing. Part 1: Techniques and applications. Critical Reviews in Food Science and Nutrition 57, 501-523.
51. Kaniganti, C.M., Emani, S., Thorat, P., Uppaluri, R., 2015. Microfiltration of synthetic bacteria solution using low cost ceramic membranes. Separation Science and Technology 50, 121-135.
52. Kim, J., DiGiano, F.A., 2009. Fouling models for low-pressure membrane systems. Separation and Purification Technology 68, 293-304.
53. Kou, X., Ke, Y., Wang, X., Rahman, M.R.T., Xie, Y., Chen, S., Wang, H., 2018. Simultaneous extraction of hydrophobic and hydrophilic bioactive compounds from ginger (*Zingiber officinale* Roscoe). Food Chemistry 257, 223-229.



TH-2589_156107040

54. Krawinkel, M.B., Keding, G.B., 2006. Bitter gourd (*Momordica charantia*): a dietary approach to hyperglycemia. Nutrition Reviews 64, 331-337.

55. Kubde, M.S., Khadabadi, S., Farooqui, I., Deore, S., 2010. *Lagenaria siceraria*: phytochemistry, pharmacognosy and pharmacological studies. Report and Opinion 2, 91-98.

56. Kubola, J., Siriamornpun, S., 2008. Phenolic contents and antioxidant activities of bitter gourd (*Momordica charantia* L.) leaf, stem and fruit fraction extracts in vitro. Food Chemistry 110, 881-890.

57. Laily, N., Kusumaningtyas, R.W., Sukarti, I., Rini, M., 2015. The potency of guava *Psidium guajava* (L.) leaves as a Functional immunostimulatory ingredient. Procedia Chemistry 14, 301-307.

58. Laorko, A., Li, Z., Tongchitpakdee, S., Chantachum, S., Youravong, W., 2010. Effect of membrane property and operating conditions on phytochemical properties and permeate flux during clarification of pineapple juice. Journal of Food Engineering 100, 514-521.

59. Laorko, A., Tongchitpakdee, S., Youravong, W., 2013. Storage quality of pineapple juice non-thermally pasteurized and clarified by microfiltration. Journal of Food Engineering 116, 554-561.

60. Li, D., Qu, Y., Liu, J., He, W., Wang, H., Feng, Y., 2014. Using ammonium bicarbonate as pore former in activated carbon catalyst layer to enhance performance of air cathode microbial fuel cell. Journal of Power Sources 272, 909-914.

61. Li, S., Li, N., 2007. Effects of composition and temperature on porosity and pore size distribution of porous ceramics prepared from Al $(OH)_3$ and kaolinite gangue. Ceramics International 33, 551-556.



TH-2589_156107040

62. Li, W., Ling, G., Lei, F., Li, N., Peng, W., Li, K., Lu, H., Hang, F., Zhang, Y., 2018. Ceramic membrane fouling and cleaning during ultrafiltration of limed sugarcane juice. Separation and Purification Technology 190, 9-24.
63. Li, Y., Fabiano-Tixier, A.S., Vian, M.A., Chemat, F., 2013. Solvent-free microwave extraction of bioactive compounds provides a tool for green analytical chemistry. TrAC Trends in Analytical Chemistry 47, 1-11.
64. Liu, J., Li, Y., Li, Y., Sang, S., Li, S., 2016. Effects of pore structure on thermal conductivity and strength of alumina porous ceramics using carbon black as pore-forming agent. Ceramics International 42, 8221-8228.
65. Lorente-Ayza, M.M., Sánchez, E., Sanz, V., Mestre, S., 2015. Influence of starch content on the properties of low-cost microfiltration ceramic membranes. Ceramics International 41, 13064-13073.
66. Lucas, E.A., Dumancas, G.G., Smith, B.J., Clarke, S.L., Arjmandi, B.H., 2010. Health benefits of bitter melon (*Momordica charantia*), Bioactive Foods in Promoting Health. Elsevier, pp. 525-549.
67. Lv, X., Li, Z., Zhu, Y., Zhao, J., Zhao, G., 2013. Effect of PMMA pore former on microstructure and mechanical properties of vitrified bond CBN grinding wheels. Ceramics International 39, 1893-1899.
68. Machado, R.M.D., Haneda, R.N., Trevisan, B.P., Fontes, S.R., 2012. Effect of enzymatic treatment on the cross-flow microfiltration of açaí pulp: Analysis of the fouling and recovery of phytochemicals. Journal of Food Engineering 113, 442-452.
69. Mashilo, J., Shimelis, H., Odindo, A., 2017. Phenotypic and genotypic characterization of bottle gourd [*Lagenaria siceraria* (Molina) Standl.] and implications for breeding: A Review. Scientia Horticulturae 222, 136-144.
70. Mason, T.J., 1996. Advances in sonochemistry. Elsevier.



TH-2589_156107040

71. Mingyi, L., Bo, Y., Jingming, X., Jing, C., 2010. Influence of pore formers on physical properties and microstructures of supporting cathodes of solid oxide electrolysis cells. International journal of hydrogen energy 35, 2670-2674.
72. Minocha, S., 2015. An overview on *Lagenaria siceraria* (bottle gourd). Journal of Biomedical and Pharmaceutical Research 4, 4-10.
73. Mirsaeedghazi, H., Emam-Djomeh, Z., Mousavi, S.M., Aroujalian, A., Navidbakhsh, M., 2010. Clarification of pomegranate juice by microfiltration with PVDF membranes. Desalination 264, 243-248.
74. Mohanta, K., Kumar, A., Parkash, O., Kumar, D., 2014. Processing and properties of low cost macroporous alumina ceramics with tailored porosity and pore size fabricated using rice husk and sucrose. Journal of the European Ceramic Society 34, 2401-2412.
75. Mondal, M., Biswas, P.P., De, S., 2016. Clarification and storage study of bottle gourd (*Lagenaria siceraria*) juice by hollow fiber ultrafiltration. Food and Bioproducts Processing 100, 1-15.
76. Mújica-Paz, H., Valdez-Fragoso, A., Samson, C.T., Welti-Chanes, J., Torres, J.A., 2011. High-pressure processing technologies for the pasteurization and sterilization of foods. Food and Bioprocess Technology 4, 969.
77. Mulder, M., 1996. Basic Principles of Membrane Technology, Kluwer Academic Publishers, Boston, USA.
78. Mura, P., Furlanetto, S., Cirri, M., Maestrelli, F., Marras, A., Pinzauti, S., 2005. Optimization of glibenclamide tablet composition through the combined use of differential scanning calorimetry and D-optimal mixture experimental design. Journal of Pharmaceutical and Biomedical Analysis 37, 65-71.
79. Nandi, B., Das, B., Uppaluri, R., Purkait, M., 2009. Microfiltration of mosambi juice using low cost ceramic membrane. Journal of Food Engineering 95, 597-605.



TH-2589_156107040

80. Nandi, B., Moparthi, A., Uppaluri, R., Purkait, M., 2010. Treatment of oily wastewater using low cost ceramic membrane: comparative assessment of pore blocking and artificial neural network models. Chemical Engineering Research and Design 88, 881-892.
81. Nandi, B., Uppaluri, R., Purkait, M., 2008. Preparation and characterization of low cost ceramic membranes for micro-filtration applications. Applied Clay Science 42, 102-110.
82. Nandi, B., Uppaluri, R., Purkait, M., 2011. Identification of optimal membrane morphological parameters during microfiltration of mosambi juice using low cost ceramic membranes. LWT-Food Science and Technology 44, 214-223.
83. Nie, L., Liu, J., Zhang, Y., Liu, M., 2011. Effects of pore formers on microstructure and performance of cathode membranes for solid oxide fuel cells. Journal of Power Sources 196, 9975-9979.
84. Nor, M., Ramchandran, L., Duke, M., Vasiljevic, T., 2015. Characteristic properties of crude pineapple waste extract for bromelain purification by membrane processing. Journal of Food Science and Technology 52, 7103-7112.
85. Obada, D.O., Dodoo-Arhin, D., Dauda, M., Anafi, F.O., Ahmed, A.S., Ajayi, O.A., 2017. Physico-mechanical and gas permeability characteristics of kaolin based ceramic membranes prepared with a new pore-forming agent. Applied Clay Science 150, 175-183.
86. Pandey, A., Belwal, T., Sekar, K.C., Bhatt, I.D., Rawal, R.S., 2018. Optimization of ultrasonic-assisted extraction (UAE) of phenolics and antioxidant compounds from rhizomes of *Rheum moorcroftianum* using response surface methodology (RSM). Industrial Crops and Products 119, 218-225.
87. Pauer, V., Csefalvay, E., Mizsey, P., 2013. Treatment of soy bean process water using hybrid processes. Central European Journal of Chemistry 11, 46-56.



TH-2589_156107040

88. Pintać, D., Majkić, T., Torović, L., Orčić, D., Beara, I., Simin, N., Mimica–Dukić, N., Lesjak, M., 2018. Solvent selection for efficient extraction of bioactive compounds from grape pomace. Industrial Crops and Products 111, 379-390.
89. Poole, C., 2009. Handbook of methods and instrumentation in separation science. Academic Press.
90. Qin, G., Lü, X., Wei, W., Li, J., Cui, R., Hu, S., 2015. Microfiltration of kiwifruit juice and fouling mechanism using fly-ash-based ceramic membranes. Food and Bioproducts Processing 96, 278-284.
91. Rahman, A.H., 2003. Bottle gourd (*Lagenaria siceraria*) a vegetable for good health. Natural Product Radiance 2, 249-250.
92. Ravi, U., Menon, L., Aruna, M., Jananni, B., 2010. Development of orange-white pumpkin crush and analysis of its physicochemical, nutritional and sensory properties. American-Eurasian Journal Agriculture and Environmental Science 8, 44-49.
93. Rawson, A., Patras, A., Tiwari, B., Noci, F., Koutchma, T., Brunton, N., 2011. Effect of thermal and non thermal processing technologies on the bioactive content of exotic fruits and their products: Review of recent advances. Food Research International 44, 1875-1887.
94. Salazar, F., De Bruijn, J., Seminario, L., Güell, C., López, F., 2007. Improvement of wine crossflow microfiltration by a new hybrid process. Journal of Food Engineering 79, 1329-1336.
95. Sarikaya, A., Dogan, F., 2013. Effect of various pore formers on the microstructural development of tape-cast porous ceramics. Ceramics International 39, 403-413.
96. Sasidharan, S., Chen, Y., Saravanan, D., Sundram, K., Latha, L.Y., 2011. Extraction, isolation and characterization of bioactive compounds from plants' extracts. African Journal of Traditional, Complementary and Alternative Medicines 8.



TH-2589_156107040

97. Sathishsekar, D., Subramanian, S., 2005. Antioxidant properties of *Momordica Charantia* (bitter gourd) seeds on Streptozotocin induced diabetic rats. Asia Pacific Journal of Clinical Nutrition 14, 153.

98. Shah, B., Seth, A., Desai, R., 2010. Phytopharmacological profile of *Lagenaria siceraria*: a review. Asian Journal of Plant Sciences 9, 152.

99. Sharma, H., Van Sumere, C., 1992. Enzyme treatment of flax. Genetic Engineering and Biotechnology News 12, 19-23.

100. Sharma, S., Puri, R., Jain, A., Sharma, M., Sharma, A., Bohra, S., Gupta, Y., Saraya, A., Dwivedi, S., Gupta, K., 2012. Assessment of effects on health due to consumption of bitter bottle gourd (*Lagenaria siceraria*) juice. The Indian Journal of Medical Research 135, 49.

101. Sharmila, G., Nikitha, V., Ilaiyarasi, S., Dhivya, K., Rajasekar, V., Kumar, N.M., Muthukumaran, K., Muthukumaran, C., 2016. Ultrasound assisted extraction of total phenolics from *Cassia auriculata* leaves and evaluation of its antioxidant activities. Industrial Crops and Products 84, 13-21.

102. Shi, C., Rackemann, D.W., Moghaddam, L., Wei, B., Li, K., Lu, H., Xie, C., Hang, F., Doherty, W.O., 2019. Ceramic membrane filtration of factory sugarcane juice: Effect of pretreatment on permeate flux, juice quality and fouling. Journal of Food Engineering 243, 101-113.

103. Shrivastava, R., AK, B., 2018. *Nyctanthes arbortristis* an Important Medicinal Plant of Madhya Pradesh State: A Review. UK Journal of Pharmaceutical and Biosciences 6, 10-15.

104. Singh, A., Vyas, B., 2018. Night Jasmine (*Nyctanthes arbortristis*). Research Journal of Pharmacognosy and Phytochemistry 10, 324-330.



TH-2589_156107040

105. Stephenson, F., 2016. Chapter 12—Centrifugation. Calculations for Molecular Biology and Biotechnology (Third Edition); Stephenson, FH, Ed, 431-438.

106. Suki, A., Fane, A., Fell, C., 1984. Flux decline in protein ultrafiltration. Journal of Membrane Science 21, 269-283.

107. Suresh, K., Pugazhenthi, G., Uppaluri, R., 2016. Fly ash based ceramic microfiltration membranes for oil-water emulsion treatment: Parametric optimization using response surface methodology. Journal of Water Process Engineering 13, 27-43.

108. Sutanto, H., Himawan, E., Kusumocahyo, S.P., 2015. Ultrasound assisted extraction of bitter gourd fruit (*Momordica charantia*) and vacuum evaporation to concentrate the extract. Procedia Chemistry 16, 251-257.

109. Tan, S.P., Kha, T.C., Parks, S.E., Roach, P.D., 2016. Bitter melon (*Momordica charantia* L.) bioactive composition and health benefits: A review. Food Reviews International 32, 181-202.

110. Tarazona-Díaz, M.P., Aguayo, E., 2013. Influence of acidification, pasteurization, centrifugation and storage time and temperature on watermelon juice quality. Journal of the Science of Food and Agriculture 93, 3863-3869.

111. Tiwari, B., O'donnell, C., Cullen, P., 2009. Effect of non thermal processing technologies on the anthocyanin content of fruit juices. Trends in Food Science & Technology 20, 137-145.

112. Trumbo, P., Schlicker, S., Yates, A.A., Poos, M., 2002. Dietary reference intakes for energy, carbohdrate, fiber, fat, fatty acids, cholesterol, protein and amino acids. Journal of the Academy of Nutrition and Dietetics 102, 1621.

113. Urošević, T., Povrenović, D., Vukosavljević, P., Urošević, I., Stevanović, S., 2017. Recent developments in microfiltration and ultrafiltration of fruit juices. Food and Bioproducts Processing 106, 147-161.



TH-2589_156107040

114. Vasanth, D., Pugazhenthi, G., Uppaluri, R., 2011. Fabrication and properties of low cost ceramic microfiltration membranes for separation of oil and bacteria from its solution. Journal of Membrane Science 379, 154-163.

115. Vladisavljević, G.T., Vukosavljević, P., Veljović, M.S., 2013. Clarification of red raspberry juice using microfiltration with gas backwashing: A viable strategy to maximize permeate flux and minimize a loss of anthocyanins. Food and Bioproducts Processing 91, 473-480.

116. Wang, L., Weller, C.L., 2006. Recent advances in extraction of nutraceuticals from plants. Trends in Food Science & Technology 17, 300-312.

117. Wang, L.K., Chang, S.-Y., Hung, Y.-T., Muralidhara, H., Chauhan, S.P., 2007. Centrifugation clarification and thickening, Biosolids Treatment Processes. Springer, pp. 101-134.

118. Wang, Z., Cui, H., Fan, S., 2020. Effect of mechanical juice extraction method on the quality of fresh-squeezed apple juice, IOP Conference Series: Materials Science and Engineering. IOP Publishing, p. 012051.

119. Xavier, L.A., de Oliveira, T.V., Klitzke, W., Mariano, A.B., Eiras, D., Vieira, R.B., 2019. Influence of thermally modified clays and inexpensive pore-generating and strength improving agents on the properties of porous ceramic membrane. Applied Clay Science 168, 260-268.

120. Xu, D.-P., Zheng, J., Zhou, Y., Li, Y., Li, S., Li, H.-B., 2017. Ultrasound-assisted extraction of natural antioxidants from the flower of Limonium sinuatum: Optimization and comparison with conventional methods. Food Chemistry 217, 552-559.

121. Xu, J., Wang, W., Liang, H., Zhang, Q., Li, Q., 2015. Optimization of ionic liquid based ultrasonic assisted extraction of antioxidant compounds from Curcuma longa L. using response surface methodology. Industrial Crops and Products 76, 487-493.



TH-2589_156107040

122. Yadav, M., Jain, S., Tomar, R., Prasad, G., Yadav, H., 2010. Medicinal and biological potential of pumpkin: an updated review. Nutrition Research Reviews 23, 184-190.

123. Yan, J.-K., Wu, L.-X., Qiao, Z.-R., Cai, W.-D., Ma, H., 2019. Effect of different drying methods on the product quality and bioactive polysaccharides of bitter gourd (*Momordica charantia* L.) slices. Food Chemistry 271, 588-596.

124. Yang, G.C., Tsai, C.-M., 2008. Effects of starch addition on characteristics of tubular porous ceramic membrane substrates. Desalination 233, 129-136.

125. Zhang, F., Lin, L., Xie, J., 2016. A mini-review of chemical and biological properties of polysaccharides from *Momordica charantia*. International Journal of Biological Macromolecules 92, 246-253.



TH-2589_156107040

TH-2589_156107040

# Chapter 2:

## Materials and Methods

TH-2589_156107040

TH-2589_156107040

# Materials and Methods

*This chapter summarizes relevant materials and adopted methods in the PhD thesis. These are (a) materials required to carry out the thesis work, (b) procedure associated with the fabrication of sawdust based low cost ceramic membranes, (c) theoretical approaches deployed for compositional optimization using Response Surface Methodology (RSM), (d) procedures and theory associated with the microfiltration of bottle gourd juices and ultrasound assisted bitter gourd juice extracts, and (e) analytical methods that were followed to evaluate the physico-chemical and nutritional parameters of the juice and extract samples.*

## 2.1 Materials

Several precursors have been procured to fabricate sawdust based low cost ceramic membranes. Sodium metasilicate nonahydrate (95 % pure) and kaolin powder (pure) were purchased from Central Drug House (P) Ltd., New Delhi, India; feldspar was acquired from National Chemicals, Gujarat, India; boric acid (99.5 % pure) was provided by Merck India. Waste wood flakes collected from local furniture shops were grounded to produce sawdust. For the analysis of nutritional parameters of vegetable juice and extract samples, sodium hydroxide pellets, sodium hypochlorite solution, oxalic acid dehydrate, sodium carbonate, aluminium chloride anhydrous, sucrose, sodium nitrite sulfuric acid (98%); Anthrone extrapure and 2, 6-dichlorophenol indophenol sodium salt (DCPIP) were purchased from SRL Pvt. Ltd., India; sodium bicarbonate was procured from Rankem, India; L-Ascorbic acid, gallic acid monohydrate and Folin-Ciocalteu phenol reagent were obtained from Sigma-Aldrich, USA. Quercetin Dihydrate (extrapure) and Bovine Serum Albumin (BSA) were

TH-2589_156107040

procured from SRL, India and Bradford Reagent was obtained from Abcam, India. Fresh bottle and bitter gourds were purchased from regional vegetable vendors.

## 2.2 Methodology

### 2.2.1 Microfiltration Experiments

#### 2.2.1.1 Membrane Fabrication

After grinding wooden flakes in mixer grinder, the sawdust was sieved through 75, 150 and 355 µm mesh sieves and also crushed using nano ball mill. The obtained sawdust was then mixed with adequate quantities of kaolin, feldspar, boric acid and sodium metasilicate using mixer grinder for 5 min. Thereafter, the mixture was placed in a membrane mould and was pressed using hydraulic press (Make: Velan Engineering, Tamilnadu, India) at 100 kgf/cm$^2$ pressure for 2 mins. The disc-shaped green membrane thus obtained was subjected to drying at room temperature at 24 h followed with drying at 100 $^o$C for 12 h and 250 $^o$C for 24 h. Finally, the sample was then finally sintered at 850$^o$C for 6 h. The heat treatments were carried out in muffle furnace. Thereafter, the samples were allowed to cool to reach room temperature by switching off the furnace (Bose and Das, 2013). Thermal characterization data being presented in the relevant prior art (Bose and Das (2013) and, Bose and Das (2014)) confirms upon the relevance of saw dust as a pore forming agent. During sintering of the saw dust, the authors opined that four major steps sequentially constitute its decomposition. These are moisture removal, hemicellulose decomposition, cellulose decomposition and lignin decomposition. Further, tradeoffs associated with respect to thermal decomposition of other raw materials and the precursor mixture for membrane fabrication with a similar composition in the reported prior art affirmed thermal stability of the pore former at the appropriate sintering temperature of 850 °C. Hence, the saw dust pore former can be inferred to be highly



TH-2589_156107040

stable and relevant towards its efficacy as a useful pore forming agent for the fabrication of kaolin based low cost ceramic membranes (Bose and Das, 2013, 2014). The fabricated low cost ceramic membranes (LCCM) were subjected to average porosity, average hydraulic permeability and flexural strength tests.

#### 2.2.1.2 Design of Experiments (DOE)

The optimization of the membrane precursor concentration was carried out using the D-Optimal mixture design. The software used for the purpose was Design Expert 7.0.0. The membranes were prepared using precursors such as: kaolin, feldspar, sawdust, boric acid and sodium metasilicate. Among these five precursors, only the concentration of kaolin, feldspar and sawdust were targeted for their optimality using mixture model design towards desired combinations of pore size, porosity and flexural strength. This is due to the fact that the binder composition (boric acid and sodium metasilicate) was optimized a priori (Bose and Das, 2014). Using RSM design expert software, optimized responses refer to average porosity, average pore size and flexural strength.

A primary advantage to conduct mixture DOE for the membrane composition is to set flexible constraints in the entire composition range. This indicates that if the concentrations of individual precursors are expressed as a fraction or percentage, they can be varied such that the total concentration can be varied between 1 and 100 %. A one-level, 3 parameter D-Optimal design was employed for the present study. Due to this reason, the RSM involved a total of 16 runs with 6 model points. Among these, 5 points were used to estimate lack of fit and five points were considered to replicate points. A generalized expression to express responses as a function of input parameters is usually represented as:

$$Y = f(X_1\ X_2\ X_3\ X_4\ X_5,\ldots\ldots X_n,) \quad (2.1)$$



TH-2589_156107040

For the RSM study involving compositional variation of kaolin, feldspar and sawdust, the maximum and minimum level of parameters were set as follows: 40 and 60 wt.% for kaolin; 20 and 30 wt.% for feldspar and 5 and 15 wt.% for sawdust. Thereby, the constraint for the total composition of these three constituents was set as 85 wt.%. In other words, the optimization involved fixed choice of other two constituents in the inorganic precursor mixture (7.5 wt.% boric acid and 7.5 wt.% sodium metasilicate)

The RSM study involved a two-step hierarchy. The first step involved optimization of raw material composition (kaolin, feldspar and sawdust) by considering average pore size and porosity as the response variables. In the second step, using the data generated from the software, further optimization was conducted by considering flexural strength as an additional response variable in addition to average pore size and porosity. Eventually, the optimized compositions from both approaches have been compared to determine upon the sensitivity of optimal compositional variations with respect to flexural strength.

#### 2.2.1.3 Membrane Characterization

***Porosity***

The porosity of the membranes were determined has been evaluated using Archimedes' Principle. Firstly, this involved measuring the dry weight of the membranes. Following this, the specimens were kept in de-ionized water for 24 h. The wet weight of the membrane was then noted by wiping off excess water from the membrane surface using tissue paper. Assuming cylindrical pores, the average porosity of the membrane was evaluated using the expression (Bose and Das, 2013):

$$\varepsilon_m = \frac{(w_2 - w_1)/\rho_w}{\pi \times (d_m/2)^2 \times T} \tag{2.2}$$



TH-2589_156107040

where, $\varepsilon_m$ is the volumetric porosity of the membrane; $w_2$ and $w_1$ are weights of wet membrane and dry membrane, respectively; $\rho_w$ is the density of water and $\pi \times (d_m / 2)^2 \times T$ is the volume of the membrane disc with thickness T.

***Average Pore Size***

In order to determine the hydraulic permeability and eventually average pore size of ceramic membranes, an indigenous permeability setup was utilized which consists of three openings namely a water/permeate inlet, a water/permeate outlet, and an opening to connect the pressure gauge and air compressor (Figure 2.1). Through the regulation of the compressor, the pressure inside the setup was varied. The membrane permeation module has two sections. While the top section is used to hold water, the bottom portion holds the fabricated membrane through which dead-end filtration was conducted. Prior to an experimental run, after enclosing the membrane, both sections of the module were connected using nut and bolt system. Silicon gaskets were used to ensure leak proof operation during a test run. To load the membrane, firstly, a circular gasket with perforations was kept in the membrane slot. The circular membrane was then placed above the gasket. Two other gaskets having a big circular hole (just smaller than the membrane diameter) were placed one above the other. After assembling the setup gas tight, water was filled in the setup and pressure was applied to check the system for prevalent leakages (Kaniganti et al., 2015).

Prior to the permeability tests, the membranes were subjected to compaction. Such experimentation involved the identification of the onset stage of the compaction. This was ensured by analyzing that a constant time duration existed to discharge an entire volume of water held in the indigenous experimental setup.



TH-2589_156107040

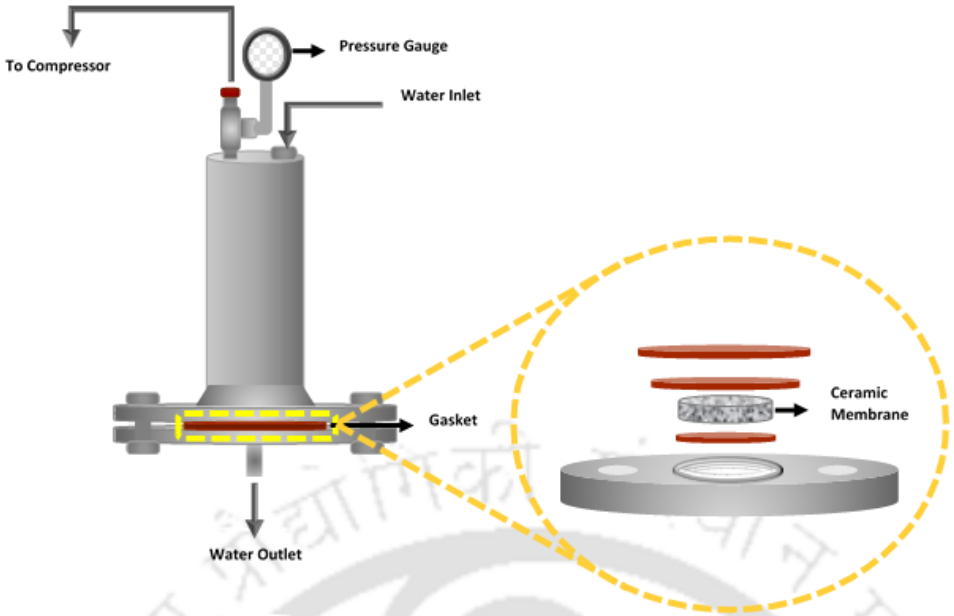


**Figure 2.1: Indigenous lab-scale membrane permeation setup.**

After compaction, the hydraulic permeability study was conducted for the compacted membranes. Thereby, the setup was completely filled with deionized water and totally avoid membrane fouling. Different pressures have been applied (viz., 103.4, 137.9 and 172.4 kPa) and the time required to discharge entire holdup water volume from the experimental setup were noted. Eventually, the average water flux was evaluated as the ratio of volume discharged per unit area and time (Nandi et al., 2009).

$$J_w = \frac{V}{A \times t} \tag{2.3}$$

where, $J_w$, $V$, $A$ and $t$ are pure water flux, discharged water volume, effective membrane area and time required for holdup water volume to get completely discharged, respectively.

Using the measured data, a graph was prepared between pure water flux and transmembrane pressure and the slope of the graph corresponds to hydraulic membrane permeability, i.e.,.

$$L_m = J_w / \Delta P \tag{2.4}$$



TH-2589_156107040

where, $L_m$ and $\Delta P$ are hydraulic permeability and applied pressure, respectively.

The average pore size of the membrane was determined using the expression:

$$d_p = \frac{8 \times \eta_w \times T \times L_m}{\varepsilon} \tag{2.5}$$

where, $d_p$, $\eta_w$ and $T$ are average membrane pore size, viscosity of water and membrane thickness respectively.

***Flexural Strength***

Three-point bend test method was deployed to determine the flexural strength (measured in MPa) of membrane specimens (55 mm × 30 mm × 5 mm) by using Universal Testing Machine (Model: 8801J4051; Make: Instron, UK). To do so, the circular discs were cut as rectangular slabs and the slabs were subsequently placed between two extreme noses of the bending setup. Thereby, a third nose was pressed on the center line of the slabs such that a fracture develops on the slabs (Bose and Das, 2014).

**2.2.1.4 Bottle Gourd Juice Preparation**

The bottle gourd juice preparation process involves washing and peeling of the bottle gourd as a first step. Thereby, the peeled bottle gourd was sliced into small pieces and fed to a mixer grinder. The grinded paste was then filtered using a cloth filter and filter paper and the filtrate was used for clarification purpose. For the study involving centrifuged juice, the filtrate was centrifuged (Centrifuge Model No.: 2-16P, Make: Sigma, Germany) at 10000 rpm for 10 min.



TH-2589_156107040

### 2.2.1.5 Microfiltration of Bottle Gourd Juice

Dead-end microfiltration study of bottle gourd juice was carried out using ceramic membranes at various applied pressures (103.4, 137.9 and 172.4 kPa). The microfiltration setup has been illustrated in section 2.2.1.3 (Figure 2.1). Both fresh juice and centrifuged juice were used for the study. Thereafter, microfiltration studies were being conducted with the compacted membranes to eventually determine the pure water flux vs pressure differential data. Eventually, hydraulic permeability and average pore size have been determined as per the procedures summarized in section 2.2.1.3 of the thesis (with the title Average Pore size). The permeation setup was then filled with adequate amount of juice. Desired trans-membrane pressure differential was applied using an air compressor. The microfiltration experiments involved collection of permeate samples at time intervals of 1 min. Pure water and permeate flux were evaluated using the expressions (Nandi et al., 2009).

$$J_w = \frac{V_s}{A_m \times t} \tag{2.6}$$

$$J_{p,t} = \frac{V_t}{A_m \times t_t} \tag{2.7}$$

where, $J_w$ = Pure water flux of the membrane, $m^3.m^{-2}.s^{-1}$

$V_s$ = Volume of the setup, $m^3$

$A_m$ = Effective permeable area of the membrane, $m^2$

$t$ = Time required for the entire water volume to discharge, s

$J_{p,t}$ = Permeate flux at time t, $m^3.m^{-2}.s^{-1}$

$V_t$ = Volume of the permeate collected at time t, $m^3$

$t_t$ = Instantaneous time, s



TH-2589_156107040

### 2.2.1.6 Flux Decline Study

The time dependent variation of the permeate flux was noted. The measured data was represented as a flux decline plot with respect to time. The flux decline plot is usually dependent on the degrees of freedom which for the considered case study refers to trans-membrane pressure differential and type of juice. The microfiltration run was terminated for an insignificant variation in the flux condition for a period of 5 min. After this step, pure water flux of the membrane was measured so as to evaluate flux decline coefficient of the membrane (FDC). The FDC is a measure of the extent of membrane fouling after microfiltration and is expressed as (Mondal et al., 2016):

$$FDC = \frac{\left(J_0 - J_p\right)}{J_0} \times 100\% \tag{2.8}$$

where, $J_0$ = Initial water Flux of the membrane, $m^3.m^{-2}.s^{-1}$

$J_p$ = Water Flux of the fouled membrane, $m^3.m^{-2}.s^{-1}$

### 2.2.1.7 Membrane Cleaning

After each microfiltration run with juice samples, the membranes were cleaned using a standard cleaning process adopted for membrane technology. This has been reported in the literature and is presented as follows (Li et al., 2018). Firstly, the fouled membranes were cleaned three to five times with Milli-Q water. Thereby, the membranes were rinsed with a mixture of 1 % NaOH and 0.5 % NaClO solution for 1 h. Subsequently, the membranes were again washed with Milli-Q water until pH of the rinsed solution reached a neutral value (pH = 7). Eventually, the membranes were rinsed with 0.5 % $HNO_3$ for 15 min. followed with a final step of membrane washing with Milli-Q water until rinsed water pH reaches a value of 7. The cleaned membranes were subjected to pure water flux evaluation test to



TH-2589_156107040

determine flux recovery ratio (FRR) (Mondal et al., 2016). FRR enables evaluation of flux recovery of the membrane after cleaning and hence cleaning efficacy. In other words, FRR indicates irreversible fouling extent of the membrane after conducting a microfiltration run. The FRR is determined using the expression:

$$FRR = \frac{J_c}{J_w} \times 100\% \tag{2.9}$$

where, $J_c$ = Pure water flux of the cleaned membrane, $m^3.m^{-2}.s^{-1}$

$J_w$ = Pure water flux of the original membrane, $m^3.m^{-2}.s^{-1}$

### 2.2.1.8 Membrane Fouling Mechanisms

The fouling mechanism of the membranes were represented with four empirical models viz., complete pore blocking, standard pore blocking, intermediate pore blocking and cake filtration, which were developed by Hermia and the models are known as Hermia models (Hermia, 1982). Constant pressure filtration law serves as the governing equation for the models and is given with the following expression:

$$\frac{d^2t}{dV^2} = K_p\left(\frac{dt}{dV}\right)^n \tag{2.10}$$

In the above equation, substitution of '*n*' with numerical values of 2, 1.5, 1 and 0 enables the models to become complete pore blocking, standard pore blocking, intermediate pore blocking and cake filtration models, respectively. During complete pore blocking, it is hypothesized that the membrane pores are completed blocked due to higher particle sizes in the feed in comparison with the membrane pore size. However, standard pore blocking and intermediate pore blocking occur for the case of feed particle sizes being smaller than membrane pores and feed particle sizes being similar to membrane pores, respectively. On



TH-2589_156107040

the other hand, cake filtration occurs for the case where feed particles accumulate on the membrane surface and form a cake that progressively obstructs flow through the membrane matrix. The following expressions sequentially represent complete, standard and intermediate and cake filtration pore blocking models (Hermia, 1982):

$$ln\left(J^{-1}\right) = ln\left(J_0^{-1}\right) + k_c t \tag{2.11}$$

$$J^{-0.5} = J_0^{-0.5} + k_s t \tag{2.12}$$

$$J^{-1} = J_0^{-1} + k_i t \tag{2.13}$$

$$J^{-2} = J_0^{-2} + k_{cf} t \tag{2.14}$$

Among the above four alternate pore blocking/filtration models, the most competent model would be chosen based on (a) fitness of measured data and (b) positive slope and intercepts of the models. Thus, model fitness involves converting measured flux decline data into $ln\left(J^{-1}\right)$, $J^{-0.5}$, $J^{-1}$ and $J^{-2}$ versus t plots and identifying the best data that fits a straight line plot with acceptable fitness parameters.

Despite Hermia models being successful to determine appropriate fouling mechanisms, they have not been useful to determine the blocking coefficients. To do so, a new set of empirical expressions have been presented by Bolton et al. (2006) for the four pore blocking models (Bolton et al., 2006). Relevant expressions have been summarized as follows:

*Complete Pore Blocking*

$$V = \frac{J_0}{K_b}\left(1 - exp\left(-K_b t\right)\right) \tag{2.15}$$

*Standard Pore Blocking*

$$V = \left(\frac{1}{J_0 t} + \frac{K_S}{2}\right)^{-1} \tag{2.16}$$

*Intermediate Pore Blocking*

$$V = \frac{1}{K_i} ln\left(1 + K_i J_0\, t\right) \tag{2.17}$$



TH-2589_156107040

*Cake Filtration*

$$V = \frac{1}{K_c J_0}\left(\sqrt{1 + 2K_c J_0^2 t} - 1\right) \tag{2.18}$$

The fitness of the above models was evaluated by conducting non-linear regression using generalized reduced gradient (GRG) method based minimization of error function in Microsoft Excel software environment. Thereby, the blocking coefficients such as $K_b$ (complete), $K_S$ (standard), $K_i$ (intermediate) and $K_c$ (cake filtration) were determined. Relevant error values have been used to judge upon the best fit model to represent the pertinent flux decline. Finally, the inferences deduced from Hermia and Bolton fouling models have been compared to choose the most appropriate model.

### 2.2.1.9 Fouling Resistances

During microfiltration, resistances for permeation occur due to time dependent membrane fouling. The total fouling resistance ($R_t$) is a measure of various factors that collectively cause resistance to the flow. It can be regarded to be the sum of hydraulic resistance ($R_m$) (resistance offered to flow by the membrane material itself and is a constant resistance throughout the microfiltration run), reversible resistance ($R_r$) (caused primarily due to formation of cake layer on the membrane surface and concentration polarization) and irreversible resistance ($R_i$) (resistance due to irreversible blocking of membrane pores). The total fouling resistance is represented with the expression (Emani, 2014):

$$R_t = R_m + R_r + R_i \tag{2.19}$$

The total fouling resistance is evaluated using measured permeate flux as:

$$R_t = \frac{\Delta P}{\eta_p J_p} \tag{2.20}$$



TH-2589_156107040

The hydraulic resistance or the membrane resistance can be determined using the pure water flux of the membrane obtained after compaction:

$$R_m = \frac{\Delta P}{\eta_w J_w} \tag{2.21}$$

The pure water flux determined after membrane cleaning is used to determine irreversible resistance of the membrane:

$$R_i = \frac{\Delta P}{\eta_w J_c} - R_m \tag{2.22}$$

Using the above permeation resistance values, the reversible resistance can be determined using the expression:

$$R_r = R_t - R_m - R_i \tag{2.23}$$

Thereby, the contribution of each of the resistances viz., $R_m$, $R_r$ and $R_i$ to the total fouling resistance could be evaluated to enable deeper insights with respect to the extent of irreversible and reversible fouling resistances during dead-end microfiltration.

**2.2.1.10 Influence of in-situ Fouling on Membrane Morphology**

During microfiltration, the membrane pores undergo fouling, which reduces the flow area. The consequent variation in the membrane morphology can be attributed to the reduction in the pore diameter, thickness and porosity of the membrane. Ideally, membrane pure water flux can be expressed in terms of membrane porosity, pore diameter and pore length using the expression (Nandi et al., 2011):

$$J_w = \frac{\Delta P}{\eta_w R_m} = \frac{\Delta P}{\eta_w} \cdot \frac{\varepsilon_m d_p^2}{32l} \tag{2.24}$$



TH-2589_156107040

During a microfiltration run, it can be assumed that the gradual membrane fouling facilitates a variation in the average morphological properties of the membrane with time. Thus, the variant membrane permeate flux can be represented using the expression:

$$J_{p,t} = \frac{\Delta P}{\eta_p R_t} = \frac{\Delta P}{\eta_p} \cdot \frac{\varepsilon_{m,t} d_t^2}{32 l_t} \tag{2.25}$$

The variation of the pore length may be considered to be negligible in comparison with the variation in cake layer thickness. Hence, the pore length may be considered to be similar throughout the microfiltration experiment. Hence, the variation in the morphological parameters with time can be obtained through the ratio of the above two expressions:

$$\frac{J_{p.t}}{J_w} = \frac{\eta_w}{\eta_p} \cdot \frac{\varepsilon_{m,t} d_t^2}{\varepsilon_m d_p^2} \tag{2.26}$$

In the above expression, terms $\varepsilon_{m,t} d_t^2$ and $\varepsilon_m d_p^2$ can be termed as the effective membrane permeability factor at time t and for the original membrane, respectively. The variant membrane effective permeability factor, $\varepsilon_{m,t} d_t^2$ indicates the extent of membrane fouling rate. In other words, a slower reduction in $\varepsilon_{m,t} d_t^2$ with time indicates lower membrane fouling rate and hence affirms promising combinations of process parameters. From the above equation, the variation in the effective membrane permeability with time t can be evaluated using the expression:

$$\varepsilon_{m,t} d_t^2 = \varepsilon_m d_p^2 \cdot \frac{J_{p,t}}{J_w} \cdot \frac{\eta_p}{\eta_w} \tag{2.27}$$



TH-2589_156107040

#### 2.2.1.11 Fitness of Empirical Models to represent Morphological Characteristics

For the fitness studies, the membrane morphological parameters namely, average pore size and porosity have been regarded to be functions of key dependent variables such as sawdust average particle size and concentration. Based on few preliminary investigations, the influence of other raw material compositions such as that of kaolin and feldspar have been found to have marginal influence on the morphological characteristics and were not considered in the modeling effort. Standard curve fitting modeling approaches have been followed. The model selection was based on a library of standard curve fitting models such as linear, quadratic, PolyRatio and Michaelis-Menten models. Higher order curve fitting models have also been attempted for their fitness. The curve fitting parameters have been obtained using Excel solver by following generalized reduced gradient (GRG) method for the minimization of the sum of the square of the error of model and experimental values of average pore size or porosity. The best fit model has been evaluated based on the $R^2$ value, which shall be maximum and close to 1. All curve fitting parameters have been regarded bounded and positive. Initial guess values for all curve fitting parameters were chosen to be one.

### 2.2.2 Ultrasound-assisted Extraction

#### 2.2.2.1 Sample Preparation and Aqueous Extraction

Bitter gourd was subjected to aqueous extraction and for that purpose, deionized water was used as the extraction medium. Small sized bitter gourd vegetables with 7-10 cm length were chosen for the experiments. To prepare the extract, firstly the vegetables were washed several times with tap water so as to ensure removal of dirt and particle traces from the skin of the vegetable. Thereafter, the vegetable was de-seeded and cut into very small pieces (5 mm



TH-2589_156107040

approx.) to subsequently place them in a beaker with precise proportions of vegetable and water. Finally, the beakers were placed in a sonication bath to carry out UAE experiments. In all experiments, the vegetables were cut afresh in order to avoid sample contamination and time bound degradation of bioactive compounds.

### 2.2.2.2 Ultrasound-assisted Extraction (UAE) Process

The ultra-sonication based extraction was carried out in a sonication bath having frequency 50/60 Hz and power 280 W (Make: Elma, Model: Elmasonic P 30H) supplemented with a water bath (Make: Amkette Industries Pvt. Ltd., Model: WB-2000) to control sonication bath temperature using a copper pipe placed inside the sonication bath and connected to the water circulation bath (Figure 2.2). The UAE extraction experiments were carried out by considering three independent variables namely extraction time, extraction temperature and vegetable to extraction media (water) ratio. Two modes of sonication, namely, normal and pulsed mode were adopted for the carried out experimental investigations to enable a comparative assessment of their competence for the enhanced extraction of said bioactive compounds.

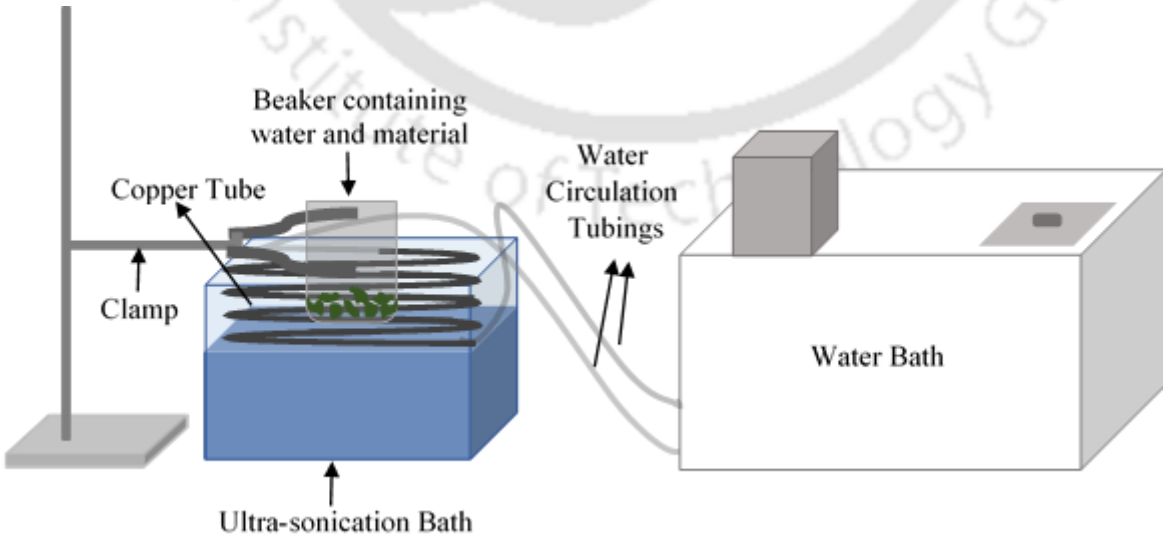


**Figure 2.2: Schematic of UAE experimental setup.**



TH-2589_156107040

Sonication as an intervention is highly effective towards reducing fouling of the membrane system due to effective pre-treatment and elimination of colloidal suspensions from the aqueous extract. The process is highly effective for those fruits/vegetables that possess minimal water content and that require larger quantities of water for the desired extraction of nutritional constituents into the aqueous phase.

#### 2.2.2.3 Experimental Design

The conducted experiments were designed using the design expert 7.0.0 software using central composite rotatable design to facilitate studies targeting the combined effect of independent variables on the desired responses or dependent variables. The inner and outer boundaries of the independent variables (temperature, time and bitter gourd to water ratio (w/v)) were selected based on the preliminary studies that were carried out prior to the design study. Accordingly, the -1 and +1 levels of these variables namely temperature, time and bitter gourd to water ratio have been set manually as 36.63 – 68.38 °C, 3.96 – 12.04 min and 0.18 – 0.42 g/mL, respectively. This ensures that the corresponding variable boundaries do not exceed the minimum and maximum values of 25 °C and 80 °C, 1 min and 15 min, and 0.1 g/mL and 0.5 g/mL, respectively. After obtaining all response variable values and subsequent fitness of suitable models, RSM model based optimization was conducted to simultaneously maximize polyphenols and antioxidant activity and minimize protein content. Further, the independent variable range was enabled to remain constant to thereby create two different designs for normal and pulsed mode sonication, respectively.



TH-2589_156107040

### 2.2.3 Juice and Extract Analysis

#### 2.2.3.1 Protein Estimation

The protein content of the juice samples was determined using Bradford Method (Bradford, 1976). For this purpose, 100 ppm BSA solution was prepared to serve as stock solution for the analysis. Using the stock solution, calibration chart was prepared to determine the protein content of unknown juice samples. For the juice sample, preparation procedure referred to dilution of 2 mL of fresh/ centrifuged/ clarified juice with 100 mL water. 1 mL of calibration samples or juice samples were mixed with 2 mL of Bradford reagent. After 30 mins, the absorbance of the samples were determined at 595 nm using UV-Visible Spectrophotometer (Model No.: UV-2600, Make: Shimadzu, Singapore).

#### 2.2.3.2 Carbohydrate Content

The carbohydrate content was determined using Anthrone's method, whose procedure is presented as follows (Agbaire and Emoyan, 2012). 1000 ppm sucrose was taken as the stock solution for calibration and 2 g fresh/centrifuged/clarified juice in 100 mL water was taken as the sample for analysis. Anthrone's reagent was prepared by dissolving 100 mg anthrone in 50 mL of ice cold 95% $H_2SO_4$. 2 mL of Anthrone's reagent was added to the solutions and was shaken for 15 min at 100 rpm. The mixture was then boiled for 30 min and was subsequently cooled. Finally, the absorbance of the sample was measured at 625 nm using UV-Visible Spectrophotometer.

#### 2.2.3.3 Vitamin C Content

The vitamin C content of a sample was determined using DCPIP method (Anjali et al., 2012). The method involves titrating standard/experimental samples with dye solution. The dye



TH-2589_156107040

solution was prepared by mixing 42 mg of sodium bicarbonate with 52 mg of DCPIP and diluting mixture with 200 mL of Milli-Q water. The working standard for the process was prepared by mixing 100 mg of ascorbic acid with 100 mL of 4 wt.% oxalic acid and then finally diluting 10 mL of this solution with 90 mL of 4 wt.% oxalic acid. 5 mL of the standard solution was mixed with 10 mL of 4 wt.% oxalic acid and was titrated against the dye solution. The volume of the dye solution required to turn the sample pink was noted ($V_1$). 1 g of sample was then taken and mixed with 100 mL of 4 wt.% oxalic acid. 5 mL of sample-oxalic acid solution was then taken and diluted with 10 mL of 4 wt.% oxalic acid and the mixture was titrated with the dye solution. The dye solution thus consumed was noted ($V_2$). Thereby, the vitamin C content of the sample was determined using expression:

$$Vitamin\,C = \frac{0.5 \times V_2 \times 100ml \times 100}{5ml \times weight\,of\,the\,sample \times V_1}\ mg/100g \tag{2.29}$$

**2.2.3.4 Total Flavonoids Content**

The total flavonoid content of the juice samples was determined using Aluminum Chloride calorimetric method (Tharasena and Lawan, 2014). Quarcetin was used as a flavonoid standard for this purpose. 1 mL of sample was mixed with 4 mL of water and 0.3 mL of 5 wt.% $NaNO_2$. After 5 min, $AlCl_3$ was added to the mixture followed with addition of 2 mL 1M NaOH solution after 6 min. The entire volume was finally made upto 10 mL. The flavonoid content of the sample was finally determined by measuring the absorbance of the samples at 510 nm with UV Visible Spectrophotometer.

**2.2.3.5 Total Phenolic Content**

The total phenol content of the juice samples was determined using Folin-Ciocalteu phenol reagent method (Tharasena and Lawan, 2014). Gallic acid was used as the standard. Firstly, 1



TH-2589_156107040

mL juice samples were mixed with 9 mL of water and then with 1 mL Folin-Ciacalteu Phenol reagent. After 5 min, 10 mL of 7 wt.% $Na_2CO_3$ was added and shaken. Finally, 4 mL of water was added to the samples and the mixture was incubated for 90 min. Finally, the absorbance of the samples was measured at 750 nm using UV Visible Spectrophotometer.

#### 2.2.3.6 Antioxidant Activity

The antioxidant activity (AA) of a extract sample was determined using DPPH scavenging method (Sutanto et al., 2015). To start with, the procedure involved the preparation of a mixture of 1.5 mL extract and 250 µM DPPH solution. Thereafter, blank and control solutions were prepared using 1.5 mL of water and ethanol each, and 1.5 mL of water and 250 µM DPPH solution each, respectively. Thereafter, all samples (blank, control and extract solution samples) were incubated for 30 min in a dark chamber at 25 $^oC$. Finally, the absorbance of control and extract samples were measured at 517 nm using UV-Visible spectrophotometer by considering the blank solution as a reference solution in the instrument system. The measured absorbance values were used to determine AA in terms of % scavenging of DPPH radical using the expression:

$$Scavenging\ of\ DPPH\ radical\ (\%) = \frac{A_{Control} - A_{Sample}}{A_{Control}} \qquad (2.30)$$

where, $A_{Control}$ is the absorbance of the control at 517 nm

$A_{Sample}$ is the absorbance of the sample at 517 nm

#### 2.2.3.7 pH, TDS and Salt Concentration

The pH, TDS and Salt concentration of the samples were determined using a digital meter (Model: AM-AL-01; Make: Aquasol, Mumbai, India).



TH-2589_156107040

### 2.2.3.8 Color and Clarity

The color and clarity of the bottle gourd juice was analyzed so as to determine the ability of microfiltration/centrifugation to clarify bottle gourd juice. The reduction of color and enhancement of juice clarity is desired and this is attributed to the removal of suspended solids during microfiltration. The color of the juice is expressed in terms of optical absorbance (A) measured using UV-Visible Spectrophotometer at a wavelength of 420 nm. The clarity of juice is expressed as percentage transmission (%T) that was evaluated using absorbance measured at a wavelength of 660 nm with the following expression (Mondal et al., 2016):

$$\%T = 100 \times 10^{-A} \tag{2.31}$$

where, $A$ = Absorbance at 660 nm

### 2.2.3.9 Microbial Analysis

To conduct microbial analysis of the juice samples, the feed and permeate samples were subjected to several fold dilution and the bacterial colonies were determined using the spread plate method. The concentration of the solutions were represented in terms of Colony Forming Units (CFU)/mL and nutrient agar was used as the growth media. The agar solution was transferred onto petri plates and was allowed to solidify. The juice samples were then spread on the plates using L-spreader instrument. The pouring of agar and spreading of the samples were carried out in a Laminar Hood set up. The prepared plates were then incubated at 37 °C for 1 – 3 days. Visible colonies in the plates were counted and were converted to CFU/mL using the following expression (Khandpur and Gogate, 2016):



TH-2589_156107040

$$CFU/mL = \frac{Number\ of\ Colonies \times Dilution\ Factor}{Amount\ Spreaded\ in\ the\ Plate\ (mL)} \quad (2.32)$$

The microbial separation efficiency of the membranes was evaluated using the expression (Kaniganti et al., 2015):

$$\%\ Rejection = \left(1 - \frac{C_p}{C_f}\right) \times 100 \quad (2.33)$$

where, $C_p$ = Microbial concentration of permeate sample, CFU.mL$^{-1}$

$C_f$ = Microbial concentration of feed sample, CFU. mL$^{-1}$

## References


1. Agbaire, P., Emoyan, O., 2012. Nutritional and antinutritional levels of some local vegetables from Delta State, Nigeria. African Journal of Food Science 6, 8-11.
2. Anjali, K.M., Singh, N., Pal, K., 2012. Effect of sulphur dioxide on plant biochemicals. International Journal of Pharma Professional's Research 3, 627.
3. Bolton, G., LaCasse, D., Kuriyel, R., 2006. Combined models of membrane fouling: development and application to microfiltration and ultrafiltration of biological fluids. Journal of Membrane Science 277, 75-84.
4. Bose, S., Das, C., 2013. Preparation and characterization of low cost tubular ceramic support membranes using sawdust as a pore-former. Materials Letters 110, 152-155.
5. Bose, S., Das, C., 2014. Role of binder and preparation pressure in tubular ceramic membrane processing: design and optimization study using response surface methodology (RSM). Industrial & Engineering Chemistry Research 53, 12319-12329.




TH-2589_156107040

6. Bradford, M.M., 1976. A rapid and sensitive method for the quantitation of microgram quantities of protein utilizing the principle of protein-dye binding. Analytical Biochemistry 72, 248-254.
7. Emani, S., 2014. Cross flow microfiltration of oil-water emulsion using kaolin based low cost ceramic membranes. Desalination 341, 61-71.
8. Hermia, J., 1982. Constant pressure blocking filtration laws: application to power-law non-Newtonian fluids. Transactions of Institution of Chemical Engineers, 60, 183-187.
9. Kaniganti, C.M., Emani, S., Thorat, P., Uppaluri, R., 2015. Microfiltration of synthetic bacteria solution using low cost ceramic membranes. Separation Science and Technology 50, 121-135.
10. Khandpur, P., Gogate, P.R., 2016. Evaluation of ultrasound based sterilization approaches in terms of shelf life and quality parameters of fruit and vegetable juices. Ultrasonics Sonochemistry 29, 337-353.
11. Li, W., Ling, G., Lei, F., Li, N., Peng, W., Li, K., Lu, H., Hang, F., Zhang, Y., 2018. Ceramic membrane fouling and cleaning during ultrafiltration of limed sugarcane juice. Separation and Purification Technology 190, 9-24.
12. Mondal, M., Biswas, P.P., De, S., 2016. Clarification and storage study of bottle gourd (Lagenaria siceraria) juice by hollow fiber ultrafiltration. Food and Bioproducts Processing 100, 1-15.
13. Nandi, B., Das, B., Uppaluri, R., Purkait, M., 2009. Microfiltration of mosambi juice using low cost ceramic membrane. Journal of food engineering 95, 597-605.
14. Nandi, B., Uppaluri, R., Purkait, M., 2011. Identification of optimal membrane morphological parameters during microfiltration of mosambi juice using low cost ceramic membranes. LWT-Food Science and Technology 44, 214-223.



TH-2589_156107040

15. Sutanto, H., Himawan, E., Kusumocahyo, S.P., 2015. Ultrasound assisted extraction of bitter gourd fruit (Momordica charantia) and vacuum evaporation to concentrate the extract. Procedia Chemistry 16, 251-257.
16. Tharasena, B., Lawan, S., 2014. Phenolics, flavonoids and antioxidant activity of vegetables as Thai side dish. APCBEE procedia 8, 99-104.

भारतीय प्रौद्योगिकी संस्थान गुवाहाटी • Indian Institute of Technology Guwahati •



TH-2589_156107040

# Chapter 3:

# Optimization of Sawdust Based Precursor Compositions during Fabrication of Low Cost Ceramic Membranes

TH-2589_156107040

TH-2589_156107040

# Optimization of Sawdust Based Precursor Compositions during Fabrication of Low Cost Ceramic Membranes

*This chapter presents the results and discussions associated to RSM based optimization of saw dust based precursor composition for the synthesis of low cost ceramic membranes. After a brief introduction in section 3.1, sections 3.2 details upon the optimal precursor composition based on membrane pore size and porosity as the response variables and subsequently, section 3.3 details upon the optimal composition by considering flexural strength as additional response variable. Section 3.4 validates the optimal compositions obtained through software analysis with additional experiments. Section 3.5 presents comparative assessment of optimal precursor compositions obtained from both cases. A comparative assessment of obtained compositions with literature data has been summarized in section 3.6. Section 3.7 provides deeper insights with respect to the dependence of critical response variables with precursor compositions. Section 3.8 summarizes the morphological, structural and thermal characteristics of the fabricated membranes followed by summary of the key findings in section 3.9[#].*

## Overview

*The relevance of D-optimal mixture model based RSM design methodology for the optimal fabrication of carbonate free low cost ceramic membranes have been discussed in this*

[#] Published Article: Chakraborty, S., Uppaluri, R., Das, C., (2018) "Optimal Fabrication of Carbonate Free Low Cost Ceramic Membranes using Mixture Model RSM Design Methodology", Applied Clay Science, 162: 101-112.

TH-2589_156107040

*chapter. The RSM design methodology was validated by targeting alterations in the composition of kaolin, feldspar and saw dust precursors during low cost ceramic membrane fabrication. Experimental findings of key dependent membrane product variables namely average pore size and average porosity have been regarded as biases to identify optimal kaolin, feldspar and saw dust precursor compositions. Further, a comparative study has been conducted to evaluate upon the sensitivity of optimal compositions while considering flexural strength as a response parameter. The RSM design methodology based theoretical and experimental investigations indicated that the optimal precursor compositions for which optimal responses were pore size and porosity varied marginally when flexural strength was also considered as additional response variable. These findings have been broadly discussed in the upcoming sections of the chapter.*

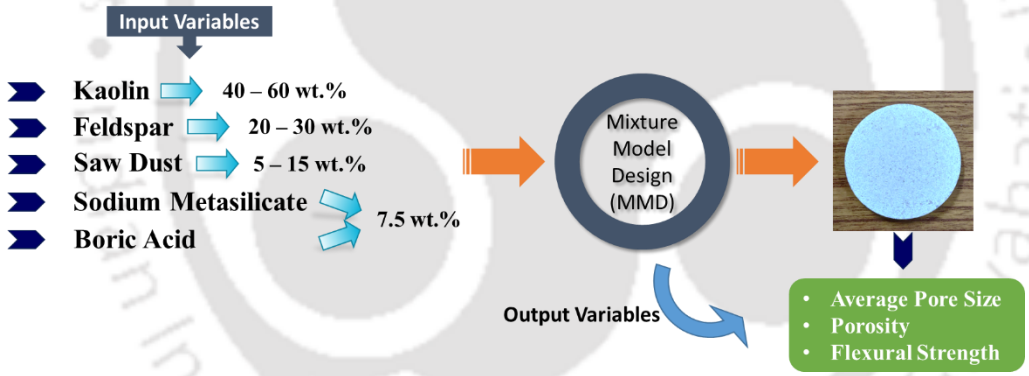


## 3.1 Introduction

This chapter elaborates upon the efficacy of mixture model design (MMD) based RSM design methodology to achieve desirable attributes of low cost ceramic membranes. Since targeting MMD for large size of the precursors is tedious and time consuming, the work targeted utilization of data available in the literature and emphasizing upon refinement in the precursor formulation. To do so, the binder composition (sodium metasilicate and boric acid) of Bose et al., 2014 was chosen to be relevant and optimization of all other inorganic



TH-2589_156107040

precursors (kaolin, feldspar and saw dust) were targeted using D-optimal mixture model (Bose and Das, 2014). The RSM design methodology targeted upon the optimality of said precursor compositional interactions on three response variables, namely, average pore size, average porosity and flexural strength. Further, the sensitivity of optimal precursor formulations with the bias of either pore size and porosity or bias involving a combination of all three response variables (including flexural strength) was addressed.

## 3.2 Optimality of Precursor Compositions and Membrane Morphology

### 3.2.1 MMD based Experimental Design

For the chosen problem specifications, a 16 run data set was generated using the MMD based RSM design approach (Table 3.1). Experimental investigations were conducted to determine the porosity and average pore size values and obtained data were presented in the last three columns of the table. The parameter values correspond to average values obtained for three different sets. Lower standard deviation values for all data sets affirm appropriate reproducibility of the data and instill confidence with respect to the parameter sets.

### 3.2.2 Selection of Best RSM Model

Various alternate models have been considered to represent the data sets involving porosity and average pore size as response variables (Tables 3.2 (a) and 3.2 (b)). For a model to be considered suitable among alternate models, the *F-value* should be as high as possible and the *p-value* should be as low as possible. Among alternate models, the special cubic model was found to be the best suited model for the case of porosity (Table 3.2 (a)).



TH-2589_156107040

**Table 3.1: D-Optimal mixture design based experimental data summary for both investigated cases.**

| Run No. | A: Kaolin (%) | B: Feldspar (%) | C: Saw Dust (%) | Response 1 (Porosity (%)) | Response 2 (Pore Size (µm)) | Response 3 (Flexural Strength MPa)) |
|---|---|---|---|---|---|---|
| 1 | 55.35 | 24.65 | 5.00 | 32.82 ± 0.43 | 1.02 ± 0.40 | 9.83 ± 0.26 |
| 2 | 59.99 | 20.00 | 5.00 | 23.32 ± 0.48 | 1.11 ± 0.02 | 9.39 ± 0.07 |
| 3 | 40.01 | 30.00 | 14.99 | 43.39 ± 2.02 | 4.01 ± 0.06 | 3.11 ± 0.10 |
| 4 | 45.15 | 28.38 | 11.47 | 32.07 ± 0.95 | 2.78 ± 0.09 | 7.12 ± 1.30 |
| 5 | 56.41 | 20.93 | 7.66 | 33.48 ± 0.21 | 1.85 ± 0.63 | 7.74 ± 0.05 |
| 6 | 47.77 | 22.23 | 15.00 | 35.99 ± 1.89 | 2.81 ± 0.08 | 5.19 ± 0.44 |
| 7 | 46.75 | 30.00 | 8.25 | 24.52 ± 0.12 | 1.79 ± 0.55 | 8.03 ± 0.32 |
| 8 | 59.99 | 20.00 | 5.00 | 24.00 ± 0.48 | 1.09 ± 0.02 | 9.29 ± 0.07 |
| 9 | 53.79 | 20.00 | 11.21 | 35.90 ± 0.64 | 1.78 ± 0.02 | 3.83 ± 0.23 |
| 10 | 40.01 | 30.00 | 14.99 | 46.24 ± 2.02 | 3.92 ± 0.06 | 3.25 ± 0.10 |
| 11 | 49.54 | 30.00 | 5.46 | 26.00 ± 0.12 | 2.09 ± 1.01 | 8.87 ± 0.50 |
| 12 | 53.79 | 20.00 | 11.21 | 36.80 ± 0.64 | 1.76 ± 0.02 | 3.51 ± 0.23 |
| 13 | 43.79 | 26.21 | 15.00 | 33.05 ± 0.82 | 3.88 ± 0.48 | 7.13 ± 1.80 |
| 14 | 49.54 | 30.00 | 5.46 | 25.83 ± 0.12 | 2.10 ± 0.03 | 8.94 ± 0.50 |
| 15 | 47.77 | 22.23 | 15.00 | 33.31 ± 1.89 | 2.92 ± 0.08 | 5.81 ±0.44 |
| 16 | 50.35 | 25.39 | 9.25 | 34.73 ± 0.39 | 2.03 ± 0.07 | 8.18 ± 0.27 |

Among all models, the *F-value* for the special cubic model was maximum (79.24) along with lowest *p-value* (<0.0001). Similar model fitness was analyzed for the case of average pore size being considered as the response variable (*F-value* = 67.15 and $p < 0.0001$).

### 3.2.3 Analysis of Variance

For the case of porosity being considered as the response variable, analysis of variable (ANOVA) results affirm upon significance of special cubic model (Table 3.3 (a)). All interactions of variables namely AB, AC, AB and ABC were found to be important with high *F-value*s. Also, this is supported with insignificant lack of fit values (*F-value* = 2.40 (low), *p-value* = 0.1815 (high)).



TH-2589_156107040

**Table 3.2: Alternate model fitness parameters for various response variables (a) porosity and (b) average pore size.**

| Source | Sum of Squares | df | Mean Square | *F-value* | *p-value* Prob > F | Comments |
|---|---|---|---|---|---|---|
| Mean vs Total | 16994.38 | 1 | 16994.38 | | | |
| Linear vs Mean | 383.80 | 2 | 191.90 | 8.92 | 0.0036 | |
| Quadratic vs Linear | 42.14 | 3 | 14.05 | 0.59 | 0.6348 | |
| Special Cubic vs Quadratic | 213.42 | 1 | 213.42 | 79.24 | <0.0001 | *Suggested* |
| Cubic vs Special Cubic | 12.62 | 3 | 4.21 | 2.17 | 0.1925 | |
| Residual | 11.62 | 6 | 1.94 | | | |
| Total | 17657.98 | 16 | 1103.62 | | | |

**(a)**

| Source | Sum of Squares | df | Mean Square | *F-value* | *p-value* Prob > F | Comments |
|---|---|---|---|---|---|---|
| Mean vs Total | 85.50 | 1 | 85.50 | | | |
| Linear vs Mean | 13.33 | 2 | 6.67 | 59.98 | <0.0001 | |
| Quadratic vs Linear | 0.55 | 3 | 0.18 | 2.06 | 0.1698 | |
| Special Cubic vs Quadratic | $1.486\times10^{-5}$ | 1 | $1.486\times10^{-5}$ | $1.497\times10^{-4}$ | 0.9905 | |
| Cubic vs Special Cubic | 0.87 | 3 | 0.29 | 67.15 | <0.0001 | *Suggested* |
| Residual | 0.026 | 6 | $4.307\times10^{-3}$ | | | |
| Total | 100.28 | 16 | 6.27 | | | |

**(b)**

Considering special cubic model as the best fitted model, obtained using model parameters, the variation in the average porosity of the membrane with variation in kaolin (A), feldspar (B) and saw dust (C) compositions could be expressed using the following equation:

$$\varepsilon = 23.55\,A - 41.35\,B - 5.62\,C + 140.58\,AB + 105.86\,AC + 271.30\,BC - 455.90\,ABC \quad (3.1)$$



TH-2589_156107040

**Table 3.3: ANOVA data summary for (a) porosity and (b) average pore size.**

| **Source** | **Sum of Squares** | **df** | **Mean Square** | ***F-value*** | ***p-value*** **Prob > F** | **Comments** |
|---|---|---|---|---|---|---|
| Model | 639.36 | 6 | 106.56 | 39.56 | < 0.0001 | *Significant* |
| *Linear Mixture* | 383.80 | 2 | 191.90 | 71.25 | < 0.0001 | |
| AB | 99.28 | 1 | 99.28 | 36.86 | 0.0002 | |
| AC | 91.33 | 1 | 91.33 | 33.91 | 0.0003 | |
| BC | 143.14 | 1 | 143.14 | 53.14 | <0.0001 | |
| ABC | 213.42 | 1 | 213.42 | 79.24 | <0.0001 | |
| Residual | 24.24 | 9 | 2.69 | | | |
| *Lack of Fit* | 15.94 | 4 | 3.98 | 2.40 | 0.1815 | *Not significant* |
| *Pure Error* | 8.30 | 5 | 1.66 | | | |
| Cor Total | 663.60 | 15 | | | | |

**(a)**

| **Source** | **Sum of Squares** | **df** | **Mean Square** | ***F-value*** | ***p-value*** **Prob > F** | **Comments** |
|---|---|---|---|---|---|---|
| Model | 14.75 | 9 | 1.64 | 380.58 | <0.0001 | *Significant* |
| *Linear Mixture* | 13.33 | 2 | 6.67 | 1547.85 | <0.0001 | |
| AB | 0.14 | 1 | 0.1z4 | 32.38 | 0.0013 | |
| AC | 0.11 | 1 | 0.11 | 25.96 | 0.0022 | |
| BC | $8.745\times10^{-3}$ | 1 | $8.745\times10^{-3}$ | 2.03 | 0.2040 | |
| ABC | 0.11 | 1 | 0.11 | 25.11 | 0.0024 | |
| AB(A–B) | 0.12 | 1 | 0.12 | 28.19 | 0.0018 | |
| AC(A–C) | 0.090 | 1 | 0.090 | 20.80 | 0.0038 | |
| BC(B–C) | 0.19 | 1 | 0.19 | 43.24 | 0.0006 | |
| Residual | 0.026 | 6 | $4.307\times10^{-3}$ | | | |
| *Lack of Fit* | 0.011 | 1 | 0.011 | 3.86 | 0.1068 | *Not significant* |
| *Pure Error* | 0.015 | 5 | $2.918\times10^{-3}$ | | | |
| Cor Total | 14.78 | 15 | | | | |

**(b)**

Results obtained from ANOVA analysis for the case with average pore size as response variable indicated a good fitness of the cubic model (Table 3.3 (b)). The ANOVA conveyed that the average pore size variation is rather a more complex function of constituents A, B and C. The *F-value*s indicated strong interaction between all variables namely AB, AC, BC,



TH-2589_156107040

ABC, AB(A–B), AC(A–C) and BC(B–C) and an insignificant lack of fit (*F-value* = 3.86 and *p-value* = 0.1068). Considering the obtained model parameters, the average pore size variation with variations in A, B and C could be expressed as:

$$d_p = 1.11\ A + 63.09\ B - 50.98\ C - 118.74\ AB - 97.86\ AC - 8.23\ BC + 53.32\ ABC + 69.80\ AB(A–B) - 50.71\ AC(A–C) - 203.08\ BC(B–C) \quad (3.2)$$

For the average porosity case, adjusted R-Squared and predicted R-Squared values were 0.939 and 0.886 respectively. Similar values were obtained for the average pore size case (adjusted value = 0.996, Predicted value = 0.90). The adequate precision was 19.116 and 57.850 for porosity and average pore size cases, respectively. An adequate precision greater than 4 was obtained and hence affirms upon the suitability of the model.

### 3.2.4 Diagnostics

For both cases, the normal plots of residuals affirm that the data points fall very closely to the straight line and convey no signs of non-normality of data points (Figure 3.1 (a) and 3.1 (b)). Hence, the data points were considered to be normally distributed for both cases. The points were located close to the diagonal line, in the predicted versus actual plots, which is the locus of similarity between predicted and actual values (Figure 3.1 (c) and 3.1 (d)). These observations infer that the expressed models were suitable to represent pertinent variations in the response variables as represented non-linear functions of kaolin, feldspar and saw dust compositions. The residual versus predicted plots for both cases affirm upon the existence of linear patterns, which is ensured by observing scattered data across the residual (horizontal central line) (Figure 3.1 (e) and 3.1 (f)).



TH-2589_156107040

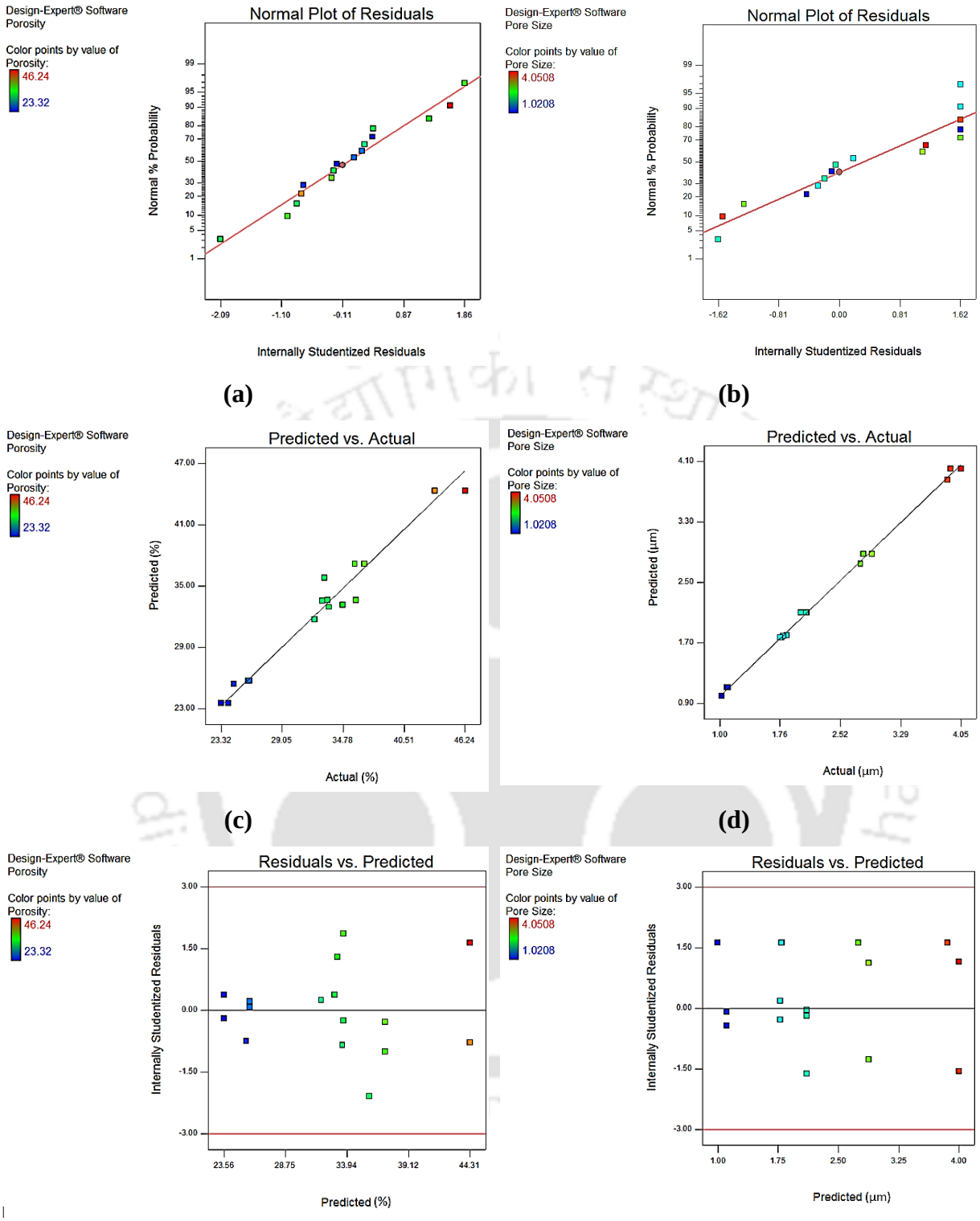


**Figure 3.1: RSM response plots for various cases (a) normal residual plot of porosity, (b) normal residual plot of average pore size, (c) porosity parity plot, (d) average pore size parity plot, (e) residuals vs predicted plot of porosity, and (f) residuals vs predicted plot of average pore size.**



TH-2589_156107040

### 3.2.5 Response Plots

Both 2D and 3D response plots confirm highly non-linear variation of the responses with variation in the compositions of constituents A, B and C in the mixture (Figure 3.2 (a – d)). With an increase in kaolin content (A), the average porosity decreased which is not the case for an increase in feldspar (B) and saw dust composition (C) (Figure 3.2 (a) and (b)). On the other hand, the average pore size increased with an increase in both kaolin (A) and saw dust (B) (Figure 3.2 (c) and 3.2 (d)). However, feldspar composition (C) did not exhibit significant influence upon average pore size of the membranes.

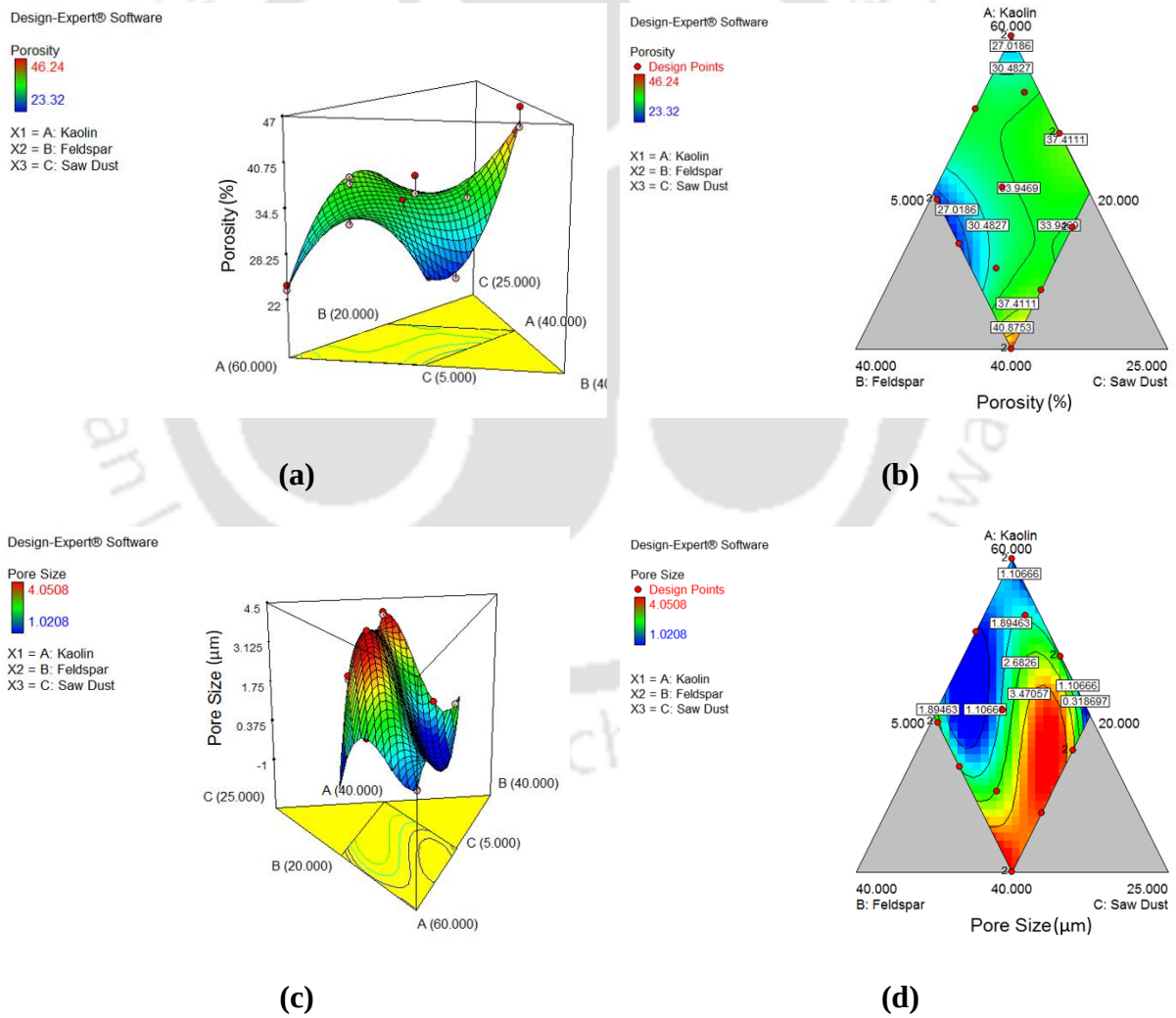


**Figure 3.2: Contour plots for various cases (a) porosity 3D plot (b) porosity 2D plot (c) average pore size 3D plot, and (d) average pore size 2D plot.**



TH-2589_156107040

The optimal set of membrane precursor composition was targeted by considering minimization of average membrane pore size. As suggested by the design, the optimum composition has been obtained as 48.19 wt.% kaolin, 28.62 wt.% feldspar and 8.19 wt.% saw dust. For the optimal composition, the average pore size and membrane porosity have been predicted to be 1.00 μm and 28.47 %, respectively.

## 3.3 Optimality of Precursor Composition, Membrane Morphology and Flexural Strength

### 3.3.1 Control and Response Variable Summary

The case involves consideration of all three variables namely average pore size, average porosity and flexural strength of the membrane as response variables for the evaluation of optimal composition of kaolin (A), feldspar (B) and saw dust (C) (Table 3.1). The needful data of flexural strength in the table were obtained by carrying out experimental investigations for the fabricated membranes with specified precursor compositions.

### 3.3.2 Identification of Best Fit Model

A comparison of various models for the system in terms of flexural strength suggested the special cubic model as the best suited model with *F-value* and *p-value* of 68.54 and <0.0001 respectively (Table 3.4 (a)).

### 3.3.3 ANOVA Parameters

The analysis of variance (ANOVA) results for porosity and average pore size were similar to that presented in section 3.2.3.



TH-2589_156107040

**Table 3.4: (a) Alternate RSM-MMD model fitness characteristics (b) ANOVA data characteristics for flexural strength case.**

| **Source** | **Sum of Squares** | **df** | **Mean Square** | ***F-value*** | ***p-value* Prob > F** | **Comments** |
|---|---|---|---|---|---|---|
| Mean vs Total | 745.36 | 1 | 745.36 | | | |
| Linear vs Mean | 56.87 | 2 | 28.43 | 13.20 | 0.0007 | |
| Quadratic vs Linear | 18.01 | 3 | 6 | 6.01 | 0.0131 | |
| Special Cubic vs Quadratic | 8.84 | 1 | 8.84 | 68.54 | <0.0001 | *Suggested* |
| Cubic vs Special Cubic | 0.64 | 3 | 0.21 | 2.46 | 0.1609 | |
| Residual | 0.52 | 6 | 0.087 | | | |
| Total | 830.24 | 16 | 51.89 | | | |

**(a)**

| **Source** | **Sum of Squares** | **df** | **Mean Square** | ***F-value*** | ***p-value* Prob > F** | **Comments** |
|---|---|---|---|---|---|---|
| Model | 83.72 | 6 | 13.95 | 108.22 | < 0.0001 | *significant* |
| *Linear Mixture* | 56.87 | 2 | 28.43 | 220.52 | < 0.0001 | |
| AB | 0.90 | 1 | 0.90 | 6.95 | 0.0271 | |
| AC | 6.58 | 1 | 6.58 | 51.00 | <0.0001 | |
| BC | 0.27 | 1 | 0.27 | 2.06 | 0.1847 | |
| ABC | 8.84 | 1 | 8.84 | 68.54 | <0.0001 | |
| Residual | 1.16 | 9 | 0.13 | | | |
| *Lack of Fit* | 0.90 | 4 | 0.22 | 4.24 | 0.0724 | *Not significant* |
| *Pure Error* | 0.26 | 5 | 0.053 | | | |
| Cor Total | 84.88 | 15 | | | | |

**(b)**

The ANOVA results obtained with flexural strength as additional response variable indicated significant interactions between the variables AB, AC and ABC (*F-value*s in Table 3.4 (b)).The lack of fit was observed to be not significant (*F-value* of 4.24 and *p-value* of 0.0724). Based on the best fitness of special cubic equation, the flexural strength variation with compositional variations of A, B and C could be expressed with the following equation:



TH-2589_156107040

$$F = 9.45\,A + 1.63\,B + 10.69\,C + 13.36\,AB - 28.40\,AC - 11.70\,BC + 92.77\,ABC \quad (3.3)$$

With good combinations of adjusted R-squared (0.977), predicted R-squared (0.963), adequate precision (28.524 which is significantly greater than a value of 4) values, the model has been inferred to be promising to represent response variables adequately in terms of the precursor compositions.

### 3.3.4 Parity Plots

The normal plots of residuals associated to flexural strength analysis depicted that the data points were located very close to the straight line and indicated no signs of non–normality (Figure 3.3 (a)).

The predicted versus actual plots indicated that the data points were located very close to the locus line and affirms the suitability of the model (Figure 3.3 (b)). Linear patterns of the residual versus predicted plots implied good fitness of the model with no non–linear relationships (Figure 3.3 (c)).

### 3.3.5 2D and 3D Response Plots

The 2D and 3D response plots of flexural strength affirm that all three precursor compositions have significant influence on the flexural strength of the membranes (Figure 3.4 (a) and (b)). The flexural strength increased with increasing compositions of saw dust, kaolin and feldspar.



TH-2589_156107040

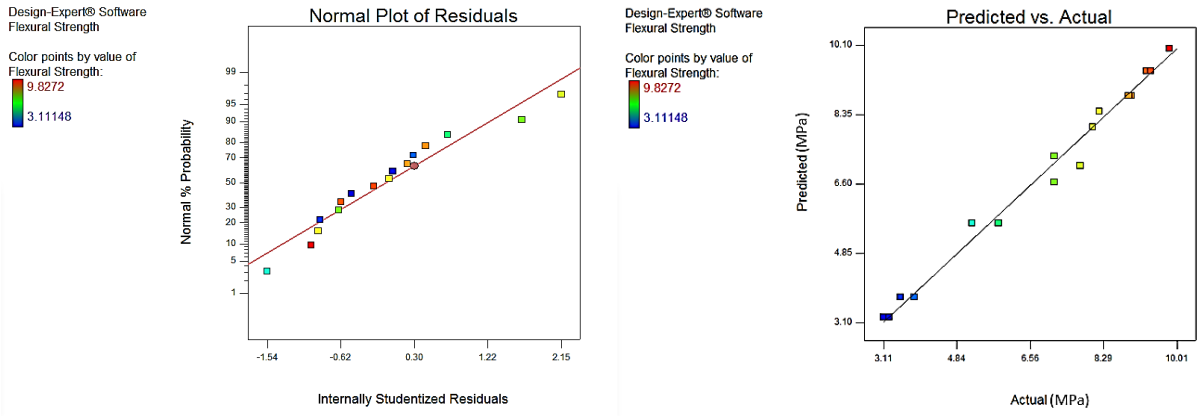


**(a)** **(b)**

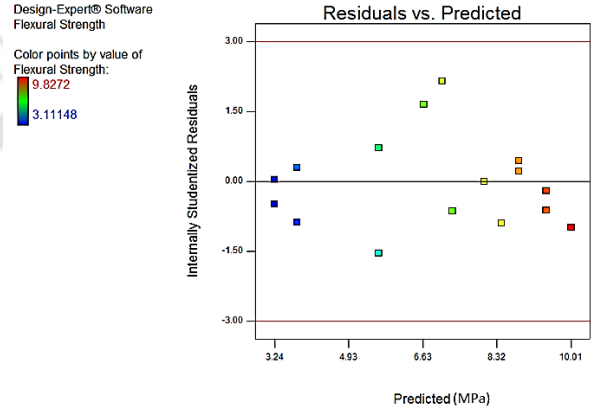


**(c)**

**Figure 3.3: Response plots for flexural strength case (a) normal residual plot (b) parity plot (c) residuals vs predicted plot.**

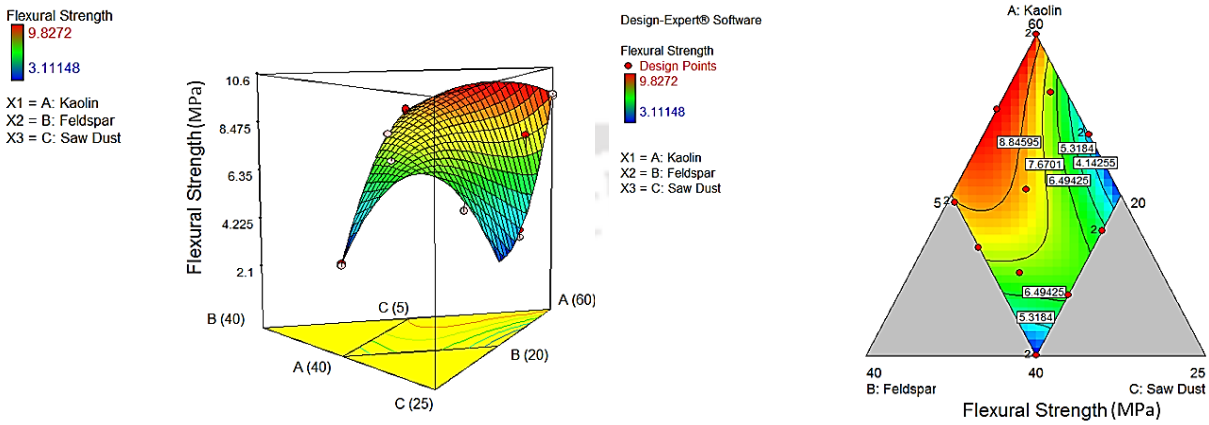


**(a)** **(b)**

**Figure 3.4: (a) 3D and (b) 2D response surface plots for flexural strength case.**



TH-2589_156107040

### 3.3.6 Precursor Composition Optimality

The bias for compositional optimality was to obtain adequate flexural strength and lower pore size of the membranes. With an objective, the mathematical optimization yielded 48 wt.% kaolin, 27.81 wt.% feldspar and 8.26 wt.% saw dust as the optimal membrane precursor composition. Corresponding response variable values are 0.93 μm average pore size, 29.98 % porosity and 8.75 MPa, respectively.

## 3.4 Comparative Analysis of Optimal Precursor Compositions

The sensitivity of the optimal precursor compositions with respect to variations in the desired responses can be evaluated from obtained data. By considering only pore size and porosity as responses, the optimal composition referred to 48.19 wt.% kaolin, 28.62 wt.% feldspar and 8.19 wt.% sawdust. These values got marginally varied to 48 wt.% kaolin, 27.81 wt.% feldspar and 8.26 wt.% sawdust as optimal formulation by considering flexural strength as additional response variable. In other words, the obtained compositions are not highly sensitive with respect to flexural strength as an additional response variable. Therefore, it was opined that flexural strength need not be considered as an additional response variable and emphasis in low cost ceramic membrane fabrication needs to be upon average pore size and porosity.

## 3.5 Validation of MMD based Optimal Formulations

The optimal composition sets obtained from the design analysis were validated experimentally in terms of the response variables namely, porosity and average pore size (Table 3.5).



TH-2589_156107040

**Table 3.5: Validity of optimal membrane characteristics with respect to experimental data.**

| S. No. | Optimal Case (Obtained from RSM) (wt.%) | Measured | | Predicted | | Error | |
|---|---|---|---|---|---|---|---|
| | | Porosity (%) | Average Pore Size (µm) | Porosity (%) | Average Pore Size (µm) | Porosity (%) | Average Pore Size (%) |
| 1 (Without Flexural Strength) | • Kaolin: 48.19<br>• Feldspar: 28.62<br>• Saw Dust: 8.19<br>• Boric Acid: 7.5<br>• Sodium Metasilicate:7.5 | 29.59 | 1.035 | 28.47 | 1.001 | 3.93 | 3.39 |
| 2 (With Flexural Strength) | • Kaolin: 48<br>• Feldspar: 27.81<br>• Saw Dust: 8.26<br>• Boric Acid: 7.5<br>• Sodium Metasilicate:7.5 | 30.56 | 1.024 | 29.98 | 0.925 | 1.93 | 10.7 |

Flexural strength data was not included in this study, since it has negligible effect on the composition sets as is evident from the minimal changes in the optimal composition for both cases. It can be analysed that for the composition not involving flexural strength as response variable, the error involved in the prediction of both average pore size and porosity is significantly low (3.39 % for average pore size and 3.93 % for porosity). However, this is not the case when flexural strength is involved as an additional response variable, since error associated with pore size was 10.7 % and for average porosity was 1.93 %, which are higher than the previous case.

## 3.6 Comparative Analysis with Prior Art

The key findings in this work have been compared with the best data being reported in the relevant prior art. It can be analyzed that compared to the membrane morphological parameters being reported by Bose et al. 2014, this work affirmed optimal composition of kaolin, feldspar and saw dust for which higher average porosity (by 9 %), comparable flexural strength (lower by 2 MPa) and higher average pore size (~1 µm compared to 0.21 µm) have been obtained (Table 3.6) (Bose and Das, 2014).



TH-2589_156107040

**Table 3.6: A summary of literature and evaluated optimal membrane precursor formulations.**

| S. No. | Inputs (wt.%) | | | | | Outputs | | | Remarks |
|---|---|---|---|---|---|---|---|---|---|
| | Kaolin | Feldspar | Saw Dust | Boric Acid | Sodium Metasilicate | Porosity (%) | Average Pore Size (µm) | Flexural Strength (MPa) | |
| 1 | 48.19 | 28.62 | 8.19 | 7.5 | 7.5 | 28.47 ± 0.29 | 1.00 ± 0.05 | – | This Work |
| 2 | 48 | 27.81 | 8.26 | 7.5 | 7.5 | 29.98 ± 1.10 | 0.93 ± 0.02 | 8.75 | This Work |
| 3 | 50 | 25 | 10 | 7.5 | 7.5 | 20.59 | 0.21 | 11.55 | Bose et al. (2014) |
| 4 | 40 | 15* | 35** | 5 | 5 | 30.1–37.4 | 2.16–3.06 | – | Emani et al. (2013) |

* Quartz 15 wt.%; ** Calcium Carbonate 25 wt.% and Sodium Carbonate 10 wt.%

Even though the average pore size and average porosity of the membrane fabricated in this work were higher than those being reported in the mentioned prior art, the work conducted in the literature did not involve a statistical design based optimization of kaolin, feldspar and saw dust compositions. However, the future scope of improvement also exists in terms of further reduction in the average pore size and average porosity. In this regard, it is important to note that while the authors of the mentioned prior art obtained lower average pore size, the optimality of compositions was not reflected, which is very important to obtain useful insights prior to conducting rigorous experimental investigations for low cost ceramic membrane fabrication with desired average properties. Other than this work, the work of Emani et al. (2013) is not relevant for comparison with the obtained data due to substantial emphasis on trial and error based precursor compositions rather than on systematic optimization (Emani et al., 2013). In summary, the trial and error based methodology followed by the authors did not provide enough scope to achieved tailored combinations of



TH-2589_156107040

average pore size and porosity. However, this is not the case in the work due to RSM based optimization methodology being duly followed in the thesis.

## 3.7 Influence of Response Variable Characteristics on Precursor Composition Optimality

Using Design Expert software and optimized membrane fabrication model, different sets of optimal membrane precursor compositions were obtained while varying membrane properties as desired. Twelve such variations were targeted in order to observe critical variations in the optimal precursor composition for alternate bias combinations set as desired objectives.

The data thus generated has been presented in Table 3.7 (a) (for sets with experimental data to assist comparison purpose) and 3.7 (b) (for sets generated without any experimental input data). Further, Table 3.7 (a) refers to minimization or maximization of pore size and maximization of porosity and flexural strength and Table 3.7 (b) refers to several relevant combinations of maximum/minimum pore size, maximum porosity and maximum flexural strength. Further, minimization of average porosity and flexural strength was not targeted in the rigorous optimization study, given the fact that these parameters are not desired attributes of a ceramic membrane. Significant insights have been obtained from such studies. A further discussion in this regard has been presented in the subsequent paragraphs.

The experimental data input referred to a minimal average pore size of 1.02 µm which can be further reduced to 0.92 µm after RSM based optimization (Table 3.7 (a)). Incidentally, the minimal average pore size indicated a reduction in saw dust composition (to 5 wt.%) with simultaneous enhancement in kaolin wt.% (from 48 to 55.35 %) and reduction in saw dust wt.% (from 8.26 to 5 %). However, the maximization of average pore size did not enhance much from the determined average pore size value (4.05 to 4.08 µm). Such variation



TH-2589_156107040

indicated a significant variation in kaolin wt.% (49.51 to 40.01 %) and feldspar wt.% (2.96 to 30 %) but not saw dust wt.% (2.53 to 14.99 %). On the other hand, the minimization and maximization of average membrane porosity using RSM design model did not involve significant variations in porosity values (24.98 % porosity predicted vis–à–vis an experimental value of 23.32 % for the minimization case and 44.31 % porosity predicted vis–à–vis an experimental value of 46.24 % for the maximization case). Among these cases, significant variation in the compositions of kaolin, feldspar and saw dust wt.% can be observed for minimization case only with respect to the corresponding compositions chosen for experimental investigations. Similarly, for maximum flexural strength, values similar to those obtained from experimental input data were obtained. However, the compositions indicated strong variation in kaolin (from 48.19 to 55.35 %), saw dust (from 8.19 to 5 %) and feldspar (from 28.62 to 24.65 %) content.

The other data set depicts the optimal kaolin, feldspar and saw dust compositions for maximum/minimum average pore size and maximum values for both porosity and flexural strength (Table 3.7 (b)). For maximum porosity, the minimal pore size was 1.29 µm which corresponds to 5.93 wt.% kaolin, 20 wt.% feldspar and 13.02 wt.% saw dust. With similar porosity, the maximum pore size of 4.05 µm indicated 49.68 wt.% kaolin, 22.85 wt.% feldspar and 12.47 wt.% saw dust. This affirms that saw dust needs to be varied significantly for a combination of optimal pore size and porosity. Similar results were obtained for optimal combinations of pore size and porosity. With combination of maximum porosity and flexural strength, the maximum pore size of 4.05 µm was obtained for 45.00 wt.% kaolin, 25.98 wt.% feldspar and 14.02 wt.% saw dust. This varied to 54.62 wt.% kaolin, 25.38 wt.% feldspar and 5.00 wt.% saw dust for the lowest pore size of 0.77 µm. The reduction in saw dust wt.% to about 5% for reduction in pore size but not porosity is questionable and further experimental investigations are required to verify the actual optimality of obtained compositions. In



TH-2589_156107040

summary, the optimal compositions obtained are reasonable and indicate a maximum or minimum pore size of 4.05 µm and 0.77 µm, respectively. This confirms that the entire compositional range being targeted for the deployed precursors (kaolin, feldspar and saw dust) and its subsequent optimality has not been addressed in the trial and error based methodology and compositional optimality being reported in the earlier works of Bose et al. 2014 and Emani et al. 2013 (Bose and Das, 2014; Emani et al., 2013). Thereby, the relevance of MMD based RSM for composition optimization of ceramic membranes is clearly evident.

**Table 3.7: Optimal data summary based on inverse engineering approach (a) validation and (b) combinatorial optimality table.**

| S. No. | Target Properties | | | Optimal Composition | | | Experimental/ Predicted |
|---|---|---|---|---|---|---|---|
| | Porosity (%) | Average Pore Size (µm) | Flexural Strength (MPa) | Kaolin (wt.%) | Feldspar (wt.%) | Saw Dust (wt.%) | |
| 1a | 29.98 | 0.93 (Minimum) | 8.75 | 48 | 27.81 | 8.26 | Predicted |
| 1b | 32.82 | 1.02 (Minimum) | 9.83 | 55.35 | 24.65 | 5.00 | Experimental |
| 2a | 34.84 | 4.08 (Maximum) | 6.42 | 49.51 | 22.96 | 12.53 | Predicted |
| 2b | 43.39 | 4.05 (Maximum) | 3.11 | 40.01 | 30 | 14.99 | Experimental |
| 3a | 24.98 (Minimum) | 1.64 | 8.46 | 47.96 | 30 | 7.04 | Predicted |
| 3b | 23.32 (Minumum) | 1.02 | 9.39 | 59.99 | 20 | 5.00 | Experimental |
| 4a | 44.31 (Maximum) | 3.99 | 3.24 | 40 | 30 | 14.99 | Predicted |
| 4b | 46.24 (Maximum) | 3.92 | 3.25 | 40.01 | 30 | 14.99 | Experimental |
| 5a | 32.29 | 1.02 | 8.96 (Maximum) | 50.87 | 26.24 | 7.89 | Predicted |
| 5b | 32.82 | 1.02 | 9.83 (Maximum) | 55.35 | 24.65 | 5.00 | Experimental |

**(a)**



TH-2589_156107040

| S. No. | Target Properties | | | Optimal Composition | | |
|---|---|---|---|---|---|---|
| | Porosity (%) | Average Pore Size (μm) | Flexural Strength (MPa) | Kaolin (wt.%) | Feldspar (wt.%) | Saw Dust (wt.%) |
| 1 | 37.26 (Maximum) | 1.29 (Minimum) | 3.11 | 51.93 | 20 | 13.07 |
| 2 | 34.94 (Maximum) | 4.05 (Maximum) | 6.35 | 49.68 | 22.85 | 12.47 |
| 3 | 33.61 | 0.67 (Minimum) | 9.84 (Maximum) | 54.14 | 25.55 | 5.31 |
| 4 | 33.88 | 4.05 (Maximum) | 7.34 (Maximum) | 47.21 | 25.07 | 12.72 |
| 5 | 33.72 (Maximum) | 3.88 | 7.46 (Maximum) | 47.02 | 25.48 | 12.5 |
| 6 | 34.65 (Maximum) | 4.05 (Maximum) | 7.02 (Maximum) | 45.00 | 25.98 | 14.02 |
| 7 | 33.74 (Maximum) | 0.77 (Minimum) | 9.97 (Maximum) | 54.62 | 25.38 | 5.002 |

**(b)**

## 3.8 Morphological, Structural and Thermal characterization

### 3.8.1 Thermogravimetric Analysis

Thermogravimetric analysis (Model: TG 209 F1 Libra, Make: NETZSCH) of the membrane precursor mixture was carried out in the temperature range of 30°C – 1000 °C. The obtained data (Figure 3.5) plot depicts three degradation stages for the precursor mixture that referred to moisture loss as first degradation stage; decomposition of hemicellulose, cellulose and lignin existent in the saw dust as second degradation stage and formation of metakaolinite from kaolinite as the third and last degradation stage. The TGA plot clearly indicates that after 850 °C, the weight % of the sample did not vary and therefore, the minimal sintering temperature can be set as 850 °C for the membrane sample.



TH-2589_156107040

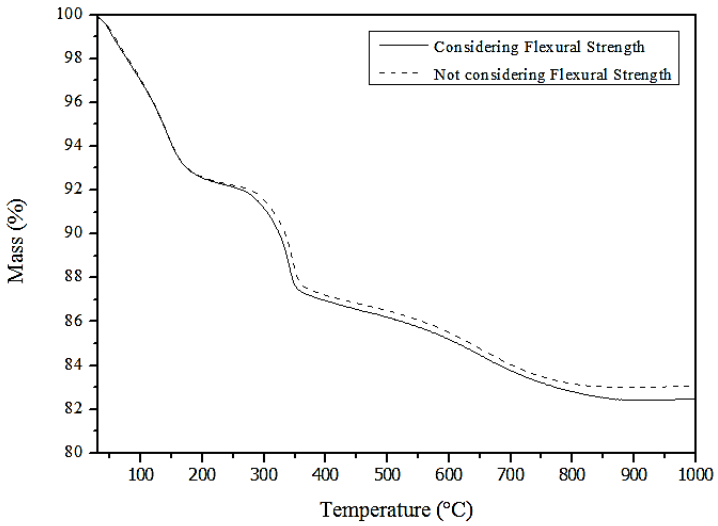


**Figure 3.5: TGA plots of optimal membrane precursor composition samples.**

### 3.8.2 Field Emission Scanning Electron Microscopy Analysis

The surface morphology of the fabricated membranes were studied using field emission scanning electron microscopy (FESEM (Zeiss)) (Figure 3.6 (a–b)). Using these images and ImageJ software, the average pore size of the fabricated membranes with optimal compositions were evaluated using procedures mentioned in the literature (Nandi et al., 2009). By considering and not considering flexural strength as additional design variables, the theoretical average membrane pore sizes (from image analysis) were obtained as 1.043 µm and 0.925 µm, respectively. Corresponding experimental values were 1.001 µm and 0.925 µm, respectively. Thus, the measurements and theoretical predictions of average membrane pore size are in good agreement with one another.



TH-2589_156107040

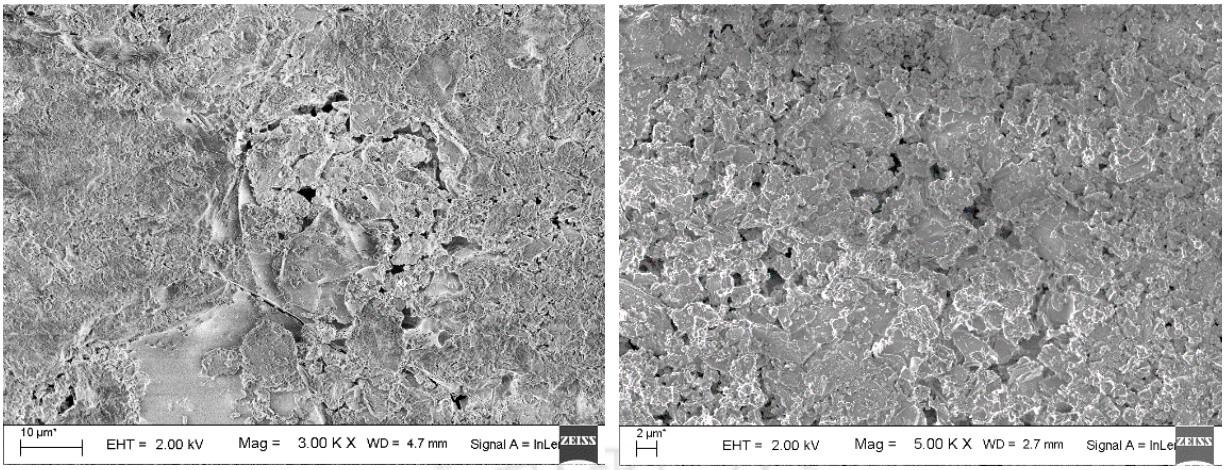


**(a)** **(b)**

**Figure 3.6: FESEM images of alternate ceramic membrane samples (a) morphological characteristics and (b) morphological and flexural strength characteristics cases.**

## 3.9 Summary

For the first time, this work considered MMD based RSM design approach for the optimization of low cost ceramic membrane precursor formulation to achieve minimal pore size. The conducted study indicated significant findings.

- The MMD was effective to evaluate upon the determination of optimal formulation of kaolin, feldspar and saw dust in a ceramic membrane formulation with fixed compositions of boric acid and sodium metasilicate.
- More complex dependence of pore size on compositional variations can be analyzed from obtained best-fit models. This was not the case for porosity.
- The consideration of flexural strength as an additional response variable can be omitted with the fact that the optimal formulations did not indicate significant variation to the composition obtained without flexural strength as response variable.



TH-2589_156107040

This work conveyed that MMD is an effective tool to deploy RSM based design methodology for further optimality of low cost ceramic membranes for microfiltration applications. Future work can target to enhance complexity of the compositions by considering variations in all precursor formulations. Thereby, ceramic membrane materials engineering research can be consolidated and refined with due insights from theoretical and simulation based insights.

## References

1. Bose, S., Das, C., 2014. Role of binder and preparation pressure in tubular ceramic membrane processing: design and optimization study using response surface methodology (RSM). Industrial & Engineering Chemistry Research 53, 12319-12329.
2. Emani, S., Uppaluri, R., Purkait, M.K., 2013. Preparation and characterization of low cost ceramic membranes for mosambi juice clarification. Desalination 317, 32-40.
3. Nandi, B., Das, B., Uppaluri, R., Purkait, M., 2009. Microfiltration of mosambi juice using low cost ceramic membrane. Journal of Food Engineering 95, 597-605.



TH-2589_156107040

TH-2589_156107040

# Chapter 4:

## Optimality of Sawdust Characteristics and Precursor Compositions during fabrication of Sub-micron Range Low Cost Ceramic Membranes

TH-2589_156107040

TH-2589_156107040

# Optimality of Sawdust Characteristics and Precursor Compositions during fabrication of Sub-micron Range Low Cost Ceramic Membranes

*In this chapter, the effect of precursor compositions and pore former characteristics have been targeted to achieve sub-micron range low cost ceramic membranes. Section 4.1 briefly presents the content relevant to the findings of the chapter. Following this, section 4.2 presents findings associated to the variations in the sawdust characteristics. Section 4.3 elaborates upon the influence of precursor compositions on the morphological characteristics of the low cost ceramic membranes. In sub-sections 4.2.1 and 4.2.2, the sawdust characteristics namely its average particle size and particle size distributions have been elaborated. Corresponding influence on membrane fluxes (section 4.2.2 and 4.3.1), average porosity (section 4.2.3 and 4.3.2), pore size and hydraulic permeability (section 4.2.4 and 4.3.3), membrane morphology (section 4.2.5) have been presented in said sub-sections, Relevance of empirical models to indicate interdependence of properties on the said precursor parameters has been presented in sections 4.2.6 and 4.3.4. A comparative assessment of findings with those available in the literature have been summarized in section 4.4. Finally, the key findings of the investigations has been presented in section 4.5*[#].

[#] Published Article: Chakraborty, S., Uppaluri, R., Das, C., (2020) "Effect of Pore Former (Sawdust) Characteristics on the Properties of Sub-micron Range Low Cost Ceramic Membranes", International Journal of Ceramic Engineering and Science, https://doi.org/10.1002/ces2.10061.

TH-2589_156107040

## Overview

*The bias for the conducted investigations is to achieve lower average membrane pore size than those obtained in the findings reported in Chapter 3. The primary sawdust characteristics considered in the study include its average particle size (brought forward through sieving with various mesh sizes) and concentration (reduced to achieve membranes with lower pore size). After achieving lowest pore size using optimal sawdust parameters, further reduction in pore size was targeted by varying precursor compositions. To do so, the sawdust content optimized in chapter 3 was taken as a basis to catalyze significant variations in the precursor composition. While pure water flux experiments were adopted to evaluate membrane permeabilities and average membrane pore size, Archimedes' principle was followed to determine porosity. Empirical models have been considered to evaluate upon the linear and non-linear dependence of measured properties with respect to said variations in either sawdust characteristics or precursor compositions.*

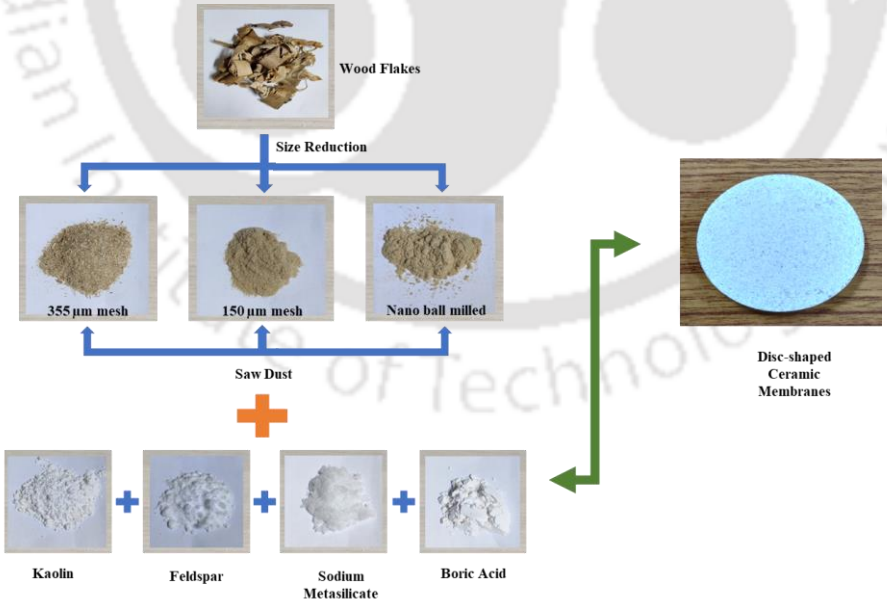




TH-2589_156107040

## 4.1 Introduction

The chapter reports findings associated to major objectives of the continued emphasis to achieve low cost ceramic membranes using sawdust precursors. The critical findings in the previous chapter report the precursor composition of CM1 membrane possessing significantly higher concentration of sawdust (8.19 wt.%). Therefore, significant scope exists to further reduce the sawdust concentration so as to achieve membranes with lower pore size. Further, the average particle size of the sawdust precursor can also be altered to further gain useful insights into the membrane morphology. Also, sawdust compositional optimality can be as well investigated upon reaching the critical limit of sawdust concentration in case further reduction in pore size is being targeted. In due course of such investigations, it became apparent that two major approaches had to be targeted. Among these the first approach refers to reduction in average pore size of the membrane through reduction in average particle size and concentration of sawdust. The second and later approach refers to the optimization of precursor composition keeping sawdust composition in a fixed proportion. In the first approach, sawdust composition was varied from 8 to 1 wt.%. Simultaneously, the average particle size of the sawdust was also varied by using various options such as sieving through 355, 150 and 75 µm mesh sieves and nano-ball milling method. The sieve size and sawdust composition was based on a trial and error based preliminary experiments. Respective nomenclature of membranes fabricated with alternate combinations of mesh size and sawdust concentration have been presented in Table 4.1. It can be noted that a minor variation in kaolin and feldspar content was as well accommodated so as to always maintain 85 wt.% of the total content of all constituents other than the binder (chosen to be fixed choice with 7.5 wt.% of both binders). Thereby, for the first approach, initially the compositional influence was investigated followed with the pore former particle size influence.



TH-2589_156107040

**Table 4.1: Summary of membranes targeted through variant sawdust characteristics.**

| S. No. | Mesh Size | Composition (wt. %) | | | Nomenclature |
|---|---|---|---|---|---|
| | | Kaolin | Feldspar | Sawdust | |
| 1 | 355 µm | 48.18 | 28.62 | 8.19 | CM1 |
| 2 | 355 µm | 50.18 | 29.81 | 5 | CM2 |
| 3 | 355 µm | 50.78 | 31.22 | 3 | CM3 |
| 4 | 355 µm | 51.78 | 32.22 | 1 | CM4 |
| 5 | 150 µm | 51.78 | 32.22 | 1 | CM5 |
| 6 | 75 µm | 51.78 | 32.22 | 1 | CM6 |
| 7 | Crushed through nano-ball mill | 51.78 | 32.22 | 1 | CM7 |

* Sodium metasilicate and boric acid were maintained at equal proportions of 7.5 wt.% each for all cases.

The fabricated membranes CM1 – CM7 have been subjected to characterizations such as pure water flux, hydraulic permeability, average porosity and average pore size.

The second and later approach adopted in the chapter refers to selection of 8.19 wt.% of sawdust as pore former composition (as affirmed in chapter 3 of the thesis and first part of the chapter) and average particle size based on 355 µm mesh sieve screening to eventually address the variation in the concentration of other components (kaolin, feldspar, boric acid and sodium metasilicate (binders)). Table 4.2 summarizes the compositions targeted to achieve sub-micron size pore size of the low cost ceramic membranes. These precursor compositions were obtained by conducting few trial and error experimental investigations to yield defect free membranes with good mechanical strength characteristics. An important perception with respect to the targeted compositional variations is with respect to the emphasis on the ratio of kaolin to feldspar ratio which was varied from about 0.48 to 2.05. This was targeted to achieve membranes with greater variation in the content of kaolin and feldspar.



TH-2589_156107040

**Table 4.2: Summary of membranes targeted through variant precursor compositions.**

| S. No. | Composition (wt. %) | | | | Nomenclature |
|---|---|---|---|---|---|
| | Kaolin | Feldspar | Boric Acid | Sodium Metasilicate | |
| 1 | 48.18 | 23.60 | 10 | 10 | VCM1 |
| 2 | 23.60 | 48.18 | 10 | 10 | VCM2 |
| 3 | 35.90 | 35.9 | 10 | 10 | VCM3 |
| 4 | 71.81 | 0 | 10 | 10 | VCM4 |
| 5 | 41.88 | 24.92 | 12.5 | 12.5 | VCM5 |
| 6 | 38.77 | 23.03 | 15 | 15 | VCM6 |

The value range of 0.48 to 2.05 was based on few trial and error investigations. Similarly, it is apparent that VCM5 and VCM6 membrane samples were targeted by considering greater content of binders (metasilicate and boric acid). For all samples VCM1 – VCM6, the sawdust content was chosen as 8.19 wt.%. Subsequently, the adopted procedures are similar to those reported for the first and former approach i.e., evaluation of pure water flux, average pore size, average porosity and hydraulic permeability.

A critical reasoning associated to selection of higher sawdust content (8.19 wt.%) for the compositions reported in Table 4.2 is due to the reason that these compositions have additional flexibility to invoke further reductions in membrane pore size, in case it is required for various applications. This will not be the case if lower sawdust concentration of 1 wt.% is considered along with finest mesh size.

## 4.2 Influence of Sawdust Characteristics on Membrane Morphological Characteristics

### 4.2.1 Sawdust Particle Characteristics

The sawdust particles were sieved using screens of various mesh sizes (355 µm, 150 µm, 75 µm). Also, a nano-ball mill process sample was also considered to evaluate upon the role



TH-2589_156107040

of nano-milling to achieve lowest average particle size and best possible reduction in average membrane pore size. Using FESEM, particle size distribution of sawdust powder were analyzed. The obtained results have been depicted in Figure 4.1. As shown, for the first three cases, compared to the nano-ball mill processed sawdust (Figure 4.1 (d)), the particle size distributions varied widely for the first three cases (Fig. 4.1 (a) – (c)). For the nano-ball mill processed sample, it can be analyzed that the particles were with even distributions and therefore possessed lower variation in size distributions. Thus, it will be interested to evaluate upon the role for particle size distributions on the pore size, porosity and hydraulic permeability of the ceramic membranes. Relevant discussions will be addressed in the later sections of the PhD thesis.

Based on the software assisted analysis, sawdust sieved through 355, 150 and 75 µm mesh sieves possessed an average particle size of 254 µm, 88 µm and 56 µm, respectively. Comparatively, the sawdust obtained from nano-ball milling possessed an average particle size of 39 µm. Thus, it is apparent that with reducing sieve size, particle size reduction can be achieved and nano-ball mill processed sample possessed lowest average particle size.

Figure 4.2 depicts the particle size distributions of sawdust powders obtained using various screens and nano-ball milled processing. These distributions have been obtained using ImageJ software. The particle size distributions varied from 138 – 559 µm, 26 – 326 µm, 12 – 167 µm and 14 – 100 µm for 355 µm, 150 µm, 75 µm and nano-ball milled cases respectively.



TH-2589_156107040

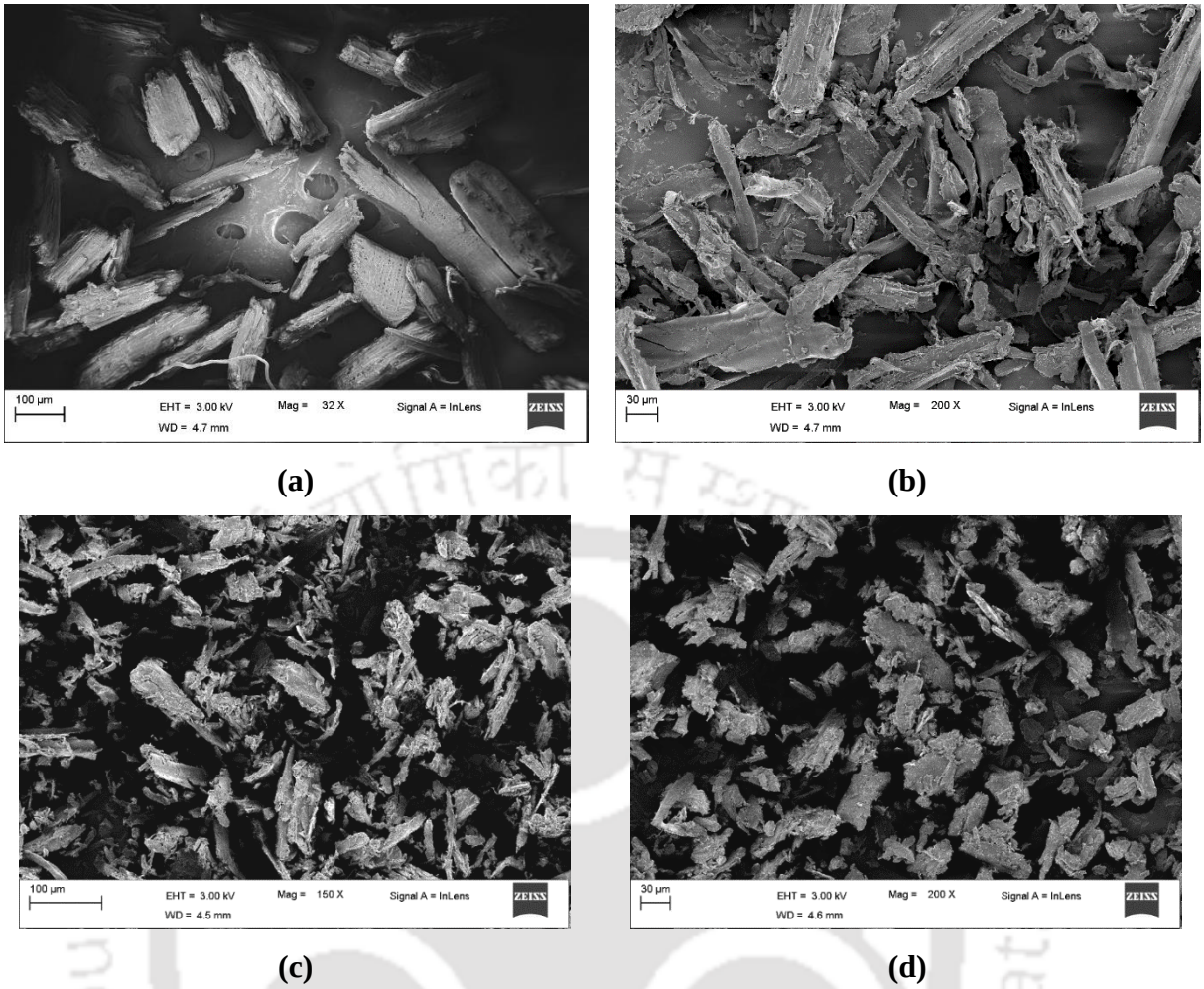


**Figure 4.1: FESEM images of sawdust samples obtained using (a) 355 µm sieve, (b) 150 µm sieve, (c) 75 µm sieve and (d) nano-ball mill**

It may be noted that the particle size of sawdust sieved through each mesh sizes, exceeds the sieve number. This shows that sieving took place both horizontally and vertically which led to increase in particle size. However, the particle size distribution plot conveys that particles larger than the sieve sizes are less predominant.

Thus, it is apparent that among all cases, the particle size distributions were significantly wider for 150 µm and 355 µm mesh sieve cases. However, further reduction in particle size distributions are apparent for the 75 µm mesh sieve case. Among all cases, the nano-ball mill processed sawdust sample possessed significantly narrow particle size distribution.



TH-2589_156107040

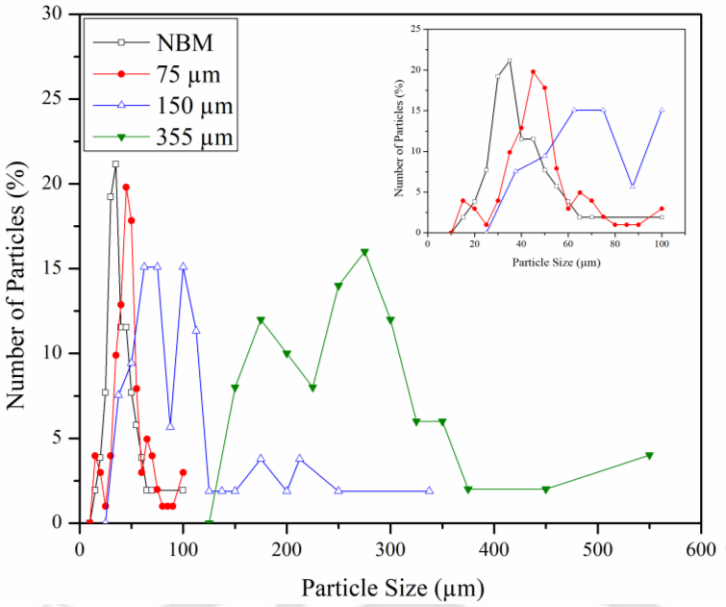


**Figure 4.2: Particle size distributions of various sawdust samples.**

Hence, with uniform particle sizes, it is very likely that the pore size distributions of the membranes fabricated with this sample would be significantly uniform.

### 4.2.2 Pure Water Flux Data

Figure 4.3 depicts the pure water flux variation with transmembrane pressure for the fabricated membranes CM1 – CM7. As shown, the pure water flux varied linearly with applied pressure and this is in accordance with the basic flux equation. The pure water flux varied from $1.50 \times 10^{-4} – 4.24 \times 10^{-4}$ $m^3.m^{-2}.s^{-1}$ , $1.06 \times 10^{-4} – 2.67 \times 10^{-4}$ $m^3.m^{-2}.s^{-1}$, $0.66 \times 10^{-4} – 1.86 \times 10^{-4}$ $m^3.m^{-2}.s^{-1}$, $0.61 \times 10^{-4} – 1.70 \times 10^{-4}$ $m^3.m^{-2}.s^{-1}$, $0.29 \times 10^{-4} – 0.87 \times 10^{-4}$ $m^3.m^{-2}.s^{-1}$, $0.28 \times 10^{-4} – 0.82 \times 10^{-4}$ $m^3.m^{-2}.s^{-1}$ and $0.17 \times 10^{-4} – 0.51\times 10^{-4}$ $m^3.m^{-2}.s^{-1}$ for CM1, CM2, CM3, CM4, CM5, CM6 and CM7 membranes, respectively.



TH-2589_156107040

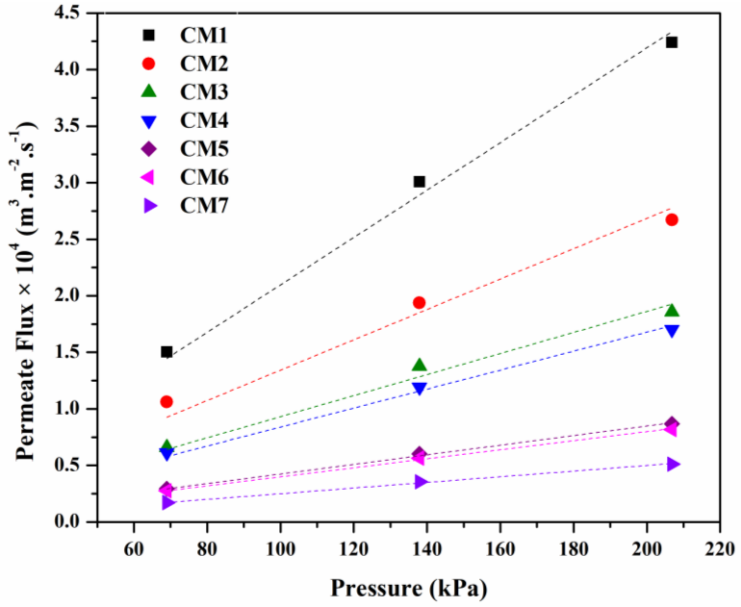


**Figure 4.3: Pure water flux plot of alternate membranes fabricated with variant sawdust characteristics.**

Thus, with increasing sawdust concentration, the pure water flux followed increased trends. Similar trends are apparent with respect to the average particle size of the sawdust samples. This is due to the reason that a reduction in sawdust concentration facilitates a reduction in both membrane porosity and pore size and hence the water flux. Similarly, a reduction in average particle size of sawdust samples is also anticipated to reduce the average membrane pore size and hence lower membrane flux.

### 4.2.3 Average Membrane Porosity

Figure 4.4 illustrates the influence of sawdust particle size and concentration on the average membrane porosity of the ceramic membranes. The average membrane porosity values of 28.47 %, 27.12 %, 23.12 %, 21.69 %, 21.08 %, 19.76 % and 16.29 % have been obtained for CM1, CM2, CM3, CM4, CM5, CM6 and CM7 membranes, respectively. Thus, it is apparent that with a reduction in sawdust concentration from 8 to 1 wt.%, the average porosity reduced from 28.47 – 21.69 % for the sawdust samples processed with 355 µm sieve. Thus, the



TH-2589_156107040

porosity reduction trends are appropriate, given that significant reduction in porosity with sawdust concentration is detrimental for the higher desired fluxes of microfiltration range membranes. Also, for the case of lower sawdust concentration of 1 wt.%, the sieve size reduction from 355 – 75 µm enabled a marginal reduction in porosity from 21.69 – 19.76 %. Such reduction is also promising for the real world microfiltration applications of fabricated low cost ceramic membranes.

The membrane prepared with best sawdust particle characteristics (nano-ball milled processed sample) possessed a lower porosity of 16.29 %. This is due to greater uniformity of sawdust particles for the case in comparison to the sieved sawdust samples. Such uniformity facilitated better synergy of all constituents during sintering process. The sieve based classification on the other hand did not facilitate uniform pore sizes. This is due to the uneven particle size distributions that translated into higher porosity of the fabricated ceramic membranes.

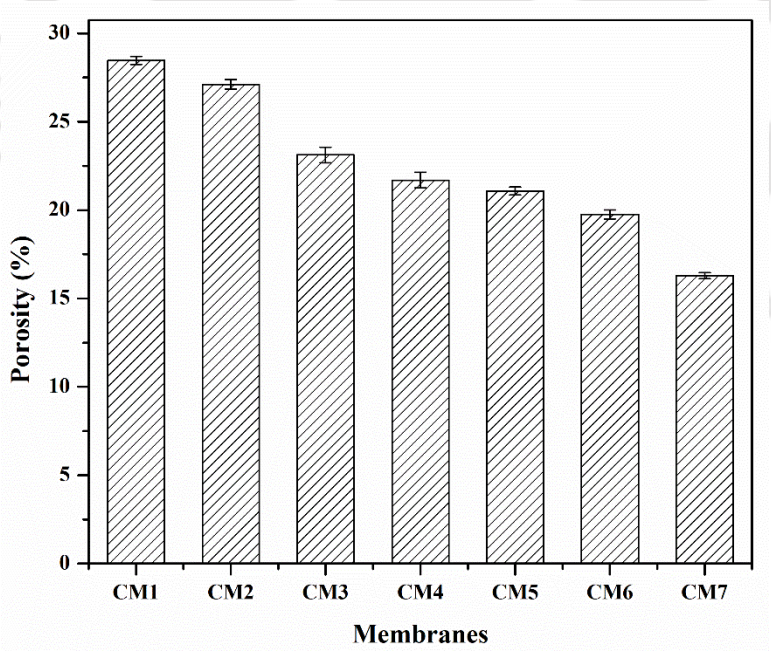


**Figure 4.4: Average porosity characteristics of membranes fabricated with variant sawdust characteristics.**



TH-2589_156107040

### 4.2.4 Average Hydraulic Permeability and Average Membrane Pore Size

Figure 4.5 (a) depicts the hydraulic permeability of CM1 – CM7 membranes. Due to significant reduction in the membrane pore size and marginal reduction in membrane porosity, the hydraulic permeability of the membranes reduced significantly from $2 \times 10^{-9}$ to $0.2 \times 10^{-9}$ $m^3.m^{-2}.s^{-1}.Pa^{-1}$. The reduction in pore size enables lower permeation rate of water through the membrane matrix. Similarly, porosity reduction provides lower void content to allow water passage and hence reduce water permeability.

The average membrane pore size was determined using average porosity and average hydraulic permeability of the membranes (Figure 4.5 (b)). As shown, for CM1 – CM3 membrane samples, the average pore size reduced from 1 – 0.74 µm. This is due to reduction in sawdust content from 8 to 1 wt.%. The findings are in good agreement with the hypothesis that lower sawdust content reduces pore former content and void formation during sintering process. Thus, it is apparent that sawdust content reduction did not catalyze significant reduction in the average membrane pore size.

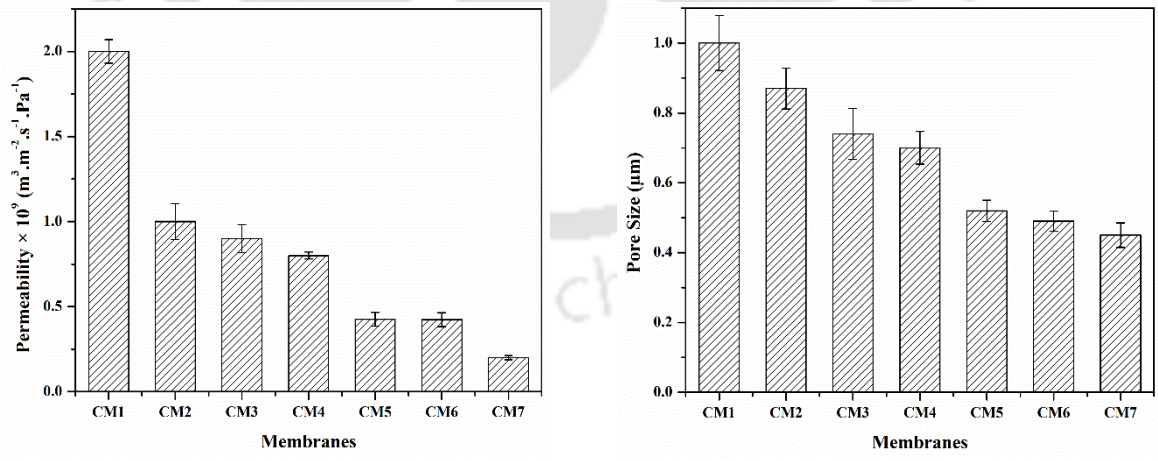


**(a)** **(b)**

**Figure 4.5: Morphological characteristics of membranes fabricated with variant sawdust properties (a) average hydraulic permeability, and (b) average pore size.**



TH-2589_156107040

Similar inferences can be deduced from CM3 and CM4 samples that indicated only a reduction by 0.04 µm in average pore size. Therefore, to further reduce pore size significantly, lower sieve size classification and nano ball milling was considered. For 1 wt.% sawdust concentration, the reduction in sieve size from 355 – 75 µm enabled a significant reduction in average membrane pore size from 0.7 – 0.45 µm (membranes CM4 and CM7). Thus, smaller pore size was achieved due to particle size reduction facilitated with lower mesh size. Further, it can be noted that the average pore size for the CM7 is marginally lower (0.45 µm) than that of CM6 obtained with 75 µm sieve (0.49 µm). In other words, nano-ball milling approach need not be followed, as significant reduction in pore size was not achieved. Finest screen can be used to achieve membranes with similar average pore size values. In summary, membranes with lower pore size of 0.45 µm can be achieved by targeting finer screen and lower pore former content (1 wt.% of sawdust). These coupled effects enabled successful reduction in void space formation during membrane sintering process.

### 4.2.5 Membrane Morphological Characteristics

The membranes CM1 – CM7 with diverse combinations of pore sizes and porosities were subjected to FESEM image analysis. The surface morphology and pore size distribution of the membranes possessing an average pore size of 1 µm, 0.7 µm and 0.45 µm (CM1, CM4 and CM7 membranes, respectively) have been presented in Figure 4.6. It is apparent that for both CM1 and CM4, the membrane pore sizes varied widely. Also, CM7 membrane possessed evenly distributed pores (Figure 4.6 (d)). This is due to the fact that the membrane was prepared using sawdust subjected to nano-ball milling process and the process indicated achievement of evenly sized particles (section 4.2.2).



TH-2589_156107040

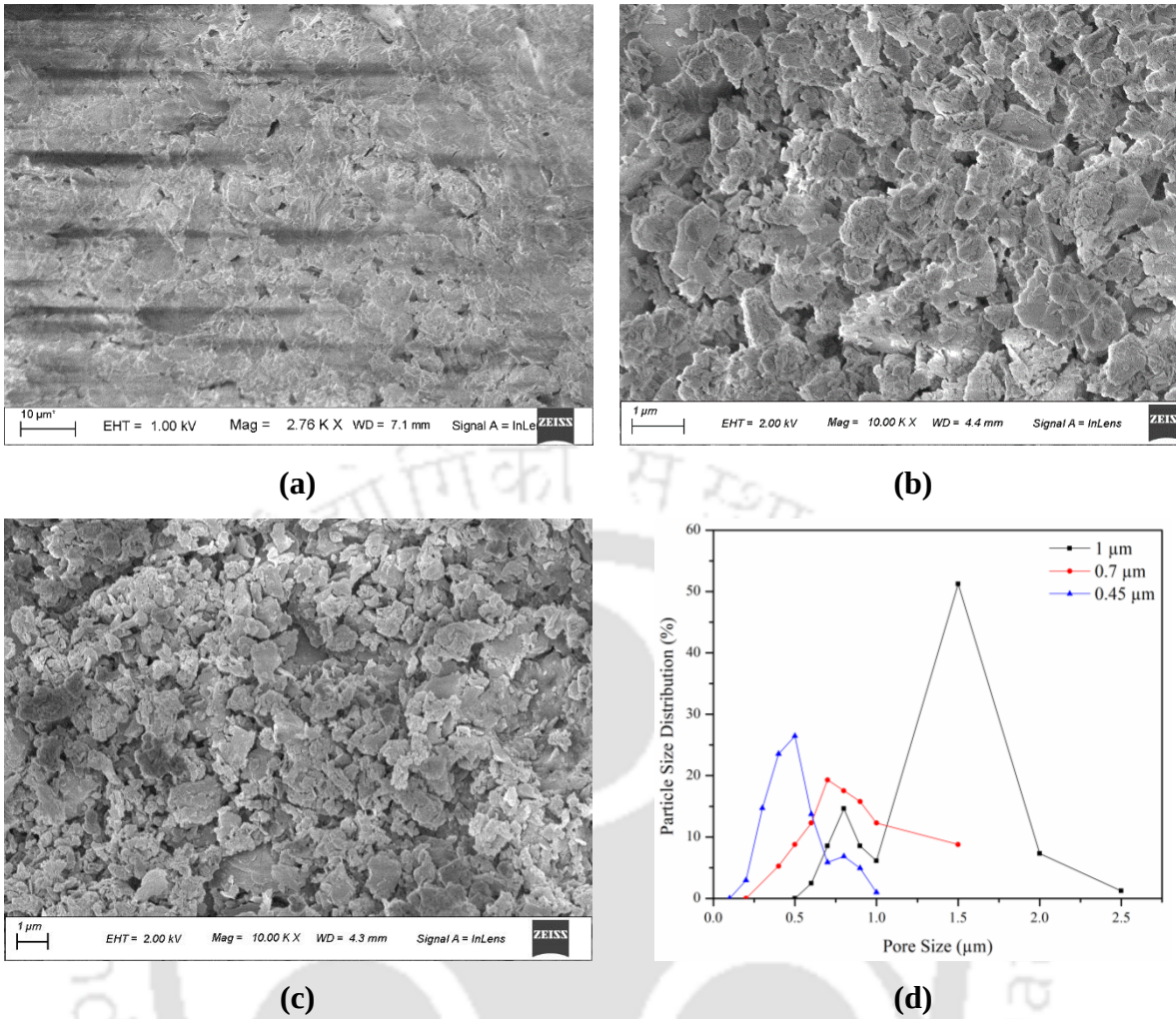


**Figure 4.6: FESEM micrographs of (a) CM1, (b) CM3, and (c) CM7 membranes; and (d) pore size distribution plot based on FESEM image analysis.**

### 4.2.6 Identification of Best Fit Empirical Models

Empirical modeling approach was adopted to judge upon the associated non-linear interaction of independent parameters (sawdust concentration and sawdust average particle size) on the average membrane porosity and pore size. Such studies would be useful to gain useful insights into the complexity associated to pore former role in achieving the desired attributes of ceramic membranes. Thus, the obtained average membrane pore size and porosity data for all membranes (CM1 – CM7) have been subjected to empirical model fitness studies using trial and error based consideration of alternate fitness models as simpler functions of sawdust



TH-2589_156107040

characteristics such as average particle size and concentration. Among various alternate models, the best fit model was a linear combination of independent parameters for pore size and a complex model of simple quadratic and Michaelis-Menten equation for the porosity. Thus, non-linear and interactive dependence on both parameters is apparent for porosity but not pore size. Table 4.3 summarizes the best fit models and their associated parameters and fitness indices. It can be analyzed that both best fit models possessed higher $R^2$ values (0.993 and 0.949) and hence the models are promising. Also, the parameter sensitivities indicate that among sawdust concentration ([SD]) and sawdust particle size ([SDPS]), the former had significant influence upon the average pore size ($d_p$) of the ceramic membranes. However, for the porosity case, the effect was contrary i.e., [SDPS] had significant impact on the parameter in comparison with [SD]. Also, [SD] significantly reduced with increasing order of the non-linear terms. The parity plots for both cases (Figure 4.7) indicate a plot close to the 45° line and affirmed good fitness of the suggested best fit empirical models. Thus, using the empirical models, the membrane morphological parameters can be predicted within the chosen range of independent parameters.

**Table 4.3: Best fit empirical models and their parameters to represent average pore size and porosity of CM1 – CM7 membranes.**

| **Models** | **Pore Size (µm)** | | | **Porosity (%)** | | | |
|---|---|---|---|---|---|---|---|
| | $d_p = k + a[SD] + b[SDPS]$ | | | $\varepsilon = a[SD] + b[SD]^2 + \frac{c[SDPS]}{d + [SDPS]}$ | | | |
| **Model Coefficients** | k | a | b | a | b | C | d |
| | 0.3778 | 0.0434 | 0.0014 | 0.9308 | $4.0215\times10^{-5}$ | 22.6054 | 15.4228 |
| **$R^2$** | | 0.993 | | | 0.949 | | |



TH-2589_156107040

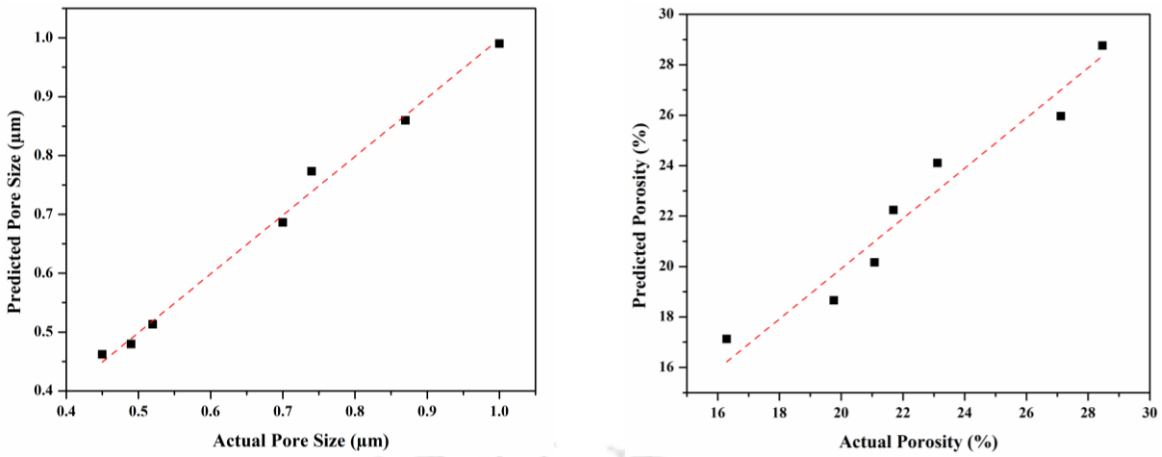


**(a)** **(b)**

**Figure 4.7: Parity plot of morphological characteristics of CM1-CM7 membranes (a) average pore size, and (b) average porosity.**

## 4.3 Influence of Precursor Compositions on Membrane Morphological Characteristics

### 4.3.1 Pure Water Flux

Figure 4.8 represents the pure water flux of VCM1 – VCM6 membranes. For all cases, the fluxes increased linearly with pressure. However, prominent variations do exist due to variation in precursor composition. The highest flux of 1.28 – 3.58 × $10^{-4}$ ($m^3.m^{-2}.s^{-1}$) was obtained for VCM4 membrane. The lowest flux of 6.89 × $10^{-7}$ – 0.18 × $10^{-7}$ was obtained for VCM6 membrane. All other membrane pure water flux were in similar range but not for VCM5, whose values are marginally lower than those obtained for other membranes. The membrane VCM4 was fabricated with zero feldspar content and with higher fluxes, the membrane indicates larger combinations of pore size and porosity of the membrane. Membranes VCM1, VCM2 and VCM3 exhibited similar pure water flux trends ranging from 1.05 – 3.78 × $10^{-4}$ ($m^3.m^{-2}.s^{-1}$).



TH-2589_156107040

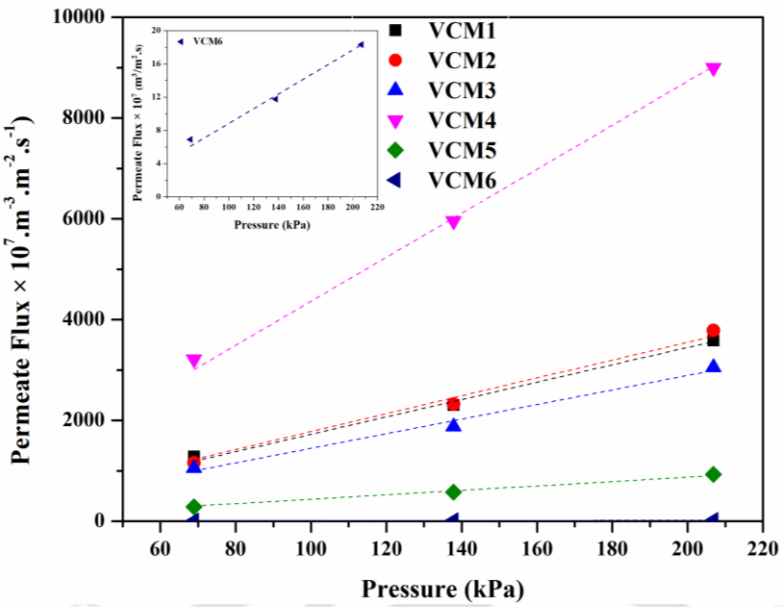


**Figure 4.8: Pure water flux plot of alternate membranes fabricated with variant precursor compositions.**

In this regard, it shall be noted that the binder composition (sodium metasilicate and boric acid) was kept 10 wt.% for each binder in VCM1 – VCM4 membranes and was increased to 12.5 wt.% and 15 wt.% each for VCM5 and VCM6, respectively. With enhanced binder composition, membrane pure water flux values reduced significantly. Upon sintering, the binders facilitate increased bonding between precursor materials and provide greater strength to the membrane structure. A significant reduction in pure water flux for the VCM5 and VCM6 membranes affirms that the binders play a significant role in varying the membrane properties and hence the flux data.

### 4.3.2 Average Porosity

The average porosity plot followed trends similar to that of the pure water fluxes reported in the previous sub-section. Figure 4.9 depicts the porosity variation for various membrane samples. The maximum and minimum porosity of 30.43 and 14.08 % were obtained for VCM4 and VCM6 membranes, respectively. For VCM5 membrane, an average porosity of



TH-2589_156107040

17.89 % was obtained which is marginally higher than that of VCM6. Thus, it is apparent that compared to feldspar content, higher kaolin content enabled higher porosities. Higher porosities also indicate lower strength of the membrane material. Since sawdust composition was kept fixed for the investigations conducted with VCM1 – VCM4 membranes, it can be assumed that its role is negligible to alter the evaluated porosity trends. On the other hand, the binder composition can be analyzed to be significant to influence the porosity. Both kaolin and feldspar content had contrasting effect on the average membrane porosity. Among these, kaolin had more positive influence on the membrane porosity. Among the membranes, kaolin content was maximum for VCM4 membrane and followed decreased trend in the order of VCM1, VCM3 and VCM2. Kaolin is well known for its plasticity towards the membrane. On the contrary, feldspar contributes towards bonding of the materials. Thus, with increasing kaolin content, the average porosity increases and with increasing feldspar content, the average membrane porosity gets reduced.

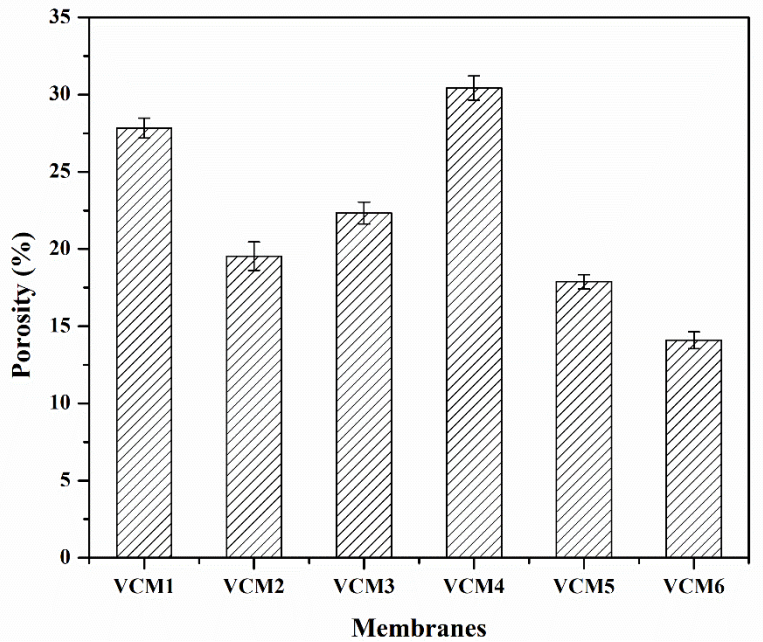


**Figure 4.9: Average porosity characteristics of membranes fabricated with variant precursor compositions.**



TH-2589_156107040

### 4.3.3 Average Hydraulic Permeability and Average Pore Size

The hydraulic permeability and average membrane pore size trends for the membranes were similar to those reported for pure water fluxes and average porosity in the earlier sub-sections (4.2.2 and 4.2.3). Figure 4.10 depicts the variations of hydraulic permeability and average membrane pore size for all membranes VCM1 – VCM6. Highest combinations of hydraulic permeability and average pore size were obtained for VCM4 membrane (1.39 µm and $40.83 \times 10^{-10}$ $m^3.m^{-2}.s^{-1}.Pa^{-1}$). The lowest combinations of these parameters were obtained for the VCM6 membrane (0.09 µm and $0.09 \times 10^{-10}$ $m^3.m^{-2}.s^{-1}.Pa^{-1}$). Ceramic membranes VCM1, VCM2 and VCM3 possess similar pore size and hydraulic permeabilities and indicate marginal variations in their values. With increasing binder concentration, the membrane pore size varied significantly. This is due to the observation that the microfiltration membranes drifted towards nanofiltration range membranes with a significant reduction in pore size from micron range to nanometer range. For VCM5, the average pore size was 0.56 µm (560 nm). The lowest average pore size of 0.09 µm (90 nm) was obtained for the VCM6 membrane. Hence, with minor variation in kaolin and feldspar content and with a smaller variation in binder content, significant variation in membrane properties can be targeted to broaden the scope of the membranes for wider application. For these cases, the hydraulic permeability values reduced significantly from $4.21 \times 10^{-10}$ $m^3.m^{-2}.s^{-1}.Pa^{-1}$ to $0.09 \times 10^{-10}$ $m^3.m^{-2}.s^{-1}.Pa^{-1}$. The lowest average pore size of 90 nm of the membrane will have a significant role in membrane fouling and hence reduced fluxes with real time applications. Such studies are to be addressed in future investigations.

An important observation among VCM1 – VCM3 membranes is that with variation in kaolin to feldspar ratio from 0.48 to 2.05, the average pore size did not vary significantly. This was not the case for porosity, with highest porosity being obtained for the case of kaolin to feldspar ratio of 0.5.



TH-2589_156107040

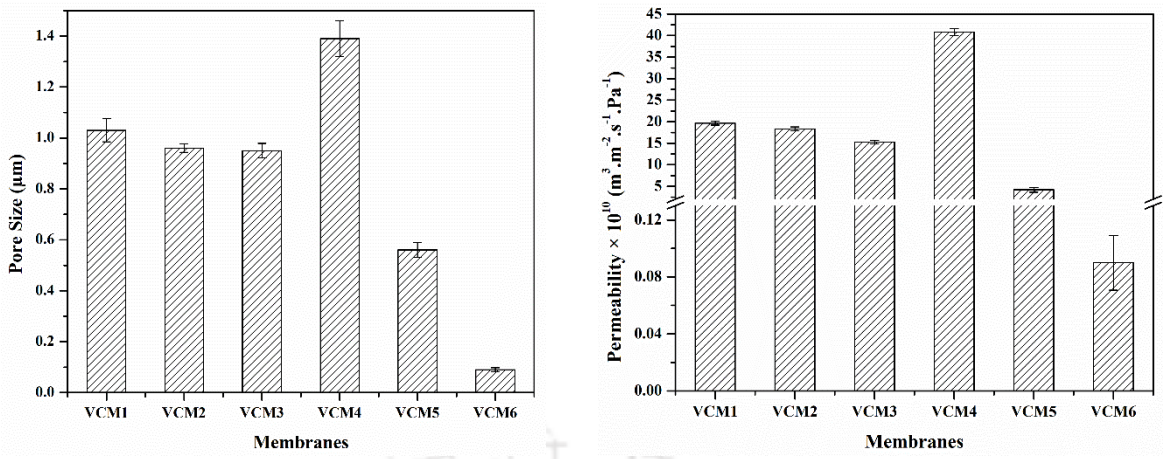


**(a)** **(b)**

**Figure 4.10: Morphological characteristics of membranes fabricated with variant precursor compositions (a) average hydraulic permeability, and (b) average pore size.**

These observations are anticipated to provide useful guidelines to further research upon the fabrication of low cost ceramic membranes with controlled and tailor made combinations of pore size and porosity.

### 4.3.4 Search for Best Fit Empirical Models

Similar to the empirical model fitness conducted for the earlier set of experimental data, empirical model fitness studies have been conducted for the determination of best fit model to represent pore size and porosity as functions of kaolin, feldspar and binder content. The best fit model was identified based on highest possible $R^2$ value of the parity plot for predicted and experimental data sets of dependent variables (pore size and porosity). The independent variables for the study refer to compositions of kaolin ([K]), feldspar ([F]), sodium metasilicate and boric acid. Since the binders (sodium metasilicate and boric acid) were taken in equal proportions for all membranes, they have been considered as a single variable ([B]).



TH-2589_156107040

To determine the best fit model, alternate models such as linear, quadratic, cubic, PolyRatio, Michaelis-Menten, cubic, special cubic and other non-linear models have been considered for the fitness studies. Since several independent variables are involved, it can be difficult to achieve the best fit model. Therefore, to ease the modeling effort and obtain useful insights with respect to the contribution of each composition, fitness studies were also considered by choosing a single variable at a time influencing the dependent variable. Thereby, a combination of such models has also been considered to obtain the best fit empirical model. Among all cases, PolyRatio model was found to be the fit model to represent the dependent variables in terms of independent variables (Equations 4.1 and 4.2). Relevant fitness parameters have been also presented in Table 4.4.

$$d_p = p + \frac{a + b[K]^{n_1}}{c + d[K]^{n_2}} + \frac{e + f[F]^{n_3}}{g + h[F]^{n_4}} + \frac{i + j[B]^{n_5}}{k + l[B]^{n_6}} \tag{4.1}$$

$$\varepsilon = p + \frac{a + b[K]^{n_1}}{c + d[K]^{n_2}} + \frac{e + f[F]^{n_3}}{g + h[F]^{n_4}} + \frac{i + j[B]^{n_5}}{k + l[B]^{n_6}} \tag{4.2}$$

It can be observed that the binders play a very important role to influence both average pore size and average porosity. This has been ascertained with the higher coefficients for the term in the modeling expression. However, the role of kaolin and feldspar are different for the both cases. For the case of porosity, the coefficients of [K] and [F] have similar influence with [F]. However, for the pore size, [F] had larger influence in comparison with [K]. Figure 4.11 (a) and (b) depict the parity plots of pore size and porosity determined with the best fit empirical models. The $R^2$ value for the porosity parity plot is 0.999 and indicates a promising trend. However, a lower but promising value of $R^2$ (0.959) was obtained for the average pore size parity plot. Significant scattering can be observed for the pore size case (Figure 4.11 (a)) in



TH-2589_156107040

comparison with the porosity case (Figure 4.11 (b)). For lower average pore size, significant variation in the predicted and measured average pore size is apparent. The model equation of pore size was found to be rather complex with larger number of coefficient terms and higher coefficient values. For lower pore size cases, complexities and interactions are likely to increase. Due to this reason, larger variation in actual vs predicted data is apparent.

**Table 4.4: Best fit empirical models and their parameters to represent average pore size and porosity of VCM1 – VCM6 membranes.**

| Model Coefficients | Pore Size ($d_p$) (µm) | Porosity ($\varepsilon$) (%) |
|---|---|---|
| $p$ | $1 \times 10^{-6}$ | $1 \times 10^{-6}$ |
| $a$ | 0.8729 | $1 \times 10^{-6}$ |
| $b$ | 0.6624 | 0.0111 |
| $c$ | 1.0072 | 4.1785 |
| $d$ | 1.5450 | 4.5319 |
| $e$ | 18.5916 | $1 \times 10^{-6}$ |
| $f$ | 0.1487 | 1.1079 |
| $g$ | 48.4956 | 5.3013 |
| $h$ | 4.0417 | 0.0021 |
| $i$ | 40318.89 | 9.2167 |
| $j$ | 5824.605 | 8.8252 |
| $k$ | 28623.22 | $1 \times 10^{-6}$ |
| $l$ | $1 \times 10^{-6}$ | 0.0001 |
| $n_1$ | $1 \times 10^{-6}$ | 2.3751 |
| $n_2$ | 5.1454 | 0.2946 |
| $n_3$ | 2.8050 | 2.5104 |
| $n_4$ | 29.1949 | 3.9675 |
| $n_5$ | $1 \times 10^{-6}$ | $1 \times 10^{-6}$ |
| $n_6$ | 2.8708 | 2.9784 |
| $R^2$ | 0.959 | 0.999 |



TH-2589_156107040

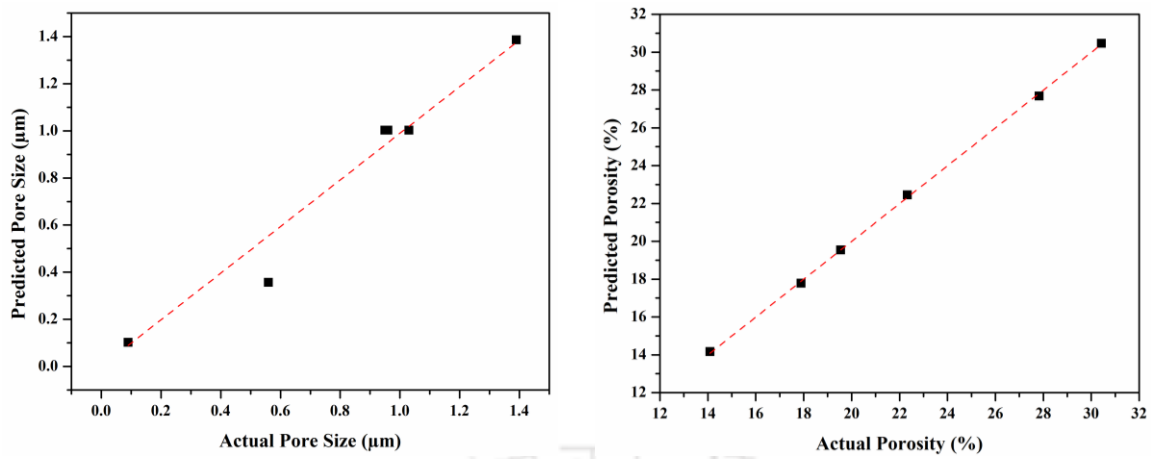


**(a)** **(b)**

**Figure 4.11: Parity plot of morphological characteristics of VCM1 – VCM6 membranes (a) average pore size, and (b) average porosity.**

## 4.4 Comparative Assessment of Membrane Morphological Characteristics

The low cost ceramic membrane morphological parameters obtained in this study have been compared with the most competent literature data that involved biological resources as pore forming agents. In the first study being addressed in this chapter, with minimal variation in the pore former composition and judicious variation in the average particle size distribution of the sawdust, the average membrane pore size has been reduced successfully from 1 to 0.45 µm. In the second study being addressed in the chapter, with minimal variation in other precursors and binder composition, the average pore size obtained was 0.09 µm. The literature reported lowest pore size is about 0.23 µm that was achieved with potato starch as pore former but with higher porosity (44.9 %) (Table 4.5). Further, it needs to be observed that for all other cases that involved biological resources as pore formers, the average pore size and porosity of the membranes were significantly higher (1 – 0.21 µm and 23.44 – 43.96 % for corn starch, ~ 4 µm and 44.9 – 67.3 % for rice husk, and 35.50 – 56.30 % for cationic manioc starch as pore formers and egg shell and natural clay as other organic precursors).



TH-2589_156107040

Thus, in the available prior art data, the data pertaining to starch pore formers is not promising due to the fact that starch is significantly expensive pore forming agent. Hence, only one prior art qualifies for a comparative assessment i.e., the data being reported using rice husk as the pore forming agent.

**Table 4.5: Data summary of ceramic membranes fabricated with low cost pore forming agents.**

| S. No. | Pore Former | Other Precursors (wt.%) | Pore Size (µm) | Porosity (%) | References |
|---|---|---|---|---|---|
| 1 | Corn Starch<br>Quantity: 0-15 wt.%<br>Average Particle Size: 53 µm | • Alumina: 75 – 90<br>• Bentonite: 10 | 1 – 2.1 | 23.44 – 43.96 | Yang and Tsai (2008) |
| 2 | Cationic manioc starch (CMS) grade Superion 300<br>Quantity: 0 – 15 wt.%<br>Average Particle Size: 23.26 µm | • Egg Shell: 0 – 15<br>• Water: 10<br>• Natural Clay: 75 – 85 | – | 35.50 – 56.30 % | Xavier et al. (2019) |
| 3 | Potato Starch<br>Quantity: 0 – 30 wt.% | • Kaolin: 35 – 50<br>• Alumina: 35 – 50 | 0.23 – 2.35 | 44.9 – 67.3 | Lorente-Ayza et al. (2015) |
| 4 | Rice Husk<br>Quantity: 5 – 40 wt.%<br>Average Particle Size: 75 – 600 µm | • Sucrose: 20<br>• Alumina: 40 – 75 | Fine pores: 4 µm<br>Interconnected Pores: 50 – 516 µm (length) | 20 – 66 | Mohanta et al. (2014) |
| 5 | Sawdust<br>Quantity: 1 – 8 wt.%<br>Average Particle Size: 39 – 254 µm | • Kaolin: 48.18 – 51.78<br>• Feldspar: 28.62 – 32.22<br>• Sodium Metasilicate: 7.5<br>• Boric Acid: 7.5 | 0.45 – 1 | 16.29 – 28.47 | This Work |
| 6 | Sawdust<br>Quantity: 8 wt.%<br>Average Particle Size: 254 µm | • Kaolin: 38.77 – 71.18<br>• Feldspar: 0 – 48.18<br>• Sodium Metasilicate: 10 – 15<br>• Boric Acid: 10 – 15 | 0.09 – 1.39 | 14.09 – 30.43 | This Work |



TH-2589_156107040

Compared to the reported data of this work, the thesis addressed comparatively lower average pore sizes of the fabricated membranes and is hence a unique novelty that needs to be advocated towards the efficacy of the saw dust pore forming agent. In summary, the research findings of this work clearly demonstrate the need for utilizing waste biological resources such as sawdust in comparison with the value added biological starch as pore former agent to successfully achieve sub-micron size pore size of the low cost ceramic membranes. This can be suitably targeted by varying the organic pore forming agent concentration and its average particle size. Thus, the literature does not provide ample scope towards customized reduction in average pore size of the membrane and target advanced applications associated with the clarification of vegetable extracts.

## 4.5 Summary

In this chapter, the utility of waste biological resource such as sawdust as well as other precursor components have been effectively investigated with the primary objective of the pore size reduction of the low cost ceramic membranes and enhanced applications of the membranes with sub-micron pore size. The key findings of the work can be outlined as follows.

- For a variation in the composition of the sawdust from 8 to 1 wt.%, the membrane pore size and porosity underwent a marginal reduction from 1 to 0.7 µm and 28.47 – 21.69 % respectively.
- A further reduction in the average membrane pore size and porosity from 0.7 – 0.45 µm and 21.69 – 16.29 % can be suitably targeted by reducing the average particle size of the sawdust from 254 to 39 µm.
- To achieve further reduction in pore size, a fundamental understanding of the contribution of all precursors is required and hence further experiments had been



TH-2589_156107040

conducted by considering variable kaolin to feldspar ratio and enhanced binder content. Such precursor composition variation facilitated significant reduction in pore size (1.39 to 0.09 µm) and porosity (30.43 to 14.09 %) of the ceramic membranes.

- It has been observed that increasing binder composition had a significant influence on the average pore size of the membranes to potentially alter them from microfiltration range to ultrafiltration range.
- The empirical model fitness studies provided useful insights. The sawdust characteristic parameters indicated a linear dependence of average pore size and non-linear dependence of average porosity upon concentration and particle size of the sawdust pore former. For increased complexity associated to the variation of precursor compositions, a highly non-linear dependence with respect to variations in the precursor compositions has been inferred.

Further research can be suitably targeted for the low cost ceramic membranes using other types of biological waste resources as pore forming agents. With these developments, it is anticipated that the low cost ceramic membrane applications can be suitably extended to finer microfiltration operations such as vegetable extract processing and microbial filtration to thereby enhance the economic competitiveness of ceramic membranes in the process industries.

## References

1. Lorente-Ayza, M.M., Sánchez, E., Sanz, V., Mestre, S., 2015. Influence of starch content on the properties of low-cost microfiltration ceramic membranes. Ceramics International 41, 13064-13073.



TH-2589_156107040

2. Mohanta, K., Kumar, A., Parkash, O., Kumar, D., 2014. Processing and properties of low cost macroporous alumina ceramics with tailored porosity and pore size fabricated using rice husk and sucrose. Journal of the European Ceramic Society 34, 2401-2412.
3. Xavier, L.A., de Oliveira, T.V., Klitzke, W., Mariano, A.B., Eiras, D., Vieira, R.B., 2019. Influence of thermally modified clays and inexpensive pore-generating and strength improving agents on the properties of porous ceramic membrane. Applied Clay Science 168, 260-268.
4. Yang, G.C., Tsai, C.-M., 2008. Effects of starch addition on characteristics of tubular porous ceramic membrane substrates. Desalination 233, 129-136.



TH-2589_156107040

# Chapter 5:

## Techno-economic Feasibility of Low Cost Ceramic Membranes for Bottle Gourd Juice Clarification

TH-2589_156107040

TH-2589_156107040

# Techno-economic Feasibility of Low Cost Ceramic Membranes for Bottle Gourd Juice Clarification

*In this chapter, the feasibility of sawdust and kaolin based low cost ceramic membranes has been targeted for the clarification of bottle gourd juice. After a brief introduction in section 5.1, the following sections elaborate upon the findings of the carried research work. Section 5.2 addresses the flux decline characteristics associated to microfiltration studies conducted with the said membranes. Following this, section 5.3 presents the findings associated to the most suitable fouling mechanism. Sections 5.4 and section 5.5, respectively detail upon the prominent membrane permeation resistances and morphological changes that occurred in due course of microfiltration. The clarified juice quality and its microbial characteristics have been addressed in sections 5.6 and 5.7, respectively. A comparative assessment with best literature data has been conveniently presented in section 5.8 so as to converge upon the efficacy of the prepared membranes towards the said application. Using the best obtained data, research findings associated to the economic evaluation of a small scale membrane process in conjunction with competent technologies have been presented in section 5.9. Finally, a summary of the key findings of the conducted research has been outlined in section 5.10*[#].

[#] Published Article: Chakraborty, S., Das, C., Uppaluri, R., (2020) "Feasibility of Low-Cost Kaolin Based Ceramic Membranes for Organic *Lagernaria siceraria* Juice Production", Food and Bioprocess Technology, 13: 1009-1023.

TH-2589_156107040

## Background

*This chapter addresses the technical and cost competitiveness of microfiltration and centrifugation to produce organic clarified bottle gourd juice. For fresh and centrifuged juices, microfiltration (MF) experiments were conducted for transmembrane pressures ranging from 103.4 -172.4 kPa. Using flux decline trend analyses, resistances in series model and recovery ratios, the microfiltration data were extensively analyzed to evaluate upon the extent of irreversible membrane fouling. Feed, centrifuged and permeate juice samples have been subjected to physico-chemical and nutritional studies.*

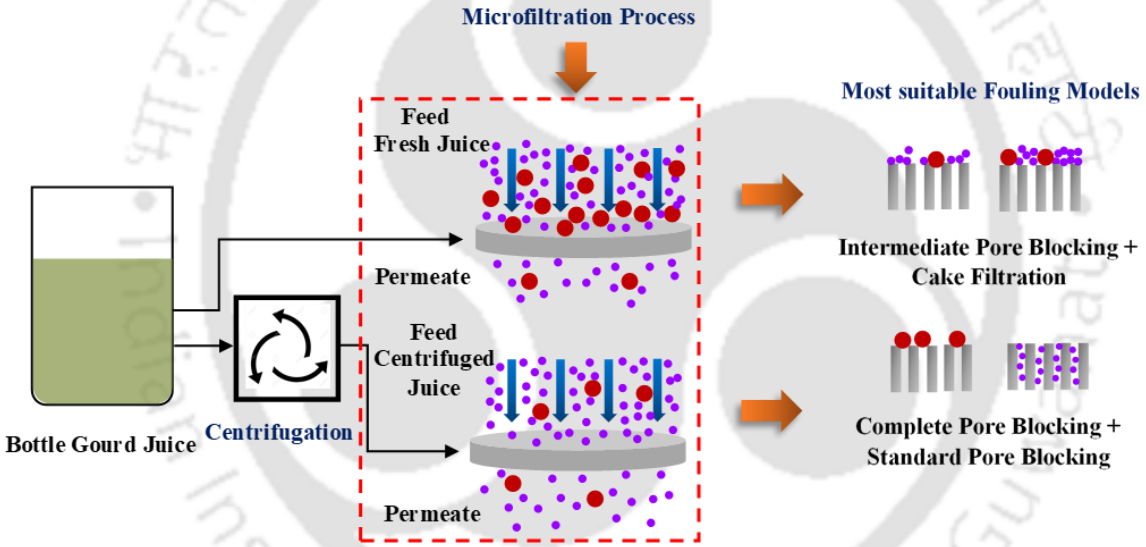


## 5.1 Introduction

With the due consideration of technical and economic evaluation of low cost ceramic membranes and centrifugation technologies as central objectives, this chapter addresses the microfiltration of bottle gourd juice using low cost ceramic membranes that were addressed in the thesis. Dead-end microfiltration studies have been conducted for the CM1 membrane reported in the Chapter 4 of the thesis. The average pore size of the CM1 membrane was



TH-2589_156107040

about ~1 µm. The rationale behind the application of the CM1 membrane towards bottle gourd juice clarification has been based on the average membrane pore size being indicated in the relevant prior art for the clarification of fruit and vegetable juices. The literatures (Emani et al. (2013) and Nandi et al. (2015)) affirmed that for raw or unprocessed fruit juice systems, the membranes possessing a sub-micron range average pore size may indicate poor membrane flux and greater membrane fouling in comparison with the membranes with an average pore size of 1 µm (Emani et al., 2013; Nandi et al., 2011). Such an analysis also corroborates with the fact that the raw/untreated juices constitute significantly higher quantities of fibrous materials and solid particulates and hence have greater tendency to contribute to irreversible membrane fouling. To further augment upon such hypothesis, the membrane performance characteristics will be addressed for variant membrane morphological characteristics in the subsequent chapters of the PhD thesis. Three different trans-membrane pressure differentials (103.4, 137.9 and 172.4 kPa) have been considered to evaluate upon membrane performance in terms of pertinent flux decline, irreversible and reversible fouling and permeate quality. Both fresh and centrifuged juice have been chosen as feed systems to evaluate membrane performance. The permeate quality of the bottle gourd juice was evaluated in terms of carbohydrate content, protein content, vitamin C content, total flavonoids, total phenol content, pH, salt content, TDS, color and clarity. The data for both fresh and centrifuged juices were measured atleast thrice. The flux data have been evaluated to exist within an error of ± 3 %.

Deploying alternate modeling approaches, the pertinent flux decline was evaluated to obtain useful insights with respect to the extent of irreversible fouling. Finally, compared to conventional polymeric membrane and centrifugation technologies, the techno-economic competitiveness of best performing low cost ceramic membrane based microfiltration technology has been addressed.



TH-2589_156107040

## 5.2 Flux Decline Analysis

Figure 5.1 (a) presents the flux decline profiles for the fresh bottle gourd juice feed system at pressure differentials of 103.4, 137.9 and 172.4 kPa. The figure conveys that the corresponding flux decline trends varied from $1.99 \times 10^{-5} - 0.17 \times 10^{-5}$ $m^3.m^{-2}.s^{-1}$, $3.12 \times 10^{-5} - 0.18 \times 10^{-5}$ $m^3.m^{-2}.s^{-1}$ and $2.14 \times 10^{-5} - 0.17 \times 10^{-5}$ $m^3.m^{-2}.s^{-1}$ for a variation in pressure differential and time from 103.4 – 172.4 kPa and 1 – 80 min respectively. Thus, the flux decline severity was maximum for 103.4 kPa case, moderately lower for 172.4 kPa case and lowest for 137.9 case. Conventionally, due to the prominence or reduction in pore blocking, corresponding flux decline severity is anticipated to either enhance or reduce uniformly with the applied pressure differential across the membrane. However, for the case, a mixed trend existed. At the lower applied pressure of 103.4 kPa, severe flux decline was very likely due to a prominent role of pore blocking. For this reason, the membrane could not enable the greater passage of the clarified juice through its modifies porous structure.

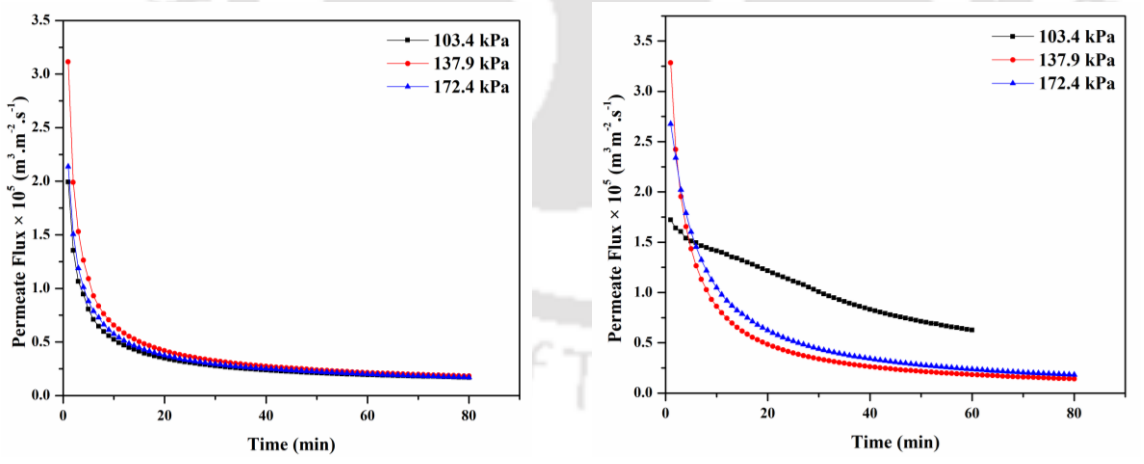


**(a)** **(b)**

**Figure 5.1: Flux decline profiles of (a) fresh and (b) centrifuged bottle gourd juice MF system.**



TH-2589_156107040

However, at the higher pressure of 172.4 kPa, the moderately improved flux decline was possibly due to the onset of cake filtration that significantly restricted enhanced pore blockage. The intermediate pressure (137.9 kPa) indicated lowest severity in flux decline and hence best flux data. This is possibly due to the optimal contribution of both pore blocking and cake filtration towards pertinent reduced flux decline.

Similar microfiltration studies have been conducted for the same membrane and for the centrifuged juice feed system. The obtained flux decline profiles have been totally different from those being obtained for the fresh feed juice system (Figure 5.1 (b)). As shown, for the centrifuged feed case, the bottle gourd juice flux varied from $1.72 \times 10^{-5} – 0.63 \times 10^{-5}$ $m^3.m^{-2}.s^{-1}$, $3.29 \times 10^{-5} – 0.14 \times 10^{-5}$ $m^3.m^{-2}.s^{-1}$ and $2.68 \times 10^{-5} – 0.18 \times 10^{-5}$ $m^3.m^{-2}.s^{-1}$ for a variation in time from 1 – 60 min for 103.4 kPa and 1 – 80 min for 137.9 and 172.4 kPa cases respectively. For comparative purposes, it can be analyzed that the flux decline profile being reported by Emani et al. (2013) for the dead-end microfiltration of mosambi juice (centrifuged) using 0.89 µm pore size membranes varied from 5.5 to $0.9 \times 10^{-5}$ $m^3.m^{-2}.s^{-1}$ in 30 min at the corresponding pressure of 206.7 kPa (Emani et al., 2013). The flux obtained in this study is thus considered to be comparable to the literature data, given the variations in the complexity of the feed constitution of the bottle gourd juice in terms of particulate matters with respect to the mosambi juice. Some flux values have been significantly higher for the centrifuged juice cases in comparison with those being obtained for the fresh feed juice. Since severe flux decline existed independently of the applied pressure, the application of cross-flow MF in lieu of the dead-end MF is anticipated to enhance the flux by about 4 to 5 times for similar process conditions (Li et al., 2018; Mondal et al., 2018).

In summary, for the fresh feed juice system, the flux decline severity was maximum for 137.9 kPa but not 172.4 kPa and 103.4 kPa. Also, comparatively higher flux was obtained for the centrifuged juice case. Thus, the juice pretreatment prior to membrane permeation can be



TH-2589_156107040

analyzed to have strongly influenced pore blocking characteristics under variant transmembrane pressure differential conditions. This may be due to fact that certain critical, heavier and complex biological macromolecules may have been omitted during the centrifugation process. These macromolecules can be thus analyzed to have a prominent role in influencing the flux decline trends of fresh juice systems. It will be interesting to evaluate upon their role on the permeate quality for both feed juice cases.

Thus, in conclusion, one can infer that the transmembrane fluxes for the best case were not significantly high to ensure upon industrial scale productivity. This may be also the case for the cross flow MF system. If such a case exists, it is important to focus towards the control morphological characteristics of the fabricated membrane. Such variations can be targeted through variations such as controlled humidity conditions, rate of heating or cooling etc., in due course of the membrane fabrication. Thus, the conducted research indicates interesting scenarios to address in due course of future research in the field of ceramic membrane based bottle gourd juice clarification.

Since transmembrane flux declined significantly for both fresh and centrifuged juice cases and applied pressure differentials, it is apparent that the flux decline did exist independently of applied pressure and for both feed systems. Hence, the membrane performance can be anticipated to significantly enhance with cross-flow mode of the operation.

Table 5.1 summarizes the flux decline coefficient (FDC) and flux recovery ratio (FRR) values for various cases. For the fresh juice, pressure variation did not have a significant effect on both FDC (91.5 – 94.13 %) and FRR (94.54 – 91.89 %). On the other hand, significant variations in FDC and FRR do exist for the centrifuged juice with respect to applied pressure.



TH-2589_156107040

**Table 5.1: FDC and FRR data of bottle gourd juice: CM1 membrane system.**

| Applied Pressure (kPa) | FDC (%) | | FRR (%) | |
|---|---|---|---|---|
| | Fresh | Centrifuged | Fresh | Centrifuged |
| 103.4 | 91.57 | 63.59 | 94.54 | 94.73 |
| 137.9 | 94.13 | 95.69 | 91.89 | 69.28 |
| 172.4 | 92.01 | 93.22 | 93.67 | 79.28 |

The lowest value of FRR (69.28 %) was obtained for the centrifuged juice at 137.9 kPa. This is possibly due to irreversible fouling that occurred due to significant pore blocking phenomena. For the same case, lowest value of FDC (63.59 %) was obtained at 103.4 kPa. This affirms that the lower pressure was favorable for the centrifuged juice. However, this needs to be further verified from the permeate quality, given the fact that higher flux need not confirm upon good permeate quality. On the other hand, for the fresh juice, the FRR values are significantly higher and indicated higher reversible fouling (about 6 – 7 %).

## 5.3 Competent Fouling Mechanisms

For fresh and centrifuged bottle gourd juice feed systems, Figures 5.2 and 5.3 respectively present the fitness plots for various Hermia flux decline models. Relevant procedures have been duly elaborated in section 2.7 of the Ph.D. thesis. Corresponding $R^2$ and fitness parameter values have been presented in Table 5.2.

For the fresh juice case, highest $R^2$ values have been obtained for cake filtration model (Table 5.2) and Figure 5.2 (d) also indicates the same. However, negative intercepts were obtained and this affirms that cake filtration model is physically invalid. Following this, the model with maximum $R^2$ values infers upon the intermediate pore blocking model. For the model, fortunately, positive slope and intercept have been obtained.



TH-2589_156107040

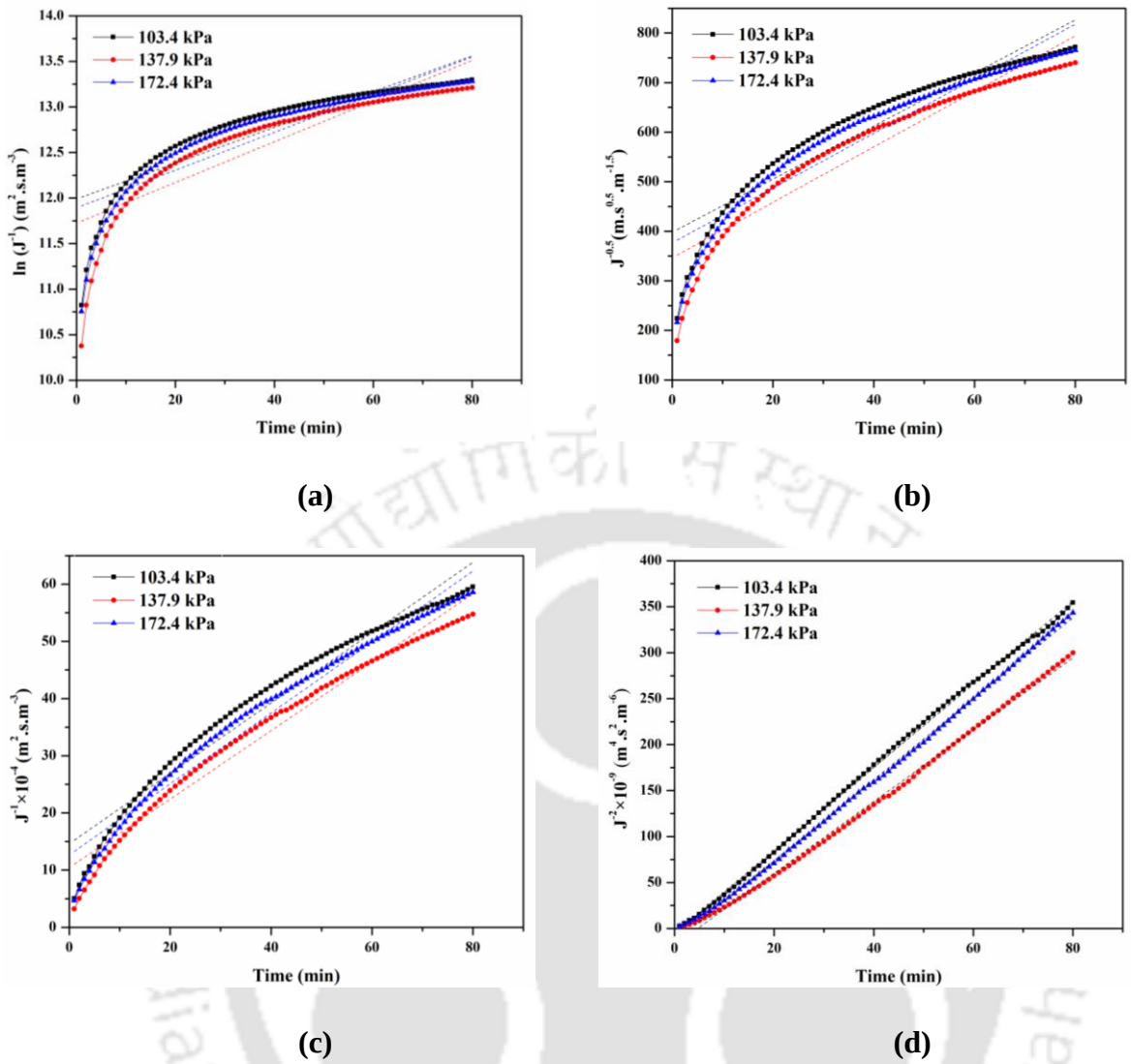


**Figure 5.2: Fitness plots of Hermia fouling models to represent pertinent flux decline during fresh bottle gourd juice MF, (a) complete pore blocking, (b) standard pore blocking, (c) intermediate pore blocking, and (d) cake filtration models.**

Overall, both Figure 5.2 and Table 5.2 affirm that any pore blocking model is unable to represent pertinent flux decline for the chosen feed juice system. Hence, short term flux decline of the fresh juice appears to have a significant deviation from the standard pore blocking models. The fitness of intermediate pore blocking model at a later stage of microfiltration for the case indicates that for the later time frame, the membrane pore sizes



TH-2589_156107040

became comparable with the particle sizes of the solutes in the feed juice constitution. Thereby, significant insitu flux decline occurred.

For the centrifuged juice case (Figure 5.3), at 103.4 kPa pressure, complete and standard pore blocking models had similar competence in terms of model fitness ($R^2$ values are very close to one another and close to 1). However, at higher pressure, intermediate pore blocking model can be analyzed to be most competent. The lack of fitness of cake filtration model conveys that the membrane morphology needs to be further engineered to achieve minimal fouling, maximum flux and appropriate permeate quality.

Further insights into the onset of various fouling mechanisms with time of microfiltration operation can be obtained by considering the flux decline profiles as a combination of short term and long-term flux declines. To do so, the flux decline data was regarded as a combination of two separate data sets obtained for two time intervals (1 – 15 min and 15 min onwards). The data set for each time duration was subjected to fitness studies using the four alternate fouling mechanism models for both feed juice cases.

**Table 5.2: Fitness parameters of alternate Hermia fouling models for fresh bottle gourd juice: CM1 membrane system.**

| Type of juice | Applied Pressure (kPa) | Complete Pore Blocking | | | Standard Pore Blocking | | | Intermediate Pore Blocking | | | Cake Filtration | | |
|---|---|---|---|---|---|---|---|---|---|---|---|---|---|
| | | $R^2$ | Slope | Intercept | $R^2$ | Slope | Intercept | $R^2$ | Slope | Intercept | $R^2$ | Slope | Intercept |
| Fresh Juice | 103.4 | 0.778 | 0.019 | 11.99 | 0.890 | 5.357 | 397.96 | 0.956 | 0.615 | 14.618 | 0.9993 | 4.526 | -5.529 |
| | 137.9 | 0.780 | 0.022 | 11.724 | 0.906 | 5.599 | 346.35 | 0.972 | 0.598 | 10.443 | 0.997 | 3.905 | -18.162 |
| | 172.4 | 0.796 | 0.020 | 11.892 | 0.906 | 5.516 | 376.66 | 0.969 | 0.620 | 12.672 | 0.999 | 4.407 | -14.468 |
| Centri-fuged Juice | 103.4 | 0.997 | 0.017 | 8.689 | 0.995 | 0.857 | 74.954 | 0.987 | 0.174 | 5.1268 | 0.953 | 0.373 | 0.438 |
| | 137.9 | 0.863 | 0.029 | 9.144 | 0.966 | 2.395 | 89.258 | 0.999 | 0.848 | 3.5177 | 0.957 | 6.351 | -75.448 |
| | 172.4 | 0.900 | 0.028 | 8.947 | 0.977 | 2.063 | 81.357 | 0.999 | 0.653 | 3.0437 | 0.952 | 3.853 | -46.097 |



TH-2589_156107040

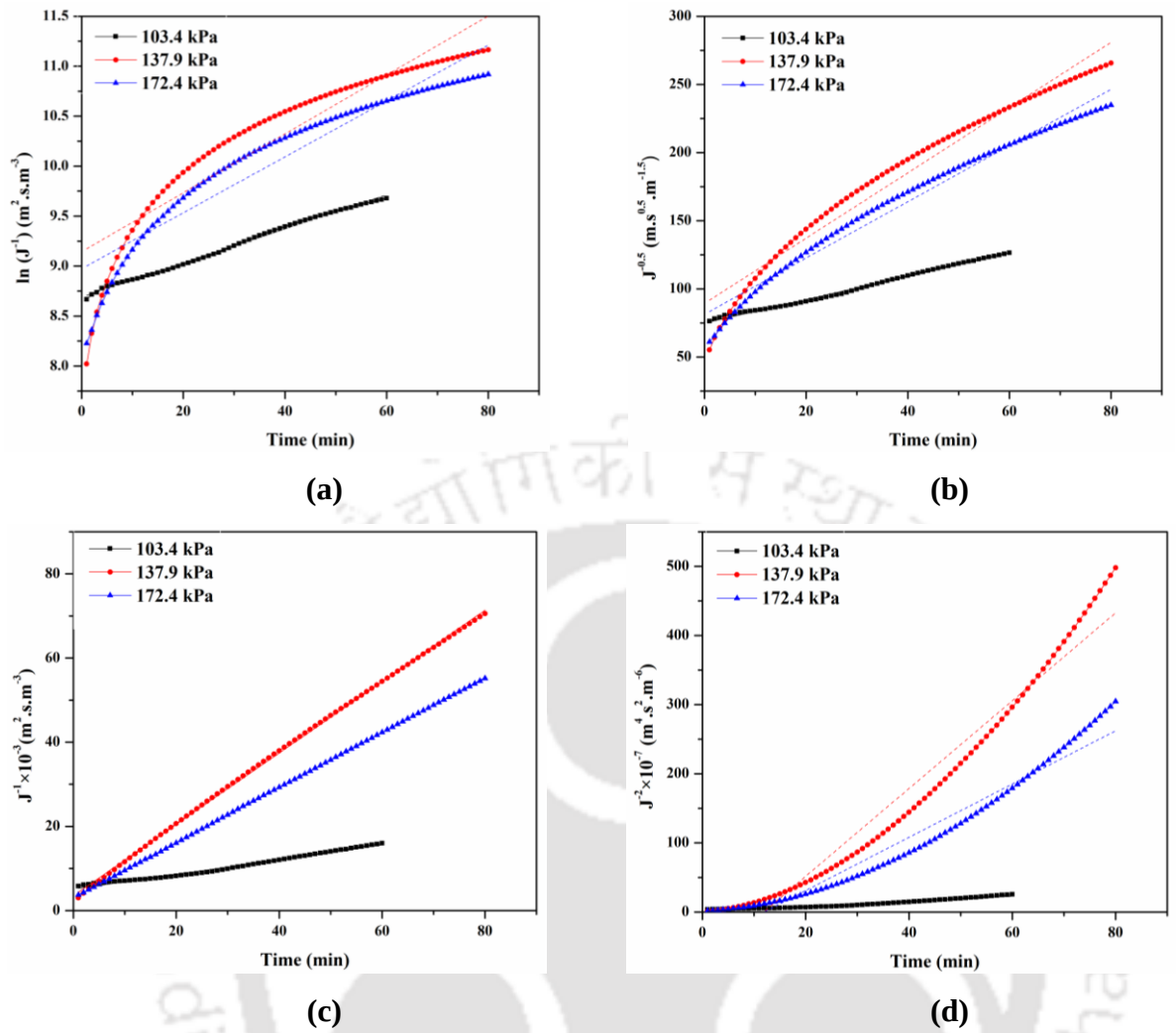


**Figure 5.3: Fitness plots of Hermia fouling models to represent pertinent flux decline during centrifuged bottle gourd juice MF, (a) complete pore blocking, (b) standard pore blocking, (c) intermediate pore blocking, and (d) cake filtration models.**

Table 5.3 (a) summarizes the $R^2$ values obtained for the alternate Hermia models for the fresh juice. The data presented in the table affirms that standard and intermediate pore blocking models have best fitness to represent initial (short term) and final (long term) flux decline profiles respectively. Similar observations are apparent for centrifuged juice feed system (Table 5.3 (b)).



TH-2589_156107040

**Table 5.3: Fitness parameters of dual Hermia fouling models to represent pertinent flux decline of (a) fresh and (b) centrifuged juice MF.**

| Models | Parameters | Applied Pressure (kPa) | | | | | |
|---|---|---|---|---|---|---|---|
| | | 103.4 | | 137.9 | | 172.4 | |
| | | Initial | Final | Initial | Final | Initial | Final |
| Complete Pore Blocking | $R^2$ | 0.893 | 0.939 | 0.887 | 0.948 | 0.904 | 0.949 |
| | Slope | 0.097 | 0.012 | 0.112 | 0.014 | 0.098 | 0.013 |
| | Intercept | 11.116 | 12.395 | 10.725 | 12.177 | 11.019 | 12.301 |
| Standard Pore Blocking | $R^2$ | 0.951 | 0.963 | 0.953 | 0.963 | 0.959 | 0.973 |
| | Slope | 17.736 | 3.981 | 17.72 | 4.283 | 17.122 | 4.212 |
| | Intercept | 249.94 | 474.66 | 212.74 | 419.7 | 237.31 | 449.37 |
| Intermediate Pore Blocking | $R^2$ | 0.985 | 0.981 | 0.989 | 0.990 | 0.989 | 0.989 |
| | Slope | 1.334 | 0.517 | 1.166 | 0.523 | 1.234 | 0.537 |
| | Intercept | 5.295 | 20.054 | 3.148 | 14.649 | 4.700 | 17.327 |
| Cake Filtration | $R^2$ | 0.997 | 0.999 | 0.991 | 0.999 | 0.993 | 0.999 |
| | Slope | 4.095 | 4.501 | 2.805 | 4.045 | 3.484 | 4.503 |
| | Intercept | -3.887 | -4.443 | -4.292 | -2.596 | -3.741 | -1.979 |

**(a)**

| Models | Parameters | Applied Pressure (kPa) | | | | | |
|---|---|---|---|---|---|---|---|
| | | 103.4 | | 137.9 | | 172.4 | |
| | | Initial | Final | Initial | Final | Initial | Final |
| Complete Pore Blocking | $R^2$ | 0.952 | 0.994 | 0.944 | 0.959 | 0.974 | 0.963 |
| | Slope | 0.016 | 0.017 | 0.109 | 0.020 | 0.085 | 0.021 |
| | Intercept | 8.692 | 8.683 | 8.202 | 9.62 | 8.262 | 9.360 |
| Standard Pore Blocking | $R^2$ | 0.960 | 0.998 | 0.985 | 0.988 | 0.993 | 0.990 |
| | Slope | 0.692 | 0.910 | 4.958 | 2.061 | 3.704 | 1.830 |
| | Intercept | 77.108 | 72.661 | 56.585 | 107.91 | 59.617 | 94.389 |
| Intermediate Pore Blocking | $R^2$ | 0.967 | 0.997 | 0.999 | 0.999 | 0.999 | 0.999 |
| | Slope | 0.113 | 0.194 | 0.931 | 0.833 | 0.652 | 0.652 |
| | Intercept | 5.929 | 4.271 | 2.275 | 4.363 | 3.000 | 3.104 |
| Cake Filtration | $R^2$ | 0.978 | 0.984 | 0.969 | 0.979 | 0.977 | 0.975 |
| | Slope | 0.154 | 0.451 | 1.806 | 7.279 | 1.074 | 4.444 |
| | Intercept | 3.471 | -2.915 | -3.364 | -127.56 | -1.035 | -79.295 |

**(b)**

## 5.4 Membrane Permeation Resistances

Figure 5.4 (a) and 5.4 (b) depict the variation of total permeation resistances for fresh and centrifuged juice feed systems respectively. As shown, the total permeation resistance increased non-linearly with increasing time for all cases. For the fresh juice, these values enhanced from 5.39 $\times 10^{12}$ to 63.92 $\times 10^{12}$ $m^2.m^{-3}$, 4.60 $\times$ $10^{12}$ to 78.40 $\times$ $10^{12}$ $m^2.m^{-3}$ and



TH-2589_156107040

$8.38 \times 10^{12}$ to $104.86 \times 10^{12}$ $m^2.m^{-3}$ respectively for 103.4 kPa, 137.9 kPa and 172.4 kPa applied pressure cases. Corresponding permeation resistances for the centrifuged juice feed system enhanced from $0.64 \times 10^{12}$ to $1.75 \times 10^{12}$ $m^2.m^{-3}$, $0.44 \times 10^{12}$ to $10.3 \times 10^{12}$ $m^2.m^{-3}$ and $0.68 \times 10^{12}$ to $10.08 \times 10^{12}$ $m^2.m^{-3}$ respectively. For all cases, the pure water permeation resistance of the membrane was evaluated to be $1.98 \times 10^{11} \pm 0.43 \times 10^{11}$ $m^2.m^{-3}$. Thus, it is apparent, that with increasing transmembrane pressure, the total permeation resistance enhanced for fresh juice case.

For centrifuged juice, total permeation resistance was minimal for 103.4 kPa case. However, the permeation resistance at 137.9 kPa and 172.4 kPa are similar to one another. Due to the presence of significant amount of large solute particles, the fresh juice offered greater permeation resistance for the transport of clarified juice. This is not the case for centrifuged juice as these large solute particles have been removed during centrifugation pretreatment step.

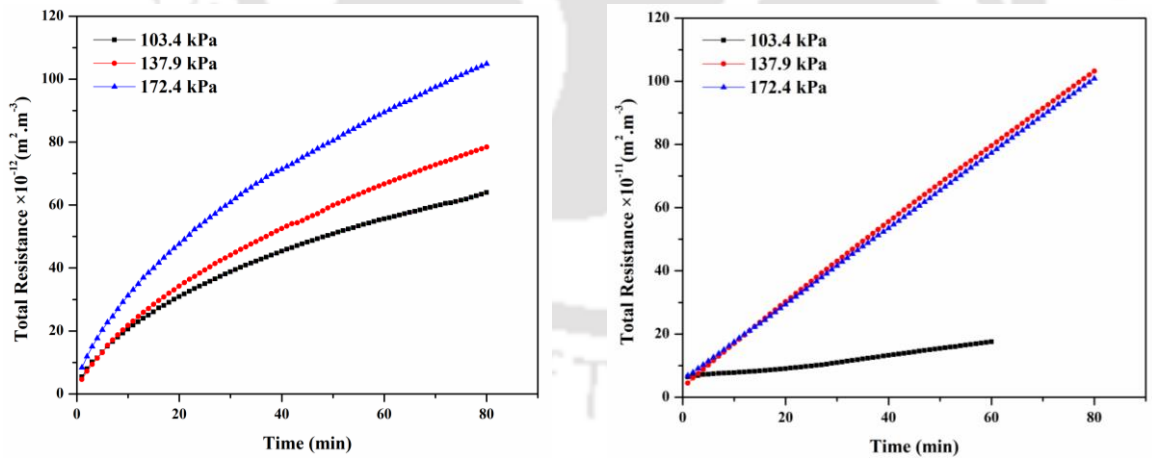


**(a)** **(b)**

**Figure 5.4: Time dependent total permeation resistance profiles associated to MF of (a) fresh and (b) centrifuged bottle gourd juice feed systems.**



TH-2589_156107040

**Table 5.4: A summary of various resistances contribution to total permeation resistance during MF of bottle gourd juice using CM1 membrane.**

| Applied Pressure (kPa) | | Contribution of Resistance to Total Resistances (%) | | | | | |
|---|---|---|---|---|---|---|---|
| | | Support | | Reversible | | Irreversible | |
| | | Fresh | Centrifuged | Fresh | Centrifuged | Fresh | Centrifuged |
| 103.4 | Onset | 4.40 | 37.22 | 95.34 | 60.72 | 0.25 | 2.07 |
| | Completion | 0.37 | 13.55 | 99.61 | 85.70 | 0.02 | 0.75 |
| 137.9 | Onset | 4.16 | 30.63 | 95.47 | 55.79 | 0.37 | 13.58 |
| | Completion | 0.24 | 1.32 | 99.74 | 98.09 | 0.02 | 0.59 |
| 172.4 | Onset | 2.23 | 28.55 | 97.51 | 63.99 | 0.16 | 7.46 |
| | Completion | 0.19 | 1.93 | 99.80 | 97.56 | 0.01 | 0.51 |

The contributions of various resistances to the total permeation resistance namely resistance of the membrane, irreversible permeation resistance and reversible permeation resistance have been evaluated. Table 5.4 summarizes the pertinent findings. For the fresh feed juice case, the reversible resistance (due to concentration polarization and cake layer formation on the support) varied from 95 to 99.7 %. However, for centrifuged juice and 103.4 kPa case, the contribution of irreversible resistance is 85.70 % and the contribution of support resistance to the total resistance was marginally higher. This is due to dominance of the irreversible membrane pore blocking in due course of time.

## 5.5 Membrane Morphological Variations during Microfiltration

The time dependent variation of effective permeability factor ($\varepsilon_{m,t}d_t^2$) as a function of the original membrane effective permeability ($\varepsilon_m d^2$), has been evaluated for fresh and centrifuged juice cases at various applied transmembrane pressure differentials (Figures 5.5 (a) and (b)). For the fresh juice, these values varied from 0.0125 – 0.0011 $m^2$, 0.0118 – 0.0007 $m^2$ and 0.0066 – 0.0005 $m^2$ for transmembrane pressure differentials for 103.4, 137.9 and 172.4 kPa, respectively. Correspondingly, for the centrifuged juice feed system, these



TH-2589_156107040

values varied from 0.1059 – 0.0385 $m^2$, 0.0872 – 0.0037 $m^2$ and 0.0813 – 0.0055 $m^2$, respectively. For both cases and for all pressure cases, the effective permeability factor reduced sharply during the first 20 – 30 min of the microfiltration run. Thereafter, the variable reduced gradually to indicate that morphological changes in the membrane might be gradual.

Among both fresh and centrifuged juice feed systems, the membrane treated with centrifuged juice was not highly susceptible to pore blocking. This is due to significant removal of larger particles from the feed system during centrifugation. For the case of centrifuged juice, the reduced applied pressure of 103.4 kPa indicated lower pore blocking and internal blockage in comparison with those evaluated at higher pressures (137.9 and 172.4 kPa). An opposite trend was obtained for the microfiltration data of fresh juice. This is due to the formation of cake layer on the membrane surface at lower applied pressure. Hence, the trends reported in Figure 5.1 (a) and 5.1 (b) are similar and in good agreement with the trends reported in Figure 5.5 (a) and Figure 5.5 (b), respectively.

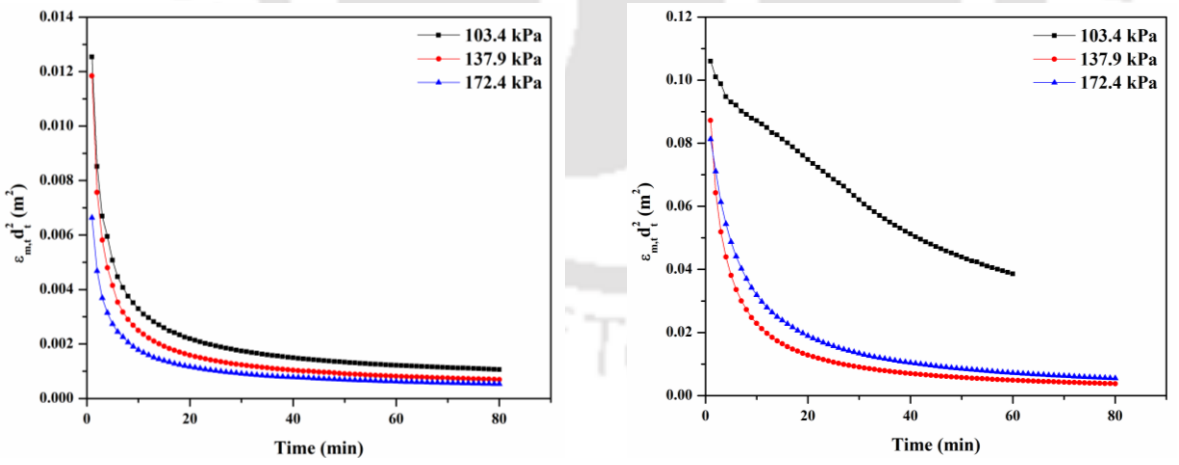


**(a)** **(b)**

**Figure 5.5: Variation of effective permeability factor with time for (a) fresh and (b) centrifuged bottle gourd juice feed systems.**



TH-2589_156107040

## 5.6 Permeate Characteristics and Clarification Efficacy

After conducting microfiltration experiments, the permeate and feed samples were tested for carbohydrate content, protein content, vitamin C content, total flavonoids, total phenol content, pH, salt content, TDS, color and clarity. Table 5.5 (a) and 5.5 (b) summarize these findings for nutritional and physico-chemical characteristics respectively. Irrespective of pressure differentials, the vitamin C content remained fairly constant (28.16 mg/g) for both feed and permeate samples. For the fresh juice, best permeate quality was obtained at 103.4 kPa in terms of highest total phenols (17.72 ± 2.54 mg GAE/100 g) and flavonoids content (120.9 ± 3.30 mg Quercetin/g) and minimal carbohydrate content (1.05 ± 0.11 g/100 mL) in the permeate. Incidentally, the membrane performance at 103.4 kPa indicated severe fouling and hence the insitu fouling can be inferred to have a strong and very important role in influencing and achieving superior permeate quality. Similar inference can be deduced for the permeate quality obtained for 137.9 kPa and fresh juice case. For the case, marginally inferior total phenols content (7.93 ± 2.12) and lower insitu fouling were obtained than those obtained at 103.4 kPa. However, the protein content was found to be comparatively lower (192.8 ± 28.23 mg/1000 mL) for 137.9 kPa applied pressure. The retention of pH is very important issue for the ceramic membranes. Prior work with carbonate precursor based ceramic membranes indicated significant alteration in the permeate pH in comparison with the feed pH  membranes (Kaniganti et al., 2015). This was not the case for the data reported in this work. Since pH retention can be observed for all permeate samples, the sawdust can be concluded to an appropriate pore forming agent to fabricate low cost ceramic membranes. On the other hand, for the centrifuged juice and all pressure differentials, the protein content in the permeate is significantly higher (318.8 ± 20.52 – 371.8 ± 10.55 mg/1000 mL) with minimal separation (5.16 – 18.70 %). While flavonoids and total phenols are significantly



TH-2589_156107040

retained in the permeate (76.60 – 96.78 % and 90.54 – 99.8 %), the presence of protein in the permeate is detrimental, as it enables significant reduction in the shelf life of the product. Complex tradeoffs exist with respect to nutritional characteristics and shelf life of an intermediate or a final food product. The existence of proteins in liquid phase products is detrimental to its shelf life. This is due to the reason that the protein serves as a nutrition source for the microbial activity and henceforth indicates the tendency towards greater spoilage with its abundant presence in the product constitution. On the other hand, adequate protein is required in any food product to ensure upon its quality of the nutrition. Therefore, a judicious approach needs to be followed i.e., in circumstances that indicate greater sensitivity of the product shelf life in comparison with the protein related nutritional content, the later could be ignored and vice-versa. This may not be the case in countries having extremely cold weather. Hence, analysis needs to be addressed on a case to case basis. Thus, the loss of nutritional value is justified for only those cases in which the shelf life is being jeopardized with the nutritional content. Such a scenario is only applicable for the liquid phase products. On the other hand, dried solid products can have such high protein content. This is due to reduced water activity of the product and hence lower risk of microbial spoilage of the solid food product. For all cases, the pH and salt content remained similar in both feed and permeate samples. Significant reduction in color (0.15 ± 0.09 and 0.45 ± 0.18) and enhancement in juice clarity (92.46 % ± 0.59 and 85.31 % ± 1.81) were observed for permeate samples obtained with fresh juice at 137.9 kPa and 172.4 kPa. For the fresh juice system, among all cases, the transmembrane pressure of 137.9 kPa can be regarded to be the best choice. This is due to optimal combinations of flux (highest among all cases) and appropriate permeate quality.

For the centrifuged juice, the juice quality was marginally higher (total phenols 20.62 ± 0.62 GAE/100g and flavonoids 153.13 ± 11.64 to 148.2 ± 1.58 mg Quarcetin/g) than the permeate



TH-2589_156107040

obtained with microfiltration. However, enhancement in clarity (73.45 – 92.46 %) and reduction in color (1.14 – 0.15 A) and protein content (371.8 – 192.8 mg/1000 mL) were pertinent in the MF clarified juice with respect to centrifuged juice (feed). Hence, centrifugation and associated costs of energy and process can be omitted by replacing centrifugation with inexpensive ceramic membrane technology for bottle gourd juice clarification.

**Table 5.5: Characteristics of feed and permeate samples associated to bottle gourd juice clarification using CM1 membrane (a) nutritional parameters, and (b) physico-chemical characteristics.**

| Juice Type | Applied Pressure (kPa) | Carbohydrate (g/100 mL) | | Protein (mg/1000 mL) | | Total Flavonoids (mg Quercetin /g) | | Total Phenolics (mg GAE/100g) | |
|---|---|---|---|---|---|---|---|---|---|
| | | Feed | Permeate | Feed | Permeate | Feed | Permeate | Feed | Permeate |
| Fresh Juice | 103.4 | 1.98 ± 0.08 | 1.05 ± 0.11 | 676.6 ± 25.32 | 305.5 ± 36.29 | 301.3 ± 2.47 | 120.9 ± 3.30 | 23.93 ± 2.37 | 17.72 ± 2.50 |
| | 137.9 | 1.98 ± 0.08 | 1.31 ± 0.09 | 676.6 ± 25.32 | 192.8 ± 28.23 | 301.3 ± 2.47 | 112.8 ±10.51 | 23.93 ± 2.37 | 7.93 ± 2.12 |
| | 172.4 | 1.98 ± 0.08 | 1.30 ± 0.17 | 676.6 ± 25.32 | 296.3 ± 29.85 | 301.3 ± 2.47 | 52.7 ±7.76 | 23.93 ± 2.37 | 13.08 ± 1.85 |
| Centri-fuged Juice | 103.4 | 1.59 ±0.05 | 1.41 ± 0.05 | 392.03 ± 1.65 | 371.8 ± 10.55 | 153.13 ± 10.42 | 122.4 ± 4.99 | 20.62 ± 0.62 | 20.51 ±1.13 |
| | 137.9 | 1.59 ±0.05 | 1.32 ± 0.15 | 392.03 ± 1.65 | 364.10 ± 11.11 | 153.13 ± 10.42 | 117.3 ± 11.64 | 20.62 ± 0.62 | 20.02 ± 0.99 |
| | 172.4 | 1.59 ±0.05 | 1.19 ± 0.15 | 392.03 ± 1.65 | 318.8 ±20.52 | 153.13 ± 10.42 | 148.2 ± 1.58 | 20.62 ± 0.62 | 18.67 ± 1.82 |

**(a)**

| Juice Type | Applied Pressure (kPa) | pH | | Salt Content (ppm) | | TDS (ppm) | | Color (A) | | Clarity (%T) | |
|---|---|---|---|---|---|---|---|---|---|---|---|
| | | Feed | Permeate | Feed | Permeate | Feed | Permeate | Feed | Permeate | Feed | Permeate |
| Fresh Juice | 103.4 | 5.46 ± 0.03 | 5.48 ± 0.01 | 2.39 ± 0.09 | 2.01 ± 0.10 | 3.13 ± 0.09 | 2.95 ± 0.12 | 2.41 ± 0.15 | 1.14 ± 0.12 | 3.78 ± 0.06 | 46.13 ± 1.08 |
| | 137.9 | 5.46 ± 0.03 | 5.46 ± 0.02 | 2.39 ± 0.09 | 1.9 ± 0.08 | 3.13 ± 0.09 | 2.5 ± 0.08 | 2.41 ± 0.15 | 0.15 ± 0.09 | 3.78 ± 0.06 | 92.46 ± 0.59 |
| | 172.4 | 5.46 ± 0.03 | 5.47 ± 0.02 | 2.39 ± 0.09 | 1.95 ± 0.18 | 3.13 ± 0.09 | 2.58 ± 0.10 | 2.41 ± 0.15 | 0.45 ± 0.18 | 3.78 ± 0.06 | 85.31 ± 1.81 |
| Centri-fuged Juice | 103.4 | 5.41 ± 0.02 | 5.43 ± 0.02 | 2.48 ± 0.17 | 2.40 ± 0.11 | 3.20 ± 0.19 | 3.01 ± 0.14 | 1.33 ± 0.04 | 1.02 ± 0.15 | 54.56 ± 3.82 | 73.96 ± 0.78 |
| | 137.9 | 5.41 ± 0.02 | 5.46 ± 0.03 | 2.48 ± 0.17 | 2.18 ± 0.17 | 3.20 ± 0.19 | 2.92 ± 0.20 | 1.33 ± 0.04 | 1.11 ± 0.08 | 54.56 ± 3.82 | 73.45 ± 0.76 |
| | 172.4 | 5.41 ± 0.02 | 5.47 ±0.01 | 2.48 ± 0.17 | 2.41 ± 0.09 | 3.20 ± 0.19 | 3.12 ± 0.02 | 1.33 ± 0.04 | 0.85 ± 0.10 | 54.56 ± 3.82 | 75.68 ± 1.84 |

**(b)**



TH-2589_156107040

## 5.7 Microbial Efficacy of Clarified Bottle gourd Juice

Using a total plate count method, the microbial analysis was conducted for fresh feed and microfiltered permeate samples (obtained at 137.9 kPa). The samples were subjected to 100 times dilution and were kept in a BOD incubator for 24 h and 37 $^{o}$C. The microbial feed concentration was evaluated as $1.76\times10^{6}$ CFU/mL for fresh feed samples (Figure 5.6 (a)).

The centrifuged juice sample was found to have a microbial concentration of $3.50\times10^{5}$ CFU/mL. Thus, about 80.11% reduction in microbial content can be achieved through the centrifugation process. The permeate samples obtained with fresh feed juice system did not exhibit visible growth after 24 h. However, after 48 h, small colonies (Figure 5.6 (b)) were observed, using which permeate microbial concentration was evaluated as $1.10\times10^{4}$ CFU/mL.

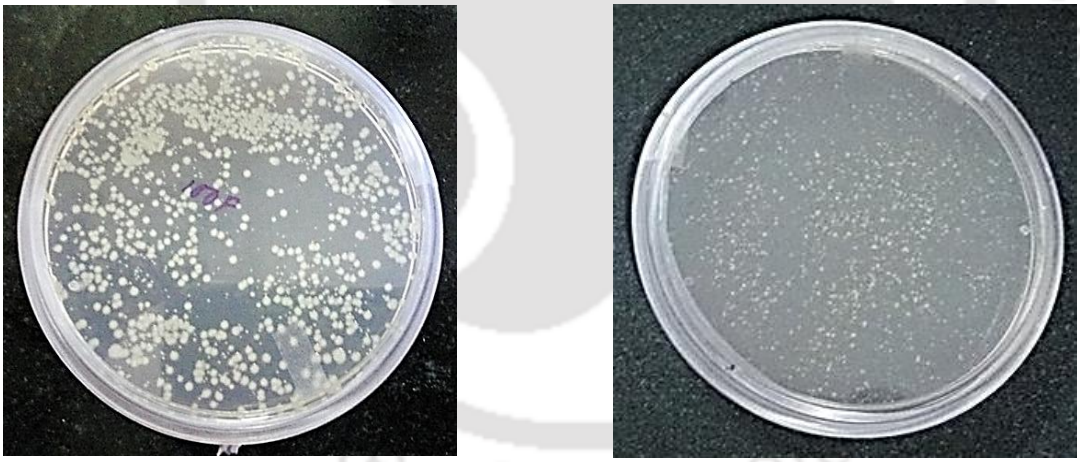

**(a)** **(b)**

**Figure 5.6: Microbial colonies obtained for various samples associated to CM1 membrane based bottle gourd juice clarification (a) fresh feed juice, and (b) permeate sample.**



TH-2589_156107040

Using these values, the membrane rejection efficiency was evaluated as 99.37%. The obtained separation efficiency is comparable to that reported in the literature for microfiltered pineapple juice with 0.2 µm hollow fiber membranes (100 % removal efficiency) (Laorko et al., 2013). Thus, it can be inferred that the low-cost ceramic membranes are suitable to retain microbes prevalent in the fresh juice samples.

## 5.8 Comparative Assessment with Prior Art

The quality of the permeate sample (in terms of various physico-chemical properties and nutrient content) obtained with microfiltration at 137.9 kPa was compared with the best available literature data for cross-flow microfiltration and microfiltration-ultrafiltration hybrid process (Mondal et al., 2016). Table 5.6 summarizes the data for comparative analysis. The permeate quality was found to be better with the dead-end microfiltration process being investigated in this research work (676.6 ± 25.32 mg/1000 mL protein, 7.93 mg GAE/100 g total phenolics, color 0.15 A and 92.46 % clarity) than the data reported in the literature for microfiltration (Mondal et al., 2016). The higher concentration of protein in the permeate obtained with the ceramic membrane is possibly due to wider pore size distribution in the ceramic membranes in comparison with the literature reported hybrid system. Compared to the hybrid or integrated microfiltration-ultrafiltration system reported in the literature, the low-cost ceramic membrane provided better FRR (93.67 % but not 85 %) but poorer FDC (40 but not 92.01). A lower FDC suggested in the literature is possibly due to the cross-flow system being deployed by the authors. However, compared to the literature, it shall be noted that 7 – 9 % higher FRR is promising and is affirming upon greater irreversible fouling of the ceramic membranes being developed in this work. It may also be noted that the data presented in the literature were obtained using polymeric membranes and cross-flow filtration module. Hence, from economics perspective, it may be deduced that the present work is



TH-2589_156107040

comparatively superior to the data being reported in the mentioned literature. However, it may also be noted that the phenolics content in the feed juice system being reported by Mondal et al. (2016) (17.7 mg GAE/100 g) was lower than that being considered in this work (23.93 mg GAE/100 g). Further, the permeate data indicates comparatively higher retention of phenolics by the ceramic membranes in conjunction with the reported data for the polymer membrane. In summary, it is very likely that the literature reported data indicates better retention of phenolic content in comparison with that being obtained and reported in this work.

**Table 5.6: A summary of optimal MF process characteristics associated to bottle gourd juice MF system.**

| S. No. | Process | Parameters | | | | | | | | | | | | Literature |
|---|---|---|---|---|---|---|---|---|---|---|---|---|---|---|
| | | Membrane Process | | | | | Permeate quality | | | | | | | |
| | | Pore Size (µm) | Applied Pressure (kPa) | FRR | FDC | Protein Removal (%) | Constituents | Total Phenolics (mg GAE/100 g) | Total Flavonoids (mg Quercetin /g) | Color (A) | Clarity (%T) | pH | Microbial Content (CFU/mL) | |
| 1 | Micro-filtration | 1.002 | 137.9 | 93.67 | 92.01 | 71.60 | Feed | 23.93 | 301.3 | 2.41 | 3.78 | 5.46 | $1.76\times10^{6}$ | This Work |
| | | | | | | | Permeate | 7.93 | 112.8 | 0.15 | 92.46 | 5.46 | $1.10\times10^{4}$ | |
| | Centrifu-gation | — | — | — | — | 57 | — | 20.62 | 153.13 | 1.33 | 54.56 | 5.41 | $3.5\times10^{5}$ | |
| 2 | Micro-filtration | 0.20 | 123 | — | — | 63.46 | Feed | 17.7 | — | 3.57 | 4.1 | 4.6 | — | Mondal et al. (2016) |
| | | | | | | | Permeate | 7.9 | — | 0.4 | 76.5 | 5.8 | — | |
| | Hybrid micro-filtration and ultra-filtration | 0.017 | 104 | 85 | 40 | 82.41 | Feed | 17.7 | — | 3.57 | 4.1 | 4.6 | — | |
| | | | | | | | Permeate | 3.9 | — | 0.14 | 94.8 | 4.7 | — | |



TH-2589_156107040

Also, the flux data reported in the literature for the hybrid, polymeric and cross-flow system at steady state was found to be approximately $8.3 \times 10^{-6}$ $m^3.m^{-2}.s^{-1}$ which is comparatively higher than that being obtained with the dead MF in this work ($1.7 \times 10^{-6}$ $m^3.m^{-2}.s^{-1}$). Deploying cross flow MF operations, the ceramic membranes flux is anticipated to enhance by about 3 to 4 times of the steady state flux indicated in this work and thereby become comparable with the literature reported best MF process flux data. In summary, the ceramic membrane proved to be highly effective due to its significant influence of pore size distribution on the clarification efficacy. Thereby, the membranes can be concluded to be applicable for the direct application towards bottle gourd juice clarification.

## 5.9 Cost Efficacy

The economic competence of centrifugation and low cost ceramic membrane process were considered based on capital and operating costs of various equipment and membrane fabrication costs. The membrane fabrication cost was evaluated as the sum of membrane raw material cost, equipment time handling costs for fabrication, electricity, manpower and miscellaneous costs with membrane shelf life assumed to be 1 year. The fixed costs associated to microfiltration sub-process include costs of compressor, permeation setup and housing cost and annual depreciation. The operating cost of the microfiltration sub-process was evaluated as a sum of membrane fabrication, cleaning and associated manpower costs. For the centrifugation process, the fixed cost corresponds to the cost of the centrifuge and operating cost correspond to the sum of electricity and manpower costs. The economic evaluation was first considered for an annual bottle gourd juice production capacity of 110 L, which was based on the membrane flux obtained after 80 min during dead end MF using the laboratory scale experimental setup. Thereafter, the economic competence of processes was evaluated for a higher throughput and juice production capacity upto 10000 L per year.



TH-2589_156107040

**Table 5.7: A summary of cost and economic parameters associated to the techno-economic feasibility study of bottle gourd juice MF process system.**

| **Membrane Precursor** | **Cost ($/kg)** |
|---|---|
| Kaolin | 3.55 |
| Feldspar | 32.09 |
| Sawdust | 0.14 |
| Boric Acid | 12.44 |
| Sodium Metailicate | 7.88 |
| **Equipment** | **Cost ($) (Shelf life 10 y)** |
| Mixer Grinder | 34.11 |
| Hydraulic Press | 1364.26 |
| Hot Air Oven | 545.70 |
| Muffle Furnace | 2728.51 |
| Sonicator | 409.28 |
| Mould | 136.43 |
| Compressor | 409.28 |
| Centrifuge | 5457.03 |
| **Equipment Power Rating (kW)** | **(Tariff: 0.098 $)** |
| Mixer Grinder | 0.75 |
| Hydraulic Press | 1.49 |
| Hot Air Oven | 2.40 |
| Muffle Furnace | 1.80 |
| Sonicator | 0.28 |
| Compressor | 0.75 |
| Power | 2.56 |
| **Dollar to Rupees Evaluation: 1 $ = ₹ 73.3** | |

Further, industrial systems may utilize booster pumps and for such cases, the MF process economics are likely to be improvised by 20 – 30% due to lower costs of the booster pump (by 30 to 40%) in comparison with the expensive compressor cost.

Therefore, the reported economic indices in this chapter could serve as useful benchmark for the cost competitive commercial processing of bottle gourd juice. Table 5.7 summarizes the relevant cost parameters for economic evaluation. The conceptual cost analysis based membrane construction costs and other operating costs have been summarized in Appendix A of the PhD thesis. However, detailed cost estimation and analysis can be considered to evaluate upon the associated variations with those being reported. Further, membrane shelf life analysis can be investigated through long term MF runs and subsequent variations in the membrane performance characteristics. The same can be also addressed in the near future.



TH-2589_156107040

Based on the assumed cost parameters (Table 5.7), the fabrication based cost for the low cost ceramic membrane was evaluated to be 440.9 $/m$^2$, which is comparable with the lower value reported in the literature (460 – 4000 $/m$^2$) (Cheryan, 1998; Koros and Mahajan, 2000; Suresh et al., 2016; Tennison, 2000). For a clarified juice production capacity of 110 L (at 137.9 kPa and 80 min processing time), the total juice processing cost has been evaluated to be 1.19 and 3.99 $/L (87.29 and 292.91 Rs/L) for microfiltration and centrifugation processes respectively. The microfiltration and centrifugation processes incur an additional processing cost of 31.26 and 79.52 %, respectively with respect to the fresh juice cost. A further introspection of involved costs has been depicted in Figure 5.7 for the microfiltration process.

As shown, the MF based clarification involved a processing cost of 0.372 $/L. For the system, the fixed and operating costs contribute to 83.13 and 16.84 % respectively. The evaluated fixed cost of the MF process (0.31 $/L) has corresponding cost contributions of compressor, membrane housing assembly and depreciation as 82.82, 8.59 and 8.59 % respectively. The evaluated operating cost of the MF process (0.06 $/L) involves the contribution of costs associated to membrane replacement, membrane cleaning and manpower cost during juice processing as 15.19, 42.41 and 42.41 % respectively. The membrane replacement cost of 0.0095 $/L involves the cost contributions of raw material, manpower, equipment, electricity and miscellaneous costs as 23.74, 40.73, 6.48, 25.48 and 3.59 %, respectively. On the other hand, the centrifugation process involved a cost of 3.54 $/L. Corresponding fixed and operating costs respectively contribute to 93.39 and 6.61% of the total cost. The evaluated fixed cost of the centrifugation process (3.31 $/L) involves the contribution of total costs due to centrifuge equipment. On the other hand, the operating cost (0.23 $/L) has cost contributions of manpower and electricity as 77.7 and 22.9 %, respectively.



TH-2589_156107040

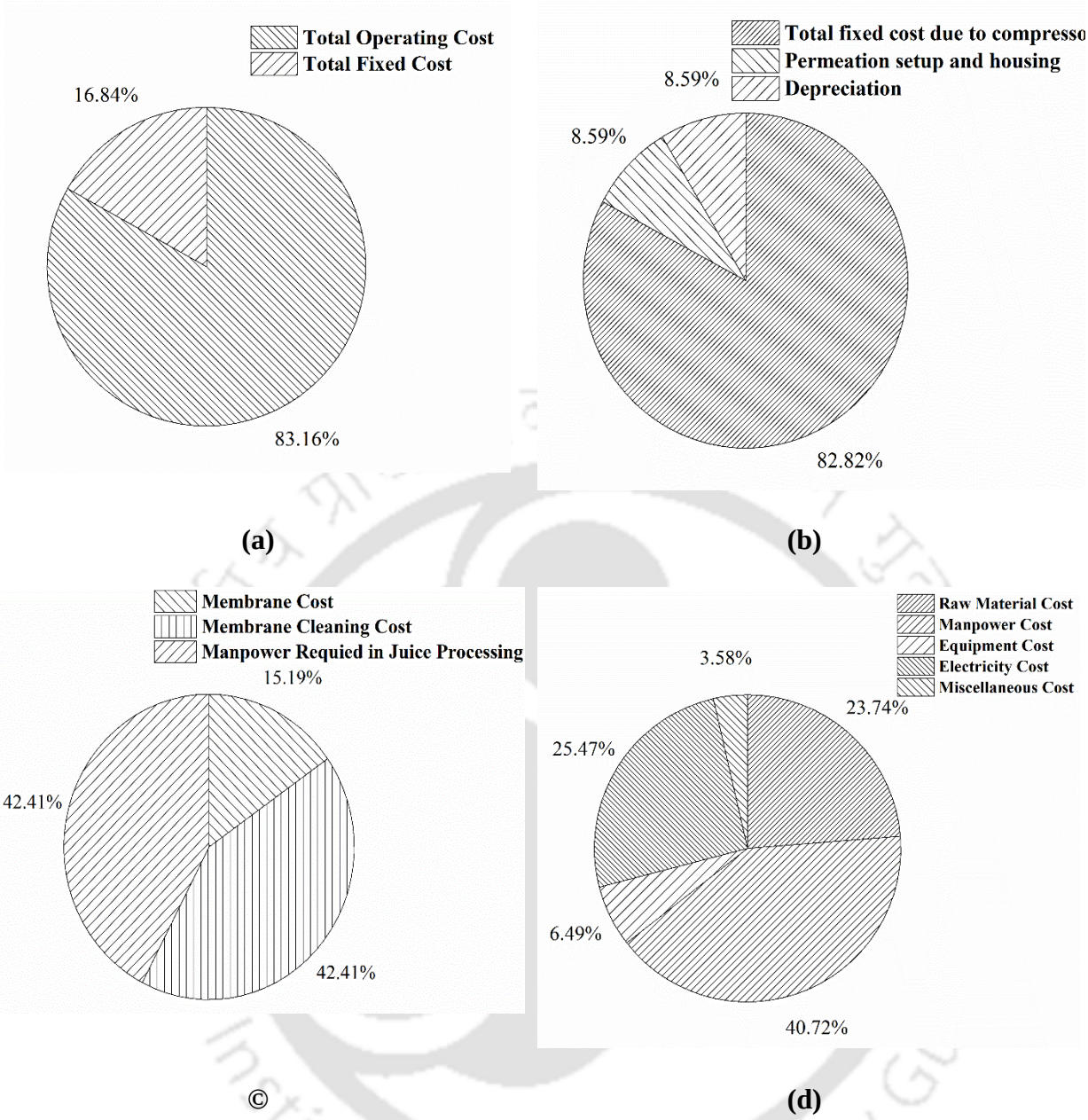


**Figure 5.7: Percent contribution of various cost heads to overall cost components of bottle gourd juice MF process system (a) total cost (0.372 $/L), (b) total fixed cost (0.31 $/L), (c) total operating cost (0.06 $/L), and (d) total membrane fabrication cost (0.0095 $/L).**

The scale-up related economic competence provided interesting insights (Figure 5.8). As shown for the MF process, the juice processing cost reduced from 1.19 to 0.37 $/L for the MF process for an enhancement in the juice production capacity from 110 – 10000 L/y. This



TH-2589_156107040

amounts to 31.27 – 26.32 % of processing cost. On the other hand, the corresponding juice processing cost reduced from 3.99 to 0.42 $/L for the centrifugation process. Incidentally, the market price of bottle gourd juice is about 2 – 5 $/L, which is significantly higher than the costs evaluated based on fresh juice and juice processing costs (1.19 – 0.37 $/L) (Weblink 1, Weblink 2).

Based on conceptual modelling approach, the Appendix C of the PhD thesis summarizes the associated energy consumption of MF vis-à-vis centrifugation coupled MF process. The conceptual cost analysis indicated that the MF process accounts for more than 75% of the total energy costs of the MF-Centrifugation process. Thus, a fractional enhancement in the energy costs needs to be evaluated in the context of the tradeoffs related to the quality attributes in terms of enhanced shelf life and better product quality. These need to be evaluated in detail in the near future.

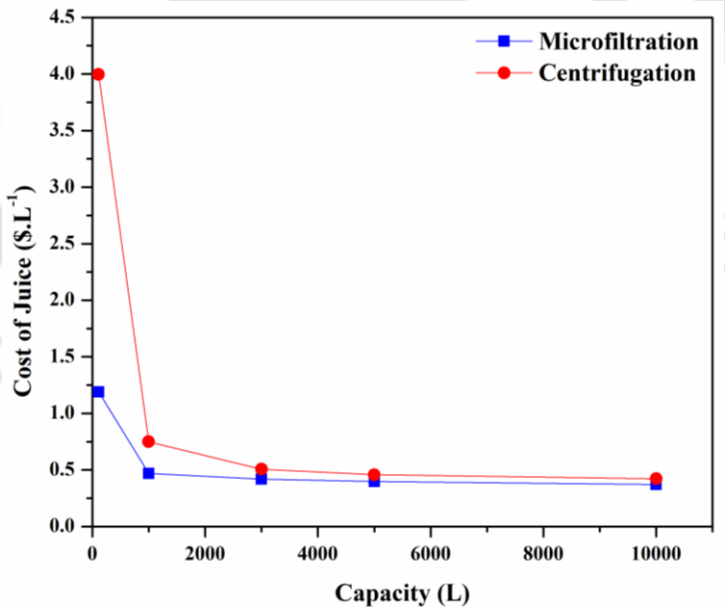


**Figure 5.8: Variation of conceptual bottle gourd juice processing cost with process capacity for MF and centrifugation processes.**



TH-2589_156107040

## 5.10 Summary

Based on the results and discussions outlined in the above sections of the chapter, following conclusions could be drawn.

- During clarification of bottle gourd juice, the sawdust based ceramic membrane CM1 (1 µm pore size and 28.47 % porosity) performed optimally at 137.9 kPa transmembrane pressure and for fresh juice. Thereby, the MF process technology omits the centrifugation process and associated process costs.
- The membrane exhibited a FDC and FRR of 91.5 – 94.13 % and 91.89 – 94.54 % respectively, at the optimum condition, despite undergoing intermediate and standard pore blocking as inferred from the Hermia Models.
- Resistance in series model shows that contribution due to reversible resistance (99.74 %) was most dominant compared to irreversible (0.02 %) and support resistance (0.24 %).
- The evaluation of effective permeability factor indicates that initial changes in membrane morphology was higher which gradually decreased with time. The effective permeability for all cases of fresh juice (0.0005 – 0.0125 $m^2$) was lower than the effective permeability of centrifuged juice (0.0037 – 0.1059 $m^2$).
- Comparing the MF data with those obtained for centrifugation, the ceramic membrane can be concluded to exhibit better clarity (92.46 %), microbial and protein rejection (99.37 % and 71.60 %) along with similar values for other nutritional parameters but not total phenolic content.
- The conceptual ceramic membrane fabrication cost has been evaluated as 440 \$/$m^2$ and thereby, the juice processing cost has been evaluated conceptually to vary from 0.37 – 1.19 \$/L. This is significantly lower than the associated costs for centrifugation and lower production capacity (110 L per year).



TH-2589_156107040

In summary, sawdust based ceramic membranes are promising technologies to serve as cost competitive microfiltration technology filter elements for the commercial clarification of bottle gourd juice.

## References

1. Cheryan, M., 1998. Ultrafiltration and microfiltration handbook. CRC press.
2. Emani, S., Uppaluri, R., Purkait, M.K., 2013. Preparation and characterization of low cost ceramic membranes for mosambi juice clarification. Desalination 317, 32-40.
3. Kaniganti, C.M., Emani, S., Thorat, P., Uppaluri, R., 2015. Microfiltration of synthetic bacteria solution using low cost ceramic membranes. Separation Science and Technology 50, 121-135.
4. Koros, W.J., Mahajan, R., 2000. Pushing the limits on possibilities for large scale gas separation: which strategies? Journal of Membrane Science 175, 181-196.
5. Laorko, A., Tongchitpakdee, S., Youravong, W., 2013. Storage quality of pineapple juice non-thermally pasteurized and clarified by microfiltration. Journal of Food Engineering 116, 554-561.
6. Nandi, B., Uppaluri, R., Purkait, M., 2011. Identification of optimal membrane morphological parameters during microfiltration of mosambi juice using low cost ceramic membranes. LWT-Food Science and Technology 44, 214-223.
7. Suresh, K., Pugazhenthi, G., Uppaluri, R., 2016. Fly ash based ceramic microfiltration membranes for oil-water emulsion treatment: Parametric optimization using response surface methodology. Journal of Water Process Engineering 13, 27-43.
8. Tennison, S., 2000. Current hurdles in the commercial development of inorganic membrane reactors. Membrane Technology 2000, 4-9.



TH-2589_156107040

9. Weblink 1: Retrieved on January 09, 2019 from: https://www.pinhealth.com/products/axiom-lauki-swaras-500-ml?gclid=EAIaIQobChMI6r65iYnE3gIVyzUrCh1MKgpbEAQYAyABEgKCx_D_BwE&utm_source=google&utm_medium=cpc&utm_campaign=1598644213&ef_id=W864ZgAAAevz8PP%40%3A20181108060836%3As&fbclid=IwAR36KnVAitF9ZSWYyqHDDqBmIdTD8 Ii-jkq5EMlpNrb-NTdYaUtoZ8fvXW8/.
10. Weblink 2: Retrieved on May 02, 2020 from: https://www.shoponn.in/bottle_gourd_lauki_juice_bg336/167868?gclid=EAIaIQobChMI6r65iYnE3gIVyzUrCh1MKgpbEAQYByABEgJv4PD_BwE&fbclid=IwAR1orgFer2ox9dNkh8xJnBDBX6bXVFuZX-fZYUDK2lEan_gW8mIISyEzNCQ.



TH-2589_156107040

# Chapter 6:

# Optimality of Membrane Morphology and Feedstock during Microfiltration of Bottle Gourd Juice

TH-2589_156107040

TH-2589_156107040

# Optimality of Membrane Morphology and Feedstock during Microfiltration of Bottle Gourd Juice

*The chapter further delineates upon the combinatorial optimality of membrane morphology and feedstock during microfiltration of bottle gourd juice. After providing relevant overview in section 6.1, the following section (section 6.2) elaborates upon the flux decline analysis. Following this, FDC and FRR analysis has been reported in section 6.3. Sections 6.4 and section 6.5 respectively summarize the findings associated to dominant fouling mechanism and permeation resistances during bottle gourd juice clarification. The permeate characteristics have been discussed in section 6.6. Based on the findings reported in sections 6.2 – 6.6, section 6.7 devotes towards the identification of best combinations of membrane and feed choice during microfiltration of bottle gourd juice. Finally, section 6.8 presents key findings of the conducted investigations[#].*

## Overview

*In the previous chapter, the efficacy of a ceramic membrane with wider average pore size has been proven to be promising for the microfiltration based clarification of bottle gourd juice. However, combinatorial optimality with respect to membrane morphology and feedstock selection was not duly addressed in the preceding chapter. Considering these as the central objectives, the chapter attempts to provide useful insights with respect to possible improvements in the membrane performance during bottle gourd juice microfiltration. Varied morphology of sawdust and kaolin based low cost ceramic membranes have been considered.*

[#] Published Article: Chakraborty, S., Uppaluri, R., Das, C., (2020) "Combinatorial Optimality of Membrane Morphology and Feedstock during Microfiltration of Bottle Gourd Juice", Innovative Food Science and Emerging Technologies, 63:102328.

TH-2589_156107040

*The feedstock variation referred to fresh, paper filtered and centrifuged juice samples. Along with the feedstock, trans-membrane pressure differential has been considered as an additional process parameter to infer upon their optimality. The combinatorial optimality of membrane pore size, feedstock and pressure differentials were determined based on the flux decline trends, fitness of fouling models, irreversible and reversible fouling data, irreversible permeation resistance and nutritional analysis of the permeate samples. An interesting feature of this work is with respect to feed constitution playing a critical role in influencing the optimal choice of membrane morphology and transmembrane pressure differentials.*

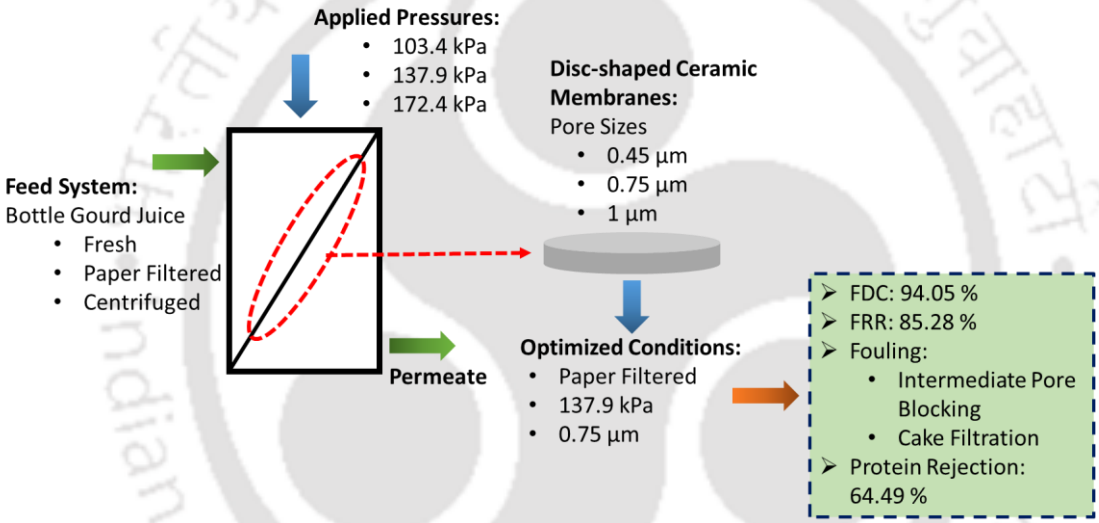


## 6.1 Introduction

The process parametric optimality during microfiltration of bottle gourd juice using low cost ceramic membranes has been addressed from membrane morphology, feedstock and applied pressure differential variability perspectives. Clay based ceramic membranes with diverse pore size distributions (0.45 (CM7 membrane), 0.75 (CM3 membrane) and 1 µm (CM1 membrane) have been considered. Three different types of feedstock namely fresh (cloth filtered), filtered (paper filtered) and centrifuged bottle gourd juice samples have been chosen. The transmembrane pressure differentials have been varied as 103.4, 137.9 and 172.4



TH-2589_156107040

kPa. Pertinent flux decline analysis was addressed using conventional Hermia fouling models and modified empirical models proposed by the research group of Bolton (Bolton, et al., 2006). The permeate product characterization involved the measurement of trans-membrane flux and other physico-chemical and nutritional parameters (such as clarity, color, protein content and polyphenols content). Permeate samples characterized with higher combinations of transmembrane flux, polyphenols content, clarity and color have been regarded to indicate the optimality of membrane morphologies, feedstocks and trans-membrane pressure differentials (TMP). Thereby, associated tradeoffs can be visualized in terms of irreversible fouling and permeate quality with said choices of the process parameters. Thereby, the ultimate objective of the thesis is to provide useful benchmarks for the low cost ceramic membrane based clarification of bottle gourd juice.

## 6.2 Flux Decline Analysis

For various combinations of membrane morphology and feedstock, Figure 6.1 illustrates bottle gourd juice dead end MF flux decline profiles at various transmembrane pressures. This refer to CM7 and centrifuged juice (case 1), CM3 and filtered juice (case 2) and CM1 and fresh juice (case 3). At 172.4 kPa, the highest flux profile ($1.19 \times 10^{-5} – 4.54 \times 10^{-5}$ $m^3.m^{-2}.s^{-1}$) has been obtained for case 1, followed by the profile for case 3 ($0.17 \times 10^{-5} – 2.14 \times 10^{-5}$ $m^3.m^{-2}.s^{-1}$) and the profile for case 2 ($0.13 \times 10^{-5} – 1.69 \times 10^{-5}$ $m^3.m^{-2}.s^{-1}$). This is due to absence of macromolecular constituents in centrifuged juice and appropriate membrane morphology. Hence, membrane morphology and feedstock selection profoundly influence vegetable juice flux decline characteristics.



TH-2589_156107040

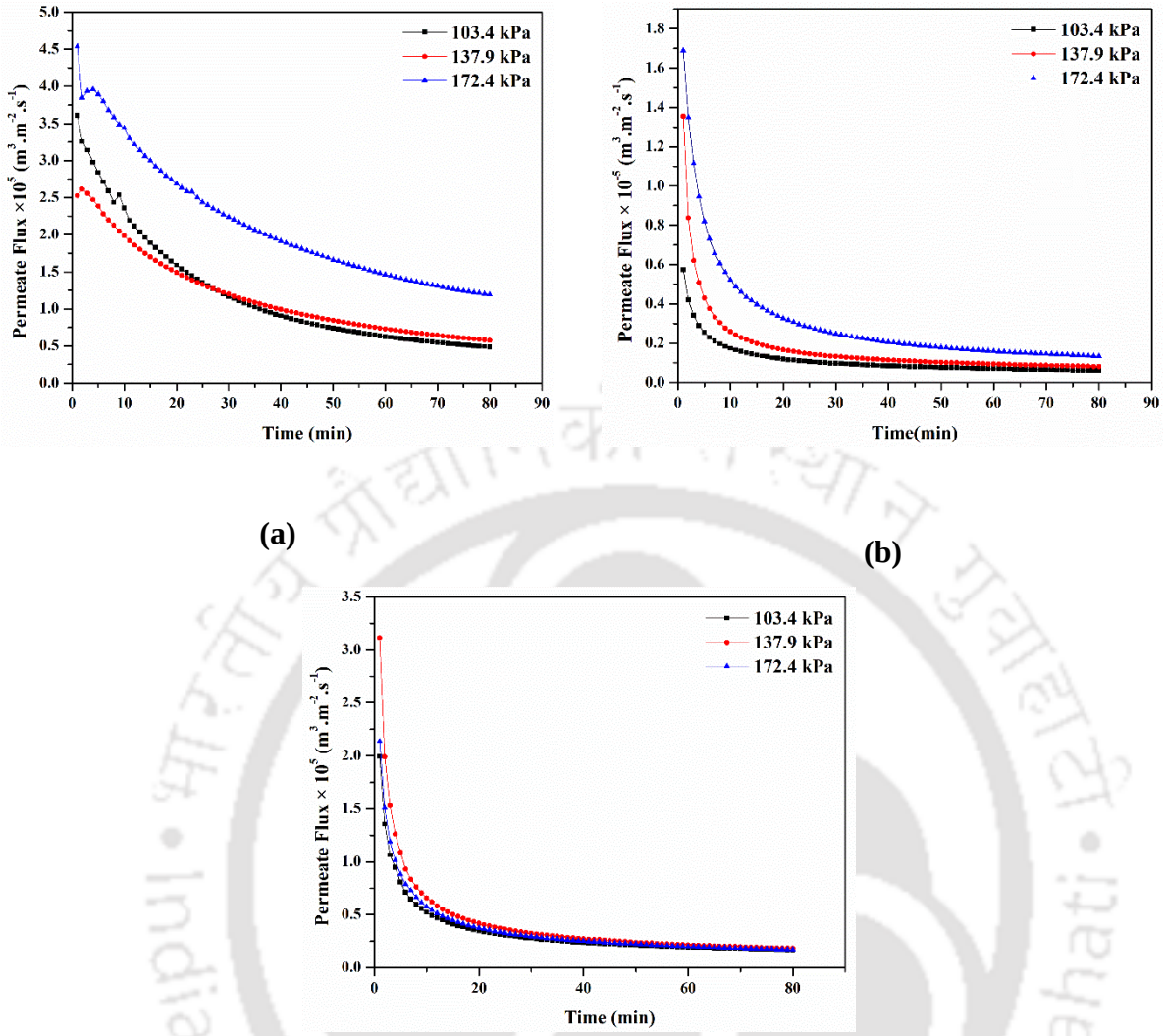


**Figure 6.1: Flux decline profiles of (a) CM7-centrifuged juice (b) CM3-filtered juice and (c) CM1-fresh juice systems.**

Compared to fresh and filtered juices adopted for CM3 and CM1 membranes respectively, the centrifuged juice processed with CM7 membrane can be analyzed to have lower tendency to block the internal pore structure of the membrane. This is due to reason that compared to the filtered and fresh juice samples, the centrifuged juice possessed lower content of the insoluble particles. The highest flux ($4.54 \times 10^{-5}$ $m^3.m^{-2}.s^{-1}$) was obtained at highest $\Delta P$ of 172.4 kPa for the case and is justified from $\Delta P$ perspective. Thus, from flux decline



TH-2589_156107040

perspective, the best choice could be CM7 membrane and centrifuged juice. However, this needs to be supplemented with appropriate FDC, highest FRR and good permeate quality. In this regard, it is important to note that the suspended particulates of the feed do have a significant influence on the permeate quality with positive contribution on the same for few cases. Therefore, the identification of optimal process condition for the low cost ceramic membrane needs to be supplemented from such analysis, which would be an interesting scenario. Such insights can be obtained from the subsequent sections.

## 6.3 FRR and FDC Characteristics

Ideally, lower FDC and higher FRR values are desired during dead end MF. However, it is very likely that higher combinations of FDC and FRR may exist due to severe insitu reversible membrane fouling during MF. Table 6.1 summarizes the FDC and FRR values for various combinations of feed juice systems and membrane morphologies. Compared to the FDC of 0.75 (89.425 – 92.10 %) and 1 µm (91.57 – 94.13 %) membrane, the FDC of 0.45 µm (73.78 – 86.62 %) membrane was low. The highest FDC of 94.13 % was obtained for 1 µm membrane. Also, feedstock choice has an important role to influence these values. It can be analyzed that for the combinations of fresh juice and higher pore sized membranes, higher FDC values have been achieved. This is due to the reason that fresh juice has larger content of suspended and insoluble solids in comparison with the paper filtered juice. Further, centrifuged juice has lowest insoluble particulate content in comparison to the fresh and paper filtered juices. Thus, these particulates can be analyzed to have a profound influence upon the pore blocking mechanisms of the membranes. They are highly favorable to the higher pore size membranes.



TH-2589_156107040

**Table 6.1: A summary of FRR and FDC values associated to bottle gourd juice using CM1, CM3 and CM7 membranes.**

| Applied Pressure (kPa) | CM1 | | CM3 | | CM7 | |
|---|---|---|---|---|---|---|
| | FDC (%) | FRR (%) | FDC (%) | FRR (%) | FDC (%) | FRR (%) |
| | Fresh | | Filtered | | Centrifuged | |
| **103.4** | 94.13 | 94.54 | 89.42 | 86.97 | 86.62 | 71.87 |
| **137.9** | 91.57 | 91.89 | 94.05 | 85.28 | 77.26 | 72.50 |
| **172.4** | 92.01 | 93.67 | 92.10 | 80.90 | 73.78 | 77.30 |

Lower FDC affirms lower combinations of reversible and irreversible fouling extent during microfiltration. Centrifugation eliminates removal of suspended and larger particles and hence lowest fouling is indicated by the FDC (73.78 – 86.62 %) among all cases. However, the FRR for the case of CM7 membrane and centrifuged juice is low (71.87 – 77.30 %) in comparison with the case of CM3 membrane and filtered juice (80.90 – 86.97 %) and CM1 membrane and fresh juice (97.89 – 94.54 %). This is due to lower pore size and internal pore blocking of the membranes that enabled a low flux recovery after membrane cleaning. For the latter two cases, larger particles tend to form an external layer on the membrane surface and minimize internal pore blocking, which was not the scenario for the first case. Such a layer can be effectively removed during membrane cleaning and hence higher FRR can be obtained. Hence, despite obtaining a very high FDC (91.57 – 94.13 %), the higher FRR (91.89 – 94.54 %) values for CM1 affirm that the membrane fouling was due to the formation of external layer with minimal internal pore blocking. A marginally lower FRR (80.90 – 86.97 %) was obtained for the CM3 membrane. This is due to the contributions of both external fouling and internal pore blocking, despite having the observation that the FDC was lower (89.425 – 94.05 %) for the case in comparison with the FDC of the CM1 membrane case (91.57 – 94.13 %).



TH-2589_156107040

With increasing pressure differentials, the FRR were found to reduce for CM3 and CM1 (from 91.89 – 94.54 % for CM1 to 80.90 – 86.97 % for CM3). This is attributed to greater penetration of comparatively smaller particles into the pore structure at higher pressure and thereby associated difficulties to clean the membrane. In other words, higher pressure is favorable for these membranes. However, for the centrifuged juice filtered with CM7 membrane, higher FRR of 77.3 % was obtained at higher pressure of 172.4 kPa. This is due to lower penetration of particles into the pores at higher (172.4 kPa) but not lower pressure (103.4 kPa). Given the highest relevance of FRR but not FDC, the best membrane among considered cases is the CM1 membrane fed fresh vegetable juice followed by CM3 fed with cloth filtered juice. However, the same needs to be supplemented from permeate quality analysis.

## 6.4 Membrane Fouling Characteristics

This section addresses fitness of appropriate pore blocking model to represent measured flux data. Figure 6.2 and Table 6.2 present the fitness plots and fitness parameters of the Hermia models for CM3 and filtered feed juice case. Among various alternate models, the cake filtration model can be inferred to the best fit model ($R^2 > 0.99$) for the case. However, the $R^2$ values (0.948 – 0.952) for the intermediate pore blocking models were also found to be acceptable. Due to the presence of large quantity of suspended solids in the feed, the effect of complete pore blocking and standard pore blocking was found to be negligible in comparison with the intermediate pore blocking and the cake filtration mechanisms. The intermediate blocking of membrane pores is possibly due to penetration of smaller particles in the feed that could enter the porous structure of the membrane. The cake layer provided hindrance to the flow and improved the membrane to serve as a composite membrane consisting of dense top layer and a porous bottom layer to restrict internal pore blocking and enhance permeate



TH-2589_156107040

quality. The FRR values for CM3 (80.90 – 86.97 %) also affirm towards this hypothesis. Except for cake filtration case, at a higher pressure of 172.4 kPa, the $R^2$ values for all fouling models (0.823 – 0.981) have been higher in comparison with those obtained at a lower pressure of 103.4 kPa (0.781 – 0.952). Hence, lower FRR (80.90 %) value was obtained for the case at high pressure.

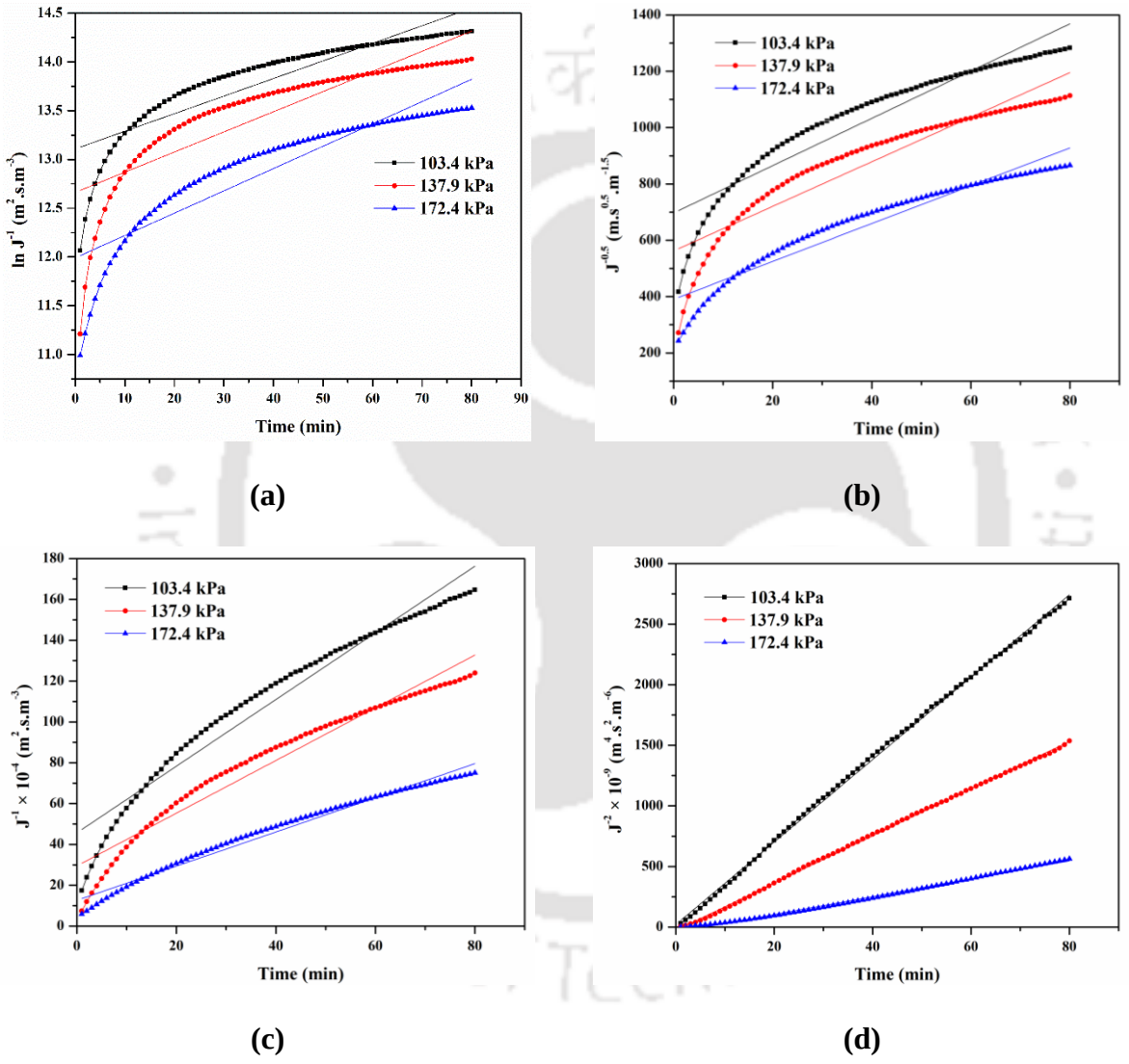


**Figure 6.2: Fitness plots of Hermia fouling models for CM3 membrane-filtered system (a) complete pore blocking, (b) standard pore blocking, (c) intermediate pore blocking, and (d) cake filtration models.**



TH-2589_156107040

**Table 6.2: Coefficient of determination ($R^2$) values for CM3 membrane-filtered juice system.**

| Models | Applied Pressure (kPa) | | |
|---|---|---|---|
| | **103.4** | **137.9** | **172.4** |
| Complete Pore Blocking | 0.781 | 0.729 | 0.823 |
| Standard Pore Blocking | 0.886 | 0.867 | 0.927 |
| Intermediate Pore Blocking | 0.952 | 0.948 | 0.981 |
| Cake Filtration | 0.999 | 0.999 | 0.995 |

Table 6.3 summarizes the fouling model coefficients predicted using Bolton's model. For all cases, it was observed that the cake filtration model has the lowest error (0.03 – 0.12) amongst all other models and hence cake filtration is the best fit model. Compared to the Hermia model, the Bolton model indicated similar result as the error for intermediate pore blocking (0.25 – 0.41) was lower than that of the complete pore blocking (0.36 – 0.57) and standard pore blocking (0.38 – 0.65) models. The coefficient for cake filtration model varied from $0.776 \times 10^{14}$ to $4.80 \times 10^{14}$ ($s^2.m^{-4}$) with an error of 0.028 to 0.117. The coefficients for complete pore blocking, standard pore blocking and intermediate pore blocking were predicted to be vary from 4.41 to 7.05, 383791.9 to 1068336 and 2036312 to 5615300 (1/m), respectively.

Similar trends were obtained for CM7 and CM1 membranes. For these two cases as well, based on the $R^2$ values of Hermia models and errors of Bolton model, cake filtration and intermediate pore blocking models were found to be dominant mechanism in comparison with standard and complete pore blocking models. In summary, the chosen combination of membrane morphology, feedstock and $\Delta P$ is promising due to dominance of cake filtration and higher FRR values.



TH-2589_156107040

**Table 6.3: Bolton pore blocking model coefficients and error values of CM3 membrane-filtered juice system.**

| Model Coefficients | Applied Pressure (kPa) | | |
|---|---|---|---|
| | **103.4** | **137.9** | **172.4** |
| $k_s$ | 1068336 | 704820.7 | 383791.9 |
| **Error** | 0.6531 | 0.3646 | 0.4719 |
| $k_b$ | 4.27 | 7.05 | 4.41 |
| **Error** | 0.5716 | 0.3653 | 0.4736 |
| $k_i$ | 5615300 | 3935572 | 2036312 |
| **Error** | 0.41 | 0.25 | 0.32 |
| $k_c$ | $4.80 \times 10^{14}$ | $2.68 \times 10^{14}$ | $0.776 \times 10^{14}$ |
| **Error** | 0.03 | 0.12 | 0.12 |

## 6.5 Permeation Resistances

For various cases, Table 6.4 summarizes contribution of support, reversible and irreversible resistances during flux decline study of bottle gourd juice using various combinations of feed juice, membrane morphology and transmembrane pressure cases. For CM7 membrane case, compared to reversible resistance (28.13 – 68.65 %), the contributions of support (22.53 – 55.53 %) and irreversible resistance (8.81 – 16.33 %) were lower. Similar results were obtained for CM3 and CM1 at all pressure differentials. With an increasing ΔP from 103.4 to 172.4 kPa, the support resistance increased significantly from 22.53 % to 55.53 % for 0.45 μm membrane (CM7 membrane). For both cases, since reversible resistance reduced significantly from 68.65 % to 28.13 %, the irreversible resistance enhanced from 8.81 % to 16.33 %. The reduced FRR for CM7 and CM3 membranes is due to the enhanced irreversible resistance (Table 6.4). For CM1, the irreversible resistance value was very low (0.01 – 0.02 %). This is also in agreement with the observations evident from membrane cleaning procedures. These observations affirmed major fouling due to external cake layer formation and not due to internal pore blocking.



TH-2589_156107040

**Table 6.4: Contributions of alternate permeation resistances to total permeation resistances of CM1, CM3 and CM7 membranes.**

| Applied Pressure (kPa) | Contribution of Resistance to Total Resistances (%) | | | | | | | | |
|---|---|---|---|---|---|---|---|---|---|
| | Support | | | Reversible | | | Irreversible | | |
| | CM1 | CM3 | CM7 | CM1 | CM3 | CM7 | CM1 | CM3 | CM7 |
| 103.4 | 0.37 | 0.73 | 22.53 | 99.61 | 98.30 | 68.65 | 0.02 | 0.95 | 8.81 |
| 137.9 | 0.24 | 0.97 | 26.82 | 99.73 | 97.72 | 63.00 | 0.02 | 1.29 | 10.17 |
| 172.4 | 0.19 | 1.61 | 55.53 | 99.8 | 96.10 | 28.13 | 0.01 | 2.28 | 16.33 |

Comparatively lower FRR (80.90 – 86.97 %) was obtained for CM3 membrane. This is due to enhanced irreversible resistance contributed by internal pore blocking. With an increase in pressure from 103.4 to 172.4 kPa, the reversible resistances reduced from 28.13 – 68.65 % and 96.10 – 98.30 % for 0.45 µm (CM7 membrane) and 0.75 µm (CM3) membranes, respectively. For the CM1 membrane, these values were observed to be similar (99.61 – 99.8 %). In summary, the obtained data are in agreement with the FRR and FDC trends elaborated previously. Among all cases, the best case corresponds to CM1 membrane operated at 103.4 kPa. For the case highest reversible resistance (99.61 %) and very low irreversible resistance (0.02 %) was apparent during dead end MF of bottle gourd juice. Similar results have been obtained for CM3 and both fresh and filtered feed.

## 6.6 Permeate Characteristics

Table 6.5 summarizes the permeate quality characteristics of bottle gourd juice samples obtained for various cases at 137.9 kPa. The clarified juice possessed maximum clarity (92.469 %) and minimum color (0.15 A) for CM1 membrane, which is similar to the permeate clarity (92.045 %) and color (0.156 A) obtained with CM3 membrane. However, the permeate sample of CM7 membrane had very low clarity (83.56 %). Despite being analyzed that the CM7 membrane permeate sample polyphenol content was the best and



TH-2589_156107040

highest in comparison with that being obtained for the permeate samples obtained from CM1 and CM3 membranes, higher color and lower clarity of the permeate sample was obtained. This affirms that the membrane was ineffective to retain suspended particles that exist in the feed juice system. Hence, CM7 can be concluded to be not suitable for the clarification of bottle gourd juice. Compared to the permeate obtained for CM1 membrane that possessed high protein content (192.83 mg/100 mL) and low polyphenols content (7.934 mg GAE/100 g), the permeate obtained from the CM3 membrane possessed lower protein content (139.173 mg/100 mL) and higher polyphenols content (10.108 mg GAE/100 mL). Microbial spoilage of clarified juice products is dependent on several factors such as moisture content, pH, acidity, redox potential and nutritional content. Since protein acts as a nutritional supplement to aid microbial growth and spoilage, lower protein content is desired to enhance shelf life of the permeate. This hypothesis is supported with the inference provided in the literature to indicate that most Gram-negative bacteria derive nutritional supplements from proteins prevalent in the food system (Jay et al., 2008).

**Table 6.5: Permeate Characteristics of CM1, CM3 and CM7 membranes and alternate bottle gourd juice feed systems.**

| Properties at 137.9 kPa applied pressure | CM1 | | CM3 | | CM7 | |
|---|---|---|---|---|---|---|
| | Fresh | Clarified | Filtered | Clarified | Centrifuged | Clarified |
| Color (A) | 2.58 | 0.15 | 0.99 | 0.16 | 1.34 | 0.47 |
| Clarity (%) | 3.81 | 92.47 | 43.83 | 92.05 | 40.55 | 83.56 |
| Proteins (mg/1000 mL) | 641.55 | 192.83 | 391.95 | 139.17 | 369.99 | 190.13 |
| Carbohydrates (g/100 mL) | 1.88 | 1.31 | 1.63 | 0.76 | 1.57 | 1.19 |
| Polyphenols (mg GAE/100 g) | 21.49 | 7.93 | 21.42 | 10.11 | 21.24 | 20.93 |



TH-2589_156107040

Further, clarified juice is very likely to have lower microbial content due to the microbial separation potential of the microfiltration system. Thus, the lower combinations of protein content and microbial content in the clarified juice system is expected to enhance the shelf life of the membrane clarified bottle gourd juice product. Hence, the permeate obtained with CM3 membrane can be analyzed to be the optimal sample from permeate quality perspective.

## 6.7 Identification of Optimal Membrane and Feed System

Based on the combinatorial characteristics of flux decline, FRR, FDC, reversible resistance, color, clarity protein content, polyphenols content and carbohydrate content, the best combinations of membrane morphology (among CM1, CM3, and CM7) and feedstock (centrifuged, filtered and fresh juices) can be inferred. Table 6.6 summarizes the membrane properties and permeate quality of the bottle gourd juice obtained with alternate membranes at an optimum pressure of 137.9 kPa.

**Table 6.6: A summary of optimal bottle gourd juice clarification characteristics of CM1, CM3, CM7 and literature reported membranes.**

| Properties | CM1 (Fresh) | CM3 (Filtered) | CM7 (Centrifuged) | Literature (Mondal et. al 2016) |
|---|---|---|---|---|
| FRR (%) | 91.89 | 85.28 | 72.50 | 86 |
| FDC (%) | 91.57 | 94.05 | 77.26 | 41 |
| Reversible Resistance (%) | 99.73 | 97.72 | 63.00 | – |
| Color (A) | 0.15 | 0.16 | 0.47 | 0.4 |
| Clarity (%) | 92.47 | 92.05 | 83.56 | 76.5 |
| Proteins (mg/1000 mL) | 192.83 | 139.17 | 190.13 | 1974 |
| Carbohydrates (g/100 mL) | 1.31 | 0.76 | 1.19 | – |
| Polyphenols (mg GAE/100 g) | 7.93 | 10.11 | 20.93 | 7.9 |



TH-2589_156107040

It may be noted that the properties portrayed by CM3 membrane and CM1 membrane were similar to each other and are better than those exhibited by CM7. However, based on lower protein content (139.17 mg/1000 mL) and higher polyphenols (10.11 mg GAE/100 g) content of the product, the membrane CM3 has been inferred to be optimum among chosen choice of feedstock and membranes morphologies.

The FRR of the CM3 was found to be similar to the values reported in the literature (85.28 % for the case and 86 % for the literature) (Mondal et al., 2016). However, the samples possessed enhanced permeate quality such as color (0.16 A), clarity (92.05 %) and lower protein content (139.17 mg/100 mL) (Table 6.6). The polyphenol content was found to be similar to that reported in the literature (10.11 mg GAE/100 g for the case and 7.9 mg GAE/100 g for the literature). In terms of permeate flux, steady state permeate flux was found to be comparable to that obtained in the literature i.e., cross flow flux of $8.3 \times 10^{-6}$ $m^3.m^{-2}.s^{-1}$ according to literature and dead end MF flux of $1.3 \times 10^{-6}$ $m^3.m^{-2}.s^{-1}$ for the CM3 membrane. Deploying cross flow MF operations, the ceramic membranes flux is anticipated to enhance by about 3 to 4 times of the steady state flux indicated in this work and thereby become comparable with the literature reported best MF process flux data. In summary, the CM3 membrane performed comparatively better than the literature reported data in terms of permeate product clarity. However, it is only in comparable terms with respect to the flux data reported in the literature. These variations are due to the deployment of ceramic membrane with wide pore size distributions in comparison with the polymer membranes that possess narrow pore size distributions.



TH-2589_156107040

## 6.8 Summary

This work investigates the best combination of applied pressure, feedstock and membrane pore size for bottle gourd juice production. The following conclusions have been drawn from the study.

- Among alternate choices of membrane morphology (0.45, 0.75 and 1 µm pore size) and feed systems (cloth filtered, paper filtered and centrifuged), 0.75 µm pore size membrane with paper filtered feed juice can be regarded to perform best in terms of fouling characteristics, color, clarity, protein content, carbohydrate content and polyphenols content. The optimum pressure was found out to be 137.9 kPa at which the best nutritional characteristics of the permeate sample have been obtained.
- For the optimized membrane, the FRR and FDC varied from 80.90 – 86.97 % and 89.425 – 92.10 % respectively.
- Both Hermia and Bolton pore blocking models infer that cake filtration and intermediate pore blocking models were the best fit models to represent the pertinent fouling characteristics of the vegetable juice microfiltration system.
- The reversible resistances were found to be dominant for both CM1 (99.61 – 99.80 %) and CM3 96.10 – 98.30 %) membranes and for all considered pressure values.
- For CM3 membrane, lowest protein content of 139.173 mg/100 mL was obtained. This is highly promising to enhance its shelf life. The considered case studies inferred that paper filtration served as an effective measure to achieve better permeate quality with CM3 membrane. On the other hand, for scalable operations, the recommended choice could be CM1 which does not require any feed pre-processing step.

Thus, during the clarification of bottle gourd juice, it is apparent that membrane morphology and feed choice significantly influence permeation characteristics of low cost ceramic



TH-2589_156107040

membranes. Therefore, it is very important to visualize the potential of combinatorial optimality investigations for the retention of desired constituents and elimination of undesired constituents in membrane processed vegetable juice systems. In summary, the research findings reported in this work can serve as a useful guideline to further enhance the application of low cost ceramic membranes for vegetable juice processing applications.

## References

1. Jay, J.M., Loessner, M.J., Golden, D.A., 2008. Modern Food Microbiology. Springer Science & Business Media.
2. Mondal, M., Biswas, P.P., De, S., 2016. Clarification and storage study of bottle gourd (*Lagenaria siceraria*) juice by hollow fiber ultrafiltration. Food and Bioproducts Processing 100, 1-15.



TH-2589_156107040

# Chapter 7:

# Sonication Assisted Optimal Extraction of Bioactive Compounds from Bitter Gourd Vegetable

TH-2589_156107040

TH-2589_156107040

# Sonication Assisted Optimal Extraction of Bioactive Compounds from Bitter Gourd Vegetable

*This chapter devotes towards the parametric optimality of ultrasound-assisted bio-active compounds extraction (UAE) from bitter gourd vegetable. Response surface methodology (RSM) was adopted to design and optimize the associated process parameters. Section 7.1 presents a brief overview of the area of research. Follow this, section 7.2 presents data sets obtained through RSM modeling based design of experiments approach. Along with the relevant discussions, sections 7.3 and 7.4, respectively elaborate upon the obtained results for normal and pulsed mode UAE respectively. Section 7.5 provides a comparative assessment of both modes of the UAE and associated hypothesis. Following this, discussion with respect to best available literature data has been considered in section 7.6 and summary of critical findings in section 7.7 of the chapter[#].*

## Overview

*In this chapter, the ultrasound-assisted extraction (UAE) of bio-active compounds (antioxidants, total phenolics and soluble proteins as response variables) has been addressed for bitter gourd (Momordica charantia). For comparative purposes, two sonication modes, namely normal and pulsed mode have been considered and the response variables have been addressed as a function of temperature, extraction time and vegetable to water ratio by targeting the design of experiments using response surface methodology (RSM). Literature*

[#] Published Article: Chakraborty, S., Uppaluri, R., Das, C., (2020) "Optimization of Ultrasound-assisted Extraction (UAE) Process for the Recovery of Bioactive Compounds from Bitter Gourd using Response Surface Methodology (RSM)", Food and Bioproducts Processing, 120: 114-122.

TH-2589_156107040

*comparison of best data indicates promising performance of the UAE in comparison with conventional extraction process.*

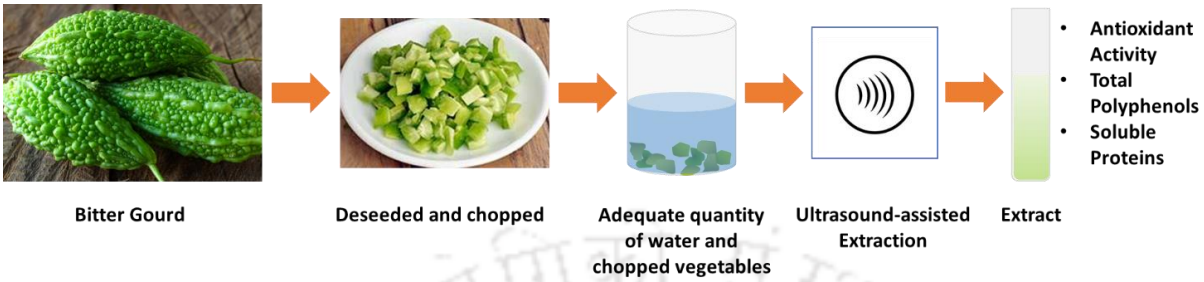


## 7.1 Introduction

Adopting water as extractant, this chapter delineates upon the RSM based UAE of bitter gourd. The critical influence of control variables (such as time of extraction, extraction temperature and bitter gourd to water ratio) on the optimality of desired combinations of bio-active constituent concentrations (maximum concentrations of antioxidant activity and polyphenols and minimum concentration of proteins) have been targeted in experimental investigations that were supplemented with RSM based ANOVA analysis. Total antioxidant activity (expressed in terms of DPPH assay) has been determined to represent the net content of various active antioxidant components (such as Isoflavones, Linolenes, Momordicine, Phenols and Vitamin C in the bitter gourd extract (Kumari et al., 2018). Central composite design (CCD) based RSM was deployed to design the experiments for subsequent model development and optimization of process variables.

## 7.2 Design of Experiments

For both cases namely normal and pulsed mode sonication, Table 7.1 summarizes the data obtained after UAE water extraction of bitter gourd vegetable associated to response



TH-2589_156107040

variables (total polyphenols, antioxidant activity and soluble proteins) and control variables (temperature (A), time (B) and bitter gourd to water ratio (C)). Analysis of variance (ANOVA) was conducted by imposing *p-value* constraints. A *p-value* < 0.05 was considered to regard models to be significant and vice-versa for insignificant lack of values. The response and control variables data sets have been regressed using a second order polynomial equation to achieve the best fit model. The model can be represented as:

$$Y_n = \beta_0 + \sum_{i=1}^{k} \beta_i X_i + \sum_{i=1}^{k} \beta_{ii} X_i^2 + \sum_{i=1}^{k} \sum_{j=i+1}^{k-1} \beta_{ij} X_i X_j \quad (7.1)$$

where, $Y_n$ denotes the response variables, $\beta_0$ the intercept, $\beta_i$ the linear regression coefficient for the $i^{th}$ factor, $\beta_{ii}$ is the quadratic and $\beta_{ij}$ is the cross-product term, $X_i$ and $X_j$ are the input variables and $k$ is the number of input variables ($k$=3).

## 7.3 Conventional UAE

### 7.3.1 Fitness of Alternate RSM Models

The mathematical models for the response variables have been represented using quadratic expressions that were deduced from the central composite design. The expressions depict the relationships between the independent and dependent variables for normal ultrasound-assisted extraction case.



TH-2589_156107040

**Table 7.1: RSM design based experimental data summary of conventional and pulse UAE processes during bioactive compound extraction from bitter gourd vegetable.**

| S. No. | Input Variables | | | Responses | | | | | |
|---|---|---|---|---|---|---|---|---|---|
| | | | | Normal Mode Sonication | | | Pulsed Mode Sonication | | |
| | Temperature (°C) (A) | Time (min) (B) | Bitter gourd to water ratio (g/mL) (C) | Antioxidant Activity (%) | Total Polyphenols (mg GAE/g) | Soluble Proteins mg/1000 mL | Antioxidant Activity (%) | Total Polyphenols (mg GAE/g) | Soluble Proteins mg/1000 mL |
| 1 | 36.60 | 3.90 | 0.18 | 10.20 | 14.50 | 36.10 | 19.30 | 19.90 | 35.10 |
| 2 | 68.90 | 3.90 | 0.18 | 68.60 | 50.10 | 34.90 | 70.90 | 56.50 | 28.80 |
| 3 | 36.60 | 12.00 | 0.18 | 14.70 | 26.40 | 36.80 | 15.70 | 15.60 | 35.70 |
| 4 | 68.40 | 12.00 | 0.18 | 75.70 | 71.20 | 33.70 | 84.80 | 86.10 | 35.50 |
| 5 | 36.60 | 3.90 | 0.42 | 43.00 | 28.30 | 55.70 | 12.70 | 28.60 | 50.70 |
| 6 | 68.40 | 3.90 | 0.42 | 62.70 | 126.00 | 55.80 | 79.10 | 125.80 | 52.80 |
| 7 | 36.60 | 12.00 | 0.42 | 61.50 | 30.80 | 54.40 | 25.70 | 28.00 | 46.90 |
| 8 | 68.40 | 12.00 | 0.42 | 83.40 | 149.60 | 55.30 | 78.70 | 171.30 | 55.80 |
| 9 | 25.00 | 8.00 | 0.30 | 20.50 | 22.50 | 48.20 | 12.60 | 13.60 | 48.30 |
| 10 | 80.00 | 8.00 | 0.30 | 89.40 | 138.50 | 45.30 | 85.60 | 151.70 | 50.60 |
| 11 | 52.50 | 1.00 | 0.30 | 54.50 | 45.10 | 42.80 | 27.40 | 39.70 | 42.50 |
| 12 | 52.50 | 15.00 | 0.30 | 76.40 | 82.80 | 50.50 | 65.60 | 81.90 | 44.80 |
| 13 | 52.50 | 8.00 | 0.10 | 13.60 | 10.30 | 27.30 | 32.40 | 25.20 | 27.10 |
| 14 | 52.50 | 8.00 | 0.20 | 48.00 | 78.00 | 59.3 | 65.10 | 88.70 | 58.20 |
| 15 | 52.50 | 8.00 | 0.30 | 18.60 | 30.90 | 43.40 | 51.70 | 30.30 | 38.60 |
| 16 | 52.50 | 8.00 | 0.30 | 18.40 | 26.90 | 46.10 | 40.60 | 26.50 | 38.40 |
| 17 | 52.50 | 8.00 | 0.30 | 17.40 | 25.20 | 41.60 | 48.20 | 25.40 | 38.40 |
| 18 | 52.50 | 8.00 | 0.30 | 19.50 | 30.70 | 44.10 | 40.90 | 23.70 | 39.80 |
| 19 | 52.50 | 8.00 | 0.30 | 17.30 | 31.30 | 48.10 | 43.60 | 29.30 | 40.90 |
| 20 | 52.50 | 8.00 | 0.30 | 18.30 | 28.00 | 43.80 | 42.60 | 27.60 | 38.00 |

The quadratic model expressions for the responses viz., antioxidant activity, total polyphenols and soluble proteins have been presented as follows:

$$Antioxidant\ Activity\,(\%) = 18.23 + 20.04A + 6.33B + 10.08C - 9.72AC + 3.45BC + 12.62A^2 + 16.13B^2 + 4.58C^2 \quad (7.2)$$

$$Total\ Polyphenols\,(mg\ GAE\ /\ g) = 28.84 + 35.56A + 8.89B + 20.70C + 3.78AB - 17.01AC + 17.07A^2 + 11.56B^2 + 4.97C^2 \quad (7.3)$$

$$Total\ Soluble\ Proteins\,(mg\ /\ 1000mL) = 44.51 + 9.66C - 0.44C^2 \quad (7.4)$$



TH-2589_156107040

**Table 7.2: Model fitness parameters (*F-value* and *p-value*) of all response variables associated to conventional UAE process.**

| Components | Antioxidant Activity | | Total Polyphenols | | Total Soluble Proteins | |
|---|---|---|---|---|---|---|
| | ***F*-value** | ***p*-value** | ***F*-value** | ***p*-value** | ***F*-value** | ***p*-value** |
| **Model** | 849.81 (Quadratic) | <0.0001 (Quadratic) | 245.85 (Quadratic) | <0.0001 (Quadratic) | 29.36 (Quadratic) | <0.0001 (Quadratic) |
| ***A*** | 2988.00 | <0.0001 | 1176.04 | <0.0001 | 1.00 | 0.3410 |
| ***B*** | 297.93 | <0.0001 | 73.53 | <0.0001 | 1.77 | 0.2133 |
| ***C*** | 755.77 | <0.0001 | 398.56 | <0.0001 | 256.96 | <0.0001 |
| ***AB*** | 1.57 | 0.2388 | 7.58 | 0.0203 | 0.031 | 0.8642 |
| ***AC*** | 401.97 | <0.0001 | 153.72 | <0.0001 | 0.69 | 0.4272 |
| ***BC*** | 50.47 | <0.0001 | 0.41 | 0.5378 | 0.049 | 0.8297 |
| $A^2$ | 1334.30 | <0.0001 | 305.07 | <0.0001 | 1.54 | 0.2432 |
| $B^2$ | 2178.96 | <0.0001 | 139.74 | <0.0001 | 1.36 | 0.2704 |
| $C^2$ | 175.83 | <0.0001 | 25.81 | 0.0005 | 0.61 | 0.4516 |
| **Lack of Fit** | 4.44 | 0.0638 | 3.89 | 0.0812 | 0.97 | 0.5143 |
| **R-Squared** | 0.998 | | 0.995 | | 0.964 | |
| **Adequate Precision** | 83.881 | | 50.891 | | 20.988 | |

The *p-values*, *F-values* and R-squared values suggest combinatorial significance of model, each independent variable and quadratic terms associated to the response variables (Table 7.2). For each case, the lack of fit was found to be not significant.

## 7.3.2 Optimality of Independent Variables

Among all control variables, a qualitative analysis of data summarized for normal mode UAE of bitter gourd vegetable affirms significant role of temperature (Figure 7.1). An enhancement in temperature favorably enhanced mass transport of polyphenols, antioxidant activity and to some extent soluble proteins into the extract phase (water). Higher concentration also favored better extraction. This is due to higher availability of such compounds with higher solute loading. Among all responses, extraction time influenced the measured responses marginally. However, since reduced time of operation significantly reduces electricity consumption, minimizing operation time is very much important during UAE of vegetables.



TH-2589_156107040

The basis for the RSM optimization is based on the maximization of both polyphenols and antioxidant activity, but not soluble proteins content in the extract. This is due to the fact that higher soluble proteins is likely to reduce the shelf life of the extract, given the fact that proteins serve to aid nutrition of microbes prevalent in the aqueous environment and contribute towards functional food spoilage.

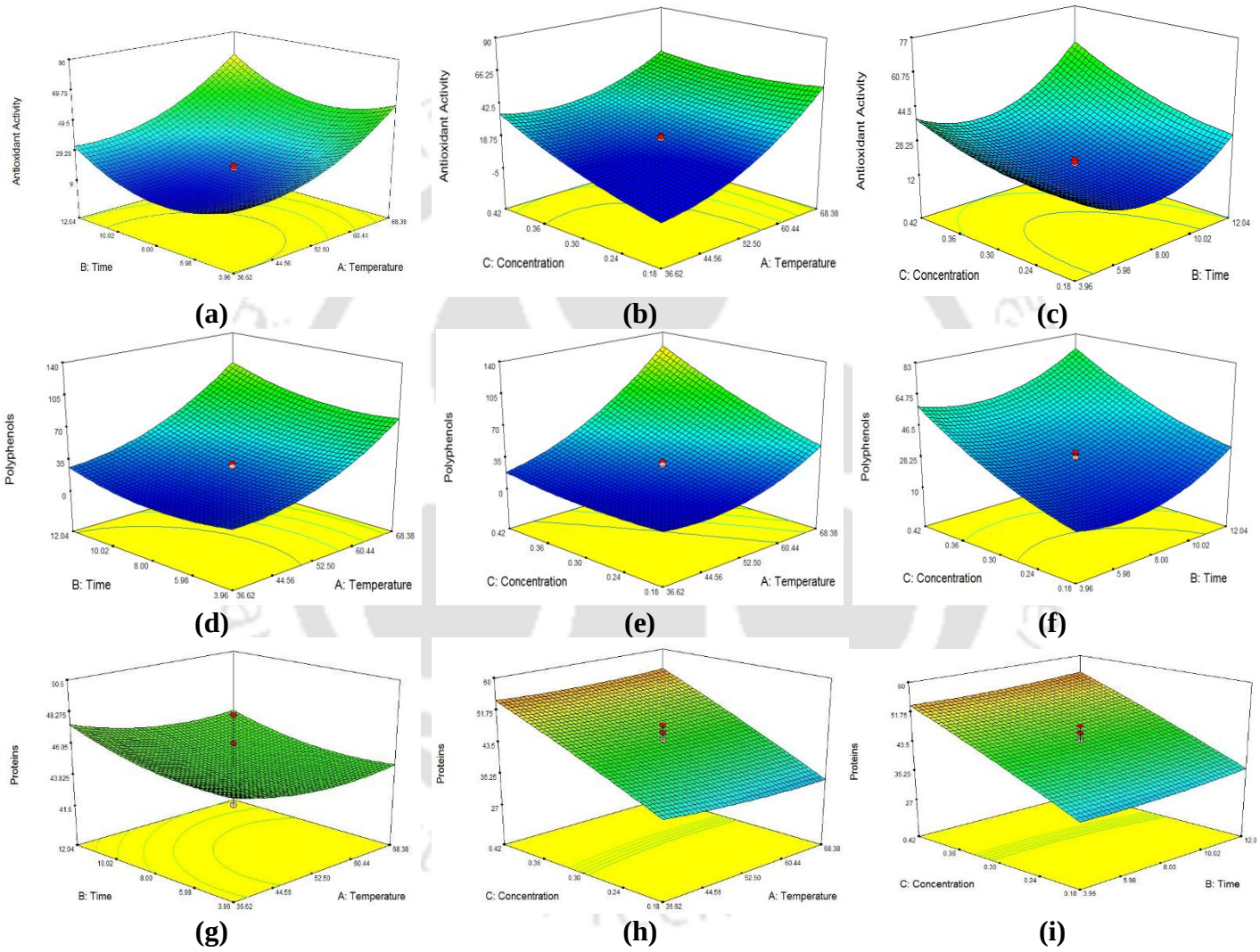


**Figure 7.1: Response surface 3D plots of antioxidant activity (a – c), total polyphenols (d – f) and soluble proteins (g – i) during conventional UAE of bitter gourd vegetable.**



TH-2589_156107040

The optimal control variable values for normal mode UAE of bitter gourd vegetable are 68.4 °C, 11.6 min and 0.3 g/L for temperature, time of extraction and vegetable to water ratio, respectively. Corresponding optimal response variable values are 103.4 mg GAE/g total polyphenols content, 69.9 % antioxidant activity and 46.2 mg/1000 mL total soluble proteins content. The experimentally obtained response variable values for the case correspond to 112.5 ± 4 mg GAE/g, 68.2 ± 2 % and 41 ± 4 mg/1000 mL, for total polyphenols, antioxidant activity and total soluble proteins, respectively. The experimentally determined values are in good agreement with those indicated by the RSM and hence the model fitness is highly relevant for the specified range of control variables.

### 7.3.3 Response Variable – Control Variable Characteristics

Figure 7.1 (a – i) depict the surface plots for various cases considered in this work. Except for concentration-time and concentration-temperature plots for proteins extraction case, the response variable surface plots for the combinations of any two variables followed a non-linear pattern. For the proteins extraction case, the effect of solute to solvent ratio is significantly high (high *F-value* of 256.96) in comparison with temperature (*F-value* of 1.00) and extraction time (low *F-value* of 1.77).

Among all responses, the fitness of antioxidant activity quadratic model is the best (highest *F-value* of 849.81 in Table 7.2) in comparison with the fitness of models associated to total polyphenols and total soluble proteins. For the case, compared to other response variable cases, the effect of temperature is comparably high. On the other hand, for both antioxidant activity and total polyphenols, compared to material to solvent ratio and extraction time, temperature had a dominant effect. For all three response variables, extraction time had a marginal effect. The lowest *F-value* for proteins extraction and each of its associated parameters indicates comparably poor fitness of model and its parameters. For soluble



TH-2589_156107040

proteins extraction, compared to temperature and extraction time, bitter gourd to water ratio had a comparatively significant effect.

For the antioxidant activity, the surface plots indicate its enhancement with an increase in temperature and concentration (Figure 7.1 (a – c)). With respect to extraction time, the surface plots affirm a reduced profile initially that later with time. Therefore, for the time variation case, the antioxidant activity fairly remained similar for initial and final extraction time values (Figure 7.1 (a) and (c)). Similar observations are evident for the surface plots of polyphenols (Figure 7.1 (d – f)) that also affirm its enhancement with an increase in temperature and concentration. Such an observation is in agreement with the *F-values* summarized in Table 7.2. However, with respect to temperature, concentration did not have a profound effect on the response variable variations (Figure 7.1 (e)). The response surface plots of proteins indicate that with an increase in bitter gourd to water ratio, proteins extraction increases. However, for increasing time and temperature, the proteins extraction enhanced marginally (Figure 1 (g – i)). Corresponding *F-values* for each control variable in Table 7.2 as well indicate greater dependence of proteins extraction on concentration, but not on temperature and time.

## 7.4 Pulse Sonication

Table 7.1 summarizes the data in terms of both control and response variables for the pulsed mode UAE case.

### 7.4.1 Identification of Best Fit Models

Unlike normal mode sonication case, the antioxidant activity for pulsed mode of sonication follows a linear model for variation in the said control variables (Table 7.3).



TH-2589_156107040

**Table 7.3: Model fitness parameters (*F-value* and *p-value*) of all response variables associated to pulse sonication based extraction of bioactive compounds.**

| Components | Antioxidant Activity | | Total Polyphenols | | Total Soluble Proteins | |
|---|---|---|---|---|---|---|
| | ***F-value*** | ***p-value*** | ***F-value*** | ***p-value*** | ***F-value*** | ***p-value*** |
| **Model** | 53.37 (Linear) | <0.0001 (Linear) | 264.47 (Quadratic) | <0.0001 (Quadratic) | 49.98 (Quadratic) | <0.0001 (Quadratic) |
| ***A*** | 146.26 | <0.0001 | 1385.15 | <0.0001 | 1.70 | 0.2210 |
| ***B*** | 8.61 | 0.0097 | 82.60 | <0.0001 | 2.62 | 0.1368 |
| ***C*** | 4.25 | 0.0559 | 328.17 | <0.0001 | 373.18 | <0.0001 |
| ***AB*** | | | 45.02 | <0.0001 | 6.96 | 0.0248 |
| ***AC*** | | | 124.96 | <0.0001 | 13.01 | 0.0048 |
| ***BC*** | | | 2.70 | 0.1311 | 2.70 | 0.1316 |
| $A^2$ | | | 301.42 | <0.0001 | 46.81 | <0.0001 |
| $B^2$ | | | 110.31 | <0.0001 | 5.86 | 0.0361 |
| $C^2$ | | | 86.65 | <0.0001 | 2.69 | 0.1322 |
| **Lack of Fit** | 4.36 | 0.0638 | 4.92 | 0.0525 | 3.68 | 0.0897 |
| **R-Squared** | 0.9091 | | 0.9958 | | 0.9783 | |
| **Adequate Precision** | 25.122 | | 53.167 | | 25.487 | |

Using the following model equations, the response variables can be represented as functions of independent variables:

$$Antioxidant\ Activity\ (\%) = -63.505 + 1.649A + 1.566B + 38.522C \quad (7.5)$$

$$Total\ Polyphenols\ (mg\ GAE\ /\ g) = 27.14 + 41.92A + 10.24B + 20.40C + 10AB + 16.66AC + 2.45BC + 18.44A^2 + 11.15B^2 + 9.88C^2 \quad (7.6)$$

$$Total\ Soluble\ Proteins\ (mg\ /\ 1000\ mL) = 39.02 + 8.92C + 1.61AB + 2.20AC - BC + 2.98A^2 + 1.05B^2 \quad (7.7)$$

### 7.4.2 Optimality of Independent Variables

For mathematical optimization, the objective function has been set to maximize extraction of antioxidants and polyphenols but minimize extraction of proteins. The optimal set of control variables refers to 68.4 °C temperature, 12 min time and 0.25 g/mL bitter gourd to water ratio. For such optimal choice of independent variables, the optimal response variables namely antioxidant activity, polyphenols and soluble proteins were 77.9 %, 104.5 mg GAE/g



TH-2589_156107040

and 42.1 mg/1000 mL, respectively. For the identified optimal control variable values, experiments have been conducted to verify the competence of the model based optimal values. Experimentation based optimal values have been analyzed as antioxidant activity of 80 ± 3 %, polyphenols content of 113.1 ± 5 mg GAE/g and protein content of 48.6 ± 5 mg/1000 mL. These are in good agreement with the model based optimal values. Hence, the best fit RSM models have been verified based on experimental fitness of optimal values.

### 7.4.3 Response Variable Characteristics

During pulsed sonication, while antioxidant activity followed a linear model, total polyphenols and total soluble proteins followed a non-linear quadratic model (Table 7.3) with respect to variation in the chosen control variables. The obtained *F-values* for all three modes affirms that the model to represent total polyphenols extraction is the best among all three models. For all cases, the temperature had a significant effect. However, the extraction time also had a reasonably significant effect and for the case of antioxidant activity, it had better effect than the vegetable to solvent ratio. Except for temperature and antioxidant activity and vegetable to solvent ratio and total soluble proteins cases, the *F-value*s of the variables are lower for antioxidant activity and total soluble proteins.

The antioxidant activity profiles indicate linear profile with greater dependency on temperature (Figure 7.2 (a) and (b)). The dependency on time and concentration can be evaluated to be minimal (Figure 7.2 (c) and corresponding *F-values* in Table 7.3). Both temperature and concentration can be analyzed to have a significant role in influencing extraction characteristics of polyphenols compared to extraction time (Figure 7.2 (d – f)). Therefore, for polyphenols case, the associated interaction parameters of *A* (temperature) and *C* (concentration) can be analyzed to be highest (Table 7.3) in comparison to the interaction parameters associated to all other control variables.



TH-2589_156107040

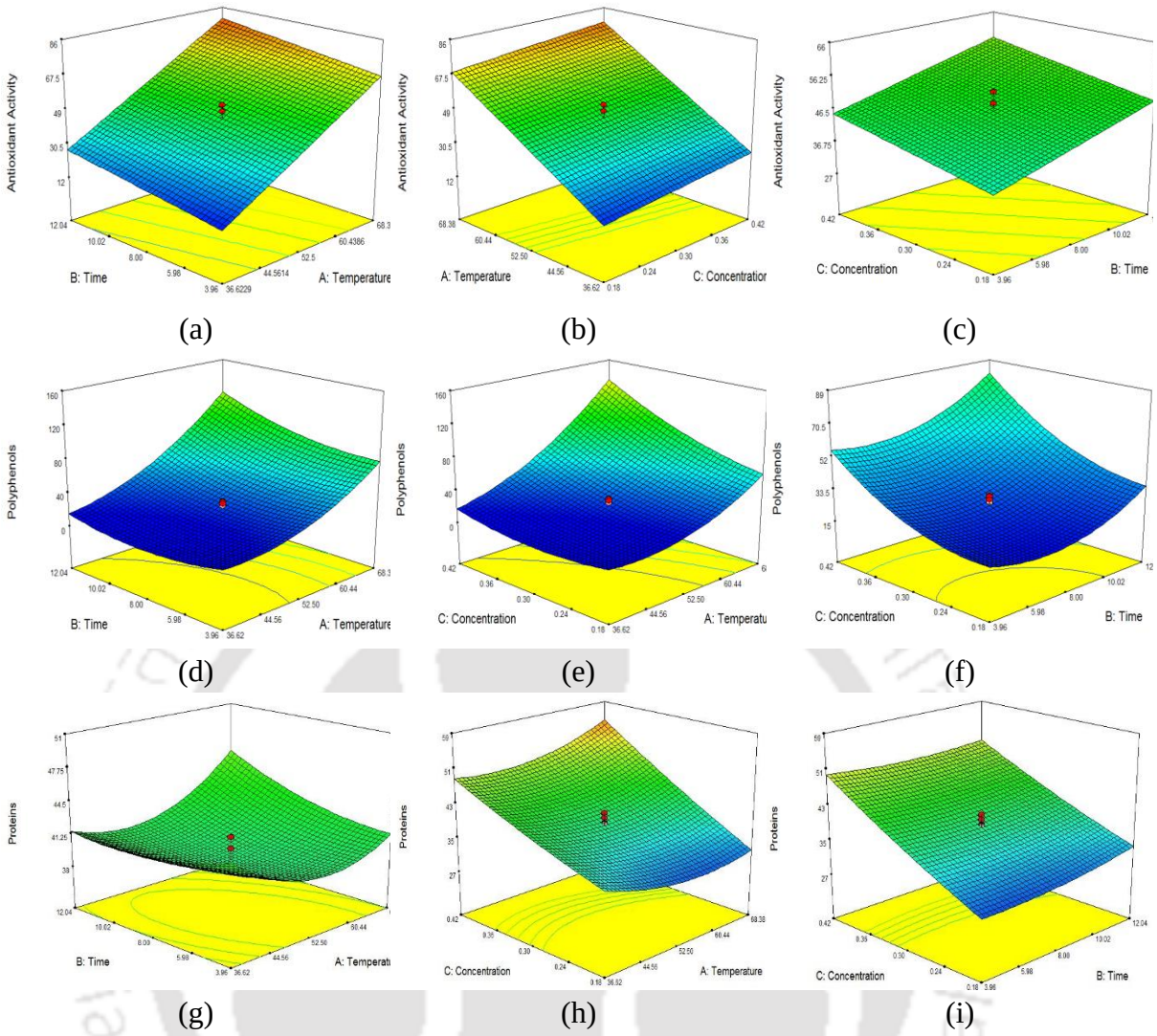


**Figure 7.2: 3D response surface plots of antioxidants (a – c), polyphenols (d – f) and soluble proteins (g – i) during pulse sonication based extraction of bioactive compounds.**

For the soluble proteins extraction case, it is evident that the effect of concentration is significant but not time and temperature (Figure 7.2 (h) and (i)).

## 7.5 Comparative Assessment of Normal and Pulsed Mode Sonication

For the pulsed UAE process, the optimal conditions of temperature, time and concentration for the chosen vegetable are 68.4 °C, 12 min and 0.25 g/mL, respectively. During conventional UAE, these values are 68.4 °C, 11.6 min and 0.3 g/mL, respectively. Significant



TH-2589_156107040

variation does not exist in the optimal values of the control variables for both cases. However, among these two, the best mode of operation can be identified based on the values obtained for the response variables. Among normal and pulsed UAE, the latter enabled better achievement of both antioxidant activity (77.9 %) and lower proteins content (42.1 mg/1000 mL) in comparison with the normal mode of UAE (69.9 % AA and 46.2 mg/1000 mL proteins content). Hence, pulsed mode can be concluded to the best among both modes of sonication, as higher AA has been achieved for similar operating conditions.

Comparing the effect of different parameters, it could be seen that in case of normal mode of ultra-sonication, only temperature and bitter gourd to solvent ratio had maximum effect, whereas time had comparatively significant effect on extraction process. However, for the pulsed mode case, extraction time also had a strong effect in addition to temperature and bitter gourd to solvent ratio (Table 7.2 and Table 7.3). This is also in agreement with the hypothesis that pulsed mode facilitates better transport of bioactive compounds from the core of the vegetable to the ruptured walls during the pulsed sonication effect. Hence, it can be concluded that pulsed mode of sonication is the best for the UAE of bitter gourd vegetable.

Sonication facilitates mass transport of bioactive compounds from the bitter gourd vegetable through the combinatorial effect of three phenomena namely, cavitation, mechanical agitation and thermology (Azmir et al., 2013). During sonication, ultrasonic waves pass through the medium by creating compression and expansion, which is referred to as cavitation. Thermology refers to elevation of temperature at various sites of the vegetable that has been brought forward due to cyclic wave compression and expansion. Insitu and restricted temperature elevation favors enhancement in diffusivity and softening of vegetable surfaces, both of which are favorable for higher mass transport. Thus, in a broader sense, cavitation can be regarded to the fundamental phenomenon that favors agitation and thermology as the driven phenomena due to cavitation. During pulsed UAE, such cavitation effect is significant,



TH-2589_156107040

given the fact that these waves pass through the medium in short time intervals and facilitate better agitation. In this work, three input parameters, namely, time and temperature of extraction and vegetable to solvent ratio have been considered for their optimality during normal and pulsed UAE. While optimal process parameters for both cases have been obtained to be similar, the pulsed UAE can be observed to be efficient to extract higher amounts of polyphenols and antioxidants in comparison with the normal UAE. During normal mode UAE, both temperature and concentration had a positive effect on antioxidant activity and polyphenol content of the extract. On the other hand, proteins extract was mostly facilitated by concentration. Similar inferences can be deduced for the pulsed UAE with higher extraction of antioxidants facilitated with the temperature. In summary, the betterment of cavitation phenomena during pulsed UAE can be inferred to be significantly influencing the extraction process efficiency.

This work adopted CCD based response surface methodology to deduce useful insights into the response surfaces and optimize the process parameters. While significant enhancement in process parametric values may not be achieved through the RSM, the RSM is a very useful technique for the chosen system, given the fact that the methodology inferred evaluation of linearity and non-linearity of specific response variables in terms of the process variables. These cannot be deduced using trial and error approaches. Thereby, parametric interactions can be understood along with identification of critical parameters and their interactions on the chosen response variables. In this regard, it is important to note that the CCD based RSM design generated lesser number of experimental runs to achieve an optimal set of process parameters for the chosen response variables during UAE based vegetable extraction.



TH-2589_156107040

## 7.6 Efficacy of Critical Findings with respect to Prior Art

Table 7.4 summarize the comparative assessment of findings of this work with respect to the limited literature data available in the field of extraction of bioactive compounds from bitter gourd (Kubola and Siriamornpun, 2008; Sutanto et al., 2015). Kubola et al. (2008) used simple boiling method for the extraction of antioxidants and polyphenols from bitter gourd. With comparable solute to solvent ratio (0.2 g/mL) as suggested by this work, lower extraction efficiency was projected indicating lower bioactive compounds in the extract. The comparative assessment affirms significantly better performance of the UAE for bitter gourd extract production. This is due to higher vegetable to water ratio and higher concentrations of bioactive compounds in the aqueous extract.

**Table 7.4: Optimal summary of process and product parameters of UAE-bitter gourd system.**

| Extraction Process | Temperature (°C) | Time (min) | Concentration (g/mL) | Antioxidant Activity (%) | Total Phenolics (mg GAE/g) | Total Soluble Protein (mg/1000 mL) | Literature |
|---|---|---|---|---|---|---|---|
| Boiling | NA | 5 | 0.2 | 53.9 ± 0.73 | 3.2 ± 1.63 | - | Kubola et. al. (2008) |
| UAE | 25 | 5 | 0.025 | 22 | 4.5 | - | Sutanto et. al. (2015) |
| Normal SLE | 65 | 5 | 0.025 | 19 | 3.7 | - | |
| Normal mode ultrasound assisted extraction | 68.4 | 11.6 | 0.3 | 69.9 | 103.4 | 46.2 | This work |
| Pulsed mode ultrasound assisted extraction | 68.4 | 12 | 0.25 | 77.9 | 104.5 | 42.1 | This work |



TH-2589_156107040

The UAE conducted by Sutanto et al. (2015) indicated 68.5 % and 95.6 % lower concentrations of antioxidants and polyphenols, respectively, along with 91.7 % lower vegetable to water concentration in comparison with the optimal findings of this work obtained with the normal UAE process (Sutanto et al., 2015). Compared to the pulsed mode of UAE, the authors obtained 71.7 % and 95.7 % lower antioxidant and polyphenols respectively using samples with 90 % comparatively lower solute concentration. Hence, the optimized UAE process suggested by this work provides better recovery efficiency compared to the literature.

Among both modes of UAE, pulsed mode UAE performed comparatively better in terms of higher antioxidants, comparable total phenolic content and lower soluble proteins content.

## 7.7 Summary

This chapter provided several important conclusions.

- Water proved to be an inexpensive non-toxic solvent for optimal extraction of bioactive compounds from bitter gourd.
- UAE of bitter gourd vegetable facilitated very good extraction profiles of bioactive compounds due to sonication. This especially refers to enhanced concentrations of polyphenols that also contribute to reduction in oxidative stress.
- Pulsed mode sonication provided best results in terms of optimal bioactive compound concentrations (antioxidant activity of 77.9 %, total polyphenols content of 104.5 mg GAE/g and total soluble proteins content of 42.1 mg/1000 mL) for optimal control variable values of 68.4 $^{o}$C temperature, 12 min extraction time and 0.25 g/mL bitter gourd to water ratio.



TH-2589_156107040

- The RSM based design and analysis yielded valuable insights as non-linear and quadratic profiles existed for several measured responses with variations in control variable values. Thereby, RSM enabled better understanding of the combined effect of the various control variables on the response variables.

In summary, the conducted study is highly promising towards furthering the application of ultrasound for the extraction of bitter gourd vegetable to produce natural functional foods for medicinal applications. Future work needs to do detail investigations to address minimizing soluble proteins content in the aqueous extract using competent membrane technologies to further enhance the value and shelf life of the aqueous bitter gourd extract.

## References

1. Azmir, J., Zaidul, I., Rahman, M., Sharif, K., Mohamed, A., Sahena, F., Jahurul, M., Ghafoor, K., Norulaini, N., Omar, A., 2013. Techniques for extraction of bioactive compounds from plant materials: A review. Journal of Food Engineering 117, 426-436.
2. Kubola, J., Siriamornpun, S., 2008. Phenolic contents and antioxidant activities of bitter gourd (*Momordica charantia* L.) leaf, stem and fruit fraction extracts in vitro. Food Chemistry 110, 881-890.
3. Kumari, P., Verma, R., Nayik, G., Solankey, S., 2018. Antioxidant potential and health benefits of Bitter gourd (*Momordica charantia* L.). Journal of Postharvest Technology 5, 1-8.
4. Sutanto, H., Himawan, E., Kusumocahyo, S.P., 2015. Ultrasound assisted extraction of bitter gourd fruit (*Momordica charantia*) and vacuum evaporation to concentrate the extract. Procedia Chemistry 16, 251-257.



TH-2589_156107040

# Chapter 8:

## Optimality of Hybrid Sonication-Microfiltration Process for Bitter Gourd Extract Production

TH-2589_156107040

TH-2589_156107040

# Optimality of Hybrid Sonication-Microfiltration Process for Bitter Gourd Extract Production

*To further improve the product quality characteristics associated to the life cycle of clarified product, the chapter details on the findings associated to the optimality of hybrid Ultrasound-assisted Extraction (UAE) – microfiltration (MF) process for the production of bitter gourd extracts. Further, morphological fitness and fouling characteristics of prepared membranes has been addressed in due course of microfiltration applied to bitter gourd extracts prepared using optimal ultrasound assisted extraction process. After elaborating upon relevant overview in section 8.1, details related to the flux decline analysis for all applicable membranes at specific choice of trans-membrane pressure differentials, has been provided in section 8.3. Following this, section 8.3 presents results associated to dominant fouling mechanisms during clarification of the said bitter gourd extract as feed system. Following this, section 8.4 devotes towards analysis of permeate product characteristics. Finally, section 8.5 summarizes key findings of the conducted research work[#].*

## Overview

*In the preceding chapter (Chapter 7), the optimization of sonication based extraction process has been elaborated to facilitate recovery of bioactive compounds from bitter gourd vegetable. However, the bitter gourd extract can be further refined in terms of product quality characteristics. To do so, the extract is regarded as a feed system to the*

[#] Submitted Article: Chakraborty, S., Uppaluri, R., Das, C., (2020) "Efficacy of Sonication-Microfiltration Hybrid Process for the Production of Clarified Bitter Gourd Extracts". Food and Bioproducts Processing, Under Review.

TH-2589_156107040

*microfiltration process to envision upon a hybrid UAE-MF process for the betterment of product quality characteristics. The efficacy of the hybrid process is the central and primary objective of the chapter. With due consideration of membrane morphology and pressure differentials, the optimality of process-product characteristics has been explored in conjunction with membrane fouling and clarified permeate characteristics.*

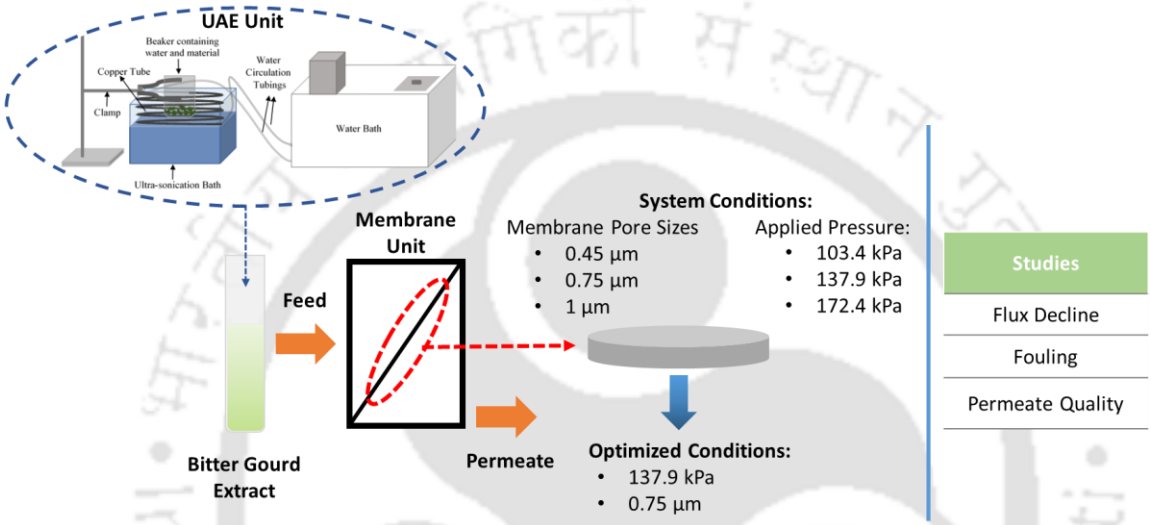


## 8.1 Introduction

In this chapter, the optimality of hybrid UAE-microfiltration process has been targeted for the production of bitter gourd extracts with better product characteristics in terms of extended shelf life of the product. Membrane morphology and trans-membrane pressure differentials have been regarded as the independent variables in the conducted experimental investigations. Three different membrane morphologies (1 µm (CM1), 0.75 µm (CM3) and 0.45 µm (CM7)) and three different trans-membrane pressures (103.4, 137.9 and 172.4 kPa) have been considered to evaluate the parametric sensitivity associated to the final extract product characteristics. The bitter gourd extract (antioxidant activity of 77.9 %, total polyphenols content of 104.5 mg GAE/g and total soluble proteins content of 42.1 mg/1000 mL) produced with optimal sonication assisted extraction process parameters (temperature



TH-2589_156107040

68.4 °C, extraction time 12 min and bitter gourd to water ratio 0.25 g/mL) summarized in the previous chapter (Chapter 7) has been chosen as the feed to the MF system. Thus, the hybrid UAE-MF system is a simple system in which the product from the UAE system is feed to the MF system. To evaluate the best choice of process parameters, flux decline behavior and identification of best fit Hermia fouling models have been addressed. The permeate product characteristics of the MF system has been evaluated in terms of the nutritional characteristics (proteins, antioxidant activity, polyphenols and carbohydrates content), color and clarity. The extract possessing minimum protein content, minimum color, maximum clarity and considerable amount of polyphenols, antioxidants and carbohydrates has been regarded to be the best choice and accordingly best choice of optimal process parameters of the MF system have been identified for the UAE-MF hybrid process.

## 8.2 Trans-membrane Flux Decline Analysis of Hybrid Process System

During MF of UAE based bitter gourd extract, the pertinent flux decline profiles for various cases (three different membranes (CM1, CM3 and CM7) at three different pressure differentials (103.4, 137.9 and 172.4 kPa)) have been depicted in Figure 8.1. For CM1, for a variation in time from 1 – 60 min, the time dependent flux varied from $9.45 \times 10^{-6}$ – $2.67 \times 10^{-5}$, $1.23 \times 10^{-6}$ – $3.97 \times 10^{-5}$ and $1.64 \times 10^{-6}$ – $6.06 \times 10^{-5}$ $m^3.m^{-2}.s^{-1}$ for pressure differential values of 103.4, 137.9 and 172.4 kPa respectively (Figure 8.1 (a)). With reducing pressure and increasing time, the flux decline can be analyzed to be gradual. Since UAE system product was used as feed to the MF process, heavier particulates and solid fibrous materials were not prevalent in the feed system. Thus, the pertinent fouling characteristics was primarily due to the presence of smaller particles in the extract. For CM3 and CM7, the flux decay profiles for 103.4 and 137.9 kPa were similar to one another (Figure 8.1 (b) and 8.1 (c)). For the 137.9 kPa and CM3 case, despite indicating higher permeate flux during the



TH-2589_156107040

onset of the MF process, the flux thereafter gradually became similar to those obtained for the membrane at 103.4 kPa. With a variation in time from 1 – 60 min, at pressure differential values of 103.4, 137.9 and 172.4 kPa, the time dependent flux varied from $7.41 \times 10^{-6}$ – $2.26 \times 10^{-5}$, $8.09 \times 10^{-6}$ – $3.34 \times 10^{-5}$ and $1.21 \times 10^{-6}$ – $4.85 \times 10^{-5}$ $m^3.m^{-2}.s^{-1}$ respectively for CM3 and from $5.59 \times 10^{-6}$ – $1.70 \times 10^{-5}$, $7.24 \times 10^{-6}$ – $2.69 \times 10^{-5}$ and $9.59 \times 10^{-6}$ – $4.41 \times 10^{-5}$ $m^3.m^{-2}.s^{-1}$ respectively for CM7 membrane. Thus, with a reduction in average membrane pore size from 1 – 0.45 µm (CM1 – CM7), the flux decline profile became severe and lowest trans-membrane flux was obtained for CM7 membrane at 103.4 kPa.

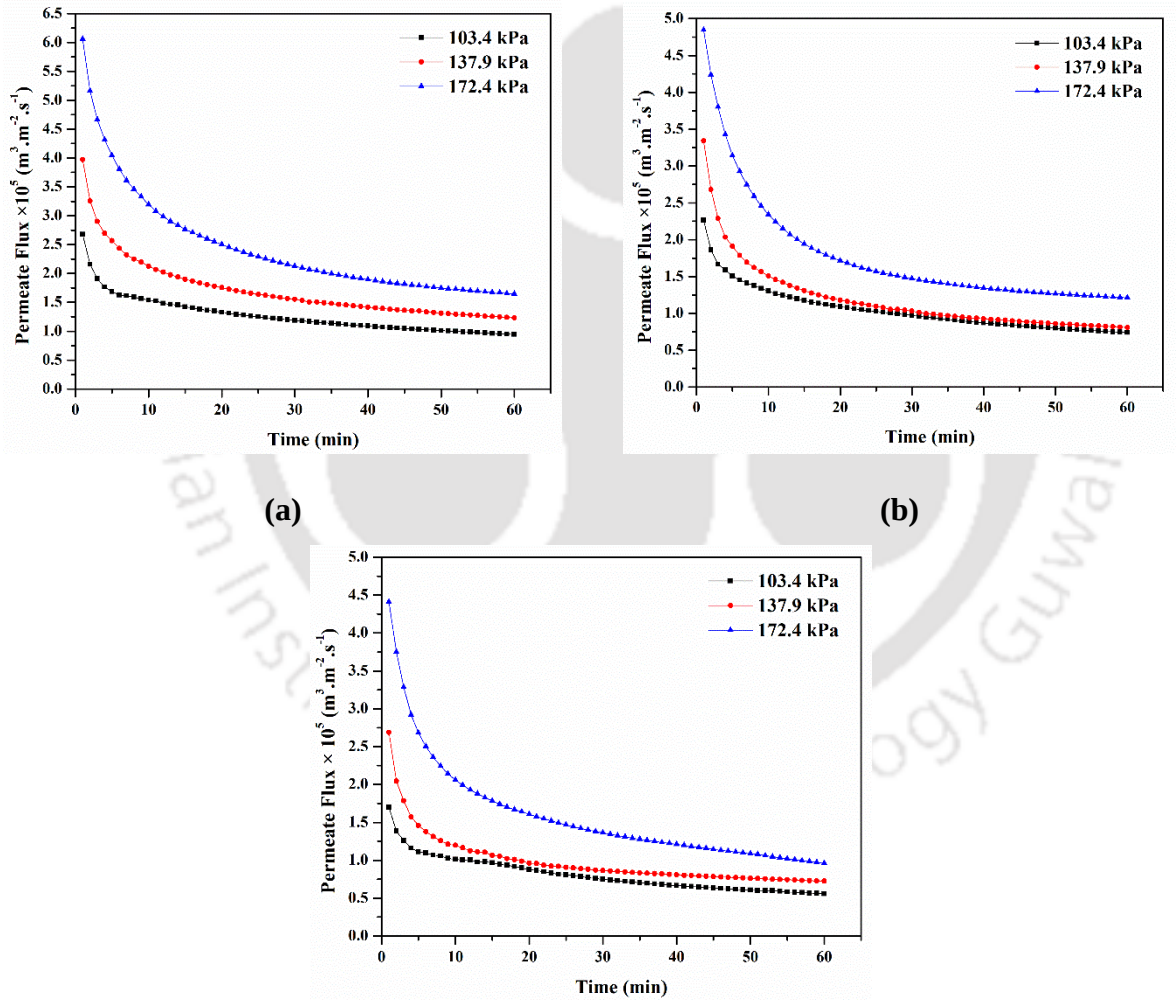


**Figure 8.1: Flux decline profiles for (a) CM1, (b) CM3, and (c) CM7 membranes in the hybrid UAE-MF process system.**



TH-2589_156107040

While higher flux is desirable for an efficient MF process, the flux decline profiles cannot be regarded as the sole concluding factors, given the fact that permeate characteristics with optimal constitution of nutritional characteristics, color and clarity is as well desired.

The flux decline study also provides data on the extent of flux decay during the microfiltration process and also about the role of different pressure differentials and membrane morphologies through FDC values (Table 8.1). The FDC calculated from the flux profiles illustrated upon the severity of fouling (increase in FDC from 64.67 to 72.84 % (CM1), 67.24 to 75.78 % (CM3) and 67.09 to 78.25 % (CM7)) occurring due to increasing trans-membrane pressures. Similar phenomena was observed for membrane morphological changes from CM1 (1 µm) to CM3 (0.45 µm) where the FDC values increased with decrease in membrane pore size. Unlike microfiltration of bottle gourd juice (Chapter 5 and 6), the FDC values were found to be lower in the present study. The use of pretreatment process (UAE) prior to microfiltration decreased the fouling propensity of the membranes to a large extent. Thus hybrid UAE-MF process not only has been anticipated to improve the product quality but also have been proven to lower the fouling of membranes during microfiltration process, which has been one of the biggest barriers in the utilization of membrane filtration process in industrial scale, till date.

**Table 8.1: Flux decay coefficients (FDC) of CM1, CM3, and CM7 membranes at alternate pressure differentials 103.4, 137.9 and 172.4 kPa during microfiltration of bitter gourd extracts.**

| Applied Pressures | FDC (%) | | |
|---|---|---|---|
| (kPa) | CM1 | CM3 | CM7 |
| 103.4 | 64.67 | 67.24 | 67.09 |
| 137.9 | 68.99 | 74.96 | 73.05 |
| 172.4 | 72.84 | 75.78 | 78.25 |



TH-2589_156107040

## 8.3 Membrane Fouling Characteristics

For membranes CM1, CM3 and CM7, Figures 8.2 (a – c), 8.3 (a – c), 8.4 (a – c) and 8.5 (a – c) respectively depict the fitness plots of flux decline profiles with respect to Hermia fouling models (standard, intermediate and complete pore blocking and cake filtration). These fitness plots affirm that the values of $J^{-0.5}$, $J^{-1}$, ln ($J^{-1}$), and $J^{-2}$ were highest for the case of lower trans-membrane pressure (103.4 kPa) and lower average pore size (CM7). This affirms that the combination of lower pressures and lower membrane pore sizes enhances the severity of membrane fouling. At lower pressure, small particulates prevalent in the feed system penetrate through the membrane and thereby enhance membrane fouling. On the contrary, at higher pressures, membrane surface is more susceptible to fouling than its inner matrix. Due to insignificant constitution of suspended solids and larger macromolecules in the feed system, it is very likely that higher pressures do not enhance membrane fouling. Hence, membrane fouling has been analyzed to be lower at higher pressure in comparison to that prevalent during low pressure operation.

With respect to average pore size, it is evident that the membrane with lower pore size (CM7) underwent significant fouling in comparison to the membrane with larger pore size (CM1). This is due to the reason that smaller particles could easily pass through larger membrane pores but do get blocked through the smaller pores to thereby enhance fouling for the CM7 membrane case.



TH-2589_156107040

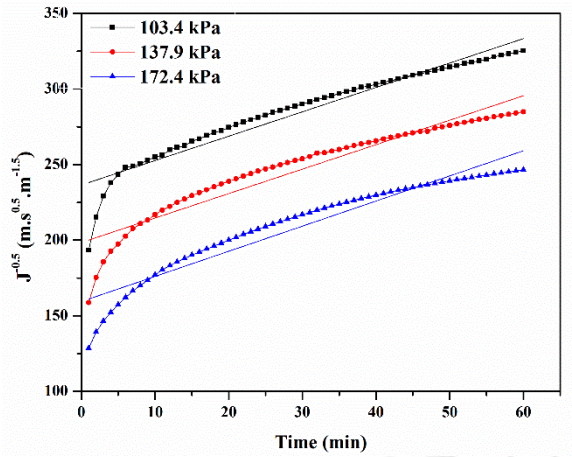


**(a)**

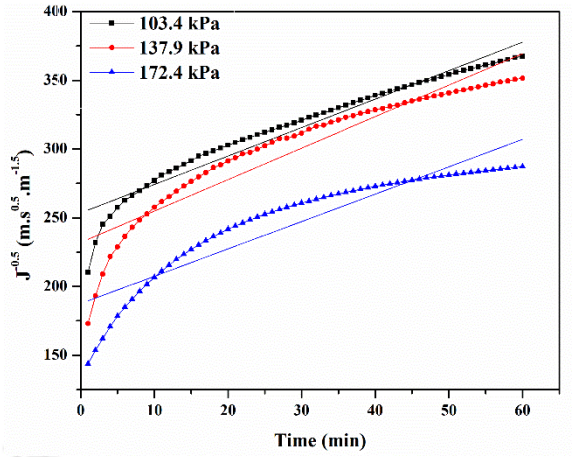


**(b)**

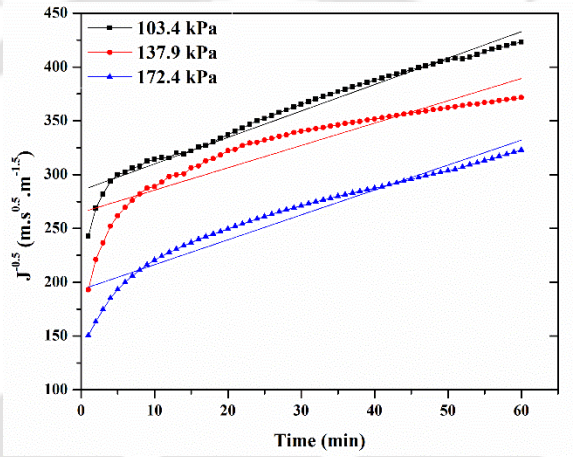


**(c)**

**Figure 8.2: Fitness plots of standard pore blocking model to represent pertinent flux decline of ceramic membranes in the UAE-MF hybrid process system (a) CM1, (b) CM3, and (c) CM7 membrane.**



TH-2589_156107040

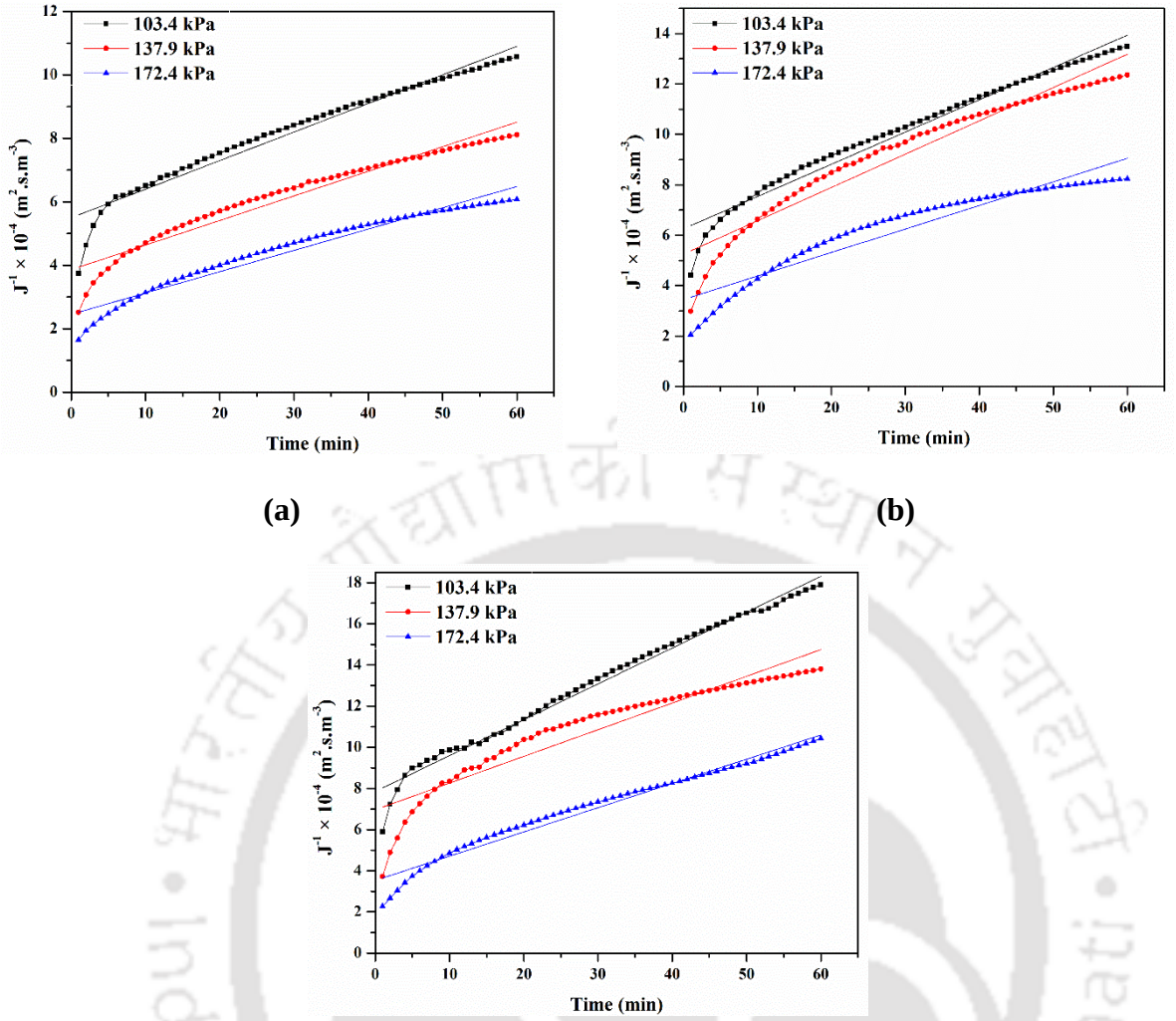


**Figure 8.3: Fitness plots of intermediate pore blocking model to represent pertinent flux decline of ceramic membranes in the UAE-MF hybrid process system (a) CM1, (b) CM3, and (c) CM7 membrane.**



TH-2589_156107040

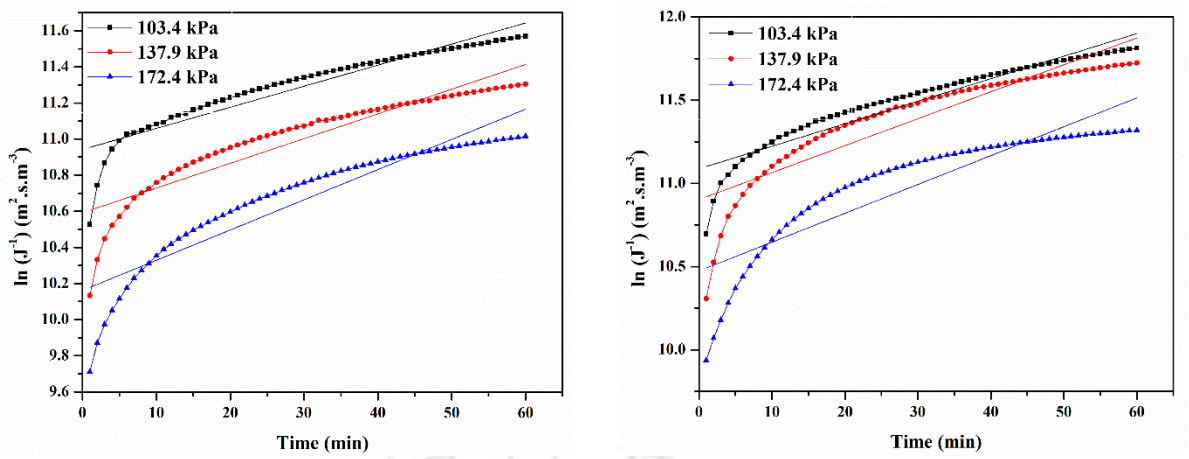


**(a)** **(b)**

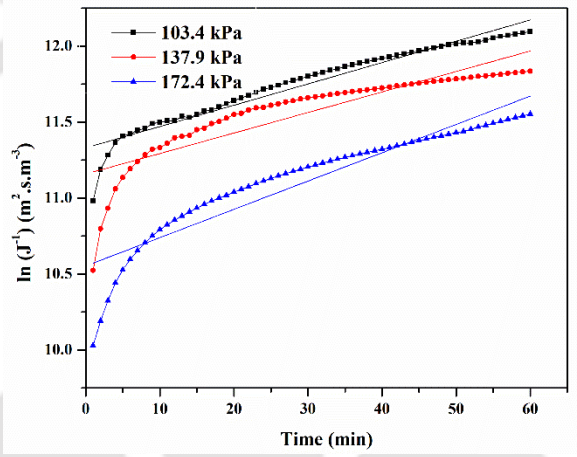


**(c)**

**Figure 8.4: Fitness plots of complete pore blocking model to represent pertinent flux decline of ceramic membranes in the UAE-MF hybrid process system (a) CM1, (b) CM3, and (c) CM7 membrane.**



TH-2589_156107040

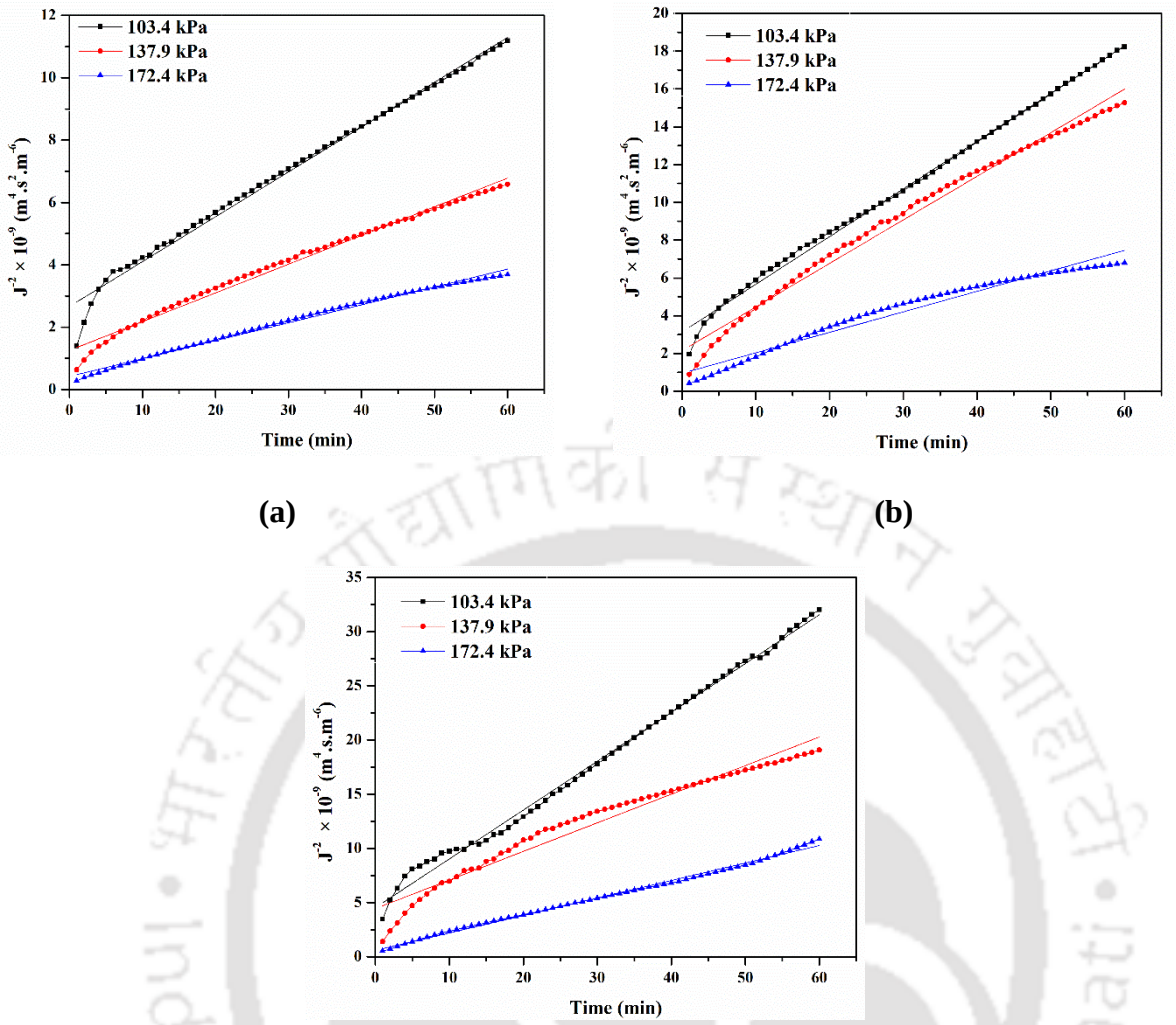


**Figure 8.5: Fitness plots of cake filtration model to represent pertinent flux decline of ceramic membranes in the UAE-MF hybrid process system (a) CM1, (b) CM3, and (c) CM7 membrane**

Table 8.2 summarizes $R^2$ values obtained for the fitness of various alternate Hermia models for all cases. Thereby, the table affirms upon the most competent fouling model that can represent pertinent flux decline for various combinations of average pore size and trans-membrane pressures as process parameters.



TH-2589_156107040

**Table 8.2: Summary of coefficient of determination ($R^2$) associated to alternate fouling models to represent CM1, CM3 and CM7 ceramic membrane flux decline data in the hybrid UAE-MF process system.**

| Fouling Models | | CM1 | | | CM3 | | | CM7 | | |
|---|---|---|---|---|---|---|---|---|---|---|
| | | 103.4 | 137.9 | 172.4 | 103.4 | 137.9 | 172.4 | 103.4 | 137.9 | 172.4 |
| Standard Pore Blocking | $R^2$ | 0.923 | 0.904 | 0.916 | 0.941 | 0.881 | 0.852 | 0.965 | 0.829 | 0.931 |
| | $k_s$ | 1.661 | 1.613 | 1.617 | 2.290 | 2.069 | 1.991 | 2.458 | 2.074 | 2.315 |
| Intermediate Pore Blocking | $R^2$ | 0.956 | 0.944 | 0.955 | 0.970 | 0.932 | 0.902 | 0.985 | 0.885 | 0.971 |
| | $k_i$ | 0.090 | 0.077 | 0.067 | 0.132 | 0.128 | 0.093 | 0.174 | 0.117 | 0.129 |
| Complete Pore Blocking | $R^2$ | 0.877 | 0.851 | 0.863 | 0.899 | 0.813 | 0.788 | 0.934 | 0.757 | 0.867 |
| | $k_c$ | 0.014 | 0.011 | 0.017 | 0.017 | 0.016 | 0.014 | 0.019 | 0.014 | 0.014 |
| Cake Filtration | $R^2$ | 0.990 | 0.988 | 0.994 | 0.996 | 0.989 | 0.966 | 0.996 | 0.957 | 0.995 |
| | $k_{cf}$ | 0.092 | 0.057 | 0.143 | 0.252 | 0.231 | 0.108 | 0.450 | 0.161 | 0.264 |

For CM1, the best fit model refers to cake filtration ($R^2$ = 0.988 – 0.994) followed with intermediate pore blocking ($R^2$ = 0.944 – 0.956), standard pore blocking ($R^2$ = 0.904 – 0.923) and complete pore blocking ($R^2$ = 0.851 – 0.877). Similar trends exist for the CM3 and CM7 membranes with cake filtration being the best fit fouling model to represent pertinent flux decline ($R^2$ = 0.966 – 0.996 (CM3) and 0.957 – 0.995 (CM7)). However, for all cases, it may be noted that for CM1 and CM7, lowest $R^2$ values were obtained for the intermediate pressure differential of 137.9 kPa. Similarly, for CM3, lowest $R^2$ values were obtained for the highest trans-membrane pressure of 172.4 kPa. For all membrane morphologies, the highest $R^2$ values were obtained for a trans-membrane pressure of 103.4 kPa for all fouling models. Thereby, the result infers upon best fitness of the fouling models for the low pressure operation case. The dominant fouling models obtained in this study viz., cake filtration and intermediate pore blocking models which are the most common fouling models found in microfiltration processes (Nandi et al., 2009; Nandi et al., 2011). However, it may be noted that the $R^2$ values obtained in this study was lower as compared to the $R^2$ values generally



TH-2589_156107040

obtained for the respective models during microfiltration. The use of pretreated extracts decreased the fouling of the membranes due to the absence of solids particulates and fibrous materials present in untreated or centrifuged juices. The coefficient values for all the models ($k_{s,}$, $k_i$, $k_c$, and $k_{cf}$) also showed similar observations and in agreement with that observed from the respective $R^2$ values. For cake filtration models, the coefficients were rather a very sensitive parameter than $R^2$, since a small variation in model $R^2$ followed a drastic change in the $k_{cf}$ value for each of the pressure and membrane cases.

The best fitness of cake filtration model to represent pertinent flux decline for all cases is affirming towards lower irreversible fouling for all cases of chosen membranes and trans-membrane pressures. Thus, the obtained results are highly promising towards the deployment of said membranes in the hybrid UAE-MF system.

The combined influence of the UAE and MF processes on the membrane stability and life needs to be determined through the conduct of the long term experimental investigations of the proposed hybrid MF process. This is due to the reason that the UAE pretreatment process reduces the pulpy or fibrous material content and solid particulates in the feed juice system. This translates into significant reduction in the membrane fouling and substantial enhancement in the membrane shelf life. Such suggested investigations need to be addressed in the near future to consolidate upon the sustainability of the hybrid UAE-MF process in conjunction with the MF process.

## 8.4 Permeate Characteristics

The findings associated to the permeate quality characteristics in terms of nutritional content, color and clarity have been summarized in Table 8.3. The best choice of membrane morphology and trans-membrane pressure has been identified based on the combinations of



TH-2589_156107040

maximum protein rejection, and better color and clarity with considerable amount of antioxidants, polyphenols and carbohydrates in the clarified permeate samples. For all pressure cases, protein rejection has been observed to reduce with decreasing average pore size of the membranes. For membranes CM – CM7, these values varied as 13.25 – 40.79 %, 25.68 – 46.74 % and 8.95 – 27.22 % at 103.4, 137.4 and 172.4 kPa, respectively. Compared to all other constituents in the feed system, proteins possess larger size. Hence, with reducing average membrane pore size, protein particles would be significantly blocked due to size exclusion principle. Hence, CM7 permeate sample possessed lowest protein content (and higher rejection) in comparison to those obtained with CM1 and CM7 membranes. However, for the pressure differential case of 137.9 kPa, protein rejection data of CM3 and CM7 are similar (46.74 and 45.58 %, respectively). It is well known that lower protein content is desirable in the product extract as higher protein content in the sample is very likely to lead to microbial spoilage upon long term storage. This is due to the reason that protein content serves as a nutrient to enhance microbial growth in the sample during long term storage. Therefore, to enhance shelf life, clarified extracts should contain lower protein content.

Other constituents of the permeate sample such as antioxidants, polyphenols and carbohydrates can be analyzed to reduce with a reduction in average membrane pore size (CM1 – CM7) and trans-membrane pressures (172.4 – 103.4 kPa). Also, the hybrid UAE-microfiltration system efficiently improved the color and clarity of the extracts. Permeate sample color reduced significantly (0.436 – 0.573 A of feed being reduced to 0.045 – 0.055 A). Similarly, clarity enhanced significantly (from 53.08 – 61.37 % to 95.78 – 98.85 %). For the case of CM3 membrane (0.75 µm average pore size) and 137.9 trans-membrane pressure differential, optimal permeate characteristics have been obtained.



TH-2589_156107040

**Table 8.3: Clarified product characteristics of the hybrid UAE-MF system.**

| Pressure (kPa) | Membrane | Protein (mg/1000 mL) | | | Antioxidant Activity (%) | | Polyphenols (mg(GAE)/g) | | Carbohydrates (mg/1000 mL) | | Color (A) | | Clarity (%T) | |
|---|---|---|---|---|---|---|---|---|---|---|---|---|---|---|
| | | Feed | Permeate | Rejection (%) | Feed | Permeate | Feed | Permeate | Feed | Permeate | Feed | Permeate | Feed | Permeate |
| 172.4 | CM1 | 44.69 | 40.69 | 8.95 | 70.83 | 66.25 | 100.87 | 88.26 | 2120.31 | 1997.89 | 0.475 | 0.048 | 55.81 | 95.78 |
| | CM3 | 46.91 | 38.45 | 18.03 | 73.54 | 61.78 | 97.64 | 84.34 | 2133.10 | 1344.03 | 0.498 | 0.046 | 58.50 | 96.58 |
| | CM7 | 49.63 | 36.12 | 27.22 | 72.30 | 50.84 | 102.70 | 84.13 | 2111.51 | 1138.19 | 0.476 | 0.045 | 56.64 | 95.82 |
| 137.9 | CM1 | 53.92 | 40.07 | 25.68 | 67.41 | 65.69 | 90.86 | 78.69 | 2022.10 | 1913.13 | 0.512 | 0.055 | 53.08 | 97.72 |
| | CM3 | 47.38 | 25.23 | 46.74 | 76.58 | 56.68 | 102.82 | 75.87 | 2173.25 | 1259.27 | 0.436 | 0.049 | 61.37 | 98.17 |
| | CM7 | 44.23 | 24.07 | 45.58 | 72.38 | 49.22 | 105.43 | 72.96 | 1919.39 | 947.59 | 0.573 | 0.045 | 54.83 | 98.85 |
| 103.4 | CM1 | 48.29 | 41.89 | 13.25 | 71.08 | 59.43 | 98.82 | 77.39 | 2103.06 | 1696.32 | 0.478 | 0.057 | 59.26 | 97.07 |
| | CM3 | 46.92 | 39.84 | 15.09 | 72.33 | 56.08 | 102.47 | 73.26 | 2112.71 | 1203.89 | 0.493 | 0.056 | 54.82 | 98.40 |
| | CM7 | 41.31 | 24.46 | 40.79 | 75.34 | 43.65 | 101.96 | 70.65 | 2038.73 | 886.15 | 0.499 | 0.053 | 57.59 | 98.76 |

These correspond to lowest protein content of 25.23 mg/1000 mL (46.74 % rejection), considerably higher antioxidant activity of 56.68 %, higher polyphenols content of 75.87 mg(GAE)/g and higher carbohydrate content of 1259.27 mg/1000 mL, color of 0.049 A and clarity of 98.17 %. Thereby, based on permeate analysis and fouling characteristics of the pertinent flux profiles, CM3 membrane being operated at 137.9 kPa has been concluded to be the best choice for the hybrid UAE-MF system. Since permeate quality is very important in comparison with fouling, moderate fouling with acceptable levels of flux decline are to be regarded to be the best choice for the UAE-MF hybrid process associated to bitter gourd extracts to produce clarified permeate product with better shelf life and nutritional characteristics.



TH-2589_156107040

## 8.5 Comparative Assessment with Prior Art Data

Table 8.3 summarizes a comparative assessment of the optimal findings of this work with those reported in the literature for the hybrid process system to extract bioactive compounds from bitter gourd vegetable. The literature reported data affirm that the authors (Jain et al. (2018)) adopted solid-liquid extraction followed with microfiltration to produce clarified bitter gourd extract (Jain et al., 2018). While the authors obtained optimal trans-membrane pressure to be similar to that obtained in this work (138 kPa), the color and clarity of the permeate sample was poor in terms of color and clarity (0.13 A and 85.38 %), given the color and clarity of the permeate sample in this work is about 0.049 A and 98.17 %, respectively. Thus, the findings in this work have better combinations of color and clarity.

The literature also affirms lower polyphenol content (0.14 mg (GAE)/g) and higher protein content (108.0 mg/1000 g) in the clarified permeate product. Thus, the permeate product needs further processing to enhance its shelf life. Contrary to this, the permeate sample obtained in this work possessed higher polyphenol content (73.26 mg (GAE)/g polyphenols content) and lower protein content (25.23 mg/1000 mL). Thus, with lower protein content and higher polyphenol content, the clarified product obtained from the hybrid UAE-MF system would have better shelf life than that obtained with the hybrid solid liquid extraction – MF system. This is due to the reason that lower protein content in the clarified juice is very likely to have lesser microbial damage (Jay et al., 2008). Antioxidant content of the clarified permeate product is about 56.68 %, which is significantly high. For comparative purpose, no literature data is available for the same. The steady state flux for the optimal conditions was found to be lower i.e., $8.09 \times 10^{-6}$ $m^3.m^{-2}.s^{-1}$ compared to $2.08 \times 10^{-5}$ $m^3.m^{-2}.s^{-1}$ in the literature. This may be due to the application of cross-flow system in the literature in comparison with the dead-end MF being deployed in this work.



TH-2589_156107040

**Table 8.3: Optimal process-product characteristics of hybrid UAE-MF process system for the production of clarified bitter gourd vegetable extract.**

| Hybrid Process | Process Parameters | | | | | | | | |
|---|---|---|---|---|---|---|---|---|---|
| | Trans-membrane Pressure (kPa) | Proteins (mg/1000 mL) | Rejection (%) | Polyphenols (mg (GAE)/ g) | Antioxidant Activity (%) | Carbohydrates (mg/1000 mL) | Color (A) | Clarity (% T) | Authors |
| SLE-MF | 138 | 108.0 | 36.91 | 0.14 | NA | NA | 0.13 | 85.38 | Jain et al. (2018) |
| UAE-MF | 137.9 | 25.23 | 46.47 | 73.26 | 56.68 | 1259.27 | 0.049 | 98.17 | This work |

Deploying cross flow MF operations, the ceramic membranes flux is anticipated to enhance by about 3 to 4 times of the steady state flux indicated in this work and thereby become comparable with the literature reported best MF process flux data. Thus, in summary, the UAE-MF performed better than the SLE-MF process and this is due to the competence of the ceramic membrane and UAE process in conjunction with the SLE and polymeric membranes being deployed in the literature.

## 8.6 Summary

This chapter addressed the efficacy of alternate UAE-MF process to achieve better clarification characteristics of bitter gourd extracts in comparison with the UAE process. Important findings of the carried out experimental and modeling investigation are as follows:

- The hybrid UAE-MF process involving UAE product as feed system to the MF affirmed upon the critical dependency of MF process fouling and permeate characteristics on the membrane morphology and trans-membrane pressure differentials.



TH-2589_156107040

- CM3 membrane (average pore size of 0.75 microns) and 137.9 kPa pressure have been identified as the optimal pressure to achieve best permeate quality and acceptable values of membrane fouling and associated flux decline.
- The CM1 membrane provided maximum flux and lower fouling. However, the membrane did not improvise upon permeate quality significantly. On the other hand, CM7 membrane provided poorer flux, higher fouling and poorer permeate quality. Thus, tradeoffs are apparent with respect to the average membrane pore size to achieve acceptable combinations of flux, fouling and permeate quality. Given these observations, the membrane with intermediate pore size has been regarded to be the optimal choice.
- Overall, hybrid UAE-MF process indicated promising performance to achieve better product-process characteristics during bitter gourd extract production.

## References

1. Jain, A., Sengupta, S., De, S., 2018. Fundamental understanding of fouling mechanisms during microfiltration of bitter gourd (*Momordica charantia*) extract and their dependence on operating conditions. Food and Bioprocess Technology 11, 1012-1026.
2. Jay, J.M., Loessner, M.J., Golden, D.A., 2008. Modern food microbiology. Springer Science & Business Media.
3. Nandi, B., Das, B., Uppaluri, R., Purkait, M., 2009. Microfiltration of mosambi juice using low cost ceramic membrane. Journal of Food Engineering 95, 597-605.
4. Nandi, B., Uppaluri, R., Purkait, M., 2011. Identification of optimal membrane morphological parameters during microfiltration of mosambi juice using low cost ceramic membranes. LWT-Food Science and Technology 44, 214-223.



TH-2589_156107040

TH-2589_156107040

# Chapter 9:

## Conclusions and Future Work

TH-2589_156107040

TH-2589_156107040

# Conclusions and Future Work

*In two sections sequentially, the chapter summarizes important conclusions of the work addressed in the PhD thesis followed with possible scope for future research.*

## 9.1 Conclusions

Based on experimental and alternate modeling efforts associated to low cost ceramic membrane fabrication, microfiltration of bottle gourd juice, ultrasound assisted extraction of aqueous bitter gourd extract and hybrid sonication-membrane process for the clarification of aqueous bitter gourd extract, the following sub-sections summarize important findings associated to the said areas of research:

### 9.1.1 Optimization of Sawdust Based Precursor Compositions during Low Cost Ceramic Membrane Fabrication

- Using MMD based response surface methodology (RSM) based design approach for the fabrication of sawdust based low cost ceramic membranes, the optimal membrane precursor composition achieved without considering flexural strength as an additional response variable were 48.19 wt.% kaolin, 28.62 wt.% feldspar and 8.19 wt.% sawdust. Corresponding optimal response variable values were 28.47 % porosity and 1.00 µm average pore size.
- Upon consideration of flexural strength as an additional response variable, the optimal precursor composition based on MMD based RSM approach only varied marginally and reached 48 wt.% kaolin, 27.81wt.% feldspar and 8.26 wt.% sawdust.

TH-2589_156107040

Corresponding optimal response variable values were 29.98 % porosity, 0.93 µm average pore size and 8.75 MPa flexural strength.

- While porosity and flexural strength response variables followed special cubic model in terms of the precursor composition, the much complex cubic model was followed by the average pore size response variable. Corresponding model *F-values* were 39.56, 108.22 and 380.58, respectively and indicate very good fitness.
- High non-linear variation of responses have been addressed for all possible combinations of the maximization and minimization of response variables to theoretically infer that the carried out is generic in nature for extension towards optimality of other independent process parameters associated to low cost ceramic membrane fabrication.
- The insignificance of flexural strength as an important response variable to influence compositional optimality is affirming to the fact that membrane researchers in the field of sawdust based low cost ceramic membrane fabrication can only regard average pore size and porosity as important response variables. Thereby, expensive instrumental facilities need not be targeted in comparison to those that can be indigenously achieved.

### 9.1.2 Optimality of Sawdust Characteristics and Precursor Compositions during sub-micron Range Low Cost Ceramic Membrane Fabrication

- For a reduction in sawdust composition from 8 to 1 %, the sawdust with an average particle size of 254 µm marginally reduced porosity (28.47 to 21.69 %) and considerably reduced average pore size (from 1 to 0.7 µm). Thus, membranes with lower pore size are anticipated to have greater utility towards microfiltration applications owing to their fitness.



TH-2589_156107040

- For the lower sawdust powder composition of 1 wt.%, a variation in average particle size from 254 to 39 µm significantly reduced the average pore size and porosity of the membranes from 21.69 – 16.29 % and 0.7 – 0.45 µm, respectively. Thus compared to sawdust composition, the particle size of the sawdust powder has a greater role to influence membrane morphology. The achievement of membranes with even lower pore size and porosity are anticipated to further widen the applicability of prepared membranes for various microfiltration applications.
- The enhanced binder composition from 7.5 to 15 wt.% (for each binder namely boric acid and sodium metasilicate) along with suitable variations in kaolin to feldspar content (from 0.5 – 2.0) facilitated a significant reduction in average pore size (from 1 to 0.09 µm) and a profound reduction in porosity (from 28.47 to 13.95 %). Thus, said compositional variations are effective to transform microfiltration range membranes to ultrafiltration range membranes with minor variations in the precursor compositions.
- The best fit empirical models for the case of sawdust composition and particle size variation indicate linear model to represent porosity ($R^2$ = 0.993) and a combination of simple quadratic and Michaelis-Menton equation ($R^2$ = 0.949) to represent average pore size. Thus, average pore size of the membrane can be visualized to have more complex dependence on the said sawdust parameters.
- The best fit empirical model to represent average pore size and porosity of the membranes for variations in kaolin, feldspar and binder composition affirm upon the relevance of complex Poly ratio models for both pore size ($R^2$ of 0.959) and porosity ($R^2$ of 0.999). Thus, composition has much complex non-linear influence on the membrane morphological parameters.



TH-2589_156107040

### 9.1.3 Techno-economic Feasibility of Low Cost Ceramic Membranes for Bottle Gourd Juice Clarification

- CM1 membrane (1 µm pore size and 28.47 % porosity) provided optimal microfiltration performance at 137.9 kPa trans-membrane pressure for the fresh bottle gourd juice system to thereby affirm that the process is competitive to replace the conventional centrifugation process. Under these conditions, the membrane flux varied from $0.18 \times 10^{-5} – 3.12 \times 10^{-5}$ $m^3.m^{-2}.s^{-1}$ for a variation in time from 0 – 80 min during dead end MF.
- Despite indicating that intermediate and standing Hermia models were the best fit models to represent pertinent flux decline, the above reported optimal process parametric conditions ensured a higher combination of FDC (94.13 %) and FRR (91.89 %). Thereby, the observation affirms greater insitu reversible fouling of the membrane in due course of the microfiltration process.
- The greater insitu reversible fouling was further confirmed through the permeation resistance analyses that affirmed negligible contribution of support (0.24 %) and irreversible (0.02 %) permeation resistances in comparison with the reversible permeation resistance (99.74 %).
- For the above mentioned optimal process parametric condition, the clarified permeate sample possessed high clarity (92.46 %), low color (0.15 A) adequate polyphenol content (7.93 mg GAE/100g), adequate flavonoid content (112.8 mg Quercetin/g), adequate carbohydrate content (1.31 g/100mL) and higher combinations of microbial (99.37%) and protein (71.6%) rejections. In other words, the sample shelf life is anticipated to be very high due to adequate constitution of nutritional parameters and reduced protein and microbial content.



TH-2589_156107040

- Based on the conceptual cost of the ceramic membrane CM1 as 440 $/m$^2$, the conceptual juice processing cost varied from 0.37 – 1.19 $/L for a variation in production capacity from 10000 – 110 L/y of the clarified bottle gourd juice product. The membrane process has been analyzed to be highly cost competitive with respect to centrifugation process whose processing cost has been correspondingly evaluated as 0.42 – 3.99 $/L.
- In summary, the insitu reversible fouling of the wider membrane morphology has been analyzed to have a promising and special role to thereby enable the realization of acceptable combinations of membrane flux, clarified permeate product with good combinations of shelf life parameters and nutritional characteristics and lower processing costs.

### 9.1.4 Optimality of Membrane Morphology and Feed Stock during Microfiltration of Bottle Gourd Juice

- Further optimization of microfiltration process parameters for the clarification of bottle gourd juice indicate 0.75 µm (CM3) membrane morphology, filtered juice and 137.9 kPa at which optimal transmembrane flux of $0.08 \times 10^{-5}$ – $1.35 \times 10^{-5}$ $m^3.m^{-2}.s^{-1}$ was obtained for variant time from 0 – 80 min during dead end MF operation.
- Optimal FDC and FRR values for the said process conditions were 94.05 and 85.23 %, respectively and affirm reversible insitu fouling.
- Both intermediate pore blocking and cake filtration model were found to be best fit fouling models with respect to Hermia and Bolton fouling models. The optimized permeation resistances indicated maximum contribution of reversible resistances (97.72 %) followed with insignificant irreversible permeation resistance (1.29 %) and support (0.97 %) resistances.



TH-2589_156107040

- For the above mentioned optimal process conditions, optimal clarified bottle gourd juice product characteristics were 0.16 A color, 92.05 % clarity, 139.17 mg/1000mL protein content, 0.76 g/100mL carbohydrate content and 10.11 mg GAE/100g polyphenol content.
- In summary, the membrane morphology of CM3 membrane performed marginally better in comparison with those of the CM1 membrane.

### 9.1.5 Sonication Assisted Optimal Extraction of Bio-active Compounds from Bitter Gourd Vegetable

- With promising performance of aqueous extraction, significant proportion of bioactive compounds have been successfully extracted using UAE.
- Amongst normal and pulse modes of the UAE, the pulse mode UAE performed better due to larger extraction of polyphenols and antioxidants at the optimal conditions.
- The optimal pulse mode UAE process parameters were 68.4 $^{o}$C temperature, 12 min extraction time and 0.25 g/mL bitter gourd to water ratio at which optimal response variable values of 77.9% antioxidant activity, 104.5 mg GAE/g total polyphenols content and 42.1 mg/1000 mL soluble protein content were obtained.
- The RSM based analysis affirmed linear variation of antioxidant activity and non-linear (quadratic) variation of total polyphenols and total soluble protein content.
- In summary, the RSM based analysis of the UAE of the bitter gourd extract provided useful insights with respect to the optimality of process conditions.



TH-2589_156107040

### 9.1.6 Optimality of Hybrid Sonication-Microfiltration Process for Bitter Gourd Extract Production

- Compared to the UAE process, the hybrid UAE-MF process yielded clarified aqueous bitter gourd extract with better shelf life parameters and marginally reduced nutritional characteristics.
- Among alternate membrane morphologies (CM1, CM3 and CM7) and pressure differentials (103.4, 137.9 and 172.4 kPa), the optimal process conditions during hybrid UAE-MF process were for the CM3 membrane operated at 137.9 kPa at which optimal permeate flux was in the range of $8.09 \times 10^{-6} – 3.34 \times 10^{-5}$ $m^3.m^{-2}.s^{-1}$.
- For the said optimal process conditions, intermediate pore blocking and cake filtration have been the best fit fouling models to represent pertinent flux decline.
- Optimal clarified bitter gourd juice extract characteristics refer to 25.23 mg/1000 mL protein content (46.74 % rejection), 56.68% antioxidant activity, 75.87 mg (GAE)/g polyphenols content, 1259.27 mg/1000 mL carbohydrate content, 0.049 A color and 98.17% clarity.

## 9.2 Future work

Based on the quantum of work addressed in the PhD thesis, the following areas of research have been identified for the needful consideration in the near future to facilitate exciting and challenging research in the field of low cost ceramic membrane based process engineering systems.

- Efficacy of other pore forming agents such as rice husk and coconut coir can be considered to evaluate their competence for the fabrication of defect free low cost ceramic membranes.



TH-2589_156107040

- Other methods of membrane fabrication such as paste method can be deployed for the said compositions and further compositional optimality can be addressed.
- Fabrication of multi-tubular membrane systems using identified compositions can be addressed to further correlate scale up related issues with the compositional optimality of the sawdust based low cost ceramic membranes.
- Other vegetables can be targeted for which microfiltration and UAE can be applied as alternate inexpensive non-thermal process technologies. Thereby, emphasis can be towards the production of organic fruit and vegetable juices and extracts with better shelf life and nutritional characteristics.
- For the processing of bottle gourd juice and bitter gourd juice extracts, other non-thermal processing methods can be addressed.
- Considering the fact that the carbohydrates separation was not achieved through the hybrid MF process, hybrid MF-NF, UAE-MF and centrifugation-MF process can be targeted to enhance the productivity of the produced juices with customized characteristics of the nutritional constituents.
- The LCCM reported in the PhD thesis can be adopted for their efficacy in sectors other than food processing such as wastewater treatment, potable water production, bio-separations and membrane bio-reactors.



TH-2589_156107040

# Appendices

TH-2589_156107040

TH-2589_156107040

# Appendix A: Cost Models and Sample Calculations associated to Techno-economic Feasibility Study

## A. Cost Model Expressions

The following sections summarizes various cost model expressions deployed for the evaluation of costs associated to membrane process system (microfiltration) and centrifugation system to produce clarified bottle gourd juice product.

a. Cost of membrane raw material

$$C_m = \left( \frac{C_a X_a + C_b X_b + C_c X_c + C_d X_d + C_e X_e}{1000} \right) \times 100 \times \text{Total quantity for 1 membrane fabrication}$$

where, $C_m$ is the membrane raw material cost

$C_a, C_b, C_c, C_d$ and $C_e$ are the cost of each components in \$/kg

$X_a, X_b, X_c, X_d$ and $X_e$ are the ratios of each component in the mixture

b. Manpower cost

$$C_{mp} = \text{Per day manpower cost} \times \text{Total number of working days}$$

where, $C_{mp}$ is the Total Manpower Cost

c. Equipment cost

$$C_{eq} = \frac{\text{Equipment price} \times \text{Hours of equipment use}}{\text{Lifespan of the equipment} \times \text{Total working hours/year}}$$

where, $C_{eq}$ is the Total equipment cost

d. Electricity cost

$$C_{ec} = \text{Equipment power rating} \times \text{Hours of equipment use} \times \text{electricity tariff}$$

where, $C_{ec}$ is the total electricity cost

e. Membrane cleaning cost = 10 % of process cost

f. Depreciation = 10 % of process cost

g. Permeation setup and housing cost = 20 % of process cost

TH-2589_156107040

## B. Sample Calculations associated to Techno-economic feasibility

### B.1. Microfiltration Process System

#### B.1.1 Membrane Cost

| Raw Material Cost | | | |
|---|---|---|---|
| **Material** | **Quantity (Fraction)** | **Calculations** | **Cost ($/kg)** |
| Kaolin | 0.4819 | | 3.55 |
| Feldspar | 0.2862 | | 32.09 |
| Saw Dust | 0.0819 | | 0.14 |
| Boric Acid | 0.075 | | 12.44 |
| Sodium Metasilicate | 0.075 | | 7.88 |
| Material required for 1 membrane = 20g | | | |
| Cost of 1 membrane ($) | | ((0.4819×3.55)+(0.2862×32.09)+(0.0819×0.14)+(0.075×12.44)+(0.075×7.88)/1000)×20 | 0.2486 |
| Membrane area (55mm dia) ($m^2$) | | | 0.002375 |
| Cost of membrane ($/$m^2$) | | 0.2486/0.002375 | **104.68** |

| Manpower cost | | | |
|---|---|---|---|
| Assuming 20 membranes could be prepared at a time | | | |
| Manpower cost per day (8 working hours) ($) | | | 6.82 |
| Total working hours | | | 10 |
| Total working days | | | 1.25 |
| Total manpower cost for 1 membrane ($/$m^2$) | | (6.28×1.25)/(20×0.002375) | **179.54** |

| Equipment Cost |
|---|
| Assuming 20 membranes could be prepared at a time |
| Lifespan of Equipments: 10 years |
| Total No. of working days in a year: 330 days |



TH-2589_156107040

**Mixer Grinder**

| | | |
|---|---|---|
| Cost of mixer grinder ($) | | 34.11 |
| Cost for 1 h use ($) | 34.11/(10×330×24) | 0.00043 |
| Time of use (h) | | 0.17 |
| Cost of equipment for making unit area of 1 membranes | 0.00043×0.17/(20×0.002375) | 0.001541 |

**Hydraulic Press**

| | | |
|---|---|---|
| Cost of Hydraulic Press ($) | | 1364.26 |
| Cost for 1 h use ($) | 1364.26/(10×330×24) | 0.0172 |
| Time of use (h) | | 1 |
| Cost of equipment for making unit area of 1 membranes | 0.01722×1/(20×0.002375) | 0.3626 |

**Hot Air Oven**

| | | |
|---|---|---|
| Cost ($) | | 545.70 |
| Cost for 1 h use ($) | 545.70/(10×330×24) | 0.00689 |
| Time of use ($) | | 12 |
| Cost of equipment for making unit area of 1 membranes | 0.00689×12/(20×0.002375) | 1.7407 |

**Muffle Furnace**

| | | |
|---|---|---|
| Cost of Muffle Furnace ($) | | 2728.5129 |
| Cost for 1 h use ($) | 2728.5129/(10×330×24) | 0.0345 |
| Time of use (h) | | 36.25 |
| Cost of equipment for making unit area of 1 membranes | 0.0345×36.25/(20×0.002375) | 26.2915 |

**Sonicator**

| | | |
|---|---|---|
| Cost of Sonicator ($) | | 409.2769 |
| Cost for 1 h use ($) | 409.2769/(10×330×24) | 0.00517 |
| Time of use (h) | | 1.5 |
| Cost of equipment for making unit area of 1 membranes | 0.00517×1.5/(20×0.002375) | 0.1632 |



TH-2589_156107040

| | | |
|---|---|---|
| **Mould** | | |
| Cost of mould ($) | | 136.4256 |
| Cost for 1 h use ($) | 136.4256/(10×330×24) | 0.00172 |
| Time of use (h) | | 1 |
| Cost of equipment for making unit area of 1 membranes | 0.00172×1/(20×0.002375) | 0.03626 |
| **Total Cost of Equipments ($/m$^2$)** | 0.001541+0.3626+1.7407+26.2915+0.1632+0.03626 | **28.59** |
| | **Electricity cost** | |
| Electricity tariff ($) | | 0.0989 |
| **Mixer Grinder** | | |
| Power (kW) | | 0.75 |
| Time of use (h) | | 0.17 |
| Electricity cost for 1 membrane ($/m$^2$) | 0.75×0.17×0.0989/(20×0.002375) | 0.2655 |
| **Hydraulic Press** | | |
| Power (kW) | | 1.492 |
| Time of use (h) | | 1 |
| Electricity cost for 1 membrane ($/m$^2$) | 1.492×1×0.0989/(20×0.002375) | 3.1073 |
| **Hot Air Oven** | | |
| Power (kW) | | 2.4 |
| Time of use (h) | | 12 |
| Electricity cost for 1 membrane ($/m$^2$) | 2.4×12×0.0989/(20×0.002375) | 59.9799 |
| **Muffle Furnace** | | |
| Total Power (kW) | | 1.8 |
| Max capacity (°C) | | 1100 |



TH-2589_156107040

| | | |
|---|---|---|
| **Time for Temp rise from 100 °C to 250 °C (average temperature 175 °C) (h)** | | 1.5 |
| Power required (kW) | (175/1100)×1.8 | 0.2864 |
| Electricity cost for 1 membrane ($/m$^2$) | 1.5×0.2864×0.0989/(20×0.002375) | 0.8946 |
| **Time at 250 °C (h)** | | 24 |
| Power required (kW) | (250/1100)×1.8 | 0.4091 |
| Electricity cost 1 membrane ($/m$^2$) | 24×0.4091×0.0989/(20×0.002375) | 20.4477 |
| **Time for Temp rise from 250 °C to 850 °C (average temperature 550 °C) (h)** | | 5 |
| Power required (kW) | (550/110)×1.8 | 0.9 |
| Electricity cost for 1 membrane ($/m$^2$) | 5×0.9×0.0989/(20×0.002375) | 9.3719 |
| **Time at 850 °C (h)** | | 6 |
| Power required | (850/1100)×1.8 | 1.3909 |
| Electricity cost for 1 membrane ($/m$^2$) | 6×1.13909×0.0989/(20×0.002375) | 17.3806 |
| Electricity cost due to muffle furnace for 1 membrane ($/m$^2$) | 0.8946+20.4477+9.3719+17.3806 | 48.0947 |
| **Sonicator** | | |
| Power (kW) | | 0.28 |
| Time of use (h) | | 1.5 |
| Electricity cost for 1 membrane ($/m$^2$) | 0.28×1.5×0.0989/(20×0.002375) | 0.8936 |
| **Total Electricity cost for 1 membrane ($/m$^2$)** | 0.2655+3.1073+59.9799+48.0947+ 0.8936 | **112.34** |

| **Miscellaneous Cost** | | | |
|---|---|---|---|
| | Quantity | Price/item ($) | |
| Sandpaper ($) | 6 | 0.0682 | 0.4093 |
| Tissue ($) | 1 | 0.3411 | 0.3411 |
| Total Miscellaneous Cost 1 membrane ($/m$^2$) | | | **15.80** |



TH-2589_156107040

| | | |
|---|---|---|
| **Total membrane cost ($/m$^2$)** | **104.6772+179.5377+28.59+112.3413+ 15.7967** | **440.94** |

**B.1.2 Overall Process Cost**

**Basis:**

1. Capacity = 109.89 L/y
2. Shelf life of membrane = 1 year

| | **Calculations** | **Costs** |
|---|---|---|
| Cost of membrane raw materials ($/m$^2$) | | 104.6772 |
| Total manpower cost for 1 membrane ($/m$^2$) | | 179.5377 |
| Total Equipment cost ($/m$^2$) | | 28.59 |
| Total Electricity cost 1 membrane ($/m$^2$) | | 112.3413 |
| Total Miscellaneous Cost 1 membrane ($/m$^2$) | | 15.7967 |
| | | |
| Compressor Electricity cost ($/y) | 0.2×112.3413 | 22.4644 |
| Equipment cost due to compressor ($/y) | 0.2×28.59 | 5.7201 |
| Total Fixed cost due to compressor ($/y) | 22.4644+5.7201 | 28.1845 |
| | | |
| Total membrane cost ($/m$^2$) | | **440.94** |
| Cost of membrane with 0.002375 m$^2$ area ($/y) | 440.9369/0.002375 | **1.05** |
| Permeate flux after 80 min (m$^3$/m$^2$.s) | | $1.83\times10^{-06}$ |
| Total working days in a year for juice processing (Assuming 80 min per run and additional 10 min for taking out the permeate, cleaning, etc.) | (80/90)×330 | =293.3333 |
| Amount processed per year (L/y) | $1.83\times10^{-06}\times1000\times0.002375\times$ | 109.8902 |



TH-2589_156107040

| | | |
|---|---|---|
| | 293.33×24×3600 | |
| Process Cost ($) | 28.1845+1.0471 | 29.2316 |
| Membrane cleaning cost ($/y) | 0.1×29.2316 | 2.9232 |
| Depreciation at 10% ($/y) | 0.1×29.2316 | 2.9232 |
| Permeation setup and housing($/y) | 0.2×29.2316 | 5.8463 |
| Total Cost of the process ($/y) | 29.2316+2.9232+2.9232+5.8463 | 40.9243 |
| Cost of 1 kg bottle gourd ($) | | 0.4093 |
| Efficiency of the process | | 0.5 |
| Required quantity of bottle gourd for 1L of Juice (1kg~1L) | | 2 |
| Cost of bottle gourd ($) | | 0.8186 |
| Raw material cost for 1 L of permeate ($) | | 0.8186 |
| Raw material cost for 109.89 L ($/y) | | 89.9510 |
| overall cost of juice separation process ($/y) | | 130.8753 |
| **Cost of juice ($/L)** | | **1.19** |
| **Cost of juice (Rs/L)** | | **87.30** |

Note: The cost of bottle gourd used for the scale-up calculations were 0.1364 $/kg (whole sale rate)

**B.2 Centrifugation Process System**

| | **Calculations** | **Costs** |
|---|---|---|
| Total centrifuged juice (L/y) | | 110 |
| Run time for single batch (min) | | 40 |
| Total juice centrifuged in single batch (L) | | 3.5 |
| With 90% efficiency of the centrifuge, total juice processed in single batch (L) | 0.9×3.5 | 3.15 |
| Batches required for 110L juice | | 34.9206 |
| Total min required for 110L (min/y) | 34.9206×40 | 1396.8254 |
| Total hours (h/y) | 1396.8254/60 | 23.2804 |
| Manpower cost per day (8 working hours) ($) | | 6.82 |
| Total Manpower Cost ($/y) | (6.82/8)×23.2804 | **19.85** |



TH-2589_156107040

| | | |
|---|---|---|
| **Centrifuge due to Cost** | | |
| Cost of centrifuge ($) | | 5457.026 |
| Lifespan (y) | | 15 |
| Total Equipment Cost ($/y) | 5457.026/15 | **363.80** |
| | | |
| **Electricity (Centrifuge) cost** | | |
| Power (kW) | | 2.56 |
| Time of use (h) | | 23.2804 |
| Total Electricity Cost ($/y) | 2.56×23.2804×0.0989(tariff) | **5.89** |
| Centrifuge efficiency | | 0.9 |
| Bottle gourds required to 110L juice (kg) | | |
| (1kg~1L) | 110/0.9 | 122.2222 |
| Total bottle gourd price ($/y) | 122.2222×0.4093 | **50.02** |
| Total Processing Cost ($/y) | 19.8503+363.8017+5.8947+50.0227 | 439.5695 |
| Cost per Litre ($/L) | | **3.99** |
| Cost per Litre (Rs/L) | | **292.91** |



TH-2589_156107040

# Appendix B: Calibration Curves for the Determination Nutritional Characteristics of Juices and Extracts

The absorbance of fresh juice, filtered juice, centrifuged juice, extracts and different permeate and extract samples was determined using a UV-Visible Spectrophotometer (Model No.: UV-2600, Make: Shimadzu, Singapore). To do so, measurements were carried out at specific wavelengths for the quantification of various nutritional parameters. Accordingly, the concentrations of proteins, carbohydrates, total flavonoids and total phenolics/polyphenols in the said samples were determined through the measurement of sample absorances at 595, 625, 510, and 750 nm, respectively. Also, a calibration curve (concentration-absorbance plot) was prepared for each constituent so as to determine the concentration of the said nutrients. For each case, the range of sample concentration was distinct for various nutrients and this was according to the measurable range associated to each nutrient. Thereby, the calibration charts have been prepared in the concentration range of 30 - 250, 100 – 750 and 10 – 80 ppm for proteins, carbohydrates and total flavonoids respectively.

The preparation procedures associated to the sample preparation has been elaborated in section 2.2.3 (Chapter 2) of the PhD thesis. The calibration curve efficacy has been fine tuned to achieve maximum $R^2$ value.

Figure A1 (a – d) depicts the obtained calibration curves of proteins, carbohydrates, total flavonoids and total polyphenols, respectively. After plotting the calibration curve, the concentrations of unknown samples could be determined with the slope of the curves. In other words, the intercept value has been taken to be zero and all curves have been fit as straight lines passing through the origin.

TH-2589_156107040

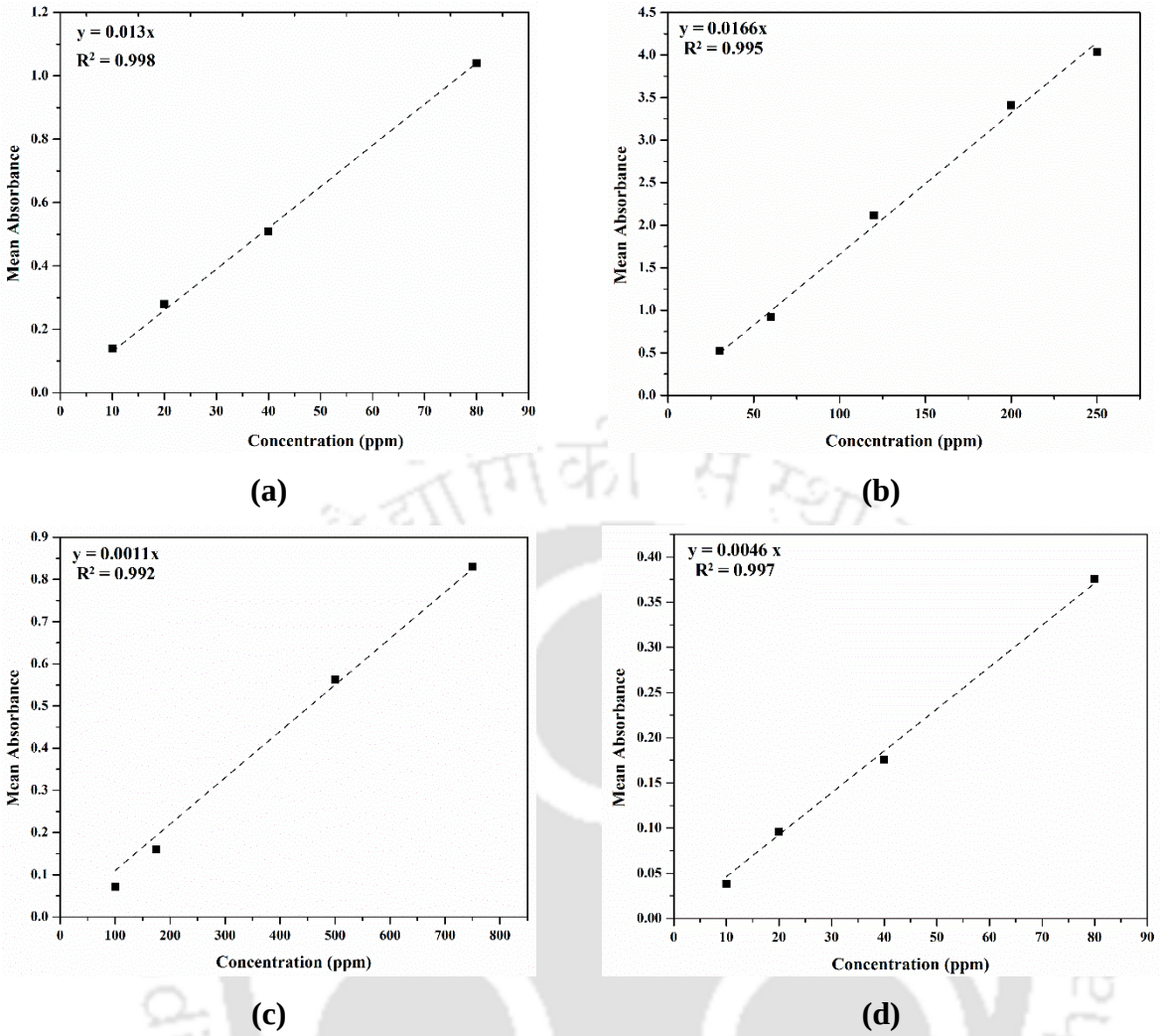


**Figure A1: Calibration curves for the determination of nutritional characteristics of feed and extract samples (a) protein, (b) carbohydrate, (c) total flavonoid, and (d) total polyphenol content**

# Appendix C: Energy Consumption in Microfiltration and Microfiltration-Centrifugation Process

## A. Membrane Preparation

| | | |
|---|---|---|
| **Mixer Grinder** | | |
| Power (kW) | | 0.75 |
| Time of use (h) | | 0.17 |
| Energy consumption 1 membrane ($kWh/m^2$) | 0.75×0.17/(20×0.002375) | 2.6842 |
| **Hydraulic Press** | | |
| Power (kW) | | 1.492 |
| Time of use (h) | | 1 |
| Energy consumption 1 membrane ($kWh/m^2$) | 1.492×1/(20×0.002375) | 31.4105 |
| **Hot Air Oven** | | |
| Power (kW) | | 2.4 |
| Time of use (h) | | 12 |
| Energy consumption 1 membrane ($kWh/m^2$) | 2.4×12/(20×0.002375) | 606.3157 |
| **Muffle Furnace** | | |
| Total Power (kW) | | 1.8 |
| Max capacity (°C) | | 1100 |
| **Time for Temp rise from 100 °C to 250 °C (average temperature 175 °C) (h)** | | 1.5 |
| Power required (kW) | (175/1100)×1.8 | 0.2864 |
| Energy consumption 1 membrane ($kWh/m^2$) | 1.5×0.2864/(20×0.002375) | 9.0442 |
| **Time at 250 °C (h)** | | 24 |
| Power required (kW) | (250/1100)×1.8 | 0.4091 |
| Energy consumption 1 membrane | 24×0.4091/(20×0.002375) | 206.7032 |

TH-2589_156107040

| | | |
|---|---|---|
| ($kWh/m^2$) | | |
| **Time for Temp rise from 250 °C to 850 °C (average temperature 550 °C) (h)** | | 5 |
| Power required (kW) | (550/110)×1.8 | 0.9 |
| Energy consumption 1 membrane ($kWh/m^2$) | 5×0.9/(20×0.002375) | 94.7368 |
| **Time at 850 °C (h)** | | 6 |
| Power required | (850/1100)×1.8 | 1.3909 |
| Energy consumption 1 membrane ($kWh/m^2$) | 6×1.3909/(20×0.002375) | 175.6926 |
| Energy consumption due to muffle furnace for 1 membrane ($kWh/m^2$) | 9.0442+206.7032+94.7368+175.6926 | 486.1768 |
| **Sonicator** | | |
| Power (kW) | | 0.28 |
| Time of use (h) | | 1.5 |
| Energy consumption for 1 membrane ($kWh/m^2$) | 0.28×1.5/(20×0.002375) | 8.8421 |
| **Total energy consumption for 1 membrane ($kWh/m^2$)** | 2.6842+31.4105+606.3157+486.1768+ 8.8421 | **1135.4293** |

## B. Power Consumption in the Overall Process

**Basis:** Single run of 80 min

### B.1 Microfiltration Process

| | | |
|---|---|---|
| **Compressor** | | |
| Power (kW) | | 1.9 |
| Time of use (h) | | 0.17 |
| Energy consumption (kWh) | 1.9×0.17 | 0.323 |
| Total energy consumption for 1 membrane ($kWh/m^2$) | | 1135.4293 |



TH-2589_156107040

| | | |
|---|---|---|
| Total energy consumption for membrane with 0.002375 $m^2$ area (kWh) | 1135.4293×0.002375 | 2.6966 |
| Total energy consumption with respect to compressor and membrane fabrication (kWh) | 0.323+2.6966 | 3.0196 |
| Energy consumption due to miscellaneous electricity usage (kWh) | 0.2×3.0196 | 0.6039 |
| **Total energy consumption due to microfiltration process (kWh)** | 3.0196+0.6039 | **3.6235** |

**B.2 Combined Centrifugation and Microfiltration Process**

| | | |
|---|---|---|
| **Centrifuge** | | |
| Power (kW) | | 2.56 |
| Time of use (h) | | 0.17 |
| Total Energy consumption (kWh) | 2.56×0.17 | 0.4352 |
| **Compressor** | | |
| Power (kW) | | 1.9 |
| Time of use (h) | | 0.17 |
| Energy consumption (kWh) | 1.9×0.17 | 0.323 |
| Total energy consumption for 1 membrane (kWh/$m^2$) | | 1135.4293 |
| Total energy consumption for membrane with 0.002375 $m^2$ area (kWh) | 1135.4293×0.002375 | 2.6966 |



TH-2589_156107040

| | | |
|---|---|---|
| Total energy consumption with respect to compressor and membrane fabrication (kWh) | 0.323+2.6966+0.4352 | 3.4548 |
| Energy consumption due to miscellaneous electricity usage (kWh) | 0.2×3.4548 | 0.6909 |
| **Total energy consumption due to combined microfiltration and centrifugation process (kWh)** | 3.4548+0.6909 | **4.1457** |



TH-2589_156107040

# Appendix D: ANOVA based analysis of Experimental Investigations

The data significance of the experimental investigations have been confirmed through the one-way ANOVA analysis for relevant responses (FDC and permeate characteristics). This is also due to the fact that the data presented in Chapters 6 and 8 of the PhD thesis have been already addressed with statistical analysis. For all relevant cases, the one-way ANOVA based data analysis summary has been presented in Tables D1-D3. The tables affirm high F-values and low p-values for the obtained data. For the bottle gourd juice clarification case, maximum F-value was obtained for reversible resistance. On the other hand, the lowest F-value was obtained for the carbohydrate content (Table D1). This is very likely due to the low content of the carbohydrate content of the juice and subsequent compromise on the evaluation efficiency to a certain extent. Table D2 denotes the ANOVA analysis of FDC using alternate membrane morphologies (CM1, CM3, and CM7) being obtained for various trans-membrane pressure differentials. The maximum F-value was obtained at 137.9 kPa and affirmed significance of the process data at this pressure condition. Statistical analysis of the hybrid system for the clarification of bitter gourd extracts indicate a marginal contradiction in comparison with the results being obtained for the bottle gourd juice clarification process. This is possibly due to the nature of the feed being clarified (Table D3). Hence, maximum F-value and lowest p-value was obtained for carbohydrates. However, for the colour case, contrary trends were being obtained. Very low value of colour in both feed and permeate samples is very likely to be the reason to achieve the relevant error in the analysis being conducted for the samples.

TH-2589_156107040

**Table D1: ANOVA analysis data of optimal bottle gourd juice clarification characteristics of CM1, CM3, and CM7 membranes with respect to (a) FRR, (b) FDC, (c) Reversible Resistance, (d) Color, (e) Clarity, (f) Proteins, (g) Carbohydrates, and (h) Polyphenols.**

| Membranes | Trail 1 | Trail 2 | Trail 3 | Mean | Standard Deviation | SE of Mean | F-Value | P-Value |
|---|---|---|---|---|---|---|---|---|
| CM1 | 94.12 | 91.3 | 90.25 | 91.89 | 2.00 | 1.16 | | |
| CM3 | 86.29 | 86.9 | 82.65 | 85.28 | 2.29 | 1.33 | 76.16 | $5.44E^{-5}$ |
| CM7 | 73.18 | 70.8 | 73.52 | 72.5 | 1.48 | 0.86 | | |

**(a)**

| Membranes | Trail 1 | Trail 2 | Trail 3 | Mean | Standard Deviation | SE of Mean | F-Value | P-Value |
|---|---|---|---|---|---|---|---|---|
| CM1 | 91.23 | 90.58 | 92.90 | 91.57 | 1.19 | 0.69 | | |
| CM3 | 86.29 | 86.9 | 82.65 | 94.05 | 1.94 | 1.12 | 55.07 | $1.37E^{-4}$ |
| CM7 | 73.18 | 70.8 | 73.52 | 77.26 | 2.87 | 1.66 | | |

**(b)**

| Membranes | Trail 1 | Trail 2 | Trail 3 | Mean | Standard Deviation | SE of Mean | F-Value | P-Value |
|---|---|---|---|---|---|---|---|---|
| CM1 | 99.77 | 99.52 | 99.9 | 99.73 | 0.19 | 0.11 | | |
| CM3 | 98.67 | 97.64 | 96.85 | 97.72 | 0.91 | 0.53 | 2388.99 | $1.97E^{-9}$ |
| CM7 | 62.47 | 63.99 | 62.54 | 63 | 0.86 | 0.49 | | |

**(c)**

| Membranes | Trail 1 | Trail 2 | Trail 3 | Mean | Standard Deviation | SE of Mean | F-Value | P-Value |
|---|---|---|---|---|---|---|---|---|
| CM1 | 0.19 | 0.15 | 0.11 | 0.15 | 0.04 | 0.02 | | |
| CM3 | 0.13 | 0.18 | 0.17 | 0.16 | 0.03 | 0.02 | 55.17 | $1.37E^{-4}$ |
| CM7 | 0.52 | 0.48 | 0.41 | 0.47 | 0.06 | 0.03 | | |

**(d)**

| Membranes | Trail 1 | Trail 2 | Trail 3 | Mean | Standard Deviation | SE of Mean | F-Value | P-Value |
|---|---|---|---|---|---|---|---|---|
| CM1 | 89.61 | 94.11 | 93.69 | 92.47 | 2.49 | 1.43 | | |
| CM3 | 90.73 | 92.81 | 92.61 | 92.05 | 1.15 | 0.66 | 76.16 | $5.44E^{-5}$ |
| CM7 | 93.85 | 82.17 | 84.66 | 83.56 | 1.27 | 0.73 | | |

**(e)**



TH-2589_156107040

| Membranes | Trail 1 | Trail 2 | Trail 3 | Mean | Standard Deviation | SE of Mean | F-Value | P-Value |
|---|---|---|---|---|---|---|---|---|
| CM1 | 190.49 | 194.31 | 193.69 | 192.83 | 2.05 | 1.18 | | |
| CM3 | 145.17 | 139.73 | 132.61 | 139.17 | 6.29 | 3.64 | 137.98 | $9.63E^{-6}$ |
| CM7 | 194.63 | 187.14 | 188.62 | 190.13 | 3.97 | 2.29 | | |

**(f)**

| Membranes | Trail 1 | Trail 2 | Trail 3 | Mean | Standard Deviation | SE of Mean | F-Value | P-Value |
|---|---|---|---|---|---|---|---|---|
| CM1 | 1.11 | 1.46 | 1.36 | 1.31 | 0.18 | 0.10 | | |
| CM3 | 0.94 | 0.73 | 0.61 | 0.76 | 0.17 | 0.09 | 12.32 | 0.007 |
| CM7 | 1.18 | 1.17 | 1.22 | 1.19 | 0.03 | 0.01 | | |

**(g)**

| Membranes | Trail 1 | Trail 2 | Trail 3 | Mean | Standard Deviation | SE of Mean | F-Value | P-Value |
|---|---|---|---|---|---|---|---|---|
| CM1 | 7.64 | 7.89 | 8.26 | 7.93 | 0.31 | 0.18 | | |
| CM3 | 10.47 | 9.84 | 10.02 | 10.11 | 0.32 | 0.19 | 130.11 | $1.14E^{-5}$ |
| CM7 | 22.95 | 20.22 | 19.62 | 20.93 | 1.77 | 1.02 | | |

**(h)**

**Table D2: ANOVA analysis data of the flux decay coefficients associated with CM1, CM3, and CM7 membranes during the clarification of bitter gourd extracts at alternate pressure differentials of (a) 103.4, (b) 137.9, and (c) 172.4 kPa**

| Membranes | Trail 1 | Trail 2 | Trail 3 | Mean | Standard Deviation | SE of Mean | F-Value | P-Value |
|---|---|---|---|---|---|---|---|---|
| CM1 | 64.58 | 64.31 | 65.12 | 64.67 | 0.41 | 0.24 | | |
| CM3 | 67.30 | 66.97 | 67.45 | 67.24 | 0.25 | 0.14 | 63.16 | $9.33E^{-5}$ |
| CM7 | 67.18 | 66.80 | 67.29 | 67.09 | 0.26 | 0.15 | | |

**(a)**

| Membranes | Trail 1 | Trail 2 | Trail 3 | Mean | Standard Deviation | SE of Mean | F-Value | P-Value |
|---|---|---|---|---|---|---|---|---|
| CM1 | 69.04 | 69.31 | 68.62 | 68.99 | 0.35 | 0.20 | | |
| CM3 | 75.26 | 75.17 | 74.45 | 74.96 | 0.44 | 0.26 | 247.58 | $1.71E^{-6}$ |
| CM7 | 73.03 | 73.18 | 72.90 | 73.05 | 0.14 | 0.08 | | |

**(b)**



TH-2589_156107040

| Membranes | Trail 1 | Trail 2 | Trail 3 | Mean | Standard Deviation | SE of Mean | F-Value | P-Value |
|---|---|---|---|---|---|---|---|---|
| CM1 | 72.74 | 73.10 | 72.68 | 72.84 | 0.23 | 0.13 | | |
| CM3 | 76.18 | 75.71 | 75.45 | 75.78 | 0.37 | 0.21 | 126.68 | $1.24E^{-5}$ |
| CM7 | 77.75 | 78.18 | 78.9 | 78.28 | 0.58 | 0.34 | | |

**(c)**

**Table D3: ANOVA analysis data of the bitter gourd extract characteristics of the hybrid UAE-MF system at 137.9 kPa pressure and for CM1, CM3, and CM7 membranes (a) Protein, (b) Antioxidant Activity, (c) Polyphenols, (d) Carbohydrates, (e) Color, and (f) Clarity.**

| Membranes | Trail 1 | Trail 2 | Trail 3 | Mean | Standard Deviation | SE of Mean | F-Value | P-Value |
|---|---|---|---|---|---|---|---|---|
| CM1 | 39.40 | 40.63 | 40.18 | 40.07 | 0.62 | 0.36 | | |
| CM3 | 24.57 | 25.01 | 26.11 | 25.23 | 0.79 | 0.46 | 548.97 | $1.61E^{-7}$ |
| CM7 | 24.17 | 24.55 | 23.49 | 24.07 | 0.54 | 0.31 | | |

**(a)**

| Membranes | Trail 1 | Trail 2 | Trail 3 | Mean | Standard Deviation | SE of Mean | F-Value | P-Value |
|---|---|---|---|---|---|---|---|---|
| CM1 | 65.04 | 66.71 | 65.32 | 65.69 | 0.89 | 0.52 | | |
| CM3 | 55.77 | 56.99 | 57.28 | 56.68 | 0.80 | 0.46 | 354.52 | $5.91E^{-7}$ |
| CM7 | 49.11 | 49.80 | 48.75 | 49.22 | 0.53 | 0.31 | | |

**(b)**

| Membranes | Trail 1 | Trail 2 | Trail 3 | Mean | Standard Deviation | SE of Mean | F-Value | P-Value |
|---|---|---|---|---|---|---|---|---|
| CM1 | 79.02 | 78.90 | 78.15 | 78.69 | 0.47 | 0.27 | | |
| CM3 | 76.69 | 75.29 | 75.63 | 75.87 | 0.73 | 0.42 | 74.34 | $5.84E^{-5}$ |
| CM7 | 72.83 | 73.50 | 72.55 | 72.96 | 0.49 | 0.28 | | |

**(c)**

| Membranes | Trail 1 | Trail 2 | Trail 3 | Mean | Standard Deviation | SE of Mean | F-Value | P-Value |
|---|---|---|---|---|---|---|---|---|
| CM1 | 1905.35 | 1936.78 | 1897.26 | 1913.13 | 20.87 | 12.05 | | |
| CM3 | 1261.57 | 1310.29 | 1210.55 | 1260.80 | 49.87 | 28.79 | 658.80 | $9.31E^{-8}$ |
| CM7 | 926.52 | 965.78 | 950.47 | 947.59 | 19.79 | 11.42 | | |

**(d)**



TH-2589_156107040

| Membranes | Trail 1 | Trail 2 | Trail 3 | Mean | Standard Deviation | SE of Mean | F-Value | P-Value |
|---|---|---|---|---|---|---|---|---|
| CM1 | 0.057 | 0.055 | 0.053 | 0.055 | 0.002 | 0.001 | | |
| CM3 | 0.048 | 0.048 | 0.051 | 0.049 | 0.001 | 0.001 | 12 | 0.008 |
| CM7 | 0.049 | 0.043 | 0.043 | 0.045 | 0.003 | 0.002 | | |

**(e)**

| Membranes | Trail 1 | Trail 2 | Trail 3 | Mean | Standard Deviation | SE of Mean | F-Value | P-Value |
|---|---|---|---|---|---|---|---|---|
| CM1 | 97.55 | 97.82 | 97.79 | 97.72 | 0.15 | 0.08 | | |
| CM3 | 98.06 | 98.34 | 98.11 | 98.17 | 0.15 | 0.09 | 37.97 | $3.92E^{-4}$ |
| CM7 | 99.00 | 98.90 | 98.65 | 98.85 | 0.18 | 0.104 | | |

**(f)**



TH-2589_156107040

TH-2589_156107040

TH-2589_156107040

# Publications

TH-2589_156107040

TH-2589_156107040

# Publications

## International Refereed Journals

**[1] Chakraborty, S.,** Uppaluri, R., Das, C., (2018) "Optimal Fabrication of Carbonate Free Low Cost Ceramic Membranes using Mixture Model RSM Design Methodology", Applied Clay Science, 162: 101-112.

**[2] Chakraborty, S.,** Uppaluri, R., Das, C., (2020) "Optimization of Ultrasound-assisted Extraction (UAE) Process for the Recovery of Bioactive Compounds from Bitter Gourd using Response Surface Methodology (RSM)", Food and Bioproducts Processing, 120: 114-122.

**[3] Chakraborty, S.,** Das, C., Uppaluri, R., (2020) "Feasibility of Low-Cost Kaolin–Based Ceramic Membranes for Organic *Lagernaria siceraria* Juice Production", Food and Bioprocess Technology, 13: 1009-1023.

**[4] Chakraborty, S.,** Uppaluri, R., Das, C., (2020) "Combinatorial Optimality of Membrane Morphology and Feedstock during Microfiltration of Bottle Gourd Juice", Innovative Food Science and Emerging Technologies, 63:102382.

**[5] Chakraborty, S.,** Uppaluri, R., Das, C., (2020) "Effect of Pore Former (Sawdust) Characteristics on the Properties of Sub-micron Range Low Cost Ceramic Membranes", International Journal of Ceramic Engineering and Science, 2:243-253.

TH-2589_156107040

## Articles Submitted/Under Preparation

**[1] Chakraborty, S.,** Uppaluri, R., Das, C., (2020) "Efficacy of Sonication-Microfiltration Hybrid Process for the Production of Clarified Bitter Gourd Extracts". Food and Bioprocess Technology, **Under Review**.

**[2] Chakraborty, S.,** Uppaluri, R., Das, C., "Influence of Precursor Composition on the Morphological Characteristics of Sub-micron Range Low Cost Ceramic Membranes".

**[3] Chakraborty,** S., Uppaluri, R., Das, C., "Ultrasound-assisted Extraction of Phytochemicals from Night Jasmine Leaves".

## Conference Presentations

**[1] Chakraborty, S.,** Das, C., Uppaluri, R., (2018) "Low Cost Ceramic Membrane Based Clarification of *Lagenaria siceraria* Juice", IJBS'17, 01-04 February, 2018, IIT Guwahati.

**[2] Chakraborty, S.,** Uppaluri, R., Das, C., (2018) "Effect of bio-pore forming agent particle size on the morphological characteristics of low cost ceramic membranes", ICAMEES'18, 14-15 December, 2018, UPES Dehradun.

**[3] Chakraborty, S.,** Uppaluri, R., Das, C., (2019) "Effect of pore former particle size and concentration on the morphological characteristics of ceramic membranes", Research Conclave'19, IIT Guwahati.

**[4] Chakraborty, S.,** Das, C., Uppaluri, R., (2019) "Preparation of Bottle Gourd Juice Using Low Cost Ceramic Membranes", Reflux'19, IIT Guwahati.

**[5] Chakraborty, S.,** Das, C., Uppaluri, R., (2020) "Influence of Precursor Composition on the Characteristics of Sub-micron Range Low Cost Ceramic Membranes", AIMS'20, BMSITM Bengaluru.



TH-2589_156107040

**[6]** **Chakraborty, S.,** Das, C., Uppaluri, R., (2020) "Morphological influence of bio pore-former characteristics during ceramic membrane fabrication", ICACC'21, Florida (Virtual).



TH-2589_156107040

TH-2589_156107040

TH-2589_156107040

TH-2589_156107040

TH-2589_156107040

TH-2589_156107040

TH-2589_156107040